

Fluorescence studies of binders used in paintings: ageing and pigment effects

By

Loreley Kirstin Cairns

Submitted in partial fulfilment of the requirements for the degree

Magister Scientiae

In the Faculty of Natural & Agricultural Sciences

University of Pretoria


Pretoria

Supervisor: Professor Patricia Forbes

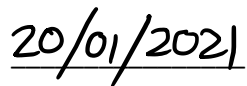
January 2021

Declaration of Authorship

I, Loreley Kirstin Cairns, declare that the dissertation; which I hereby submit for the degree Magister Scientiae at the University of Pretoria, is my own work and has not previously been submitted by me for a degree at this or any other institution.

A handwritten signature in black ink, appearing to read "Loreley Cairns", written over a horizontal line.

Signature

A handwritten date "20/01/2021" in black ink, written over a horizontal line.

Date

*“To develop a complete mind:
study the science of art, and
study the art of science.
Learn how to see, and
realise that everything connects to everything else.”*

~ Leonardo da Vinci

Summary

A large range of binding materials are used in paintings, some of which are characterised by their fluorescence (e.g. drying oils) and others in which the fluorescence is poorly understood (e.g. synthetic binders). This study aims to identify the fluorescence of binding media (proteinaceous, polysaccharide, synthetic binders and drying oils), as well as determine any changes in fluorescence which are resultant of ageing and pigment effects.

Drying oils were identified as having the highest fluorescence intensity of all binders used in this study, and the fluorescence was found to bathochromically shift as the dried film aged (after 2 years of natural ageing). To fully understand the changes in fluorescence, four different commercially available oils (namely linseed, water-miscible linseed-, stand- and poppyseed oil) were analysed using UV-visible absorption and fluorescence spectroscopy. Both liquid and cured, solid film oils were analysed. Liquid oils showed a structured absorption pattern, of which only two weakly absorbing peaks (λ_{ex} 300 and 315 nm) resulted in fluorescence emission (λ_{em} 330 and 410 nm). The solid film lacked the structured pattern seen in the liquid oil's absorption spectrum, showing instead a broad absorption peak. At an excitation wavelength (λ_{ex}) of 365 nm, the cured film normally fluoresces at λ_{em} 440 nm, but was seen to shift to λ_{em} 550 nm due to yellowing.

Artificial ageing techniques (exposure to UV light, elevated temperatures, and ammonia vapour) were applied to the drying oils to induce the bathochromic fluorescence shifts. As the oils aged a yellow to brown discolouration developed. A correlation between the degree of discolouration and the shift in fluorescence was identified. As the oils change colour so does the fluorescence and the fluorescence shifts from blue (λ_{em} 440 nm) to green (λ_{em} 550 nm) and sometimes even yellow.

In addition to the artificial ageing of drying oils, five different pigments were mixed individually with various binders. The five pigments used in this study were: lamp black, Indian yellow, oriental blue, phthalo blue and alizarin crimson. Characterisation and fluorescence studies of each of these pigments were done, and it was found that alizarin crimson (AC) has a characteristic green fluorescence (λ_{em} 550 nm) in solutions that facilitate hydrogen bonding. The pigment-binder mixtures were then analysed using fluorescence spectroscopy to determine whether the pigments caused changes in fluorescence of the binder it was mixed with. It was found that the pigments caused a slight hypsochromic shift in egg-based binding media. However, most binders were unaffected by the non-fluorescent pigments. Interestingly, the drying oils created a newly fluorescent compound with AC, in which three peaks were

identified in the fluorescence spectra: the drying oil (λ_{em} 450 nm), the green fluorescence of AC (λ_{em} 550 nm) and a new orange fluorescent peak (λ_{em} 630 nm).

The results of this study indicate that fluorescence spectroscopy is a non-invasive technique which can be used in the analysis of paintings. Fluorescence spectroscopy can be used to determine the class of binding medium used, as well as the yellow discolouration of drying oils. Non-fluorescent pigments do not affect the fluorescence of binding media, and thus confirms the validity of fluorescence spectroscopy as an analytical tool in conservation studios.

Acknowledgements

I would like to start by thanking the most important people that helped me complete this dissertation. Firstly, to Prof Forbes, without your belief in me and trusting me with the lab work and write up, I would not have achieved all I have in these two years. Secondly, to my chemistry family for always being someone I can bounce ideas off; Shane, Clarissa, Wynand, Simphiwe, Jessie and Leylene. Thank you for constantly listening and giving advice to help solve problems. Thirdly, thank you to my family, Mamma, Daddy, Kaylen and Gawain, Pilot, Chicco and Splash (WYLKG-PCS), thank you for helping me relax and take a break.

The University of Pretoria Museums are acknowledged for the support and donations of binding media. My conservation family, Maggi, Isabelle, Sandra and Salome, are thanked for reminding me why I started this masters in the first place. Thank you for helping me remember the importance and relevance of my research. I would also like to thank my high school art teacher, Juffrou Gesie. Dankie! Sonder Juffrou sou ek nooit van hierdie navorsingsveld geleer het nie. Dankie vir Juffrou Morrison wat altyd in my geglo het en my oortuig het om wetenskap te swot en 'n manier te vind om my twee liefdes (kuns en wetenskap) te kombineer.

My lab and office colleagues, for all the coffee and cake with birthday celebrations. A BIG thank you to the best librarian ever, Rianie van der Linde. Thank you so much for always helping me find articles from ages long past. Thank you to Daniel for helping me gain confidence in my writing. Thank you, Dr Selepe, Rendani, Madelien and Babalwa for your help in HPLC analysis.

I would also like to thank my friends and church family, too numerous to mention, for all the dance evenings, zoom calls and game nights. Lastly, an extra special thanks to Leo. Without you this last year would have been impossible, thank you for helping me find motivation in the final stages of the write up!

Table of Contents

Declaration of authorship	ii
Summary	iv
Acknowledgements	vi
List of Figures	ix
List of Tables	xiii
List of Abbreviations	xiv
Chapter 1: Background to the Study	1
1.1 Analysis of paintings	1
1.2 Aims and objectives of this study	3
1.3 Justification of this study	4
1.4 Structure of the dissertation	4
1.5 References	4
Chapter 2: Literature Review	11
2.1 Introduction	11
2.2 Ultraviolet fluorescence imaging as an art forensic tool	11
2.3 Principles of ultraviolet fluorescence	13
2.4 Ultraviolet fluorescence spectroscopy	15
2.5 Instrumentation	18
2.6 Application	23
2.6.1 Binders	23
2.6.2 Pigments	30
2.6.3 Limitations of fluorescence spectroscopy on paintings	33
2.7 Case study from literature	33
2.8 References	35
Chapter 3: Experimental Methodology	45
3.1 Overview	45
3.2 Sample preparation	47
3.2.1 Binders	47
3.2.2 Pigments	48
3.2.3 Solid samples	51
3.2.4 Ageing of samples	52
3.2.5 Powder samples	56
3.2.6 Liquid samples	56
3.3 Instrumentation	58
3.3.1 UV-induced fluorescence imaging	58
3.3.2 Absorption and fluorescence spectroscopy.	57
3.3.3 Infra-red spectroscopy	57

3.3.4	X-ray fluorescence spectroscopy	59
3.3.5	Powder X-ray diffraction	59
3.3.6	Chromatography	59
3.4	References	60
Chapter 4: Results and Discussion		62
4.1	Fluorescence study of lipid binders	62
4.1.1	Absorption and fluorescence studies	62
4.1.2	Chromatography studies	67
4.1.3	Ageing studies	69
4.2	Fluorescence study of pigments	77
4.2.1	Characterization of the pigments.	79
4.2.2	Fluorescence spectroscopy of pigments.	88
4.3	Fluorescence study of binder and pigment mixtures	93
4.3.1	Lamp black	93
4.3.2	Oriental blue	95
4.3.3	Phthalo blue	96
4.3.4	Indian yellow	98
4.3.5	Alizarin crimson	100
4.3.6	Comparison of pigments in different binders	103
4.4	References	104
Chapter 5: Conclusion		110
5.1	Final remarks and conclusion	110
5.2	Recommendations and future work	111
Addenda		
Addendum A:	Additional graphs for lipid studies	A1
Addendum B:	Additional graphs for pigment characterisation	B1
Addendum C:	Fluorescence images of alizarin crimson	C1
Addendum D:	Fluorescence images of lamp black	D1
Addendum E:	Fluorescence images of oriental blue.	E1
Addendum F:	Fluorescence images of phthalo blue.	F1
Addendum G:	Fluorescence images of Indian yellow	G1
Addendum H:	Summary of fluorescence of binders from previous studies	H1
Addendum I:	Outputs of previous studies	I1
Addendum J:	Published journal paper	J1

List of Figures

Fig. 2.1	Winged youth, Roman wall painting at the British Museum. VIS) Visible image; UVR) UV reflected image; UVF) UV-induced luminescence where the dark areas are due to previous restoration work.	12
Fig. 2.2	The electronic structure of an arbitrary system. Indicating various radiative/non-radiative degradation paths that result in a lower energy emission than the absorption energy.	14
Fig. 2.3	A 3D fluorescence map of a film of gum Arabic.	16
Fig. 2.4	Fluorescence life-time imaging of a section of damaged painted wall painted by Masolino da Panicale, in the Collegiata of Catiglione Olona - a Renaissance church near Varese; a) intensity map; b) life-time map; c) HSV map.	18
Fig. 2.5	Chemical monomers of selected synthetic binders.	30
Fig. 2.6	Fluorescence of Salome's face painted by Masolino di Panicale. a) Visual image; b) UV-induced fluorescence excited at 365 nm with an UV-A low pressure mercury lamp.	34
Fig. 3.1	Overview of project layout shown in relation to research done in previous years.	46
Fig. 3.2	Example of microscope slides covered in canvas. These samples are coated with the respective drying oil, the drying oils are not cured in this image.	52
Fig. 3.3	A photo of the chamber which is saturated with ammonia vapour from a 25% ammonia solution.	53
Fig. 3.4	Summary of the samples used in the artificial ageing experiments.	55
Fig 3.5	An example of the powder sample holder for the fluorescence measurements which is filled with Indian yellow pigment.	56
Fig. 4.1	UV-Vis absorption spectra of the liquid drying oils dissolved in ethanol. All spectra were blank corrected and normalised to 1.	63
Fig. 4.2	Fluorescence and absorption spectra of cured drying oils (once they formed a solid film). All oils studied showed the same peaks.	63

Fig. 4.3	Absorption spectra of liquid linseed oil dissolved in ethanol (red) and corresponding fluorescence spectra, at an excitation wavelength (λ_{ex}) 300 nm (black) and λ_{ex} 315 nm (blue), respectively.	64
Fig. 4.4	UV chromatograms of methanol extracts of cured LO film (top) and liquid LO (below) at different wavelengths: 240 nm – green; 260 nm – red; 280 nm – navy blue; 300 nm – light blue.	67
Fig. 4.5	Absorption and fluorescence spectra of the most optically active fractions in linseed oil collected by HPLC-PDA-SPE.	68
Fig. 4.6	Yellowing of oils after 24 hours of UV-light exposure, and subsequent storage in a dark drawer. The colour changes that occur over time are evident, from freshly painted oil (A), to 7 days (B), 14 days (C) and 4 months (D) of storage in the dark drawer.	70
Fig. 4.7	Changes in the fluorescence spectrum of aged linseed oil, exposed for 24 hr to UV light and subsequently stored in a dark drawer. The excitation wavelength for all measurements was 360 nm. The bathochromic shift (to a longer emission wavelength) is a result of yellowing as the sample ages.	70
Fig. 4.8	Rate of the fluorescence emission maximum changes of linseed oil after various exposure times to UV light (254 nm) and then subsequent storage in dark drawers. The excitation wavelength was 360 nm for all measurements.	71
Fig. 4.9	Rate of fluorescent changes of linseed oil after exposure to ammonia vapor, and subsequent storage in a dark drawer. The excitation wavelength was 360 nm for all measurements.	73
Fig. 4.10	Bleaching of yellowed linseed oil after 8 hr exposure to sunlight. The excitation wavelength was 360 nm for all measurements.	75
Fig. 4.11	Powder X-ray diffraction pattern of lamp black pigment.	78
Fig. 4.12	FTIR-ATR spectrum of lamp black pigment.	79
Fig. 4.13	Experimental PXRD pattern of oriental blue pigment sample (black line), where the overlaid blue lines indicate 2 theta values for ultramarine (pigment blue 29) from the ICDD database.	80
Fig. 4.14	Chemical structure of phthalocyanine blue, the metal (M) being copper in the blue variety.	81

Fig. 4.15	X-ray fluorescence spectrum of phthalocyanine blue, using 30 kV excitation energy with a rhodium X-ray tube.	82
Fig. 4.16	FTIR spectrum of phthalocyanine blue.	82
Fig. 4.17	Chemical structures of Indian yellow colourants: a) euxanthic acid; b) acid orange 1; c) acid yellow 23; d) acid yellow 63.	83
Fig. 4.18	FTIR-ATR spectrum of Indian yellow.	84
Fig. 4.19	Structures of the anthraquinone derivatives responsible for the red colour in madder lake. a) alizarin; b) purpurin; c) pseudopurpurin.	85
Fig. 4.20	FTIR-ATR spectrum of alizarin crimson. The spectrum was obtained from 4000 cm ⁻¹ to 400 cm ⁻¹ .	85
Fig. 4.21	Positive ion mass chromatograms from red pigments dissolved in methanol.	87
Fig. 4.22	Fluorescence spectra of powder pigments under 254 nm excitation (not normalised).	88
Fig. 4.23	Fluorescence spectra of powder pigments under 360 nm excitation (not normalised)	89
Fig. 4.24	The fluorescence image of pigments in ethanol under 365 nm UV light.	89
Fig. 4.25	The absorption (black) and fluorescence spectra (red) of alizarin crimson in different solvents.	91
Fig. 4.26	The fluorescence image of alizarin crimson (AC) in different solvents under 365 nm UV light.	92
Fig. 4.27	Fluorescence spectra of lamp black-binder mixtures at excitation wavelength 254 nm.	94
Fig. 4.28	Fluorescence spectra of drying oils mixed with lamp black (LB) pigment.	94
Fig. 4.29	Fluorescence of oriental blue (OB) mixed with drying oils (λ_{ex} 360 nm).	95
Fig. 4.30	Fluorescence spectra of phthalo blue-binder mixtures at excitation wavelength 254 nm.	97
Fig. 4.31	Fluorescence spectra of phthalo blue (PB) mixed with drying oils (λ_{ex} 360 nm).	97

Fig. 4.32	Fluorescence spectra of Indian yellow-binder mixtures at excitation wavelength 254 nm.	98
Fig. 4.33	Fluorescence spectra of Indian yellow (IY) mixed with drying oils (λ_{ex} 360 nm).	99
Fig. 4.34	Fluorescence image of alizarin crimson-binder samples painted onto microscope slides visualised under 254 nm ultraviolet light. The green fluorescence of alizarin crimson mixed with paraloid B72 is evident.	100
Fig. 4.35	Fluorescence spectra of alizarin crimson-binder mixtures at an excitation wavelength of 360 nm.	101
Fig. 4.36	Fluorescence spectra of alizarin crimson (AC) mixed with drying oils (λ_{ex} 360 nm).	103

List of Tables

Table 2.1	Light sources used as excitation source for fluorescence measurements of paintings.	19
Table 2.2	Detectors generally used in fluorescence spectroscopy.	22
Table 2.3	A summary of the fluorescence from various paint binders found in literature.	24
Table 2.4	The fatty acid content of drying oils typically present in paintings.	26
Table 2.5	Summary the excitation wavelength and emission peaks of known fluorescent pigments found in literature.	30
Table 3.1	Summary of artists materials used. The preparation method and the abbreviations used for each binder and pigment are described.	48
Table 4.1	Shifts in absorption and emission bands of the liquid sample, cured film, ethanol extract and the oil film after ethanol extraction, as well as the two purified HPLC fractions in methanol.	65

List of Abbreviations

Alphabetized according to the first letter of the abbreviation.

Abbr.	Description	Abbr.	Description
AC	Alizarin crimson	OB	Oriental blue
ACN	Acetonitrile	OX	Ox gall
ATR	Attenuated total reflection	P67	Paraloid P67
BA	Butyl acrylate	P72	Paraloid P72
BMA	Butyl methacrylate	PAA	Polyacrylic acid
c	Speed of light	PB	Phthalo blue
CCD	Charge-coupled device	PDA	Photodiode array
CMOS	Complementary metal oxide semiconductor	Phe	Phenylalanine
DEE	Diethyl ether	PMT	Photomultiplier tube
DI.H₂O	Deionised water	PO	Poppy seed oil
DMF	Dimethyl formamide	PR83	Alizarin crimson, light
DMSO	Dimethyl sulfoxide	PR112	Alizarin crimson, dark
DOPA	Dihydroxyphenylalanine	PVAC	Polyvinyl acetate
DSLR	Digital single-lens reflex	PVAL	Polyvinyl alcohol
EM	Electromagnetic	PVB	Polyvinyl butyral
EMA	Ethyl methacrylate	PXRD	Powder X-ray diffraction
EtOAc	Ethyl Acetate	QTOF	Quadrupole time of flight
EtOH	Ethanol	QY	Quantum yield
EW	Egg white	RGB	Red-Green-Blue
EY	Egg Yolk	rpm	Rotations per minute
FG	Fish glue	RSG	Rabbit skin glue
FLIM	Fluorescence lifetime imaging	S₀	Ground state
FTIC	Fluorescein isothiocyanate	S₁	First excited state
FTIR	Fourier-transform infrared	S₂	Second excited state
FWHM	Full width at half maximum	SA	South Africa

GA	Gum Arabic	SFS	Synchronous fluorescence spectroscopy
GM	Gilding milk	SO	Stand oil
GT	Gum Tragacanth	Trp	Tryptophan
h	Planck's constant	TR-LIF	Time resolved laser induced fluorescence
HPLC	High performance liquid chromatography	Tyr	Tyrosine
HSV	Hue-saturation-value	UK	United Kingdom
ICDD	International Centre for Diffraction Data	UPLC	Ultra-performance liquid chromatography
IPCH	Institute for the Preservation of Cultural Heritage	USA	United States of America
IR	Infrared	UV	Ultraviolet
IY	Indian yellow	UVA	UV light between 315-400 nm
KG	Klusel G	UVB	UV light between 280-315 nm
Las	Lascoux	UVC	UV light between 100-280 nm
LB	Lamp black	UVF	UV-induced fluorescence
LED	Light emitting diode	UVL	UV luminescence
LEDμSF	LED micro spectrofluorometer	UVR	UV reflectance
Lidar	Light detection and ranging	WE	Whole egg
LIF	Laser induced fluorescence	WLO	Water-miscible linseed oil
LISSA	Lissamine rhodamine B sulfonyl chloride	XRF	X-ray fluorescence
LO	Linseed oil	μSPE	Micro solid phase extraction
MA	Methyl acrylate	λ	Wavelength
MeOH	Methanol	λ_{em}	Emission wavelength
Mi	Mowiol 18-88	λ_{ex}	Excitation wavelength
MMA	Methyl methacrylate	3D	Three dimensional
Mt	Mowital B30H	Δf	Polarizability orientation
n	Refractive index	μ_G	Ground state dipole moment

NCPD	Non-conjugated polymer dots	μ_E	Excited state dipole moment
Nd:YAG	Neodymium-yttrium aluminium garnet	$\bar{\nu}_A$	Absorption wavenumber
NFK	N-formylkynurenine	$\bar{\nu}_F$	Fluorescence wavenumber
NR9	Madder lake, genuine	ϵ	Dielectric constant

Chapter 1: Background to the Study

1.1 Analysis of paintings

There is often the misconception that paintings are static and unchanging objects. However, paintings are dynamic systems that are constantly changing, and are expected to be observed a hundred years or more after the artist painted it. Over time, degradation reactions can cause significant colour changes in the painting from what was originally painted [1-4]. Scientific research can be used to identify these changes and predict further degradation reactions. Chemical analysis (ranging from spectroscopic to chromatographic techniques) can give information on the context, historical significance, provenance, and the exhibition history of a painting, and can help historians develop a comprehensive technical background of the work [5]. Research and chemical analysis can explore the history of the painting by identifying situations/environmental factors that the painting was exposed to, which led to colour changes and thereby degradation reactions.

A recent technical study on the famous *Girl with the Pearl Earring*, painted by Johannes Vermeer, clearly showcases the importance of research [6-15]. The original study, entitled: *Girl Illuminated*, was done in 1994, when the painting, which was in a very poor condition, was obtained by the Mariutshuis museum. The study was motivated by the need to understand the physical and chemical state of the painting, to advise conservators of the best conservation treatment [6, 16]. In 2018 the second study, entitled: *The Girl in the Spotlight*, was done to develop a better understanding of the history of the painting, i.e. what materials were used and how they are distributed in the painting [8-14]. When the material properties of the painting were identified, they could be related to the broader historical and technical context of Vermeer's work [15]. These two major research projects on the same painting were conducted for two distinctly different reasons, highlighting the importance of the chemical analysis of paintings.

There are several ways in which scientific research on paintings can be done, and these can be classified into two broad groups which are of importance to conservators: destructive and non-destructive methods [17]. As the name suggests, destructive methods damage the object being analysed, either through the removal of sample material from a rare object or through ablating the material, which leaves a hole in the object [18, 19]. Both scenarios are best avoided, especially considering that some heritage artefacts might only be broken shards of a few centimetres cubed in size. When several

samples are needed for various tests, the artefact quickly becomes depleted and destroyed. For this reason, several conservation governance bodies have strict guidance on when it is ethical to take a sample for research purposes [20, 21].

As invasive destructive analysis is generally unwanted, there is a great incentive to develop non-destructive sampling methods for the chemical analysis of works of art [22, 23]. These non-destructive techniques rely mostly on spectroscopy, in which electromagnetic radiation (EM) is used to irradiate a sample, and the reflectance, transmission or fluorescence of these EM rays are detected [22].

Several EM radiation techniques aimed at painting characterisation have employed X-rays [24-27] or infrared (IR) radiation [28-35], measuring the reflection, absorption and fluorescence of these EM rays. Similar techniques such as Raman spectroscopy, electron microscopy and various ion beam analysis techniques [36-40] have also been employed to obtain an in-depth analysis of the painting. This study is focussed on developing an ultraviolet (UV) fluorescence technique, which is achieved by irradiating a sample with ultraviolet light and measuring the resultant visible light fluorescence.

Ultraviolet fluorescence imaging/photography is a technique which has been used in chemical art analysis since the early 1930's [41], however in the last few years hand-held spectrometers have been developed which allow the fluorescence spectra of a painting to be measured, and not only the fluorescence colour from images [42, 43]. Though fluorescence of paintings is a known phenomenon, paintings have a complex composition which changes depending on the artist's painting style. Ultraviolet-induced fluorescence is dependent on the energy levels within a molecule. These energy levels can change with electron withdrawing or donating groups being introduced into the system, and therefore the fluorescence is dependent on the chemical composition of the painting. There is ongoing research aimed at identifying these changes in fluorescence and the underlying chemical composition which causes them [44-51].

1.2 Aims and objectives of this study

This study aims to develop a better understanding of the chemistry behind the fluorescence of paintings. This is essential if fluorescence spectroscopy is to not only be used as a diagnostic test of the binders, but to understand the complexity of the painter's materials and the interaction between pigments and binders. This will aid conservators in better interpreting ultraviolet-induced fluorescence images when faced with an unconventional fluorescence result. The focus of this study is to determine the changes in fluorescence of the binding media used in paintings, as a result of ageing and pigment effects. Four main groups of binders were investigated, namely: drying oils, proteinaceous binders, polysaccharide binders and synthetic binders.

In a preliminary study, the four different groups of binders were prepared, aged, and mixed with non-fluorescent inorganic pigments. Inorganic pigments do not dissolve in the binder and remain in their crystalline form. Therefore, to further develop the technique, organic pigments with possible fluorescent characteristics, as well as pigments which dissolve in the binder and thus lead to larger pigment-binder interactions, were mixed with the different binders.

The objectives of this study were to:

- Identify the fluorescent changes (if any) after two years of natural ageing of the various binders.
- Induce artificial ageing in lipid binders through exposure to elevated temperatures, ultraviolet light, and ammonia gas. Thereafter identify and/or characterise the fluorescent changes that result from the different artificial ageing mechanisms.
- Prepare paint samples that are mixtures of binders and organic pigments, and to characterise the changes in fluorescence of binders caused by the pigments.
- Use chromatographic techniques to understand the chemical processes that cause changes in fluorescence of lipid binders, and that occur due to ageing or pigment-binder interactions.

1.3 Justification of this study

Given the widespread use of ultraviolet-induced fluorescence photography of historical artefacts, this study is crucial to identify the accuracy and viability of these techniques. Several studies have identified the fluorescence of either a binder [44, 52-54] or pigment [55-57] in isolation, however, few studies that treat paintings as a complex mixture of various binders and pigments have been done [51, 58]. This study aims to characterise the fluorescence of each drying oil, and to determine how the fluorescence changes as a function of time. Furthermore, this study will determine how the fluorescence of a various binders changes in mixtures with fluorescent and non-fluorescent organic pigments.

1.4 Structure of the dissertation

This dissertation is structured into five chapters, in which the fluorescence of binders and the induced chemical changes that they undergo through the action of pigments and ageing, are presented. Chapter 2 reviews the literature of UV-induced fluorescence and the recent advances made in painting analysis using ultraviolet light. It also includes a short section on the known chemical changes that occur in the binders and pigments that were used in this study. Chapter 3 provides an overview of the experimental techniques used in this study. The results and discussion are presented in Chapter 4, where the results for the drying oils are analysed first (no interference from pigments). Thereafter the pigments are discussed and how pigment-binder mixtures affect the fluorescence methods of binder identification that utilise fluorescence measurements. Chapter 5 concludes the discussion of the results and provides recommendations for future studies.

1.5 References

1. Kirchner E, Geldof M, Hendriks E, Gaibor P, Ness A, Janssens K, et al. Recreating Van Gogh's original colors on museum displays. *IS&T International Symposium on Electronic Imaging*. 2019;77:1-5. Doi: 10.2352/ISSN.2470-1173.2019.14.COLOR-077.
2. Geldof M, Gaibor ANP, Ligterink F, Hendriks E, Kirchner E. Reconstructing Van Gogh's palette to determine the optical characteristics of his paints. *Heritage Science*. 2018;6(17):1-20. Doi: 10.1186/s40494-018-0181-6.

3. Kirchner E, van der Lans I, Ligterink F, Geldof M, Megens L, Meedendorp T, et al. Digitally reconstructing Van Gogh's Field with Irises near Arles part 3: Determining the original colors. *Color Research and Application*. 2018;43:311-327. Doi: 10.1002/col.22197.
4. Berns RS, Byrns S, Casadio F, Fiedler I, Gallagher C, Imai FH, et al. Rejuvenating the color palette of Georges Seurat's A Sunday on La Grande Jatte—1884: A simulation. *Color Research and Application*. 2006;31(4):278-293. Doi: 10.1002/col.20223.
5. Arslanoglu J, Centeno SA, Digney-Peer S, Duvernois I. "Picasso in the Metropolitan Museum of Art": an investigation of materials and techniques. *Journal of the American Institute for Conservation*. 2013;52(3):140-155. Doi: 10.1179/1945233013Y.0000000007.
6. Vandivere A, Wadum J, van den Berg KJ, van Loon A. From 'Vermeer Illuminated' to 'The Girl in the Spotlight': approaches and methodologies for the scientific (re-) examination of Vermeer's Girl with a Pearl Earring. *Heritage Science*. 2019;7(66):1-14. Doi: 10.1186/s40494-019-0307-5.
7. Vandivere A. The technical (re-) examination of Vermeer's Girl with a Pearl Earring. *Heritage Science*. 2020;8(26):1-4. Doi: 10.1186/s40494-020-00370-7.
8. Vandivere A, van Loon A, Dooley KA, Haswell R, Erdmann RG, Leonhardt E, et al. Revealing the painterly technique beneath the surface of Vermeer's Girl with a Pearl Earring using macro-and microscale imaging. *Heritage Science*. 2019;7(64):1-16. Doi: 10.1186/s40494-019-0308-4.
9. Delaney JK, Dooley KA, van Loon A, Vandivere A. Mapping the pigment distribution of Vermeer's Girl with a Pearl Earring. *Heritage Science*. 2020;8(4):1-16. Doi: 10.1186/s40494-019-0348-9.
10. De Meyer S, Vanmeert F, Vertongen R, van Loon A, Gonzalez V, van der Snickt G, et al. Imaging secondary reaction products at the surface of Vermeer's Girl with the Pearl Earring by means of macroscopic X-ray powder diffraction scanning. *Heritage Science*. 2019;7(67):1-11. Doi: 10.1186/s40494-019-0309-3.
11. Elkhuisen WS, Callewaert TW, Leonhardt E, Vandivere A, Song Y, Pont SC, et al. Comparison of three 3D scanning techniques for paintings, as applied to Vermeer's 'Girl with a Pearl Earring'. *Heritage Science*. 2019;7(89):1-22. Doi: 10.1186/s40494-019-0331-5.

12. van Loon A, Gambardella AA, Gonzalez V, Cotte M, De Nolf W, Keune K, et al. Out of the blue: Vermeer's use of ultramarine in Girl with a Pearl Earring. *Heritage Science*. 2020;8(25):1-18. Doi: 10.1186/s40494-020-00364-5.
13. van Loon A, Vandivere A, Delaney JK, Dooley KA, De Meyer S, Vanmeert F, et al. Beauty is skin deep: the skin tones of Vermeer's Girl with a Pearl Earring. *Heritage Science*. 2019;7(102):1-10. Doi: 10.1186/s40494-019-0344-0.
14. Vandivere A, van Loon A, Callewaert T, Haswell R, Gaibor ANP, van Keulen H, et al. Fading into the background: the dark space surrounding Vermeer's Girl with a Pearl Earring. *Heritage Science*. 2019;7(69):1-19. Doi: 10.1186/s40494-019-0311-9.
15. Vandivere A, Wadum J, Leonhardt E. The Girl in the Spotlight: Vermeer at work, his materials and techniques in Girl with a Pearl Earring. *Heritage Science*. 2020;8(20):1-10. Doi: 10.1186/s40494-020-0359-6.
16. Wadum J, Costaras N. Johannes Vermeer's 'Girl with a pearl earring': de- and re-restored. *Preprints of ARAAFU's 4th international symposium; 1995*.
17. Rizzutto M, Curado J, Bernardes S, Campos P, Kajiya E, Silva T, et al. Analytical techniques applied to study cultural heritage objects. *2015 International Nuclear Atlantic Conference – INAC*. 2015. ISBN: 978-85-99141-06-9.
18. Giussani B, Monticelli D, Rampazzi L. Role of laser ablation–inductively coupled plasma–mass spectrometry in cultural heritage research: a review. *Analytica Chimica Acta*. 2009;635(1):6-21. Doi: 10.1016/j.aca.2008.12.040.
19. Grönlund R, Lundqvist M, Svanberg S. Remote imaging laser-induced breakdown spectroscopy and remote cultural heritage ablative cleaning. *Optics Letters*. 2005;30(21):2882-2884.
20. Quye A, Strlič M. *Ethical sampling guidance*. London: Institute of Conservation (ICON); 2019.
21. Adriaens M, Degryny C, Cassar J. *Benefits of non-destructive analytical techniques for conservation*: Office for Official Publications of the European Communities; 2005.
22. Janssens K, Dik J, Cotte M, Susini J. Photon-based techniques for nondestructive subsurface analysis of painted cultural heritage artifacts. *Accounts of Chemical Research*. 2010;43(6):814-825.

23. Janssens K, Van Grieken R. *Non-destructive micro analysis of cultural heritage materials*. Amsterdam: Elsevier; 2004.
24. Alfeld M, Janssens K, Dik J, de Nolf W, van der Snickt G. Optimization of mobile scanning macro-XRF systems for the in situ investigation of historical paintings. *Journal of Analytical Atomic Spectrometry*. 2011;26(5):899-909.
25. Hocquet FP, del Castillo HC, Xicotencatl AC, Bourgeois C, Oger C, Marchal A, et al. Elemental 2D imaging of paintings with a mobile EDXRF system. *Analytical and Bioanalytical Chemistry*. 2011;399:3109-3116. Doi: 10.1007/s00216-010-4281-8.
26. Malmqvist KG. Comparison between PIXE and XRF for applications in art and archaeology. *Nuclear Instruments and Methods in Physics Research Section B: Beam Interactions with Materials and Atoms*. 1986;14(1):86-92.
27. Mosca S. Identification of pigments in different layers of illuminated manuscripts by X-ray fluorescence mapping and Raman spectroscopy. *Microchemical Journal*. 2016;124:775-784. Doi: 10.1016/j.microc.2015.10.038.
28. Moon T, Schilling MR, Thirkettle S. A note on the use of false-color infrared photography in conservation. *Studies in Conservation*. 1992:42-52.
29. Mairinger F. The infrared examination of paintings. *Radiation in Art and Archeometry*. Eds DC Creagh, DA Bradley, Elsevier. 2000:40-55.
30. Cosentino A. Effects of different binders on technical photography and infrared reflectography of 54 historical pigments. *International Journal of Conservation Science*. 2015;6(3):287-298.
31. Derrick MR, Stulik D, Landry JM. *Infrared spectroscopy in conservation science*. Los Angeles: The Getty Conservation Institute; 2000.
32. Legrand S, Alfeld M, Vanmeert F, De Nolf W, Janssens K. Macroscopic reflection Fourier Transformed Mid-Infrared (MA-rFTIR) scanning, a new technique for in situ imaging of painted cultural heritage artifacts. *Analyst*. 2014;139:2489-2498.
33. Ricciardi P, Delaney JK, Facini M, Zeibel JG, Picollo M, Lomax S, et al. Near infrared reflectance imaging spectroscopy to map paint binders *in situ* on illuminated manuscripts. *Angewandte Chemie International Edition*. 2012;51(23):5607-5610.

34. Rosi F, Miliani C, Braun R, Harig R, Sali D, Brunetti BG, et al. Noninvasive analysis of paintings by mid-infrared hyperspectral imaging. *Angewandte Chemie International Edition*. 2013;52(20):5258-5261.
35. Thoury M, Delaney JK, de la Rie ER, Palmer M, Morales K, Krueger J. Near-infrared luminescence of cadmium pigments: in situ identification and mapping in paintings. *Applied Spectroscopy*. 2011;65(8):939-951.
36. Casadio F, Daher C, Bellot-Gurlet L. Raman spectroscopy of cultural heritage materials: overview of applications and new frontiers in instrumentation, sampling modalities, and data processing. *Analytical Chemistry for Cultural Heritage*. 2017:161-211.
37. Ghirardello M. Time-resolved photoluminescence microscopy combined with X-ray analyses and Raman spectroscopy sheds light on the imperfect synthesis of historical cadmium pigments. *Analytical Chemistry*. 2018;90(18):10771-10779.
38. Rosi F. UV–Vis–NIR and micro-Raman spectroscopies for investigating the composition of ternary $\text{CdS}_{1-x}\text{Se}_x$ solid solutions employed as artists' pigments. *Microchemical Journal*. 2016;125:279-289.
39. Smith GD, Clark RJH. Raman microscopy in art history and conservation science. *Studies in Conservation*. 2014;46:92-106.
40. Vandenabeele P, Wehling B, Moens L, Edwards H, De Reu M, Van Hooydonk G. Analysis with micro-Raman spectroscopy of natural organic binding media and varnishes used in art. *Analytica Chimica Acta*. 2000;407(1-2):261-274.
41. Rorimer JJ. *Ultra-violet rays and their use in the examination of works of art*, New York: Metropolitan Museum of Art; 1931.
42. Romani A, Clementi C, Miliani C, Brunetti B, Sgamellotti A, Favaro G. Portable equipment for luminescence lifetime measurements on surfaces. *Applied Spectroscopy*. 2008;62(12):1395-1399.
43. Mounier A, Lazare S, Le Bourdon G, Aupetit C, Servant L, Daniel F. LED μ SF: a new portable device for fragile artworks analyses. Application on medieval pigments. *Microchemical Journal*. 2016;126:480-487.
44. de la Rie ER. Fluorescence of paint and varnish layers (Part I). *Studies in Conservation*. 1982;27(1):1-7.

45. de la Rie ER. Fluorescence of paint and varnish layers (Part II). *Studies in Conservation*. 1982;27(2):65-69.
46. de la Rie ER. Fluorescence of Paint and Varnish Layers (Part III). *Studies in Conservation*. 1982;27(3):102-108.
47. Dhenadhayalan N, Mythily R, Kumaran R. Fluorescence spectral studies of gum Arabic: multi-emission of gum Arabic in aqueous solution. *Journal of Luminescence*. 2014;155:322-329.
48. Marinelli M, Pasqualucci A, Romani M, Verona-Rinati G. Time resolved laser induced fluorescence for characterization of binders in contemporary artworks. *Journal of Cultural Heritage*. 2017;23:98-105.
49. Miyoshi T. Fluorescence from oil colours, linseed oil and poppy oil under N₂ laser excitation. *Japanese Journal of Applied Physics*. 1985;24(3):371-372.
50. Romani A, Clementi C, Miliani C, Favaro G. Fluorescence spectroscopy: a powerful technique for the noninvasive characterization of artwork. *Accounts of Chemical Research*. 2010;43(6):837-846.
51. Verri G, Clementi C, Comelli D, Cather S, Piqué F. Correction of ultraviolet-induced fluorescence spectra for the examination of polychromy. *Applied Spectroscopy*. 2008;62(12):1295-1302.
52. Nevin A, Cather S, Anglos D, Fotakis C. Analysis of protein-based binding media found in paintings using laser induced fluorescence spectroscopy. *Analytica Chimica Acta*. 2006;573:341-346.
53. Nevin A, Cather S, Burnstock A, Anglos D. Analysis of protein-based media commonly found in paintings using synchronous fluorescence spectroscopy combined with multivariate statistical analysis. *Applied Spectroscopy*. 2008;62(5):481-489.
54. Nevin A, Comelli D, Valentini G, Anglos D, Burnstock A, Cather S, et al. Time-resolved fluorescence spectroscopy and imaging of proteinaceous binders used in paintings. *Analytical and Bioanalytical Chemistry*. 2007;388(8):1897-1905.
55. Artesani A, Ghirardello M, Mosca S, Nevin A, Valentini G, Comelli D. Combined photoluminescence and Raman microscopy for the identification of modern pigments: explanatory examples on cross-sections from Russian avant-garde paintings. *Heritage Science*. 2019;7(17):1-13.

56. Cesaratto A. Analysis of cadmium-based pigments with time-resolved photoluminescence. *Analytical Methods*. 2014;6:130-138.
57. Comelli D, MacLennan D, Ghirardello M, Phenix A, Schmidt Patterson CM, Khanjian H, et al. The degradation of cadmium yellow paint – New evidence from photoluminescence studies of trap states in Picasso’s *Femme (Époque des “Demoiselles d’Avignon”)*. *Analytical Chemistry*. 2019;91(5):3421-3428.
58. Verri G, Comelli D, Cather S, Saunders D, Piqué F, editors. Post-capture data analysis as an aid to the interpretation of ultraviolet-induced fluorescence images. *Proceedings of SPIE – The International Society for Optical Engineering*. 2008;6810:1-12.

Chapter 2: Literature Review

2.1 Introduction

This study investigates the intrinsic fluorescence of binding media used in paintings. Though this study is scientifically based, fluorescence imaging of paintings is a common photographic technique used in conservation studios. To fully understand the fluorescence of binding media it is important to acknowledge the importance and history of the imaging technique along with the principles of fluorescence spectroscopy. A review and summary of previously published studies on the applications of fluorescence spectroscopy in paintings is included in this Chapter.

2.2 Ultraviolet fluorescence imaging as an art forensic tool

Ultraviolet (UV) induced fluorescence imaging of paintings is a common method used in conservation studios and is one of the first diagnostic tests in art forensics. This technique is often employed in crime series or movies (for example *White Collar S01E05* and *Hawaii Five-0 S05E11*), due to the eye-catching quality of seeing a painting illuminated. However, contrary to how Hollywood presents it, ultraviolet imaging is only the first of many steps in art forensics.

Ultraviolet light has been used from the early 20th century to analyse paintings [1], of which ultraviolet induced fluorescence (UVF) imaging is the most common technique. A sample/painting is irradiated with UV light which causes the painting to emit radiation in the visible light range. UV light absorbance can also be measured through detecting the reflection of UV rays. The ultraviolet reflection (UVR) image obtained is a black and white photo (Figure 2.1), which is used to identify the intensity of reflected UV light. Both UVR and UVF images can be taken using a digital camera, each with its own set of modifications. An UVR photo measures the intensity of reflected UV light and therefore the UV-filter in the camera should be removed and a visible light and infrared filter should be installed to cancel out all visible and infrared light. In contrast, UVF images (also known as UV luminescence, UVL) are taken with an UV-filter which removes the UV excitation wavelength, to prevent any reflected UV light from obscuring the photo [2].

UVF is commonly used in conservation studios to observe heterogeneities on the surface of paintings, such as craquelure, biological attack, or areas of previous restoration which is not always visible to the

naked eye [3]. Retouched paint from previous restoration has similar optical properties as original paint and cannot be distinguished by the naked eye but can be distinguished by its behaviour under UV light, where it commonly appears darker (Figure 2.1). UVF can also identify and characterise strongly fluorescent pigments such as Indian yellow and madder lake, which have known fluorescence properties [4-7].

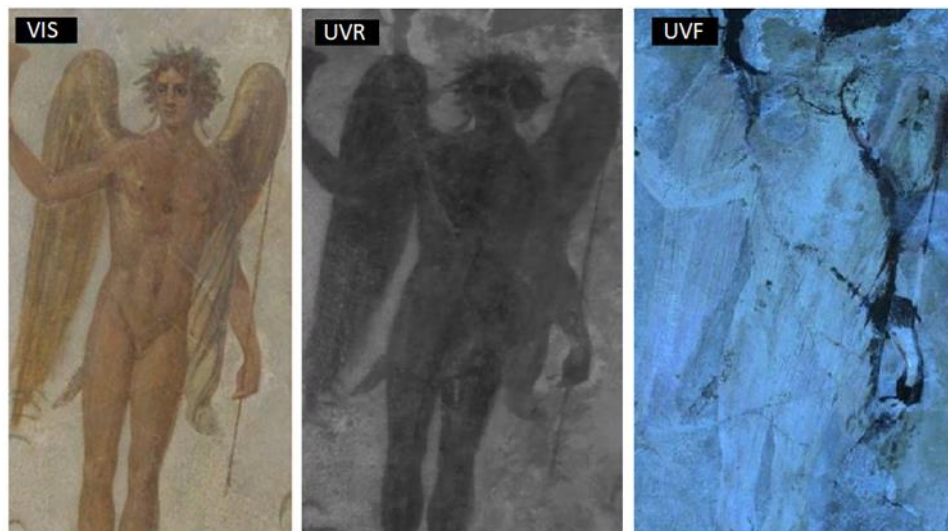


Figure 2.1: *Winged youth, Roman wall painting at the British Museum. VIS) Visible image; UVR) UV reflected image; UVF) UV-induced fluorescence where the dark areas are due to previous restoration work [8].*

Studies have attempted to classify pigments and binding media based on their luminescent colours [9-13]. However due to ageing, degradation, and substrate effects this has proved difficult to summarise. Drying oils have been identified by both yellow [14] and blue luminescence [15]. Whereas blue-green fluorescence is indicative of proteinaceous binders (egg white and animal glues) [14]. Strongly fluorescent pigments, which are more fluorescent than the binders that encase them, can easily be identified. For example, madder lake which is known for its pinkish-orange fluorescence can easily be detected, even when the red colourant is not visible to the naked eye [16], see Section 2.7. However, poorly fluorescent pigments, such as zinc white, are not so easily detected in an UVF image [17].

The discrepancies and overlap between the different luminescent colours have led to the development of multispectral imaging and fluorescence spectroscopy techniques to aid in identification [16, 18]. Combinations of UV-induced fluorescence, reflected UV light, reflected IR and infrared-induced fluorescence imaging have been shown to increase the accuracy of identification of specific pigments or

binders [10, 18]. Flow chart methods are used to relate the colours observed by the different multispectral techniques to a specific binder or pigment [18].

2.3 Principles of ultraviolet fluorescence

It is important to understand the basic principles of fluorescence and to not just fawn over the colourful fluorescence images that this technique produces. The fluorescence process is initiated when an object is illuminated with electromagnetic (EM) rays. For this study, the EM rays will be ultraviolet light which has a wavelength between 200 and 400 nm. The UV lamps are often called Wood lamps in art circles, or black lights, as ultraviolet light is not visible to the naked eye and is therefore (incorrectly) named black light [1]. By illuminating an object with UV light, electrons in the upper layer of the object are excited to a higher energy state. As these electrons fall back to the ground state, they undergo various decay mechanisms [19]. One of the possible decay mechanisms is radiative decay, in which lower energy EM rays are emitted. Ultraviolet induced fluorescence generally emits visible light fluorescence.

The process is illustrated in Figure 2.2; incident light (λ_{ex}) is absorbed by the sample which causes an electron to move from the ground state (S_0) to the first excited state (S_1) or second excited state (S_2). The latter of the two is less common and rarely seen [11]. These electronic transitions are quantised and can be experimentally determined through UV-Visible light absorption studies. When the specific quantised energy is absorbed it results in an excited state molecule, therefore this specific absorbed wavelength can also be referred to as the excitation wavelength (λ_{ex}).

Once in the excited state, the molecule can undergo both non-radiative and radiative transitions. A radiative transition from an excited state to a lower energy ground state is known as luminescence. Luminescence can be classified into two different groups, phosphorescence and fluorescence. Phosphorescence, which is typically employed in commercial glow-in-the-dark items, can glow (luminesce) for several minutes after excitation, while fluorescence has a shorter lifetime of typically a few nano seconds (ns).

The energy of fluorescence emission of a system differs from its absorption energy, due to the presence of non-radiative transitions leading to energy loss. The energy difference between the absorption and emission energy is known as the Stokes shift [19]. The smaller this Stokes shift, the fewer non-radiative relaxation pathways the molecule has undergone.

The non-radiative transitions are dependent on the molecular structure of the excited species and its chemical environment. All molecules undergo internal conversions and vibrational relaxation, which result in a lower emission energy (Figure 2.2) compared to the excitation energy [19]. The most common non-radiative transition is solvent relaxation, where the fluorescence colour (and therefore emission wavelength) of a sample changes depending on the polarity of the solvent. The solvent relaxation is mathematically described by the Lippert equation [19], which predicts that polar solvents cause a greater relaxation, and therefore a larger Stokes shift, in the fluorescence of the molecular system.

In Figure 2.2, the colours of the energy transitions are representative of energy changes. The wavelength of light is inversely proportional to the energy of the photons. When the excitation wavelength (λ_{ex}) is in the blue range (shortest wavelength with higher energy), the resulting fluorescence will be slightly red-shifted to a green colour emission (λ_{em} ; longer wavelength with a lower energy). Ideally there would be no difference between the absorbed and emitted wavelength, however in reality there is always some energy difference which leads to a Stokes shift. In Figure 2.2, the green emission would have the smallest Stokes shift, and red the largest Stokes shift.

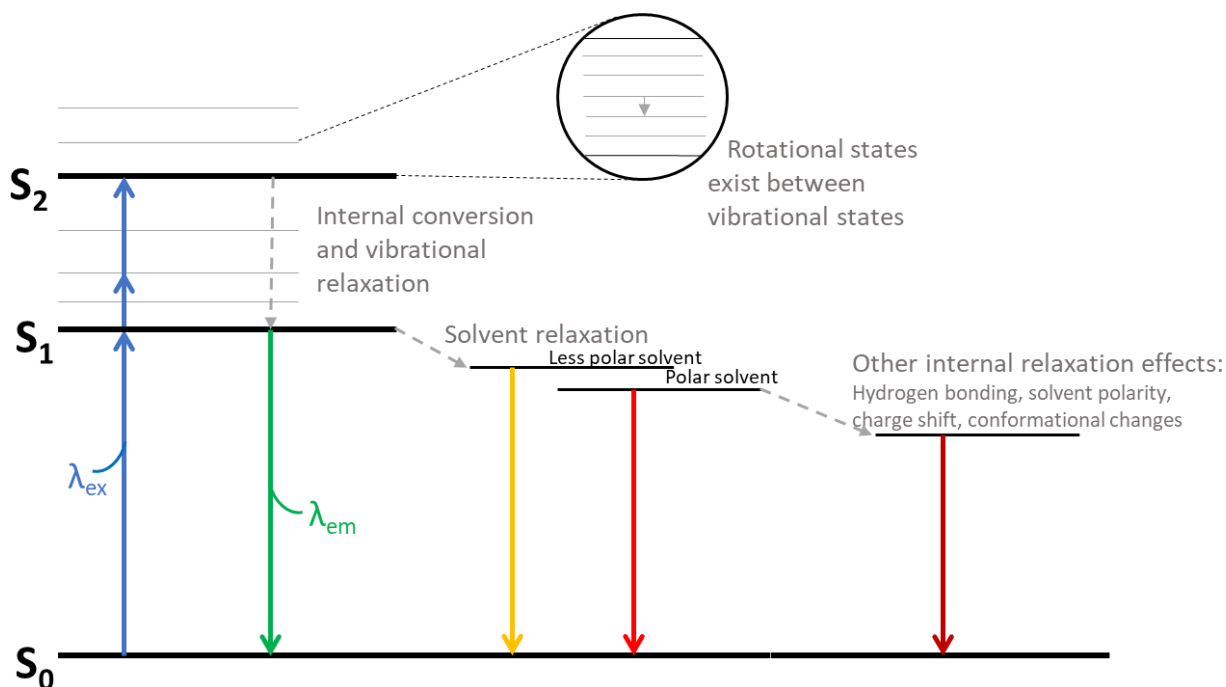


Figure 2.2: The electronic structure of an arbitrary system indicating various radiative/non-radiative degradation paths that result in a lower energy emission than the absorption energy. Adapted from [19].

Since energy is quantised, the absorption and emission lines should be sharp peaks, however this is not the case (Section 4.1). Between each electronic state, there exists several vibrational states, and within those exist different rotational states. The rotational states are so fine that they do not have a large impact on the absorption or fluorescence of a system. However, the vibrational state can change the initial ground state energy of a molecule, such that the energy of absorption is lower or higher than expected from the electronic ground state (S_0).

The emission spectrum is independent of excitation wavelength [19]. Light sources often emit wavelengths represented by a sharp gaussian curve, thus the excitation wavelength they generate can be considered as the peak of this curve. This results in various wavelengths being emitted, as this excitation wavelength overlaps with the specific energy required for absorption, the sample becomes excited. This is true of a single molecule, but when working with mixtures (e.g. paintings), the emission spectrum can vary drastically from the pure sample due to intrinsic effects from the microenvironment [8, 19]. The microenvironment of the sample changes the availability of non-radiative decay pathways. This often results in fluorescence quenching, however this can also lead to electron transfer between different molecules, which in turn can enhance the fluorescence [19]. Additionally, in mixtures there are several molecules that can be excited to emit fluorescence, leading to complex spectra which are dependent on the excitation wavelength.

2.4 Ultraviolet fluorescence spectroscopy

Fluorescence spectroscopy is different to fluorescent imaging techniques as it measures the spectrum (intensity of each wavelength) of emitted light rather than the visible light colours. Spectroscopy has the advantage of measuring low intensity peaks, where the individual colours would not always be visible in a photograph or to the naked eye [16]. Human eyes perceive a mixture of wavelengths as one colour and not the individual colours (see Section 2.7). Therefore, spectroscopy is a promising technique as the results are not subject to an individual's personal interpretation of colour.

In traditional spectroscopy techniques, a sample is irradiated with an excitation source of a specific wavelength. The spectrum of fluorescence is measured at a 90° angle from the incident light and represents the intensity of emitted light. The emission intensity is typically measured from a wavelength 10 nm longer than the excitation wavelength and can be recorded up to any desired wavelength, based on the detector employed. For UV-induced fluorescence, the emission spectrum is often measured in the visible range (400-750 nm) or near infra-red region (750-2500 nm).

In a sample containing a single molecular species, the emission wavelength can be attributed to the electronic states, which are deduced from the molecular structure and functional groups. This fluorescence wavelength remains constant regardless of the excitation wavelength used. However, in a more complex sample as would be found in binding media, these energy levels cannot as easily be attributed to a specific molecule or functional group, and as a result the fluorescence can change drastically from one excitation wavelength to the next. In a sample with multiple chemical species, a specific excitation (λ_A) can result in fluorescence from species A, while another excitation wavelength (λ_B) will result in fluorescence from species B. The two different excitation wavelengths (λ_A and λ_B) could differ by as little as 10 nm and result in drastically different fluorescence spectra [19].

These changes in fluorescence of complex mixtures are identified by using 3D fluorescence mapping. The 3D map is created by systematically increasing the excitation wavelength (ordinate) and measuring the resulting intensity of fluorescence at a range of emission wavelengths (abscissa). The intensity of fluorescence is depicted on this map as contours or through colour dependant intensity changes [20], for example, Figure 2.3 depicts a 3D fluorescence map. It is clearly seen that gum Arabic has an optimal excitation wavelength of 280 nm, and results in a fluorescence emission around 300 nm. This indicates that gum Arabic has one fluorophore that can be detected in the emission range (290 – 450 nm).

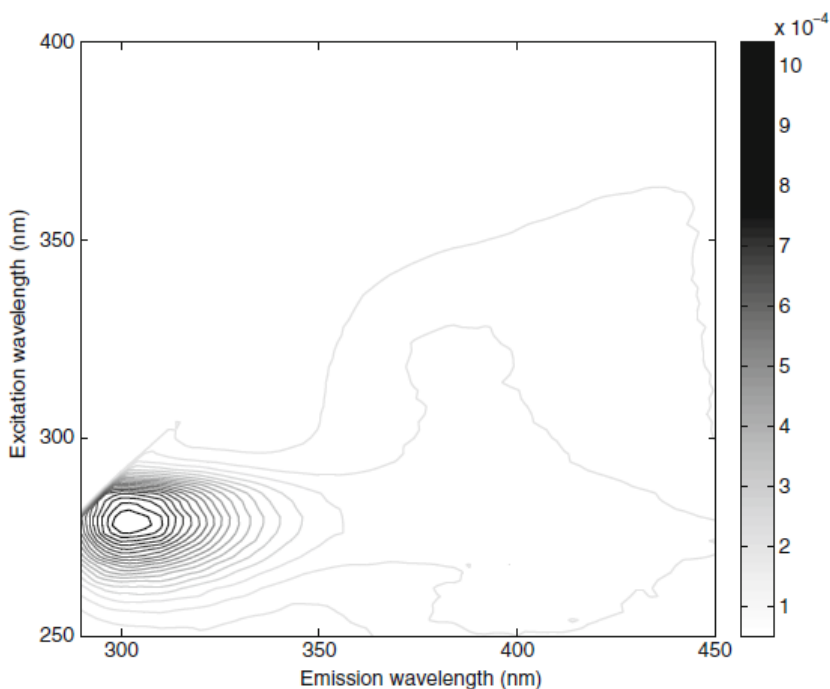


Figure 2.3: A 3D fluorescence map of a film of gum Arabic [20].

In addition to traditional fluorescence spectroscopy where a single excitation wavelength is used and the emission spectrum is measured, synchronous fluorescence spectroscopy (SFS) can be used. SFS is the analysis of both excitation and emission spectra simultaneously with a fixed wavelength difference ($\Delta\lambda$) between λ_{ex} and λ_{em} . A peak in SFS does not indicate that a specific excitation wavelength results in fluorescence, but rather that with a fixed $\Delta\lambda$ there is an increased fluorescence at an excitation wavelength. For example, an excitation wavelength of 250 nm will result in a poor fluorescence at λ_{em} 270 nm while at λ_{ex} 570 nm there will be a strong peak at λ_{em} 590 nm. This does not indicate that λ_{ex} 250 nm does not produce any fluorescence.

SFS poses several advantages over the traditional spectroscopy method as it provides spectral simplification, reduced scattering interference, bandwidth narrowing and improved resolution [21]. It has proved to be slightly more successful in differentiating between binders of the same chemical class, particularly in combination with multivariate statistics [22, 23]. For example, traditional fluorescence spectroscopy could not distinguish between linseed, poppyseed or walnut oil (which are all drying oils), however SFS could distinguish between these three oils by small differences in relative peak height [24].

Fluorescent lifetime imaging (FLIM) is another useful technique in identifying fluorescent samples and can classify binders more accurately than traditional and synchronous fluorescence spectroscopy. Binders of the same group can prove difficult to identify based on fluorescence spectra [25]; for example proteinaceous binders, egg white and animal glues contain tyrosine and tryptophan as fluorophores [26]. Fluorescence spectroscopy will show the presence of the fluorophores and their intensity of fluorescence whereas the fluorescent lifetimes are different for each binder based on the chemical matrix that the fluorophore is in. The fluorescent lifetime can be defined as the time a molecule is in the excited state [27]. The microenvironment may affect the path of non-radiative decay and thus the population of molecules in the excited state, leading to a decreased fluorescent lifetime. Fluorescent lifetimes have been found to be powerful in differentiating between pigments of the same chemical class, as in a recent study which was conducted to show differences in fluorescent lifetimes in anthraquinoid pigment dyes [28].

FLIM can be used as a spectroscopic technique [28] but is more commonly used as an imaging technique [29]. The sample is analysed pixel by pixel to record the fluorescence lifetime (only a few nanoseconds) and the intensity of the fluorescence. These maps are then combined into one to produce a hue-saturation-value (HSV) map (Figure 2.4). The HSV model has been adapted specifically for FLIM, where

the colour (hue) indicates the fluorescent lifetime of the area, and the darkness indicates a lower intensity of photons, making it is easy to characterise areas of different composition [29].

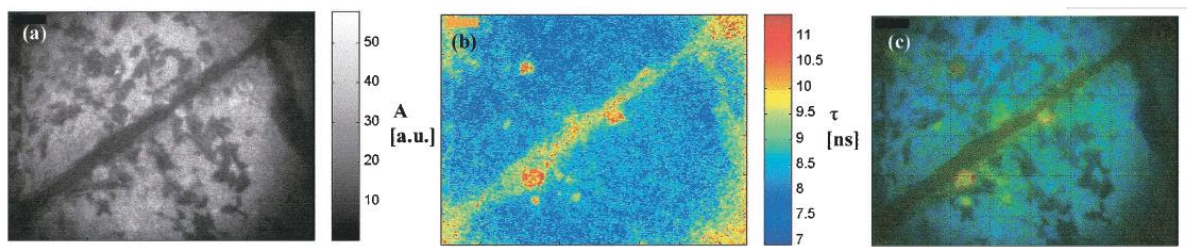


Figure 2.4: Fluorescence life-time imaging of a section of damaged painted wall painted by Masolino da Panicale, in the Collegiata of Catiglione Olona - a Renaissance church near Varese; a) intensity map; b) life-time map; c) HSV map [29].

Time-resolved laser induced fluorescence (TR-LIF), also known as time-resolved photoluminescence (TRPL), is another method that is based on the principle of luminescent decay time. Instead of measuring the exact fluorescent lifetime, TR-LIF makes use of two spectra recorded at different times [30]. The first spectrum is recorded at no time delay from when the sample was irradiated, whilst the second is recorded sometime after irradiation, for example 30 ns. By comparing the two spectra, any changes in relative peak height would indicate a different fluorescent lifetime. This is particularly useful in identifying different fluorophores that emit at a similar wavelength and are superimposed to give one broad peak in real time fluorescent measurements [31]. As is the case for Primal B-60 (a contemporary binder), which showed a broad peak at 294 nm in real time while the delayed time spectrum showed that the peak shifted to 280 nm. This showed the presence of two fluorophores with different fluorescent lifetimes [31].

2.5 Instrumentation

As discussed, there are several different fluorescence spectroscopy techniques. These techniques generally have very similar specifications in instrumentation, and have intrinsic differences with sensitivity of detectors for life time measurements. For all techniques, an excitation light source is needed. UV-induced fluorescence spectroscopy specifies that an ultraviolet light (200-350 nm) is used and is typically produced using halogen lamps and LED lights. However, several applications have started using lasers as excitation wavelength (laser-induced fluorescence, LIF) due their higher intensity and narrow emission wavelength range which provides selectivity [32]. The intensity of the laser source

allows samples to be analysed from distances up to ten meters away [3]. This has created an ideal method to analyse historic buildings, sculptures, and roof paintings where ladders and scaffolding are otherwise needed to take samples. LIF instruments can specifically be developed for outdoor and distance analysis in the form of *fluorescence lidar* (light detection and ranging). Fluorescence lidar is designed to measure fluorescence in full daylight and is used in several environmental monitoring applications [33]. It is important to note that although the laser sources are advantageous in distance analysis, they can cause unwanted photo-oxidation of pigments if the light intensity is too high [34].

The light source employed in fluorescence spectroscopy determines the excitation wavelength (Table 2.1). Halogen lamps have a broad-spectrum emission which requires the use of multiple filters and slits to obtain a specific excitation wavelength. The main advantage of halogen lamps is that they allow any excitation wavelength to be chosen. Laser sources have a few set wavelengths at which they can excite which is dependent on the composition of the gain medium. The most common laser source used in art conservation applications is the Nd:YAG laser, which is an isomorph of a yttrium aluminium garnet (YAG) crystal where a portion of the yttrium (Y) atoms are replaced with neodymium (Nd) atoms which allows enhanced photon intensity [35]. Excimer lasers have proved to be valuable tools in the conservation of paintings as they can remove the varnish layer of objects without causing thermal alterations and minimal light penetration [34].

LEDs (light emitting diodes) are composed of a semiconducting material (such as aluminium gallium arsenide) which emits light when activated by an external energy source. To obtain the different wavelengths in LED lights, impurities are added to change the band gap width, which changes the energy and therefore the wavelength that is emitted. Therefore, only certain excitation wavelengths are provided by a single LED source [36]. The advantages of LED lights are that they are small, of low cost and are easily interchangeable [37].

Table 2.1: *Light sources used as excitation source for fluorescence measurements of paintings.*

Light source		Excitation wavelengths possible (nm)	Filters needed*	Reference
Halogen lamps	Xenon arc Lamp (Jobin-Yvon/Horiba Fluoromax-P)	All λ possible (continuous source) 1 nm and 5 nm slits used to obtain the needed λ . Examples: 260, 280, 335, 355	-	[24, 38]
	High pressure mercury lamp. (HBO 100W)	Continuous source, 1 and 5 nm slits used 365	10 nm bandwidth interference filter (365FS 10-25) coupled with ND400 (Nikon) dichroic mirror	[39]
Laser sources	Nd:YAG laser	1054, 532, 355, 266, 213	Density filter	[3, 38, 40-41]
	KrF Excimer laser (TUI Laser AG BraggStar 200)	248	-	[38]
	Nitrogen laser (LN203C Laser Photonic)	337	-	[29]
	XeCl Excimer laser	308	-	[42]
LED	Light emitting diodes	375	455 nm filter	[37]
		285	320 nm filter	

In fluorescence imaging, the source and detector are often separate components. Large UV lamps (the light source) can be found in most conservation studios, the detector for imaging is commonly a DSLR (digital single-lens reflex) camera that captures the fluorescence emission of a painting. However, in fluorescence spectroscopy, the light source and detector may be found in the same instrument. This aids in better calibration between the excitation wavelength and the emitted light as well as reducing the background light and enhances the reproducibility.

The detector plays a critical role in the sensitivity and resolution of spectroscopy measurements. A range of different detectors are used (Table 2.2), although they all follow the same basic principle. The detectors consist of an array of pixels that act as transistors to convert a photon signal into a digital (electron) signal. This digital signal is used to plot the spectrograph. The most common detector in spectrometers is a charge-coupled device (CCD) which is also found in DSLR cameras [43]. In competition with the CCD, a complementary metal-oxide semiconductor (CMOS) detector could be used, as it has a lower power consumption and costs less than a CCD. However, a CMOS has a lower sensitivity than the CCD, which is disadvantageous particularly in fluorescence measurements [43]. Fluorescence emission is often only a tenth of the intensity of the incident light, therefore high sensitivity is needed in fluorescence detectors. This brings us to the third most common detector; the photo-diode array (PDA).

Photo-diode array detectors consist of an array of pixels that make them ideal to measure an entire spectrum in a short amount of time. When compared to a CCD detector, a PDA detector has a lower charge to voltage conversion efficiency, which means that it is less sensitive to low light levels. However, the PDA has a high photo saturation charge which allows higher intensities of light to be measured at high accuracies. Therefore, CCD is ideal for very low light applications whilst PDA detectors are ideal due to their large photodetection range [44].

Table 2.2: Detectors generally used in fluorescence spectroscopy.

Detector		Range (nm) [†]	Filters used	Reference
CCD detectors	CCD camera (Retiga 2000)	400-720	Liquid tuneable filter	[16]
	Time-gated intensified CCD camera	370-870	FKB-VIS-40 band-pass transmission filters	[30]
	Thorlabs Spectrometer CCS200/M, CCD line array	200-1000	-	[37]
	Ocean Optics HD4000 Spectrophotometer (CCD)	250-600	290 nm cut off filter	[38]
	CCD Multichannel spectral analyser (PMA 11-C5966)	400-800	Residual excitation light removed by GG400 long pass filter	[39]
PDA detectors	Jasco Fluorescence spectrometer, silicon photodiode array	250-480	Excitation and emission monochromator	[24]
	Time-resolved optical multichannel analyser (OMA) with silicon photodiode array detector	400-800	Cut-off filter (Kodak Wratten #2E) to remove reflected excitation light	[29]
	Photocathode detector	350-800	-	[28]

[†] Range of recorded spectrum, this does not necessarily indicate the full range of the detector.

Ideally, any analysis that is done on artworks should be non-destructive and done *in situ*. This means that the artwork can remain in the museum and is analysed with minimal handling. This has led to the development of the LED micro-spectrofluorometer (LED μ SF) and other handheld spectrofluorometers which have allowed for more sophisticated spectroscopic analysis [16, 28, 37, 45, 46]. The handheld instruments have interchangeable LED lights as excitation sources and CCD detectors [28, 37]. In

addition, Peltier cooling can be used to improve sensitivity in CCD detectors for handheld instrumentation [47].

2.6 Application

Fluorescence spectroscopy is a surface analysis technique [10]. Therefore, UV-induced fluorescence is limited to the analysis of the surface of a painting, i.e. the varnish and paint layer. This study focuses on the fluorescence of paint binding media, with mixtures including pigments, whilst the fluorescence of varnish layers was not studied. There have been extensive studies on the fluorescence of the varnish layer, which the reader is referred to for further information [48-50]. It is important to note that the fluorescence discussed in this dissertation refers to the intrinsic fluorescence (also known as autofluorescence) of materials and is not induced by chemical stains. Fluorescence-staining is a technique whereby dyes are applied to a sample, these dyes (e.g. fluorescamine, LISSA, FITC and many others) bond to certain functional groups resulting in a fluorescent sample [51]. Although this staining technique is highly efficient, it is an invasive technique which could lead to irreversible damage to paintings.

To fully investigate the fluorescence of paint materials, it is important to firstly understand the intrinsic fluorescence of binders in a pure model sample that contains no pigments. Thereafter, the intrinsic fluorescence of pigments needs to be studied. Once all the components of paint are considered individually, they can be investigated together as a mixture.

2.6.1 Binders

Binders are as the name suggests, the adhesive medium that binds the pigment to the substrate of the painting. Binders consist of complex organic mixtures that form a film through solvent evaporation or polymer formation. Paint properties, such as curing time, gloss, rheology and application thickness depend on the choice of binder and binder-to-pigment ratio. This leads to the different painting techniques, for example drying oils are used in oil paints while polysaccharide materials are often used in water paint, and eggs in tempera painting [52].

Many binders are extracts from natural materials, which results in complex mixtures of chemicals. Therefore, there could be multiple compounds present that lead to the fluorescence of a single binder. Several studies have attributed certain chemicals to the fluorescence; however, many fluorophores are still unknown (Table 2.3).

Table 2.3: A summary of the fluorescence from various paint binders found in literature.

Binder		Excitation (nm)	Emission (nm)	Identified fluorophores	Reference
Drying oils	Linseed oil	365	480-540	1-amino-3-iminopropene	[53]
		337	480-550		[54]
		363.8	492-685		[55]
	Poppy seed oil	337	440-500		[54]
Proteinaceous binders	Animal glues	248	305, 385	Tyrosine, pentosidine and pyridinoline	[38]
		355	415, 440, 480	di-tyrosine, pyridinoline, dihydroxyphenylalanine (DOPA)	[38]
		337	430-440		[56]
		337	430		[25]
	Casein	248	340, 420	Tryptophan, di-tyrosine	[38]
		280	348	n-acetyl tryptophan	[38]
		355	450		[3]
	Egg white	248	340, 420	Tryptophan, di-tyrosine	[38]
		355	420, 435	di-tyrosine, tryptophan, and oxidation products e.g. N-formylkynurenine (NFK) and kynurenine	[38]
		300	325, 425		[26]
		266	333	Tryptophan	[57]
		363.8	588		[55]
		355	520		[3]
		337	410		[25]
	Egg yolk	248	515-440		[38]
		266	333, 520, 450	Aromatic amino acids, phospholipids and photo-oxidation products	[57]
		355	515,440	Phospholipids	[58]
		350	425		[25, 34]
	Whole egg	363.8	480		[55]
		308	500		[42]

	Calcium caseinate	337	460		[29]
	Parchment glue	260	301	Tyrosine and n-acetyl tyrosine ester	[38]
		335	385, 415	Pentosidine, di-tyrosine	[38]
	Rabbit skin glue	355	435, 480	Lysine adducts and DOPA	[38]
		355	520		[3]
		266	333, 310	Tyrosine and tryptophan	[57]
Polysachharides	Gum Tragacanth	363.8	450		[55]
	Gum Arabic	363.8	450		[55]
		278	302	Tyrosine, tryptophan, phenolic compounds (caffeic acid and ferulic acid)	[20]
		278	315	Tyrosine and tryptophan	[59]
Synthetic binders	Paraloid B72	266	335		[3]
	Mowilith 50	266	330		[3]
	Calaton	266	330		[3]
	Primal AC ₃₃	266	315		[3]
	Primal B60	220	294		[31]
	Vinavil	266	340		[3]
	PVAc	337	460		[29]
	Acrytal C ₁₂	220	280		[31]
	Vinil Pritt	220	280		[31]
Mixtures	Whole egg + Linseed oil	363.8	550		[55]

2.6.1.1 Lipid binders

Drying oils have been used in paintings as a binding medium since the 16th century. Their ability to dry and form a solid film under ambient conditions [60] can be attributed to the unsaturation in oils, which facilitates polymerization [61]. Linseed-, poppyseed-, as well as walnut- or safflower-oil, which are commonly used in paintings, contain high concentrations of the unsaturated fatty acids moieties, such as linolenic and linoleic acid (Table 2.4) [52]. Linseed oil is extracted from the flax plant (*Linum*

usitatissimum), which contains large amounts of unsaturated fatty acid moieties [62]. Water-miscible linseed oil contains an emulsifier which makes the oil hydrophilic, allowing for the use of water, instead of toxic organic solvents, to rinse paint brushes [61]. Stand oil is a form of linseed oil that has been pre-polymerised through heat treatment. Poppy seed oil is extracted from *Papaver somniferum* seeds and contains lower concentrations of unsaturated fatty acid moieties [63]. The properties of each oil are largely dependent on the type of fatty acids present; for example, oils with a high unsaturated fatty acid content dry faster but have a greater tendency to yellow with age [62, 64-67].

Table 2.4: *The fatty acid content of drying oils typically present in paintings [65, 68, 69].*

Fatty acids	Linseed oil (%)	Poppyseed oil (%)	Walnut oil (%)	Safflower oil (%)
Palmitic acid (C16:0)*	6-8	8-12	3-7	5.5-7
Stearic acid (C18:0)	3-6	2-3	0.5-3	2-3
Oleic acid (C18:1)	14-24	12-17	9-30	10-35
Linoleic acids (C18:2)	14-19	55-65	57-76	55-81
Linolenic acid (C18:3)	48-60	3-8	2-16	0-1

*C16 indicates the number of carbons in the chain (in this case, 16 carbons), while the second number indicates the degree of unsaturation (number of double bonds).

The fluorescence of drying oils is beneficial as it can aid in diagnostic tests that identify areas of previous restoration [2, 70]. Aged drying oils develop a very characteristic blue coloured fluorescence which is seen over the entire painting, while newly applied paint (from restorations) will have no fluorescence, making the new, unaged paint (and milk proteins) easy to detect. The fluorescence of drying oils has been related to the degree of yellowing: the fluorescence shifts from blue to green as the samples age and yellow [53, 71, 72].

Drying oils are clear to translucent when applied to paintings, but gradually develop a yellow discoloration over time. This discoloration is an unavoidable property of oil paint [61]. The chemical basis of the yellow colour remains poorly understood, despite the wide range of reported compounds that are suspected to play a role in this regard [53, 61, 62, 71, 73-77]. The currently accepted view is that the yellowing is a result of two compounds, one which reflects yellow light, and another which fluoresces yellow, although their identities are still unknown [53]. Since the discoloration and fluorescence are so closely related, it is important to understand the discoloration trends.

Although little is known of compounds responsible for the yellowing of oils, there are a few trends associated with this yellowing process. Firstly, a high degree of unsaturation in the oil leads to significant discolouration. Therefore, linseed oil will yellow to a greater extent than poppy seed oil, which is less unsaturated [61, 78]. Secondly, the yellowing has been found to be accelerated by certain metal-containing pigments, such as lead white, copper carbonate and various cobalt pigments [14, 71, 78-80]. Thirdly, the discolouration is reversible and can go through cycles, depending on the storage conditions; light exposure reverses the yellowing, while dark conditions promote yellowing, which suggests that photodegradation reactions reverse the discolouration (and possibly the associated yellow coloured fluorescence) [71, 80].

2.6.1.2 Proteinaceous binders

Proteinaceous binders (animal glues and egg-based media) are derived from animal sources. Animal glues are natural polymers derived from collagen, the major structural protein of skin, cartilage, and bones. Egg-based media are egg yolk, egg white and whole egg mixed with oil, gum or mastic resin to produce a tempera painting once mixed with pigments [81]. Tempera paintings can be done with egg alone, but often contain additives to change the painting properties. Other protein samples such as animal glue have been mixed in tempera as an additive (or alone to form glue-tempera), but egg-based materials are the main component of tempera. Tempera paints were a popular painting technique in the 14-15th centuries [81].

Fluorescence studies are often used as a diagnostic test for proteins, however there is often a misconception when referring to fluorescence studies of proteins. Fluorescence-staining, where dyes (e.g. Fluorescamine, LISSA and FITC) are used, indicate where certain proteins are present [82-85]. Dyes are added to protein samples which bond covalently to the primary amines in amino acids, and this bond formation results in a fluorescent dye. Fluorescamine results in a blue fluorescence (λ_{em} 470 nm; λ_{ex} 390 nm), LISSA in a yellow red colour (λ_{em} 590 nm; λ_{ex} 570 nm) and FITC reacts with sulfhydryl groups to form a green coloured fluorescence (λ_{em} 519 nm; λ_{ex} 495 nm) [51]. The staining technique is highly efficient, and is typically done on embedded and polished (cross section) paint samples. The staining is not done on the larger painting, but the removal of paint samples is an invasive technique which leads to irreversible damage to paintings. Fortunately, proteins have an intrinsic fluorescence by which the chemical components of proteins are fluorescent [86]. It is this intrinsic fluorescence that becomes important in a cultural heritage setting.

In fresh (newly applied) protein samples, the most prominent fluorophores are the aromatic amino acids: tryptophan (Trp, λ_{em} 348 nm), tyrosine (Tyr, λ_{em} 303 nm) and phenylalanine (Phe, λ_{em} 282 nm) [38]. Tryptophan has the highest quantum yield (QY) and will result in the majority of the observed fluorescence, whilst phenylalanine has the smallest QY and is rarely seen in fluorescence spectra [38]. As the proteinaceous samples dry and stabilize, they form new crosslinked structures, of which some are fluorophores. In egg and casein samples, crosslinked products formed through the Maillard reaction (between proteins and saccharides) result in strongly fluorescent pentosidine (λ_{em} 385 nm) and pyridinoline (λ_{em} 440 nm) products [38]. In addition, fluorescent photo-oxidation products can be found in dried paint samples, such as di-tyrosine (λ_{em} 415 nm), dihydroxyphenylalanine (DOPA, λ_{em} 480 nm), N-formylkynurenine (NFK, λ_{em} 440 nm) and kynurenine (λ_{em} 435 nm) of which the latter two are tryptophan oxidation products [38, 87, 88]. Although these are the main fluorophores in proteinaceous samples, they do not all fluoresce at the same intensity due to variations in quantum yields. Studies have been done to deconvolute fluorescence spectra to characterise the contribution of each protein fluorophore [22].

2.6.1.3 Polysaccharide binders

Gum Arabic and Gum Tragacanth are well known polysaccharide materials. They are extracts from *Acacia Senegal* trees and *Astragalus* shrubs, respectively. Gums consist mainly polymer chains of saccharide materials such as galactose, arabinose and rhamnose, along with peptide chains (containing hundreds of amino acids) that are attached to the polysaccharide blocks. Some of these polysaccharides can contain proteins within the polymer chain. The protein content can vary from 2 to 25 % (w/w), and this variation is attributed to the source of tree sap (location and tree species), as well as the age of the tree [59].

Few fluorescence studies have been done on polysaccharide materials [20, 55, 59], in these studies the fluorophores in polysaccharides have been identified as tyrosine and tryptophan residues [20, 59]. Dhenadhaylan, et al. [59] has proved that increasing the acidity of gum Arabic allows the amino acids to precipitate out of the polymer chain which results in an increase in fluorescence intensity. Therefore, although gum materials are polysaccharides, their fluorescence can be comparable to the proteinaceous binders.

2.6.1.4 Synthetic binders

Synthetic binders are long chains of polymers, including polyvinyl acetate (PVAC), polyvinyl alcohol (PVAL), derivatives of polyacrylic acid (PAA) and acrylic homopolymers (poly (n-butyl methacrylate) as well as acrylic copolymers (with methyl methacrylate (MMA) and either ethyl acrylate (EA) or n-butyl acrylate (nBA)). Synthetic binders have not been on the market for a very long time compared to traditional binders which have been used for centuries [52]. Due to this time scale, the long-term chemical degradation of synthetic binders is still poorly understood [89]. A few studies have aimed to aid chemical understanding. As fluorescent imaging is generally the first diagnostic test undertaken, studies have recently started focusing on the fluorescence of synthetic binders [46]. Fantoni et al. (2013) [3] and Marinelli et al. (2017) [31] have contributed significantly to the identification of the differences in fluorescence of synthetic binders. These studies have, however, focused on identifying differences in fluorescent colours or spectra and have not attributed the fluorescence to chemical species [3, 31].

In this project, a select few synthetic binders were studied based on their availability and use in conservation studios. The binders studied were thus: mowiol 18-88, mowital B30H, lascoux, paraloid B72 and paraloid B67. Mowiol 18-88 is a PVAL polymer, which is partially hydrolysed [89, 90]. Mowital B30H is a polyvinyl butyral (PVB) in which butyraldehyde (noted by the B in B30H) is used and has a relatively high degree of acetalization (noted by the H). Lascoux is a thermoplastic acrylic resin composed of a water-based dispersion of a copolymer of butyl acrylate (BA) and methyl methacrylate (MMA), which is thickened with acrylic butylester.

Paraloid is the trade name for polymethacrylate synthetic binders. The exact composition percentages of each paraloid are not well known, however all paraloids share similar reversible adhesive properties. Paraloid B72 is the most studied and is a copolymer of 30% methyl acrylate (MA) and 70% ethyl methacrylate (EMA) with a small amount (about 2%) of butyl methacrylate (BMA) [91]. Paraloid B72 is weakly fluorescent at 335 nm (λ_{em}) when excited at 266 nm (λ_{ex}) [3]. The polymer structures of these materials are depicted in Figure 2.5.

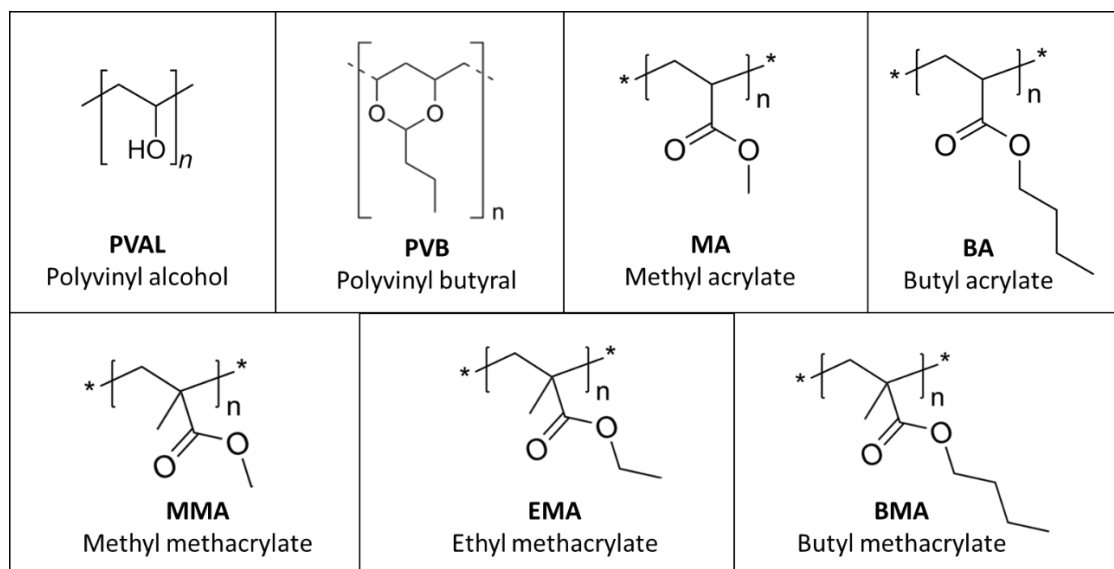


Figure 2.5: Chemical monomers of selected synthetic binders.

2.6.2 Pigments

Pigments are the substances that give colour to paint and can be classified as either inorganic, organometallic or organic pigments. The inorganic pigments are pigments that contain metals and can consist of mineral pigments (e.g. natural ultramarine, derived from lapis lazuli, a semi-precious stone), synthetic mineral pigments (e.g. synthetic ultramarine) and other metal-based complexes (e.g. cadmium sulphide). Organic pigments are carbon based chemical structures, which consist of dyes extracted from plants (e.g. madder) and synthetic organic pigments (e.g. arylamide yellow).

It is important to note that not all pigments fluoresce. Similar to the binders, specific conditions and chemical structures are needed for fluorescence to occur. Table 2.5 summarises the pigments of known fluorescence, which can be found in literature.

Table 2.5: Summary the excitation wavelength and emission peaks of known fluorescent pigments found in literature.

Pigment	Excitation wavelength (nm)	Emission wavelength (nm)	Reference
Zinc White (ZnO)	248	285	[34]
	337	385	[92]
	355	380-400	[30]
	355	385	[93]
Titanium white (TiO ₂)	337	381	[92]
	355	473	[93]
	355	400 ^a	[30]
	355	500 ^b	[30]
Lead white (PbCO ₃) ₂ ·Pb(OH) ₂	248	490	[34]
	355	547	[93]
Hydrocerussite 2PbCO ₃ ·Pb(OH) ₂	248	590-610	[94]
	355	480-580*	[30]
Cerussite PbCO ₃	248	458-443	[94]
	355	500-550	[30]
Cadmium yellow (CdS)	337	520	[92]
	355	483	[93]
	355	470-510	[30]
Lemon yellow (BaCrO ₄)	337	383, 520	[92]
Citron yellow (ZnCrO ₄ ·K ₂ CrO ₄ ·ZnO)	337	383, 520	[92]
Chrome yellow citron (PbCrO ₄ ·PbSO ₄)	248	560	[34]
	337	540	[92]
Hansa yellow (C ₁₆ H ₁₂ Cl ₂ N ₄ O ₄)	337	382, 550	[92]
Aureolin (K ₃ Co(NO ₂) ₆ ·3H ₂ O)	337	550	[92]
Naples yellow	355	538	[93]

Cadmium red	337	600	[92]
	355	568	[93]
	355	550-630	[30]
Red lead	355	568-600	[93]
Vermillion	308	620	[42]
	337	600	[92]
	337	630	[56]
	532	600	[95]
Barite	355	450	[30]
Calcite	355	450	[30]
Egyptian blue	355	910*	[30]
Madder lake	365	455-540	[5]
	490	540-560	[6]
	440	630	[7]
		630	[16]
Curcumin	248	560	[34]
Azurite	248	380	[34]
Indian yellow (euxanthic acid)	435	535	[4]

^a Titanium white in rutile polymorph

^b Titanium white in anatase polymorph

*Fluorescence not related to the band gap energy and is rather an effect of intrinsic defects of the crystal structure

Organic pigments fluoresce due to the presence of conjugated double bonds which lead to electron delocalization. This can be due to the presence of several aromatic rings or long alkene conjugation paired with aromatic rings or di-azo bonds [32]. However, not all organic pigments contain this conjugation, and therefore will not fluoresce. Inorganic pigments lack conjugation that leads to the delocalization of electrons, however certain inorganic pigments can fluoresce where the band gap is small enough to be excited [96, 97]. The appropriate band gap is commonly found in semi-conductor pigments and can be enhanced by the presence of impurities. For example, yellow cadmium-based pigments ($\text{CdSe}_x\text{S}_{1-x}$) have shown to fluoresce at longer wavelengths as the concentration of selenium increases [97].

2.6.3 Limitations of fluorescence spectroscopy on paintings

There are a few limitations of determining the fluorescence of binders in painted objects, especially considering that a multitude of fluorescent and non fluorescent pigments may be added to the binder. Firstly, it is important to note that pigments are often particles immersed in the binder film; this can result in reflection of the incident light from the crystal surfaces. This has been accounted for in literature by the use of the Kubelka Munk theory, which is an equation that corrects the fluorescence spectra for scattering effects [8]. However, pigments are often ground to fine powders to ensure an even coloured paint, and this can create a multitude of submicron sized pigment particles, which do not fluoresce [97].

Secondly, the emission spectrum of binders may undergo bathochromic shifts (to longer wavelengths), through the presence of different pigments [98] and the various painting techniques [25]. It is also known that certain pigments can accelerate the production of fluorescent species, e.g. lead white in linseed oil [8, 53]. Thirdly, pigments can greatly affect the fluorescence spectrum by absorbing the emitted light from binders [8, 15, 99]. At low binder to pigment ratios, the binder's fluorescence is often not observed. This can be due to chemical quenching, masking effects or the absorption of emitted light by pigments [25].

2.7 Case study from literature

There are numerous examples which illustrate the power of fluorescence spectroscopy in art conservation. One of these is a case study done by Comelli, *et al.* [16] on a fresco at the Baptistery of Castiglione Olona (Italy) painted by Masolino da Panicale in 1435, has showed the advantages of measuring a fluorescence spectrum along with analysing a visual image. In addition, this case study shows the importance of understanding binder and pigment fluorescence in a single object.

In the visible image (illuminated by white light, i.e. no fluorescence) the headpiece in the painting seems to look the same, with only a slight difference in colour and lustre (Figure 2.6a). However, the fluorescence image shows a bright, orange-coloured fluorescence (Figure 2.6b). When the fluorescence spectrum was measured, two distinct peaks were found, λ_{em} 480 and 630 nm. The first fluorescence at 480 nm was identified as the binder which is similar to the fluorescence in other parts of the painting, as is seen by the blue glow, while the orange fluorescence at 630 nm has been identified as the pigment,

madder lake. Madder lake is a very saturated red organic colourant, which consists of a base anthraquinone structure which leads to the bright fluorescence [100].

The visual image of the painting (Figure 2.6a) did not have the saturated red colouration which is associated with madder lake. However, through fluorescence spectroscopy, the madder lake was identified. This discovery suggests that the madder lake was previously added as decorative means and could have been removed by previous restoration attempts. Though most of the colour was removed, traces of the strongly fluorescent pigment were still identified. This level of detail was only possible after spectral studies were done, as the luminescence photograph (Figure 2.6b) could not characterise the fluorescence wavelength. In addition, when looking at this fluorescence image, no fluorescence is seen from the binder under the orange fluorescence. Fluorescence spectroscopy is a very sensitive technique which should always be used in conjunction with fluorescence imaging.



Figure 2.6: *Fluorescence of Salome's face painted by Masolino di Panicale. a) Visual image; b) UV-induced fluorescence excited at 365 nm with an UV-A low pressure mercury lamp [16].*

This case study demonstrates the importance of fluorescence spectroscopy when interpreting fluorescence images. To accurately use fluorescence spectroscopy as an identification technique, it is important to understand the chemical nature of each fluorophore, and how changes in the chemical environment result in different fluorescent peaks. This will be achieved in this study by using a range of destructive and non-destructive techniques to characterise the chemical changes induced in model samples. The experimental methodology employed is discussed in the following chapter.

2.8 References

1. Rorimer JJ. *Ultra-violet rays and their use in the examination of works of art*, New York: Metropolitan Museum of Art; 1931.
2. Cosentino A. Practical notes on ultraviolet technical photography for art examination. *Conservar Património*. 2015(21): 53-62. doi:10.14568/cp2015006.
3. Fantoni R, Caneve L, Colao F, Fiorani L, Palucci A, Dell'Erba R, et al. Laser-induced fluorescence study of medieval frescoes by Giusto de' Menabuoi. *Journal of Cultural Heritage*. 2013;14(3):S59-S65. doi: 10.1016/j.culher.2012.10.025.
4. Feller RL. *Artist's pigments: a handbook of their history and characteristics, Vol. 1*, London: Archetype Publications; 1986. ISBN: 978-1-904982-74-6.
5. Dyer J, Sotiropoulou S. A technical step forward in the integration of visible-induced luminescence imaging methods for the study of ancient polychromy. *Heritage Science*. 2017;5(24):1-24.
6. Claro A, Melo MJ, de Melo JSS, van den Berg KJ, Burnstock A, Montague M, et al. Identification of red colorants in van Gogh paintings and ancient Andean textiles by microspectrofluorimetry. *Journal of Cultural Heritage*. 2010;11(1):27-34. doi: 10.1186/s40494-017-0137-2.
7. Clementi C, Nowik W, Romani A, Cibir F, Favaro G. A spectrometric and chromatographic approach to the study of ageing of madder (*Rubia tinctorum* L.) dyestuff on wool. *Analytica Chimica Acta*. 2007;596(1):46-54. doi:10.1016/j.aca.2007.05.036.
8. Verri G, Comelli D, Cather S, Saunders D, Piqué F, editors. Post-capture data analysis as an aid to the interpretation of ultraviolet-induced fluorescence images. *Proceedings of SPIE – The International Society for Optical Engineering*. 2008;6810:1-12.
9. Carden ML. Use of ultraviolet light as an aid to pigment identification. *APT Bulletin*. 1991;23(3):26-37.
10. Dyer J, Verri G, Cupitt J. *Multispectral imaging in reflectance and photo-induced luminescence modes: A User Manual*. London: British Museum; 2013.
11. Mairinger F. UV-, IR-and X-ray imaging. *Comprehensive Analytical Chemistry*. 2004;42:15-71.

12. Verri G. An investigation of corrected UV-induced fluorescence for the examination of polychromy M.A Dissertation, Courtauld Institute of Art, London; 2007.
13. Mazzinghi P, Pelagotti A, Aldrovandi A, Masotti L. Digital fluorescence imaging for the restoration of painting. *Proceedings of International Conference EVA'96 Electronic Imaging and the Visual Arts*; 1996.
14. Mounier A, Belin C, Daniel F. Spectrofluorimetric study of the ageing of mixtions used in the gildings of mediaeval wall paintings. *Environmental Science and Pollution Research*. 2011;18(5):772-782.
15. Verri G, Clementi C, Comelli D, Cather S, Piqué F. Correction of ultraviolet-induced fluorescence spectra for the examination of polychromy. *Applied Spectroscopy*. 2008;62(12):1295-1302.
16. Comelli D, Valentini G, Nevin A, Farina A, Toniolo L, Cubeddu R. A portable UV-fluorescence multispectral imaging system for the analysis of painted surfaces. *Review of Scientific Instruments*. 2008;79(8):086112:1-3.
17. Artesani A. Photoluminescence properties of zinc white: an insight into its emission mechanisms through the study of historical artist materials. *Applied Physics and Material Science Processes*. 2016;122.
18. Cosentino A. Identification of pigments by multispectral imaging; a flowchart method. *Heritage Science*. 2014;2(1):8.
19. Lakowicz JR. *Principles of fluorescence spectroscopy*. New York: Plenum Press; 1983.
20. Brambilla L, Riedo C, Baraldi C, Nevin A, Gamberini M, D'andrea C, et al. Characterization of fresh and aged natural ingredients used in historical ointments by molecular spectroscopic techniques: IR, Raman and fluorescence. *Analytical and Bioanalytical Chemistry*. 2011;401(6):1827.
21. Li Y-Q, Li X-Y, Shindi AAF, Zou Z-X, Liu Q, Lin L-R, et al. Synchronous fluorescence spectroscopy and its applications in clinical analysis and food safety evaluation. *Reviews in Fluorescence*. 2012; 95-117.

22. Nevin A, Cather S, Burnstock A, Anglos D. Analysis of protein-based media commonly found in paintings using synchronous fluorescence spectroscopy combined with multivariate statistical analysis. *Applied Spectroscopy*. 2008;62(5):481-489.
23. Nevin A, Comelli D, Valentini G, Cubeddu R. Total synchronous fluorescence spectroscopy combined with multivariate analysis: method for the classification of selected resins, oils, and protein-based media used in paintings. *Analytical Chemistry*. 2009;81(5):1784-91.
24. Mannino MR, Orecchio S, Gennaro G. Microanalytical method for studying paintings by use of fluorescence spectroscopy combined with principal component analysis. *Microchemical Journal*. 2013;110:407-16.
25. Comelli D, Nevin AB, Verri G, Valentini G, Cubeddu R. Time-resolved fluorescence spectroscopy and fluorescence lifetime imaging for the analysis of organic materials in wall painting replicas. In: Pique F, Verri G. *Organic Materials in Wall Paintings*. Los Angeles: The Getty Conservation Institute; 2015.
26. Nevin A, Comelli D, Valentini G, Anglos D, Burnstock A, Cather S, et al. Time-resolved fluorescence spectroscopy and imaging of proteinaceous binders used in paintings. *Analytical and Bioanalytical Chemistry*. 2007;388(8):1897-1905.
27. Nevin A, Cesaratto A, Bellei S, D'Andrea C, Toniolo L, Valentini G, et al. Time-resolved photoluminescence spectroscopy and imaging: new approaches to the analysis of cultural heritage and its degradation. *Sensors*. 2014;14(4):6338-6355.
28. Romani A, Clementi C, Miliani C, Brunetti B, Sgamellotti A, Favaro G. Portable equipment for luminescence lifetime measurements on surfaces. *Applied Spectroscopy*. 2008;62(12):1395-1399.
29. Comelli D, D'Andrea C, Valentini G, Cubeddu R, Colombo C, Toniolo L. Fluorescence lifetime imaging and spectroscopy as tools for nondestructive analysis of works of art. *Applied Optics*. 2004;43(10):2175-2183.
30. Artesani A, Ghirardello M, Mosca S, Nevin A, Valentini G, Comelli D. Combined photoluminescence and Raman microscopy for the identification of modern pigments: explanatory examples on cross-sections from Russian avant-garde paintings. *Heritage Science*. 2019;7(1):17.

31. Marinelli M, Pasqualucci A, Romani M, Verona-Rinati G. Time resolved laser induced fluorescence for characterization of binders in contemporary artworks. *Journal of Cultural Heritage*. 2017;23:98-105.
32. Nevin A, Spoto G, Anglos D. Laser spectroscopies for elemental and molecular analysis in art and archaeology. *Applied Physics A*. 2012;106(2):339-361.
33. Raimondi V, Cecchi G, Lognoli D, Palombi L, Grönlund R, Johansson A, et al. The fluorescence lidar technique for the remote sensing of photoautotrophic biodeteriogens in the outdoor cultural heritage: A decade of in situ experiments. *International Biodeterioration & Biodegradation*. 2009;63(7):823-835.
34. Castillejo M, Martín M, Oujja M, Silva D, Torres R, Manousaki A, et al. Analytical study of the chemical and physical changes induced by KrF laser cleaning of tempera paints. *Analytical Chemistry*. 2002;74(18):4662-4671.
35. Fan T, Byer R. Modeling and CW operation of a quasi-three-level 946 nm Nd: YAG laser. *IEEE Journal of Quantum Electronics*. 1987;23(5):605-612.
36. Zheludev N. The life and times of the LED—a 100-year history. *Nature Photonics*. 2007;1(4):189.
37. Mounier A, Lazare S, Le Bourdon G, Aupetit C, Servant L, Daniel F. LED μ SF: a new portable device for fragile artworks analyses. Application on medieval pigments. *Microchemical Journal*. 2016;126:480-487.
38. Nevin A, Cather S, Anglos D, Fotakis C. Analysis of protein-based binding media found in paintings using laser induced fluorescence spectroscopy. *Analytica Chimica Acta*. 2006;573:341-346.
39. Matteini P, Camaiti M, Agati G, Baldo M-A, Muto S, Matteini M. Discrimination of painting binders subjected to photo-ageing by using microspectrofluorometry coupled with deconvolution analysis. *Journal of Cultural Heritage*. 2009;10(2):198-205.
40. Syvilay D, Bai X, Wilkie-Chancellier N, Texier A, Martinez L, Serfaty S, et al. Laser-induced emission, fluorescence and Raman hybrid setup: A versatile instrument to analyze materials from cultural heritage. *Spectrochimica Acta Part B: Atomic Spectroscopy*. 2018;140:44-53.

41. Ciofini D, Oujja M, Cañamares MV, Siano S, Castillejo M. Detecting molecular changes in UV laser-ablated oil/diterpenoid resin coatings using micro-Raman spectroscopy and laser induced fluorescence. *Microchemical Journal*. 2018;141:12-24.
42. Castillejo M, Martin M, Oujja M, Silva D, Torres R, Domingo C, et al. Spectroscopic analysis of pigments and binding media of polychromes by the combination of optical laser-based and vibrational techniques. *Applied Spectroscopy*. 2001;55(8):992-998.
43. Gilchrist JR. Choosing a Scientific CCD Detector for Spectroscopy [https://www.photonics.com/Articles/Choosing a Scientific CCD Detector for/a12010](https://www.photonics.com/Articles/Choosing_a_Scientific_CCD_Detector_for/a12010): Photonics.com; 2002 [Accessed July 2020].
44. Choi H. Advantages of photodiode array. Korea: *Manual SCINCO Co Ltd*; 2011.
45. Romani A, Clementi C, Miliani C, Favaro G. Fluorescence spectroscopy: a powerful technique for the noninvasive characterization of artwork. *Accounts of Chemical Research*. 2010;43(6):837-846.
46. Fuster-López L, Stols-Witlox M, Picollo M. UV-Vis Luminescence imaging techniques/Técnicas de imagen de luminiscencia UV-Vis. *Colección Conservation 360º*. 2020.
47. Dominec F. Design and construction of a digital CCD spectrometer. PhD Thesis, Czech Technical University, Prague; 2010.
48. Kirchner E, van der Lans I, Ligterink F, Hendriks E, Delaney J. Digitally reconstructing van Gogh's field with irises near Arles. Part 1: varnish. *Color Research & Application*. 2018;43(2):150-157.
49. Rogge CE, Lough K. Fluorescence fails: analysis of uva-induced visible fluorescence and false-color reflected UVA images of tintype varnishes do not discriminate between varnish materials. *Journal of the American Institute for Conservation*. 2016;55(2):138-147.
50. de la Rie ER. Fluorescence of paint and varnish layers (Part I). *Studies in Conservation*. 1982;27(1):1-7.
51. Dallongeville S, Garnier N, Rolando C, Tokarski C. Proteins in art, archeology, and paleontology: from detection to identification. *Chemical Reviews*. 2016;116:2-79.
52. Smith R. *The artist's handbook*. London: Dorling Kindersley; 1990.

53. de la Rie ER. Fluorescence of paint and varnish layers (Part II). *Studies in Conservation*. 1982;27(2):65-69.
54. Miyoshi T. Fluorescence from oil colours, linseed oil and poppy oil under N₂ laser excitation. *Japanese Journal of Applied Physics*. 1985;24(3):371-372.
55. Larson LJ, Shin K-SK, Zink JI. Photoluminescence spectroscopy of natural resins and organic binding media of paintings. *Journal of the American institute for Conservation*. 1991;30(1):89-104.
56. Miyoshi T. Fluorescence from colours used for japanese painting under N-laser excitation. *Japanese Journal of Applied Physics*. 1988;27(part 1):627-630.
57. Gaspard S, Oujja M, Moreno P, Méndez C, García A, Domingo C, et al. Interaction of femtosecond laser pulses with tempera paints. *Applied Surface Science*. 2008;255(5):2675-2681.
58. Baij L, Astefanei A, Hermans J, Brinkhuis F, Groenewegen H, Chassouant L, et al. Solvent-mediated extraction of fatty acids in bilayer oil paint models: a comparative analysis of solvent application methods. *Heritage Science*. 2019;7(31):1-8.
59. Dhenadhayalan N, Mythily R, Kumaran R. Fluorescence spectral studies of gum Arabic: multi-emission of gum Arabic in aqueous solution. *Journal of Luminescence*. 2014;155:322-329.
60. White R. *The organic chemistry of museum objects*. London: Buttersworth. 1994.
61. Poth U. Drying oils and related products. *Ullmann's Encyclopedia of Industrial Chemistry*. 2001.
62. van den Berg J. *Analytical chemical studies on traditional linseed oil paints*. PhD Thesis, Univeristy of Amsterdam, Amsterdam; 2002. ISBN 90-801704-7-X.
63. Izzo FC. 20th century artists' oil paints: a chemical-physical survey. PhD Thesis, Ca' Foscari University of Venice: Venice; 2011.
64. van Dam EP, van den Berg KJ, Gaibor ANP, van Bommel M. Analysis of triglyceride degradation products in drying oils and oil paints using LC-ESI-MS. *International Journal of Mass Spectrometry*. 2017;413:33-42.
65. Colombini MP, Modugno F. *Organic mass spectrometry in art and archaeology*. Pissa: John Wiley & Sons; 2009.

66. van der Doelen GA, van den Berg KJ, Boon JJ. Comparative chromatographic and mass-spectrometric studies of triterpenoid varnishes: fresh material and aged samples from paintings. *Studies in Conservation*. 1998;43(4):249-264.
67. Levison HW. Yellowing and bleaching of paint films. *Journal of the American Institute for Conservation*. 1985;24(2):69-76.
68. Katkade M, Syed H, Andhale R, Sontakke M. Fatty acid profile and quality assessment of safflower (*Carthamus tinctorius*) oil. *Journal Pharmacogn Phytochemistry*. 2018;7:3581-3585.
69. Coşge B, Gürbüz B, Kiralan M. Oil Content and fatty acid composition of some safflower (*carthamus tinctorius L.*) varieties sown in spring and winter. *International Journal of Natural & Engineering Sciences*. 2007;1(3): 11-15.
70. Pelagotti A, Pezzati L, Bevilacqua N, Vascotto V, Reillon V, Daffara C, editors. A study of UV fluorescence emission of painting materials. *Art '05–8th International Conference on Non-Destructive Investigations and Microanalysis for the Diagnostics and Conservation of the Cultural and Environmental Heritage Lecce, Italy; 2005*.
71. Mallécol J, Lemaire J, Gardette J-L. Yellowing of oil-based paints. *Studies in Conservation*. 2001:121-131.
72. Bayliss S, van den Berg KJ, Burnstock A, de Groot S, van Keulen H, Sawicka A. An investigation into the separation and migration of oil in paintings by Erik Oldenhof. *Microchemical Journal*. 2016;124:974-982.
73. Privett O, Blank M, Covell J, Lundberg W. Yellowing of oil films. *Journal of the American Oil Chemists' Society*. 1961;38(1):22-27.
74. Geldof M, Gaibor ANP, Ligterink F, Hendriks E, Kirchner E. Reconstructing Van Gogh's palette to determine the optical characteristics of his paints. *Heritage Science*. 2018;6(1:17):1-20. doi:10.1186/s40494-018-0181-6.
75. Chio K, Tappel AL. Synthesis and characterization of the fluorescent products derived from malonaldehyde and amino acids. *Biochemistry*. 1969;8(7):2821-2827.
76. Franks F, Roberts B. Quantitative study of the oxidative discoloration of ethyl linoleate. I. Oxidation in the bulk phase. *Journal of Applied Chemistry*. 1963;13(7):302-309.

77. O'Neill L, Rybicka S, Robey T. Yellowing of drying oil films. *Chemistry and Industry*. 1962:1796-1797.
78. Rakoff H, Thomas F, Gast L. Reversibility of yellowing phenomenon in linseed-based paints. *Journal of Coatings Technology*. 1979;51(649):25-28.
79. Ioakimoglou E, Boyatzis S, Argitis P, Fostiridou A, Papapanagiotou K, Yannovits N. Thin-film study on the oxidation of linseed oil in the presence of selected copper pigments. *Chemistry of Materials*. 1999;11(8):2013-2022.
80. Kumarathasan R, Rajkumar AB, Hunter NR, Gesser HD. Autoxidation and yellowing of methyl linolenate. *Progress in Lipid Research*. 1992;31(2):109-126.
81. Casoli A, Berzioli M, Cremonesi P. The chemistry of egg binding medium and its interactions with organic solvents and water. In: *New Insights into the Cleaning of Paintings: Proceedings from the Cleaning 2010 International Conference*; 2013.
82. Dallongeville S, Richter M, Schäfer S, Kühnlenthal M, Garnier N, Rolando C, et al. Proteomics applied to the authentication of fish glue: application to a 17th century artwork sample. *Analyst*. 2013;138(18):5357-5364.
83. Sandu ICA, Roque ACA, Matteini P, Schäfer S, Agati G, Correia CR, et al. Fluorescence recognition of proteinaceous binders in works of art by a novel integrated system of investigation. *Microscopy Research and Technique*. 2012;75(3):316-324.
84. Sandu ICA, Schäfer S, Magrini D, Bracci S, Roque CA. Cross-section and staining-based techniques for investigating organic materials in painted and polychrome works of art: a review. *Microscopy and Microanalytics*. 2012;18:860-875. doi:10.1017/S1431927612000554.
85. Kuckova S, Sandu ICA, Crhova M, Hynek R, Fogas I, Schafer S. Protein identification and localization using mass spectrometry and staining tests in cross-sections of polychrome samples. *Journal of Cultural Heritage*. 2013;14(1):31-37.
86. Nevin A, Anglos D, Cather S, Burnstock A. The influence of visible light and inorganic pigments on fluorescence excitation emission spectra of egg-, casein- and collagen-based painting media. *Applied Physics A: Materials Science & Processing*. 2008;92(1):69-76.

87. Deyl Z, Mikšik I, Zicha J. Multicomponent analysis by off-line combination of synchronous fluorescence spectroscopy and capillary electrophoresis of collagen glycation adducts. *Journal of Chromatography A*. 1999;836(1):161-171.
88. Dallongeville S, Garnier N, Rolando C, Tokarski C. Proteins in art, archaeology, and paleontology: from detection to identification. *Chemical reviews*. 2016;116(1):2-79.
89. Okada Y, Kawanobe W, Hayakawa N, Tsubokura S, Chujo R, Fujimatsu H, et al. Whitening of polyvinyl alcohol used as restoration material for Shohekiga. *Polymer Journal*. 2011;43(1):74-77.
90. Sulzbach, Hessen. *Technical brochure: Mowiol - Polyvinyl Alcohol*. Clariant GmbH1999.
91. Vinçotte A, Beauvoit E, Boyard N, Guilminot E. Effect of solvent on PARALOID® B72 and B44 acrylic resins used as adhesives in conservation. *Heritage Science*. 2019;7(1):42.
92. Miyoshi T, Ikeya M, Kinoshita S, Kushida T. Laser-induced fluorescence of oil colours and its application to the identification of pigments in oil paintings. *Japanese Journal of Applied Physics*. 1982;21(7R):1032-1036.
93. Borgia I, Fantoni R, Flamini C, Di Palma TM, Guidoni AG, Mele A. Luminescence from pigments and resins for oil paintings induced by laser excitation. *Applied Surface Science*. 1998;127:95-100.
94. Gonzalez V, Gourier D, Calligaro T, Toussaint K, Wallez G, Menu M. Revealing the origin and history of lead-white pigments by their photoluminescence properties. *Analytical Chemistry*. 2017;89:2909-2918. doi: 10.1021/acs.analchem.6b04195.
95. Miliani C, Rosi F, Burnstock A, Brunetti BG, Sgamellotti A. Non-invasive in-situ investigations versus micro-sampling: a comparative study on a Renoirs painting. *Applied Physics A*. 2007;89(4):849-856.
96. Pronti L, Felici AC, Ménager M, Vieillescazes C, Piacentini M. Spectral behavior of white pigment mixtures using reflectance, ultraviolet-fluorescence spectroscopy, and multispectral imaging. *Applied Spectroscopy*. 2017;71(12):2616-2625.
97. Ghirardello M, Mosca S, Marti-Rujas J, Nardo L, Burnstock A, Nevin A, et al. Time-resolved photoluminescence microscopy combined with X-Ray analyses and Raman spectroscopy sheds

- light on the imperfect synthesis of historical cadmium pigments. *Analytical Chemistry*. 2018;90(18):10771-10779.
98. de la Rie ER. Fluorescence of Paint and Varnish Layers (Part III). *Studies in Conservation*. 1982;27(3):102-108.
99. Clementi C, Miliani C, Verri G, Sotiropoulou S, Romani A, Brunetti BG, et al. Application of the kubelka—munk correction for self-absorption of fluorescence emission in carmine lake paint layers. *Applied Spectroscopy*. 2009;63(12):1323-1330.
100. Diaz AN. Absorption and emission spectroscopy and photochemistry of 1,10-anthraquinone derivatives: a review. *Journal of Photochemistry and Photobiology, A: Chemistry*. 1990;53:141-167.

Chapter 3: Experimental Methodology

3.1 Overview

The experimental scheme of the project is presented in Figure 3.1, which shows the inter-relationship between the components of this study. All binders were prepared in 2017 and naturally aged for two years. The fluorescence spectra of these 2017 samples were analysed in 2017 (as freshly dried binders), and subsequently in 2018 and 2019 to identify any shifts in fluorescence spectra resultant of natural ageing. Drying oils showed interesting results (as discussed in Section 4.1) and were therefore specifically chosen to undergo artificial ageing experiments (Section 3.2.4). Various artificial ageing mechanisms (UV light, sunlight, dark drawer, and exposure to ammonia vapour) were applied based on suggestions from literature [1, 2]. High performance liquid chromatography (HPLC) and other chromatographic techniques were then employed to further characterise the fluorophore in drying oils.

In addition to the ageing studies, in 2018 mixtures of binder and inorganic pigments were prepared and analysed to characterize any fluorescent changes resultant of pigment interactions (Section 4.3). Inorganic pigments do not dissolve in the binder and remain in their crystalline form. Therefore, pigment effects from inherently fluorescent pigments and pigments which will dissolve into the binder leading to larger pigment-binder interactions, were investigated (Section 3.2.2).

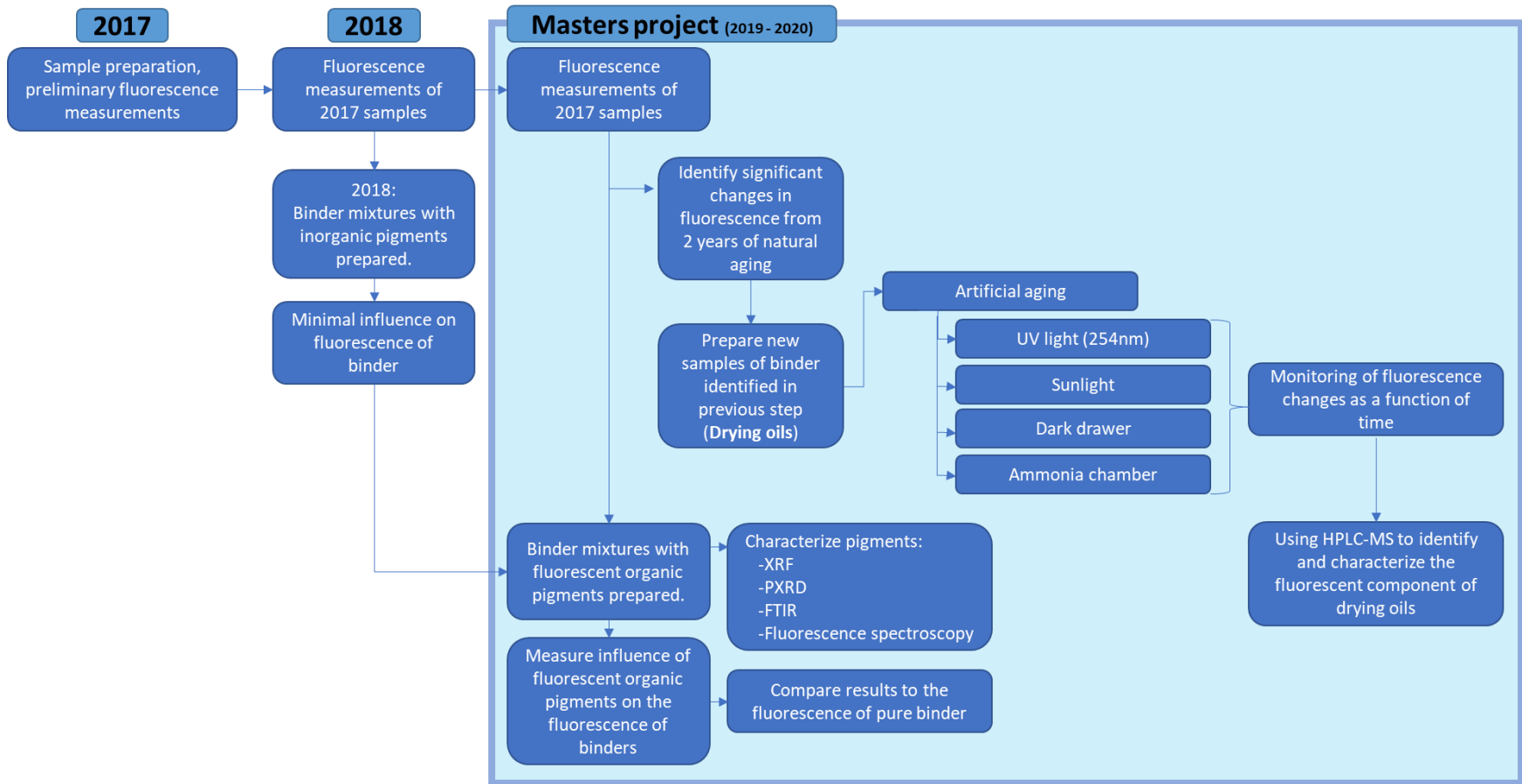


Figure 3.1: Overview of project layout shown in relation to research done in previous years.

3.2 Sample preparation

3.2.1 Binders

The binders were made up according to traditional recipes [3]. Three different variations of chicken egg samples were tested: whole egg, egg white and egg yolk. Egg white was obtained by separating the egg yolk and egg white, the egg white was then used directly. Egg yolk was obtained by drying the egg yolk casing with paper towel and then piercing the casing to allow the yolk to drip out, this ensures no contamination from egg white. Whole egg was prepared by scrambling the entire egg (including the egg yolk casing) with a clean spatula.

Rabbit skin glue (BluePrint, SA) was dissolved in deionised water (DI.H₂O) to a 5% (w/w) concentration, following traditional recipes [3, 4] (Table 3.1). The deionised water was obtained from a Millipore Direct-Q 3 UV system (Molsheim, France). Fish glue (Sennelier, France) was ready made to a 50% dry extract solution in water and required no sample preparation. Ox gall (Winsor & Newton, UK) required no sample preparation, and is an additive to paint which will be studied for its binding properties. These binders, along with the egg samples, are classified as proteinaceous binders.

Gum Arabic (Winsor & Newton, UK) was ready-made and required no additional sample preparation. Gum Tragacanth (University of Pretoria Museums) was made up by dissolving the powder in deionised water at a 1:27 weight to volume ratio and heated to 80°C on a hot plate (Heidolph, Labotec, SA) for 2 hr ensure complete dissolution, as was instructed on the sample bottle. Klucel G powder (University of Pretoria Museums) was dissolved in deionised water at 80% (w/w), stirred with a magnetic stirrer bar and heated on a hotplate for 1 hr. It was then left-over night (24 hrs) before painting of the model sample. These binders are classified as polysaccharides but will be further discussed in tandem with the proteinaceous materials.

Lascoux (a medium for consolidation 4176, BluePrint, SA) and gilding milk (LUKAS, Germany) were ready to use, and required no sample preparation. Paraloid B72 and paraloid B67 (BluePrint, SA) were made up by dissolving 0.3 g of the resin beads in 10 mL of methanol (HPLC grade - Sigma Aldrich, SA) to produce a 30% paraloid solution, following guidelines given by the conservators at University of Pretoria museums. Mowital (BluePrint, SA) and mowiol 18-88 (BluePrint, SA) were dissolved in deionised water and made up to a 60% (w/w) solution before applying the binder onto various substrates. These binders (lascoux, paraloid, mowital and mowiol) are classified as synthetic binders.

Four different drying oils were analysed, all of which were ready to use and required no additional sample preparation. The oils used were linseed oil (LO), water-miscible linseed oil (WLO), stand oil (SO) and poppy seed oil (PO) all from Winsor & Newton, UK. These will further be referred to as lipid binders.

3.2.2 Pigments

Five different pigments were used: alizarin crimson (PCM545), lamp black (PCM559), Indian yellow (PCM557), phthalo blue (PCM565) and oriental blue (PCM563) all from BluePrint, the South African Institute for Heritage Science & Conservation. In addition, reference samples of alizarin crimson were used: namely alizarin crimson dark (PR83 58000, Kremer pigments), alizarin crimson light (PR 112 12370, Kremer pigments) and madder lake (NR9 75330, 75420, Kremer pigments). The reference samples were donated by the Institute for the Preservation of Cultural Heritage (IPCH) at Yale to the Tangible Heritage Conservation (THC) program at the University of Pretoria. A summary of all artist materials used in this project can be found in Table 3.1.

Table 3.1: Summary of artists' materials used. The preparation method and the abbreviations used for each binder and pigment are described.

Binder		Abbr.	Preparation method	Supplier
Proteinaceous	Whole egg	WE	Whole was prepared by mixing the egg (without removing the egg yolk casing).	Supermarket eggs
	Egg white	EW	Obtained by separating the egg white from the egg yolk.	Supermarket eggs
	Egg yolk	EY	Obtained by separating the egg yolk from the egg white and drying the egg yolk casing with paper towel and then piercing the casing to allow the yolk to drip out.	Supermarket eggs
	Rabbit skin glue	RSG	Dissolved in DI.H ₂ O to 5% (w/w) solution.	BluePrint, SA
	Fish glue	FG	Ready-made to 50% solution.	Sennelier, France
	Gilding milk	GM	-	LUKAS, Germany
	Ox gall	OX	-	Winsor & Newton, UK
Polysaccharide	Gum Arabic	GA	-	Winsor & Newton, UK
	Gum Tragacanth	GT	Dissolved in DI.H ₂ O to 1:27 volume ratio.	University of Pretoria Museums, SA
	Klucel G	KG	Dissolved in DI.H ₂ O to 80% (w/w) solution, stirred and heated for 1 hr. Left for 24 hrs before painting of the model samples.	University of Pretoria Museums, SA
Synthetic	Mowital	Mt	Dissolved in DI.H ₂ O to 60% (w/w) solution.	BluePrint, SA
	Mowiol 18-88	Mi		BluePrint, SA
	Lascoux	Las	-	BluePrint, SA

	Paraloid P67	P67	Dissolved 0.3 g of the resin beads in 10 mL MeOH to provide a 30% (w/v) paraloid solution.	BluePrint, SA
	Paraloid P72	P72		BluePrint, SA
Drying oils	Linseed oil	LO	-	Winsor & Newton, UK
	Poppy seed oil	PO	-	Winsor & Newton, UK
	Stand oil	SO	-	Winsor & Newton, UK
	Water-miscible linseed oil	WLO	-	Winsor & Newton, UK
Pigments		Abbr.	Preparation method	Supplier
Alizarin crimson		AC	-	BluePrint, SA
Lamp black		LB	-	BluePrint, SA
Indian yellow		IY	-	BluePrint, SA
Phthalo blue		PB	-	BluePrint, SA
Oriental blue		OB	-	BluePrint, SA
Alizarin crimson, light		PR83*	-	Kremer pigments, Germany
Alizarin crimson, dark		PR112*	-	Kremer pigments, Germany
Madder lake, genuine		NR9*	-	Kremer pigments, Germany

*When the exact chemical nature of a pigment is known it can be ascribed an index number based on the extensive colour index database, where PR indicates 'Pigment Red' and NR a 'Natural Red'.

3.2.3 Solid samples

3.2.3.1 Microscope slides

3.2.3.1.1 Painted samples

Solid samples of all binders were prepared in 2017 by painting the binders onto glass microscope slides (76 x 26 mm, Labocare, UK) to cover an area of roughly 55 x 15 mm dimension. These films were cured in a dark drawer under ambient conditions (20 ± 5 °C and 50 ± 20 % relative humidity (RH), where fluctuations were the result of seasonal changes). These solid samples were aged for two years in dark drawers.

3.2.3.1.2 Spin-coated samples

The drying oils were prepared as uniform films on microscope slides using a spin-coater (model WS-650MZ-23NPPB, Laurell, USA) to ensure a smooth surface. 1 mL of drying oil was spread evenly over a microscope slide and spin-coated for 10 sec at 500 rpm (rotations per minute) at an acceleration of 300 rpm/min. The process was repeated a second time, using only 0.5 mL of drying oil. This ensured a thin film which could dry homogenously, without any wrinkling, and could then be used further for absorption studies.

3.2.3.1.3 Binder-Pigment samples

Paint mixtures were made up to a ratio of 5-10% mass of pigment to mass of binder and applied using an impasto technique onto a glass microscope slide using a spatula. Impasto is the technique whereby paint is applied thickly to the substrate. A spatula was used instead of a paint brush to prevent contamination from poorly cleaned paint brushes and to ensure a reasonably smooth surface without brush strokes. These samples were dried in a dark drawer for 3 months before analysis.

3.2.3.2 Canvas

Samples for artificial ageing were prepared by painting the drying oils onto microscope slides covered with pieces of painter's canvas (Archneer, SA; Figure 3.2). This was done to facilitate the accelerated ageing with minimal alligator skin formation (wrinkling of paint caused by rapid drying of the upper layers of drying oil). These samples were solely used for fluorescence studies and to monitor the changes in fluorescence during artificial ageing.

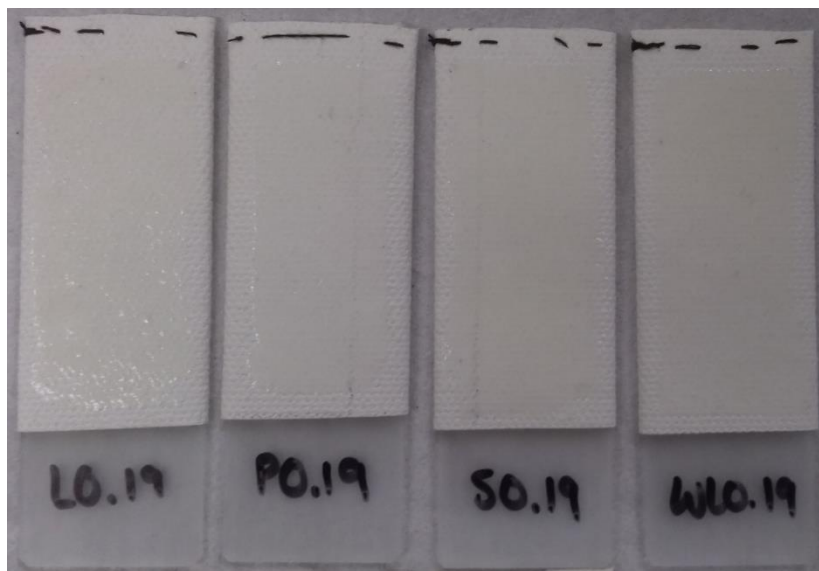


Figure 3.2: Example of microscope slides covered in canvas. These samples were coated with the respective drying oil, the drying oils are not cured in this image.

3.2.3.3 Bulk samples

At a later stage in the research it was identified that the fluorescence of drying oils showed interesting results. Extraction of the solid oils was done (Section 3.2.4.2), however the amount of binder sample on the microscope slide was not enough for efficient extraction. Therefore, bulk samples were prepared by pouring a large amount of linseed oil into a glass petri dish. The sample was artificially aged under ultraviolet light for 24 hrs before drying in a dark drawer. The oil layer was roughly 1 mm thick and showed severe wrinkling and yellowing. The upper layer was touch dry within a few weeks, but the lower layers were still wet. A scalpel was used to cut a grid pattern (10 x 10 mm blocks) into the upper layer, which allowed oxygen to diffuse into the lower layers and thereby allow the entire oil sample to dry.

3.2.4 Ageing studies

The 2017-samples were left to naturally age in a dark drawer under ambient conditions (20 ± 5 °C and 50 ± 20 % RH, where fluctuations were as a result of seasonal changes). A year of natural ageing showed minimal fluorescent changes, and of all the binders investigated, the drying oils showed the most drastic changes from ageing. Therefore, the drying oils were subject to both artificial accelerated ageing and natural ageing to determine which processes would lead to the most changes.

Artificial ageing was achieved by exposing the samples to elevated temperatures, artificial light, and a saturated chamber of ammonia vapour. An ammonia chamber was prepared to induce yellowing. The wooden chamber (25 x 25 x 60 cm) was sealed with rubber and had a glass window through which the colour change could be monitored (Figure 3.3). A beaker containing 40 mL of 25% ammonia solution (Merck, USA) was placed in the chamber to saturate the air with ammonia vapour. Two main sets of samples were treated; the first set of samples was exposed to various ageing environments while wet and the samples were cured under these ageing conditions. The second set was first cured in a dark chamber for 3 months after which they were exposed to the artificial ageing conditions.



Figure 3.3: A photo of the chamber which was saturated with ammonia vapour from a 25% ammonia solution.

Within each set there were various times for which a sample was exposed to the ageing conditions (Figure 3.4). The first set of 44 samples was cured under the following ageing conditions: two samples for each oil (a total of eight samples) were cured exposed to an elevated temperature (80°C) in an oven, with one sample exposed for 3 hr and the other for 6 hr. Another set of 5 samples per oil were cured for either 24 hr, 1 week, 2 weeks, 3 weeks or 1 month under a UVC lamp (254 nm, UVP UVGL-58 Analytikjena, USA), thereafter they were placed in a dark drawer. Another set of four samples for each oil was cured in the ammonia chamber under ambient indoor light conditions, for either 24 hr, 1 week, 2 weeks or 1 month, and thereafter placed in a dark drawer.

The second set of 24 samples was cured in a dark drawer for 3 months before being exposed to the different ageing conditions. Two samples for each oil were placed under the UV lamp for either 24 hr or 1 week, and thereafter were placed in a dark drawer. Another set of four samples for each oil were placed in the ammonia chamber for either 24 hr, 1 week, 2 weeks or 1 month and thereafter were stored in a dark drawer before analysis.

The third set consisted of reference samples that were cured in controlled environments to ensure that the change in fluorescence was due to the artificial ageing conditions and not a fundamental change that occurs in drying oils. All together there were five reference samples prepared for each oil (20 samples in total). They were placed under various lighting conditions and were not exposed to any of the artificial ageing conditions: the first set (4 samples) were placed in the dark drawers along with all other samples. Two sets (8 samples) were placed in the office - void of any additional chemical vapours that could possibly be present in the laboratory environment, the first set was placed under ambient office lighting conditions (fluorescent lamps which were on daily for roughly 12 hrs) and the second was placed in a dark box. There were also two sets (8 samples) placed in the undergraduate laboratory which receives the most sunlight during the day as it is on the top floor with north-facing windows. The first set was placed on a windowsill directly in the sun, while the second set was placed in a dark box on the windowsill – to ensure that they experienced the same heat fluctuations as those on the windowsill. In addition to the oil reference samples, a blank canvas was prepared and kept in the dark drawer with the bulk of the oil samples, this was tested throughout the study to confirm that the blank canvas did not develop any fluorescence.

Bleaching studies were done on severely yellowed drying oils. The samples which produced the fastest yellow discolouration were chosen, namely samples 11, 12 and 13 which were all cured under UV light and subsequently stored in a dark drawer. These samples developed severe discolouration, and a bleaching study was done to determine the reversibility thereof (Section 4.3). As the number of samples were limited only three methods were used to determine the reversibility of the discolouration. Three main light sources were used: ambient sunlight, 254 nm and 365 nm UV light. The sunlight exposure was done in open air, starting at midday in summer. The exposure to sunlight was limited due to the unpredictable thunderstorms in the summer, which led to an initial exposure time of 3 hr, followed the next day by another 5 hrs. UV light was more easily monitored and exact exposure times of 8 and 24 hr were used.

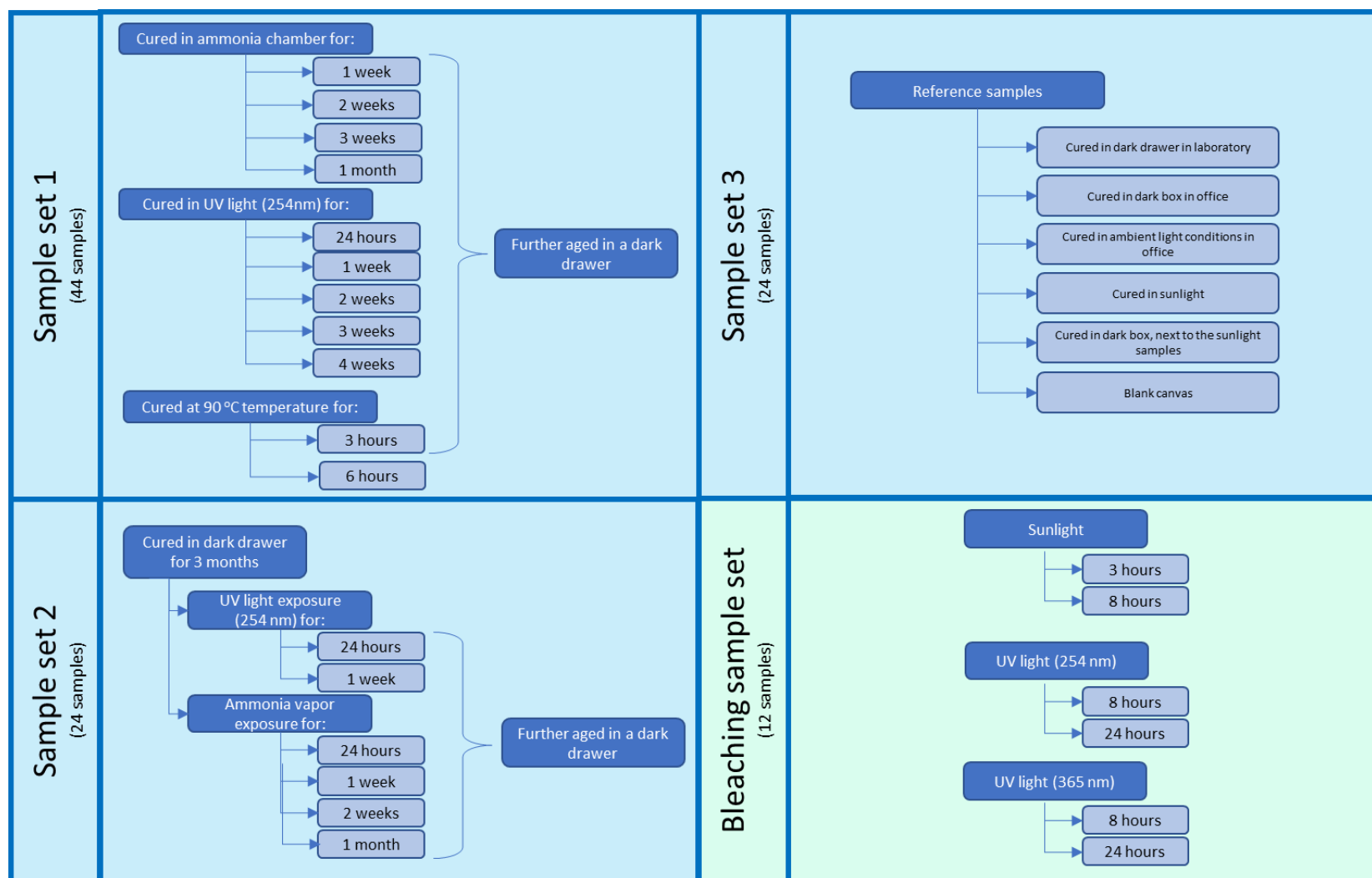


Figure 3.4: Summary of the samples used in the artificial ageing experiments, where each grey block represents a set of the four oils (i.e. each block represents a set of LO, SO, WLO & PO). The bleaching sample set contained only three sample subsets, where the grey blocks represent the different times after which the fluorescence was measured.

3.2.5 Powder samples

No additional preparation was needed for the powder samples. For fluorescence measurements the pigments were packed into a powder sample holder (Figure 3.5), using a clean spatula. All pigments, except OB, were stable in the sample holder when placed vertically in the spectrofluorometer. The oriental blue was covered with a microscope slide, to prevent the powder particles from falling out.

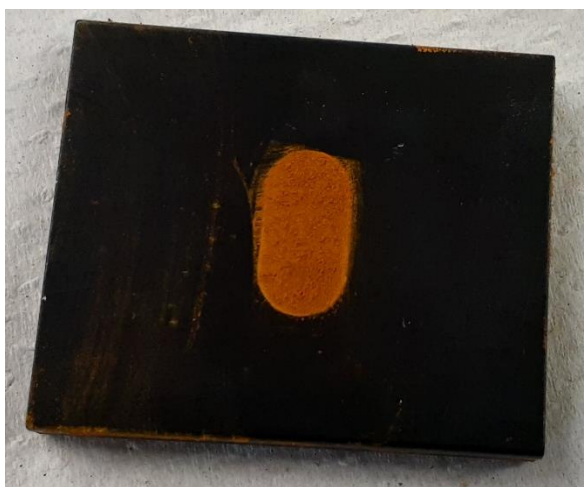


Figure 3.5: *An example of the powder sample holder for the fluorescence measurements which in this example is filled with Indian yellow pigment.*

3.2.6 Liquid Samples

3.2.6.1 Binders

Liquid samples were prepared by dissolving 10 μL of the binder in 1000 μL of solvent. For proteinaceous binders (GM, OX, GA, GT, WE, EW, EY, RSG, FG and KG) deionised water was used as solvent. Chloroform (99.5% RadChem, SA) was used for the synthetic binders (Mi, Las, P67 and P72) and ethanol (95% ACE Chemicals, SA) for the lipid binders (LO, WLO, SO, PO).

Liquid samples were prepared by dissolving 10 μL of the liquid oil in 1000 μL of solvent. The solvents used were: diethyl ether (90% SAR Chem, SA), ethanol, dichloromethane, and toluene at 95% purity (ACE Chemicals, SA), acetonitrile, hexane and methanol were HPLC grade (99.9% Sigma Aldrich, SA), while cyclohexane and chloroform were 99.5% purity (RadChem, SA).

3.2.6.2 Extraction techniques

Solid-liquid extraction was performed on the dried oils by placing 0.500 mg cured oil into a vial with 1000 μ L ethanol. The sealed vial was then ultrasonicated at a high frequency (50 Hz) for 30 min using a Scientech ultrasonic bath (Labtec, SA). Additionally, the solid film on a microscope slide and from the bulk sample (removed from the petri dish) was extracted through Soxhlet extraction. The microscope slide samples contained \pm 0.20 g naturally dried linseed oil. Quartz wool was used to prevent any solid particles from entering the siphon. Thereafter subsequent extractions were done using \pm 0.20 g of bulk sample placed in a 25 mm x 90 mm glass microfibre thimble (Whatman, UK). For all Soxhlet extractions 100 mL methanol was used and the extraction took place over 24 hrs, resulting in a bright yellow solution and a severely cracked oil film.

3.2.6.3 Pigments

Alizarin crimson was tested for any fluorescent anomalies after unexpected fluorescence results were obtained from the pigment-binder mixtures (Section 4.2.2). Alizarin crimson (\pm 0.0135 g) was dissolved in 3 mL of solvent. The solvents used were chloroform, toluene, DCM, DMSO, ACN, acetone, DMF, methanol, ethanol, DI.H₂O, diethyl ether, hexane and cyclohexane (of the same purity as those used in the binders sample preparation (Section 3.2.4.1)). The solution was ultrasonicated for 5 min and then filtered through 0.22 μ m PTFE Clarinert syringe filters (Agela technologies, USA) to remove all remaining pigment particles. The resultant transparent solution was analysed using UV-Vis absorption and fluorescence spectroscopy.

3.2.6.4 HPLC and UPLC sample preparation

Oil samples were prepared for HPLC analysis by placing \sim 1.5 mg of the solid film oil or 10 μ L liquid oil into 1 mL of HPLC grade methanol (Sigma Aldrich, USA). The samples were ultrasonicated for 30 min at high frequency and allowed to settle. Once settled the solvent layer was removed and transferred to 1.5 mL glass vials to be analysed. 0.22 μ m PTFE Clarinert syringe filters (Agela technologies, USA) were used to remove all remaining solid film particles prior to injection.

The alizarin crimson sample and reference samples were dissolved in 1 mL HPLC grade methanol and filtered through a 0.22 μ m PTFE Clarinert syringe filter. The resultant solution was then diluted by using 10 μ L in 990 μ L of methanol. This final solution had a faint red discolouration which could hardly be seen.

3.3 Instrumentation

3.3.1 UV-induced fluorescence imaging

Samples were irradiated with UV light using an Analytik Jena UVP UVGL-58 lamp (USA) at 254 nm and 365 nm excitation wavelength, housed in a dark box. The visual fluorescence was captured using a Samsung galaxy A20 cell phone equipped with a 13 MP F1.9 camera.

3.3.2 Absorption and fluorescence spectroscopy

During both absorption and fluorescence studies, liquid samples were held in 10 mm path length quartz cuvettes, which were washed between each experiment using 10% Piranha solution. For fluorescence studies, painted samples on microscope slides were analysed in a slide-holder at a 30° angle to the incident light, to prevent reflected incident light from entering the detector.

All spectra were normalised to one (unless stated differently) and have been smoothed using a 20-point Savitzky-Golay method in Origin Pro 2016.

3.3.2.1 Fluorescence spectrometer

Fluorescence measurements were made on a Fluoromax-4 spectrofluorometer (Horiba, Japan) with a continuous 150 W xenon lamp and photodiode detector. A single monochromator was used for excitation and emission wavelengths, with a slit width of 5 nm for both the light source and the detector.

3.3.2.2 UV-Visible light absorption spectrometer

UV-Visible absorption measurements were done using a Cary 100-Bio UV-Visible spectrophotometer (Varian, USA) equipped with a visible light source lamp and a deuterium lamp, which switched at 350 nm. Scans were measured from 800-200 nm with a Czerny-Turner 0.28 m monochromator equipped with a R928 photomultiplier tube (PMT) detector.

3.3.3 Infra-red spectroscopy

Fourier-transform infrared spectroscopy (FTIR) was performed using a Bruker Alpha FT-IR spectrophotometer fitted with an attenuated total reflection (ATR) platinum diamond accessory. The transmittance spectra were recorded with 4 cm⁻¹ resolution in 64 scans, measuring from 4000-400 cm⁻¹.

3.3.4 X-ray fluorescence spectroscopy (XRF)

X-ray fluorescence measurements were done using a Bruker Tracer Si handheld spectrometer (Bruker, Germany), equipped with a Rhodium X-ray tube excitation source and a silicon drift detector (SDD) allowing measurement of elements from magnesium to uranium. Spectra were collected using the oxide-3 phase factory calibration where three scans with excitation energy changing from 15, 30, and 50 kV, with automatically adjusted microamps (μA) using a titanium-aluminium (Ti: 25 μm and Al: 300 μm) transmission filter. The samples were not infinitely thick, nor matrix matched, therefore quantitative data was not provided but rather the spectra were used for qualitative identification. Pigments were placed in small polyester plastic sleeves, and major elements were identified through comparative studies to a blank sleeve. Data reduction was done on Bruker Artax software (v. 8.9.9.476).

3.3.5 Powder X-ray diffraction (PXRD)

Powder X-ray diffraction of all pigments was done using a Bruker 2D Phaser powder diffractometer (Bruker, Germany) at room temperature. Cu K α radiation was generated at 30 kV and 10 mA with a wavelength of 1.54 Å. Small amounts of powder were used on a low background silicon quartz sample holder. Patterns were collected in a range from 5-60° 2 θ in steps of 0.05° and a counting time of 3 s per step. The powder patterns were matched to confirm the composition using Diffrac.Eva software (version 2.0) which provided comparison to the ICDD (The International Centre for Diffraction Data) database.

3.3.6 Chromatography

3.3.6.1 HPLC-PDA-SPE

Samples were analysed using a 1260 Infinity binary high-performance liquid chromatography (HPLC) system (Agilent, USA), equipped with an Agilent 1260 auto sampler and a XSelect® HSS T3 5 μm (4.6 mm x 150 mm) reverse phase column (Waters, SA). The 1260 Infinity Photodiode-Array Detector (PDA) (Agilent, USA) used a deuterium lamp (wavelength range 190 to 640 nm), with an optical slit of 4 nm. Chromatograms were monitored using selected wavelengths: 240, 260, 280, 300, 315 and 400 nm.

Separation was achieved by means of a reverse phase step gradient using acetonitrile (A) and water (B) both with 0.1% formic acid, at a 4.00 $\mu\text{L}/\text{min}$ flow rate. Initial conditions were: 20% A: 80% B, ramped up to 100% A within 12 min, held constant for 14 min. Thereafter, the gradient was rapidly changed back to the initial conditions of 20% A in 2 min and then held constant for another 2 min (total run time of 20

min). The HPLC system was fitted with a re-usable online micro solid phase extraction (μ SPE) collection unit. Two fractions were manually collected between 12.6 - 13.0 min (fraction 1) and 13.05 – 13.4 min (fraction 2) onto polydivinyl-benzene polymer Hysphere-GP 20 x 2 mm μ SPE cartridges (Spark Holland, The Netherlands) and were then eluted using HPLC grade methanol (Sigma Aldrich, SA) into 1.5 mL glass vials.

3.3.6.2 UPLC-QTOF

In order to obtain high resolution molecular information about the fractions collected from the HPLC analysis, they were subsequently analysed using a Waters Synapt G2 high definition mass spectrometry (HDMS) system (Waters Inc., USA). The system comprises of a Acquity Ultra Performance liquid chromatograph (UPLC[®]) coupled to a quadrupole time of flight mass spectrometer (QTOF) (Waters Inc., USA). This system enables high chromatographic resolution at high pressures and allows for enhanced peak detection and accurate mass identification. The accuracy was controlled by an internal lock mass standard of 2 pg/ μ L solution leucine enkephalin (m/z 555.2693), which was directly infused into the source through a secondary orthogonal electrospray ionisation (ESI) probe allowing intermittent sampling. The internal control was used to compensate for instrumental drift, ensuring good mass accuracy throughout the duration of the runs. Resolution of 20 000 at m/z 200 full width at half maximum (FWHM) and mass error within 0.4 mDa were obtained.

A Waters UPLC[®] C₁₈ Ethylene Bridged Hybrid (BEH) column (1.7 μ m particle size, 100 mm length \times 2.1 mm internal diameter) was used. Injection volumes were set at 5 μ L with an autosampler. Separation was achieved by means of a reverse phase step gradient using water (A) and acetonitrile (B) both with 0.1% formic acid (HPLC grade, Romil, UK), at 0.3 μ L/min flow rate. Initial conditions were: 95% A: 5% B, with a linear ramp up to 100% B within 13 min, held constant for 1 min. Thereafter, the gradient was rapidly changed back to the initial conditions of 95% A in 0.5 min. The column was then washed with 95% A: 5% B for 1 min followed by conditioning and re-establishment of the initial conditions to allow for equilibration before the start of the next run. This resulted in a total run time of 16 min. The column temperature was kept constant at 40 °C. The positive and negative ion mass spectra were collected in separate chromatographic runs (employing the same separation conditions).

Mass spectral scans were collected every 0.3 s. The raw data was collected in the form of a continuous profile. The mass spectral discharge electrode was set at 2.6 kV and 2.0 kV for positive and negative ionisation, respectively. The source temperature was set at 120 °C, the sampling cone voltage at 25 V,

extraction cone voltage at 4.0 V and cone gas (nitrogen) flow at 10.0 L/hr. The desolvation temperature was set at 350 °C with a gas (nitrogen) flow of 600.0 L/hr. Mass to charge ratios (m/z) between 50 and 1200 Da were recorded. QuanLynx™, an application manager included in the MassLynx™ software (version 4.1; Waters Inc., USA), was used for analyte identification.

3.4 References

1. de la Rie ER. Fluorescence of paint and varnish layers (Part II). *Studies in Conservation*. 1982;27(2):65-69.
2. Schaeffer TT. *Effects of light on materials in collections: data on photoflash and related sources*. Los Angeles: The Getty Conservation Institute; 2001.
3. Cennini C, Thompson DV. *The craftsman's handbook*. New York: Dover Publications; 1954.
4. Smith R. *The artist's handbook*. London: Dorling Kindersley; 1990.

Chapter 4: Results and Discussion

4.1 Fluorescence study of lipid binders

4.1.1 Absorption and fluorescence spectroscopic analysis

The UV-Vis absorption spectra of drying oils were recorded for the liquid oils (dissolved in ethanol) and the solid films. There were few differences in the UV-absorption spectra between the four different drying oils in solution (Figure 4.1). All oils have two strongly UV-absorbing peaks, one between 200 and 215 nm while the second, less intense peak occurred at 230 nm. The absorption at 200-215 nm indicates the presence of polyenes and unsaturated α,β -ketones [1, 2]. Between 250 and 350 nm, the oils show weak absorptive peaks indicating the presence of an unconjugated chromophore containing a heteroatom [3].

The spectra of linseed oil (LO) and water-miscible linseed oil (WLO) are the most similar: both show peaks at about 280, 300 and 315 nm, while the peak at 269 nm (in the presence of another peak at 315 nm) is characteristic of WLO. The spectral similarity between LO and WLO are not surprising, considering the fact that WLO is LO with an added emulsifier that increases its solubility in water, but other than that, the two are chemically identical [4]. Poppy seed oil (PO) has three additional moderately absorbing peaks, at 258, 269 and 279 nm, of which the first peak is characteristic of PO and does not appear in either LO or WLO. Stand oil (SO) does not have any peaks in the range between 250 to 350 nm, suggesting that the compounds that would normally give rise to peaks in this area may have reacted during the pre-polymerization process [5]. In contrast to the absorption spectra of samples in solution, the cured films show only a broad peaked absorption at 300 nm (Figure 4.2).

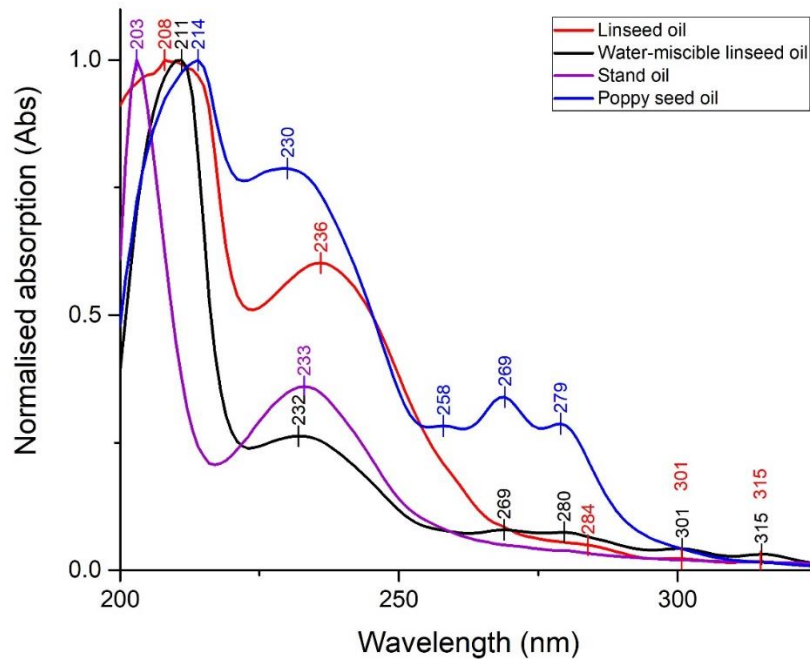


Figure 4.1: UV-Vis absorption spectra of the liquid drying oils dissolved in ethanol. All spectra were blank corrected and normalised to 1.

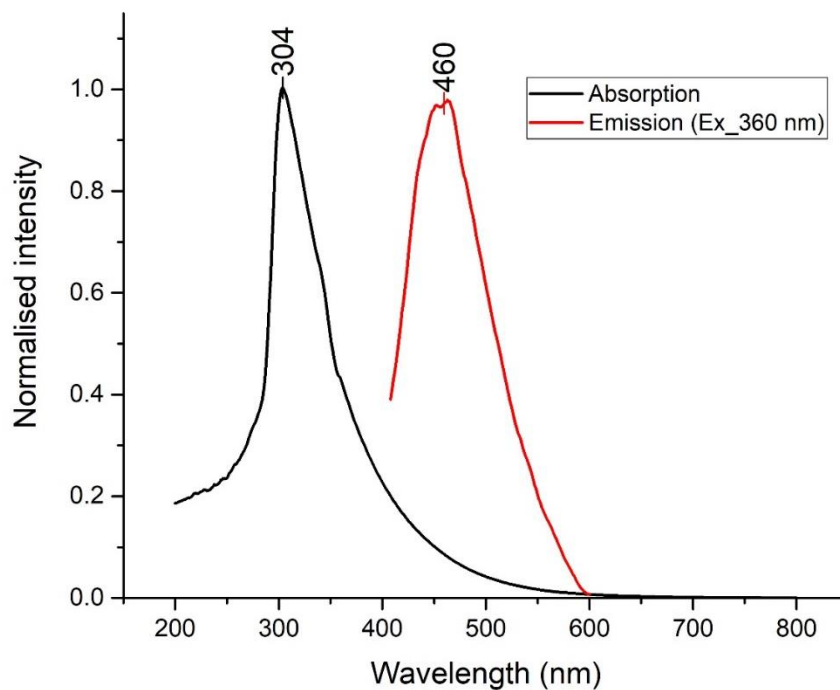


Figure 4.2: Fluorescence and absorption spectra of cured drying oils (after formation of a solid film). All oils studied showed the same peaks.

The absorption patterns give an indication of the excitation wavelength which will result in optimal fluorescence. Of the five distinct absorption peaks in liquid linseed oil, only two resulted in fluorescence. Excitation (λ_{ex}) at 300 nm results in a two-peaked fluorescence signal (Figure 4.3) while excitation at 315 nm gives only one. The emission at 330 nm only appears upon excitation at 300 nm, while the peak at 410 nm appears when both excitation wavelengths (λ_{ex} 300 and 315 nm) are used. Although PO and SO show no absorption at 300 and 315 nm, both excitation wavelengths give the same fluorescence spectra as LO, and no additional fluorescence is observed.

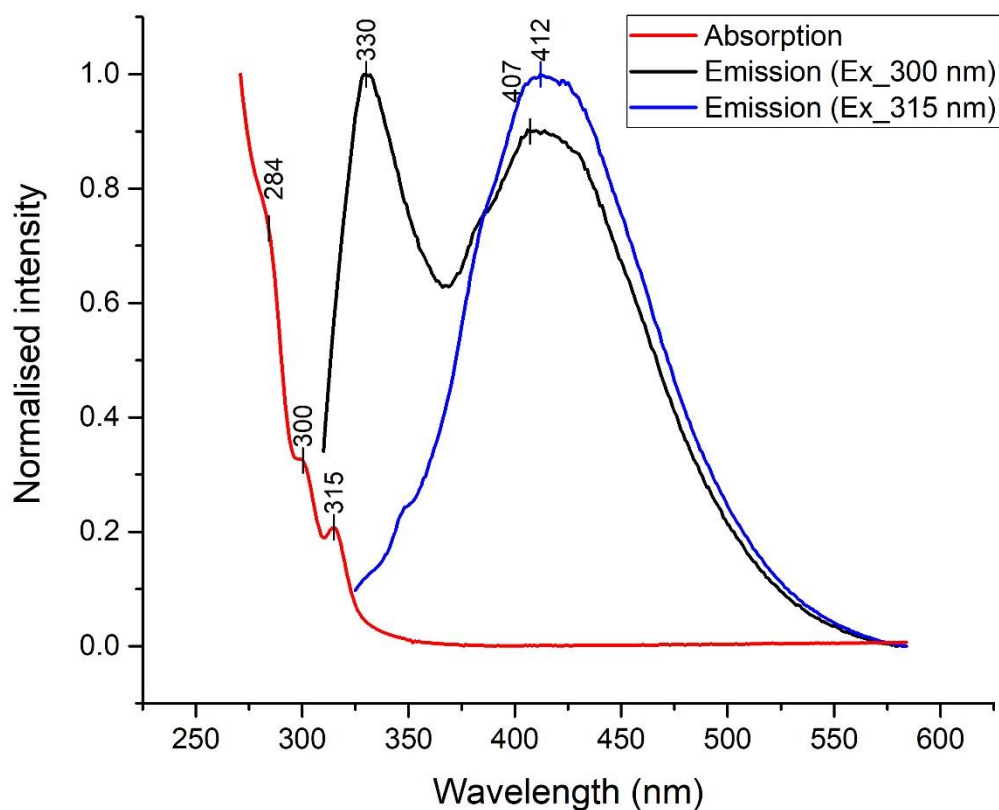


Figure 4.3: Absorption spectra of liquid linseed oil (LO) dissolved in ethanol (red) and corresponding fluorescence spectra, at an excitation wavelength (λ_{ex}) 300 nm (black) and λ_{ex} 315 nm (blue), respectively.

Curing of the liquid-phase samples shifts the fluorescence from a weak ultraviolet emission (330 and ~410 nm) to a strong blue-green fluorescence in the solid film (Figure 4.2). Bathochromic shifts (shifts to longer wavelengths) of such magnitude (50 to 100 nm) are not uncommon and are often induced through changes in solvent polarity or hydrogen bonding [4]. Drying oils are cured through an auto-

oxidation process which results in a change from a nonpolar liquid oil to a polar polymer network [1]. To determine whether the bathochromic shift is a result of a polarity change, the Lippert equation can be used [4]. The equation assumes that no external factors interact with the fluorophore; additional interactions, such as hydrogen bonding or the formation of charge-transfer states, can be detected as deviations from this generalised state. In this case, applying the Lippert equation revealed no trend, indicating that the bathochromic shift is not a result of polarity changes (Addendum A, Figure A1). Interestingly, the intensity of the two fluorescent peaks from the liquid samples is found to be solvent-dependent. Polar solvents result in both peaks having similar fluorescence intensities, whereas nonpolar solvents halve the intensity of the first peak (330 nm) while the second peak (410 nm) remains at a reasonably constant intensity (Addendum A, Figure A2).

The solvent-extractable components of the cured LO were analysed. The cured linseed oil film does not fully dissolve, regardless of the polarity of solvent used. The following solvents were used to dissolve LO: ethanol, methanol, chloroform, DMSO, water, hexane, and a chloroform-methanol-water (1:2:1) mixture. Ethanol yields the largest fluorescent intensity, confirming literature reports of it being the most efficient solvent for extracting compounds from LO [6]. The extracts (derived from Soxhlet- and ultrasonic-extractions) showed a single absorption peak (315 nm) which corresponds to that of the liquid oil, with the absence of the absorption peak at 300 nm. The yellow extract was found to be stable, with no noticeable colour changes having occurred after a month. The fluorescence of the extract was tested directly after extraction, as well as a month later, to determine whether any degradation or instability had occurred, but was found to have remained stable at 418 nm.

The fluorescence peak of the extract at 418 nm corresponds to liquid LO and not its solid phase (Table 4.1). The remaining solid film remained strongly fluorescent under UV light, and showed no change in fluorescence emission. However, the film was severely cracked and could not be used for further absorption studies.

Table 4.1: Shifts in absorption and emission bands of the liquid LO sample, cured film, ethanol extract and the oil film after ethanol extraction, as well as the two purified HPLC fractions in methanol from the ethanol extract.

	Absorption band maximum; λ_{ex} (nm)	Emission band maximum; λ_{em} (nm)	Stokes shift; Δ (nm)
Liquid	207	-	-
	236	-	-
	283	-	-
	300	329, 412	29, 112
	315	412	97
Cured oil film	300	445 → 550*	145 → 250*
Ethanol extract from cured oil	318	418	100
Cured oil film after ethanol extraction	-	445	-
Fraction 1	232	-	-
	275	315	40
Fraction 2	275	315	40

* Fluorescence of cured oil changes upon ageing; discussed in Section 3.2.

4.1.2 Chromatography analysis

The ethanol extract of the cured LO oil was fractionated using high performance liquid chromatography (HPLC) coupled to a photodiode array detector (PDA) to identify the most optically active fractions. The chromatograms were monitored using a range of absorption wavelengths, as no peaks were seen using 315 nm. Interestingly, only 280 nm showed peaks on the chromatogram. For both the liquid and cured oil extracts, two fractions were collected corresponding to the detection of two large absorption peaks (Figure 4.4), at 12.8 min (fraction 1) and 13.2 min (fraction 2) respectively.

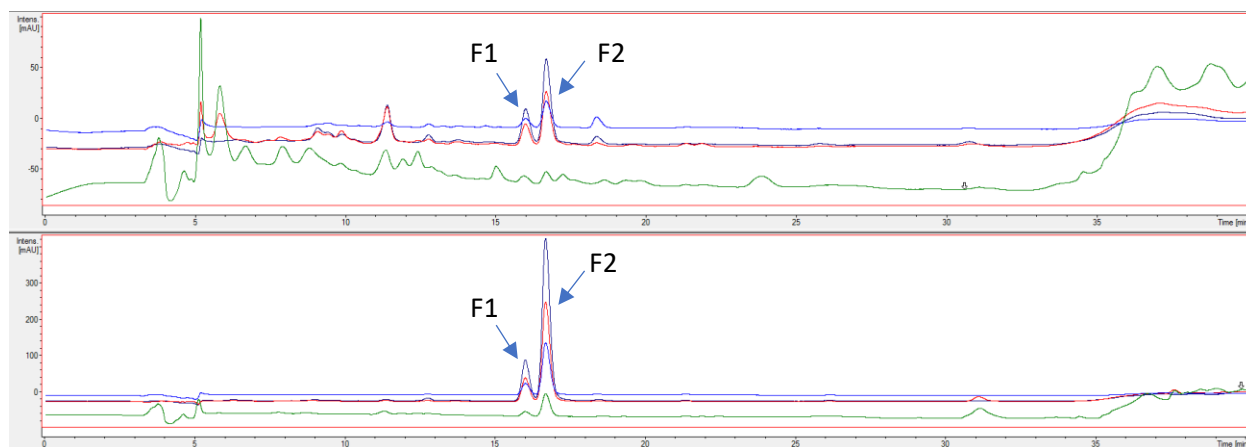


Figure 4.4: UV chromatograms of methanol extracts of cured LO film (top) and liquid LO (below) at different wavelengths: 240 nm – green; 260 nm – red; 280 nm – blue; 300 nm – light blue.

Both fraction 1 and 2 have the same strong absorption peak at 275 nm, while fraction 1 has an additional peak at 232 nm (Figure 4.5 and Table 4.1). The fluorescence emission of the two fractions are both at 315 nm (λ_{ex} 275 nm; Δ 40 nm), which does not correspond to that of the liquid or cured oil (Table 4.1). This suggests that the absorption at 315 nm is dependent on the oil matrix, and that once the compounds are isolated, they show different excitation spectra. The fractions have a smaller Stokes shift than the liquid oil and the extract of cured oil, suggesting that the isolated compounds are not the same as those that result in the fluorescence of the cured oil.

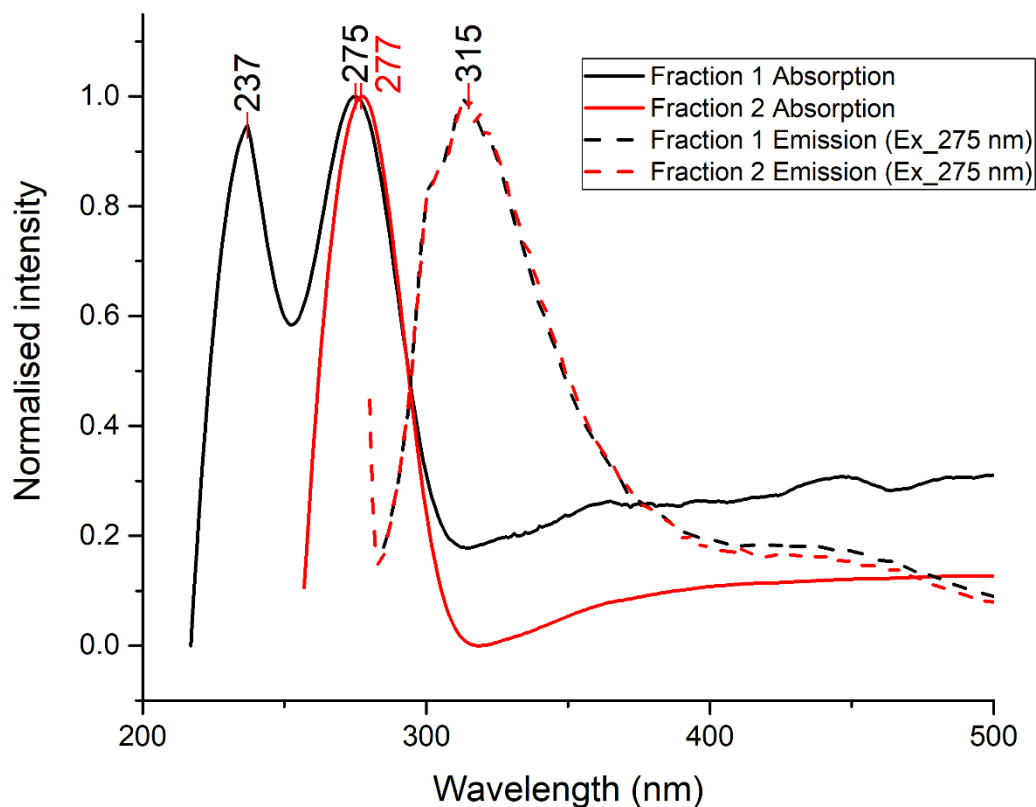


Figure 4.5: Absorption and fluorescence spectra of the most optically active fractions in linseed oil collected by HPLC-PDA-SPE.

The preceding findings indicate that the compound giving rise to the first peak in liquid oil, at λ_{ex} 300 nm; λ_{em} 330 nm, reacts as part of a polymer structure, and cannot be extracted. While the second compound, which gives rise to the second peak at λ_{ex} 315 nm; λ_{em} 410 nm, remains unreacted in the cured oil, and emits only in solution. This could be interpreted to mean that the first peak contributes significantly to the strong blue fluorescence in the solid phase, which is stabilised during the polymerization process. This is commonly seen in non-conjugated polymer dots (NCPDs) where poorly fluorescent subfluorophores (heteroatom-containing double bonds; C=O, C=N, N=O) are enhanced through chemical linking or physical immobilisation [7]. Subfluorophores have an intrinsically weak fluorescence, although it increases drastically with vibrational and rotational restriction. NCPDs have a characteristic blue fluorescence and can develop a bathochromic shift when the electron density over the subfluorophore increases [8]. This bathochromic shift in drying is seen as the oil ages (as is further explained in Section 4.1.3).

Thus, the fluorophore in drying oils is likely a carbonyl subfluorophore from the unsaturated fatty acids and triglycerides. This carbonyl does not react in the oxidative polymerisation process [9] and therefore becomes immobilised.

4.1.3 Ageing studies

Oils that were cured under UVC light (254 nm) showed immediate alligator skin formation and bleaching. The accelerated curing of oils exposed to UV light is due to a radical mechanism which is initiated by light [8, 10, 11]. After exposure to UV light, the cured samples were placed in dark drawers, which visibly accelerated the yellowing of the oils (Figure 4.6). As the samples aged, the fluorescence was measured in weekly intervals, for two months, and then monthly, for another six months. Note that the ageing methods employed in this study were extreme exposure to light and dark, which does not represent typical light conditions in museums. However, the dark experimental conditions were similar to storage rooms of museums where paintings can reside for months in the dark. The extreme experimental light conditions accelerated all ageing reactions, which allowed for a short-term monitoring of changes in fluorescence [12, 13].

With ageing, a bathochromic shift in the spectra of the oil is observed, which can be related to the yellowing effect (Figure 4.7) [14-18]. The fluorescence emission maximum is initially at 460 nm but increases exponentially to 500 – 510 nm (a green colour) upon ageing, and then reaches a plateau (Figure 4.8). An additional few months in the dark drawer was found to increase the emission further to 550 nm, imparting a yellow-green fluorescent colour to the sample (Addendum A, Figure A3). This is the general trend found for samples cured under ultraviolet light in this study. The formation of a plateau of constant emission indicates that there are two processes that cause the bathochromic shift. These findings illustrate the fact that oil paintings are continuously changing, but that there are multiple steps in the ageing process that can be initiated later in the lifetime of the drying oils.

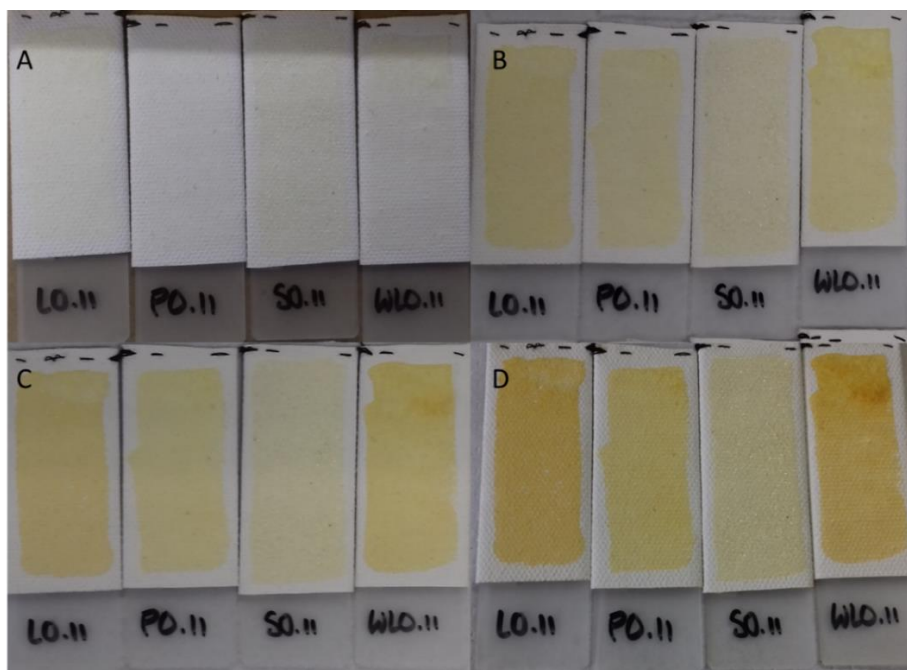


Figure 4.6: Yellowing of oils (LO, PO, SO and WLO) after 24 hours of UV-light exposure, and subsequent storage in a dark drawer. The yellowing that occurs with time during storage in a dark drawer: (A) freshly painted oil, (B) 7 days, (C) 14 days and (D) 4 months.

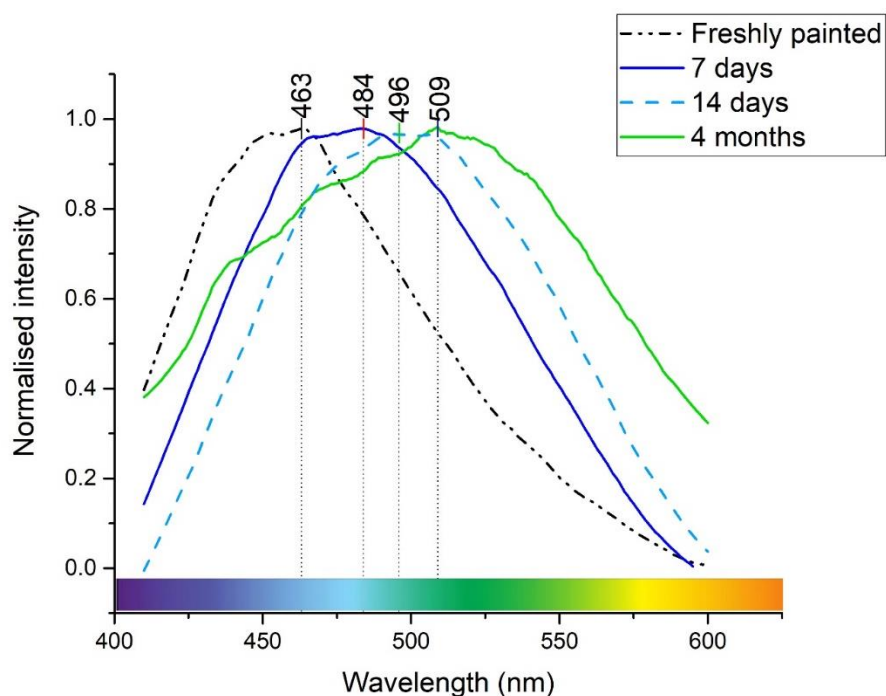


Figure 4.7: Changes in the fluorescence spectrum of aged linseed oil, exposed for 24 hr to UV light and subsequently stored in a dark drawer. The excitation wavelength for all measurements was 360 nm. The bathochromic shift (to a longer emission wavelength) is a result of yellowing as the sample ages.

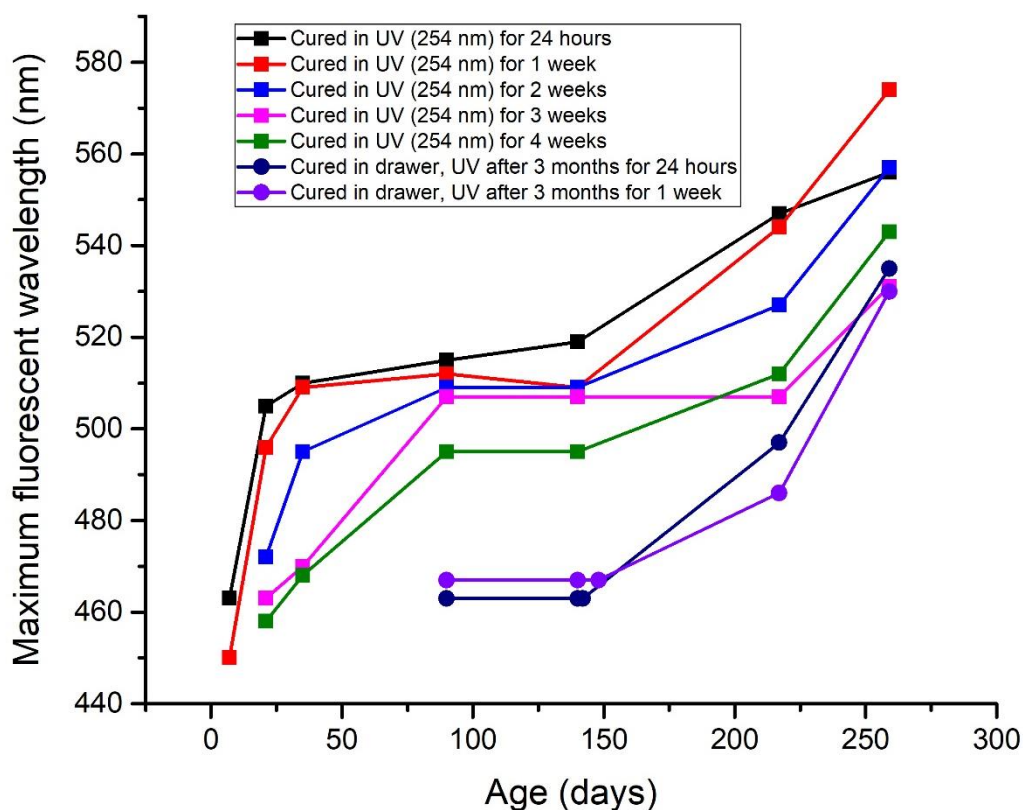


Figure 4.8: Rate of the fluorescence emission maximum changes of linseed oil after various exposure times to UV light (254 nm) and then subsequent storage in dark drawers. The excitation wavelength was 360 nm for all measurements.

Drying oils that have been cured under ambient conditions (dark drawer at 20 ± 5 °C and 50 ± 20 %RH) and then exposed to UV light after 3 months, show a different trend in their fluorescence spectra. Instead of reaching a plateau, a steadily increasing emission wavelength is observed, that passes from blue (450 – 490 nm), to green (495 – 570 nm) and to yellow (570 - 590 nm) fluorescence (Figure 4.8). Samples that were cured in sunlight did not show any yellowing, and thus no changes in fluorescence. Ageing under dark conditions causes discolouration, however, without sunlight or UV-light exposure the discolouration takes much longer to develop. It was found that natural ageing can take up to two years to develop the same kind of discolouration that UV-light causes within 2 weeks.

The curing of drying oils in an ammonia chamber appears to inhibit the drying process, as the oils appeared to be as viscous as when they were initially applied. Drying oils that were cured in the dark showed some degree of drying within the same time frame as those kept in the ammonia chamber. Interestingly, uncured samples that were in the ammonia chamber for a longer period (1 month)

showed accelerated yellowing once cured (after 4 months), while a short exposure time to ammonia while the oil was still liquid did not affect the yellowing rate (Figure 4.9). This could be because the ammonia is absorbed into the liquid oil, and once the oils are cured, the ammonia reacts with the cured product resulting in a yellow discolouration.

When the ambiently cured oils were placed (after 3 months of curing) in the ammonia chamber, the colour of the oil changed rapidly. Within 24 hrs, the saturated ammonia chamber changed all four oils to an orange-brown colour. The ammonia chamber caused the same degree of yellowing as UV-light treatment did, but within a 24-hr period, rather than a month (Figure 4.10). This supports the hypothesis that the presence of ammonia is a main cause for the acceleration of the yellowing found in oil paintings [14], and thus stresses the need to use ammonia-free cleaning products in museum environments. Previous studies have suggested the formation of a fluorescent aminoenamine in oils, which is responsible for bathochromic shifts [19, 20]. However, recent studies have shown that these isolated adducts may in fact not be fluorescent [21]. It is, nonetheless, still possible that the nitrogen-containing vapours are responsible for the colour changes through the formation of a fluorescent compound, as there have been studies that demonstrate using infrared spectroscopy that the nitrogen content in drying oils increases as the oils age [22].

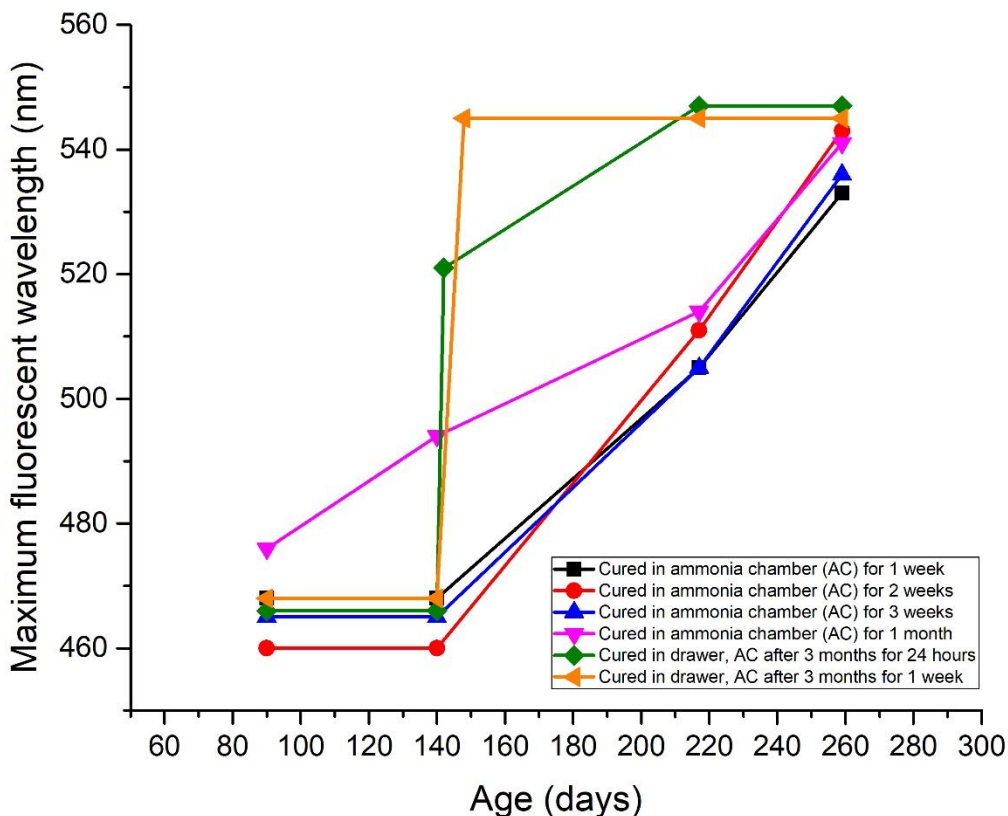


Figure 4.9: Rate of fluorescent changes of linseed oil after exposure to ammonia vapor, and subsequent storage in a dark drawer. The excitation wavelength was 360 nm for all measurements.

All stages of yellowing (identified by green and yellow fluorescence) were reversible in sunlight within 8 hrs of exposure, as is evident from the hypsochromic shift in fluorescence (Figure 4.10). The yellowing is not reversed under neither 254 nor 365 nm UV light (in a 24 hr period), indicating that a broad light spectrum is needed to reverse the yellowing effects. Artificial ageing under UV light accelerates the rate of yellowing but yellowing cannot be used as a measure of age as the painting can be bleached. A bleached painting will thereby appear younger while a freshly painted portrait might look old if stored in the dark. The yellowing cycle can be repeated numerous times and still undergo the same degree of yellowing and bleaching [23], the bleaching process is faster than the yellowing. This suggests a hysteresis curve, in which the extent of yellowing is related to the light exposure history of the painting. Previous studies that have monitored the discolouration over several years have found a repetitive nature of the yellowing and bleaching of oils [24, 25]. Even though the bleaching is cyclic, it is important

to stress that it is a photodegradation reaction and therefore affects the integrity of the paint and should be avoided. The yellowing indicates a formation of new compounds/bonds in drying oils, while the bleaching indicates the deactivation or destruction of these compounds. Based on the assumption that the fluorophore is a carbonyl subfluorophore, the formation of yellowing compounds causes an increase in electron density around the carbonyl which results in the bathochromic shift [7]. The destruction of these yellow compounds will then remove the electron density from the carbonyl, resulting in a hypsochromic shift.

Although all drying oils showed a similar trend in their rate of yellowing, they did not all yellow to the same extent. Linseed oil (both LO and WLO) shows the most intense colour changes, while poppy seed oil yellows less, and stand oil hardly shows any yellowing. Poppy seed oil reaches a maximum fluorescence emission at 530 nm as a result of yellowing, while stand oil remains at 510 nm (Addendum A, Figure A4-A5 for poppy seed oil and Figure A6-A7 for stand oil). WLO takes longer to cure, but once cured, yellows much more rapidly than LO, reaching its maximum fluorescence emission at 570 nm (the same as LO; Addendum A, Figure B8-B9). During the curing process of all oils, no noticeable yellowing occurred, whereas once cured, the rate of change in yellowing and fluorescence were a result of the ageing mechanism employed.

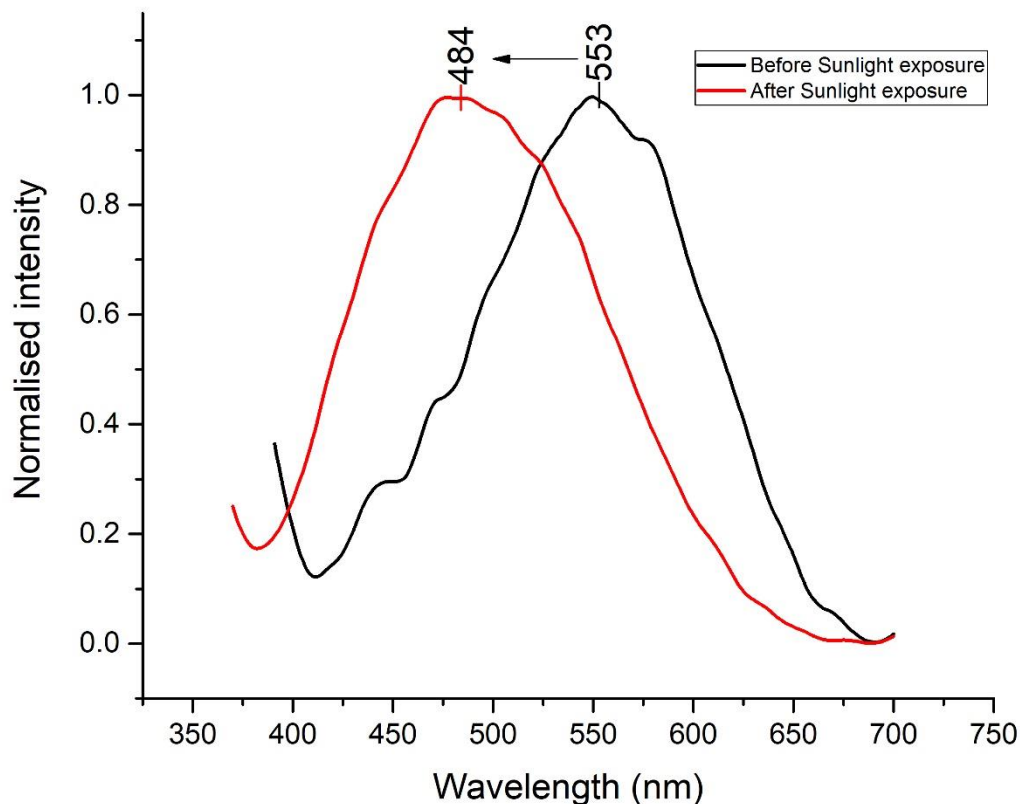


Figure 4.10: Fluorescence spectra of bleached yellowed linseed oil, after 8 hr exposure to sunlight. The excitation wavelength was 360 nm for all measurements.

The two-step process in fluorescence development was also observed in the colour changes, whereby the first incline lead to a yellow (Figure 4.6a-d) and the second to a brown discolouration (Addendum A, Figure A3). The brown discolouration became evidently visible with the discolouration from ammonia vapour, but occurs over several months in all samples. A shorter wavelength fluorescence (blue, 460 nm) indicates a yellow discolouration, while a longer wavelength (green or yellow, 500-550 nm) indicates that the oil has started to turn brown in colour. Although these observed changes were drastic, they are not unknown- paintings degrade over time [26, 27], which leads to colour changes. These colour changes can be a result of varnish discolouration [28], pigment degradation [29-31], or binder discolouration [27, 32, 33]. Pigments are commonly used for colour reconstructions, as pigment degradation (which leads to colour changes) is often irreversible [34]. Varnish is also known to be a major factor in the discolouration of paintings due to its yellowing tendencies and the formation of

micro-cracks which turn the varnish a milky colour [35]. This can be corrected by having a conservator remove the varnish layer. However, the process to determine the original colour of the binding medium is not as easily achieved, due to the cyclic nature of the discolouration. Some binding media have a yellow colour when originally painted, this does not affect the colour of the painting other than that of the white coloured paints. Determining the original colour of the binding medium will help to establish whether the binder discolouration is significant in the colour reconstruction process.

Drying oils are found to bleach in light, whereas dark conditions accelerate discolouration. As there is no measure of the amount of 'darkness' a painting receives, the measure of the discolouration of binder is often misinterpreted. By relating the discolouration of drying oils to the fluorescence, the discolouration of drying oils can be accurately calculated regardless of the age of the painting or the light conditions to which it has been exposed.

4.2 Fluorescence study of pigments

4.2.1 Characterisation of the pigments

Pigments can be classified using a specific number from the colour index [36], that identifies them based on their chemical composition, lightfastness and chemical stability. By classifying pigments according to their chemical composition, the confusion that arises from the existence of different manufacturer trade names for the same pigment, is avoided. The pigments purchased for this study have not been classified according to the colour index, and therefore could be any range of chemical compounds which provide the specific colour. Therefore, characterisation studies were required to confirm the chemical nature of these pigments and to subsequently determine their fluorescent properties.

Characterisation was achieved using X-ray powder diffraction (PXRD), X-ray fluorescence (XRF) and Fourier transform infrared spectroscopy (FTIR). In some cases, the pigments could not be classified using these techniques, and were then analysed using ultra high-performance liquid chromatography (UPLC) coupled to a quadrupole time-of-flight mass spectrometer (Q-TOF MS).

4.2.1.1 Lamp black (LB)

Lamp black is a general name given to black pigments of carbon soot material, collected from an open flame by placing an object above the flame to collect the soot material [37]. Lamp black analysed by PXRD spectroscopy shows a single peak in the powder diffraction pattern at $16.71\ 2\theta$ (Figure 4.11). This peak corresponds to pure carbon (from the ICDD database) confirming that lamp black is a carbon soot material. The XRF spectrum showed no significant peaks (Appendix B, Figure B1-B2) and the FTIR spectrum showed very weak signals of large amorphous nature (Figure 4.12). This confirms that lamp black is, as the name suggests, a carbon-based pigment with no chemical characteristics that are predicted to fluoresce. The FTIR peak at $1738\ \text{cm}^{-1}$ is indicative of a carbonyl bond, however carbonyl bonds are generally strongly absorbent [38]. Therefore, the weak absorption indicates that the carbonyl is likely not part of the main structure of the soot but may arise from adsorbed compounds derived from the combustion process that contain carbonyl bonds [39]. The peaks in the FTIR spectrum can be attributed to impurities within the pigment. The carbon structure could closely resemble that of graphite, where the large surface area allows for the absorption of chemical species from the air [39], which results in the amorphous peaks seen in the PXRD and FTIR spectra.

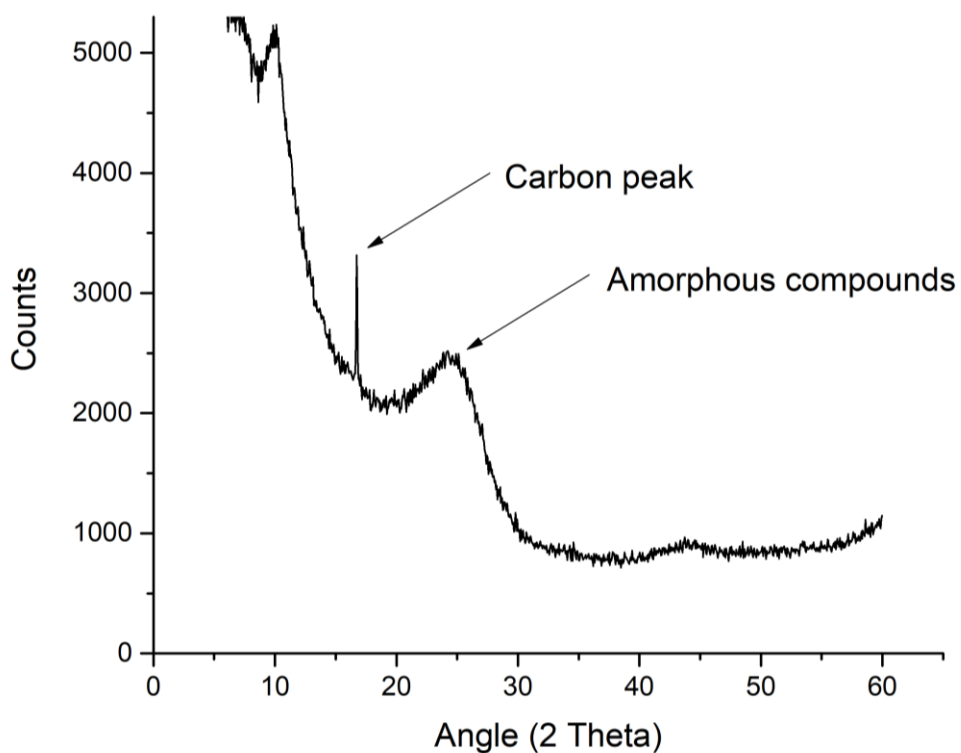


Figure 4.11: Powder X-ray diffraction pattern of lamp black pigment.

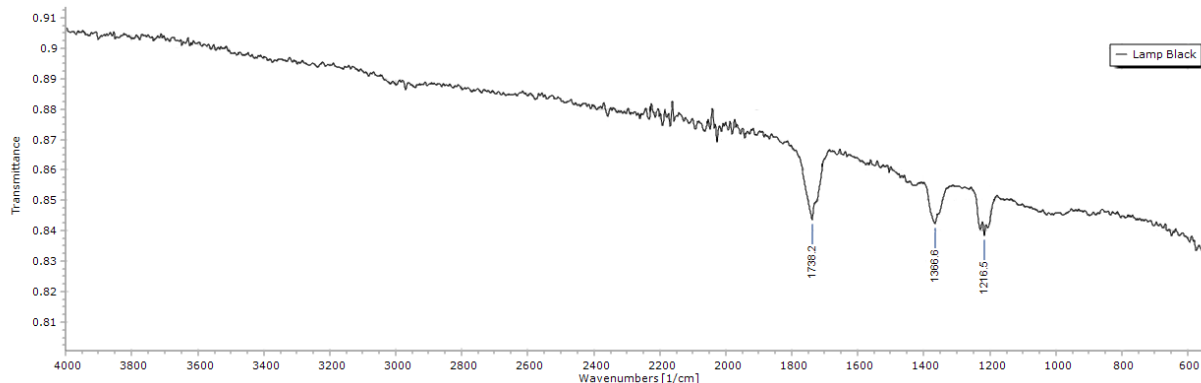


Figure 4.12: FTIR-ATR spectrum of the lamp black pigment. The spectrum was obtained from 4000 cm^{-1} to 400 cm^{-1} but did not show any peaks at higher frequencies ($4000 - 2500\text{ cm}^{-1}$).

4.2.1.2 Oriental blue (OB)

The PXRD pattern of oriental blue was perfectly matched on the ICDD database and was confirmed to be pigment blue 29: Ultramarine, $\text{Na}_7\text{Al}_6\text{Si}_6\text{O}_{24}\text{S}_3$ (Figure 4.13). Oriental blue is often a trade name for ultramarine mixed with Prussian blue. The ultramarine is typically identified by PXRD, and the Prussian blue through a characteristic FTIR peak at 2085 cm^{-1} . This characteristic FTIR peak was not present in this case (Addendum B, Figure B7), confirming that the pigment is ultramarine. Ultramarine is a pigment which is not known to fluoresce [37, 40], which was experimentally confirmed (Section 4.2.2).

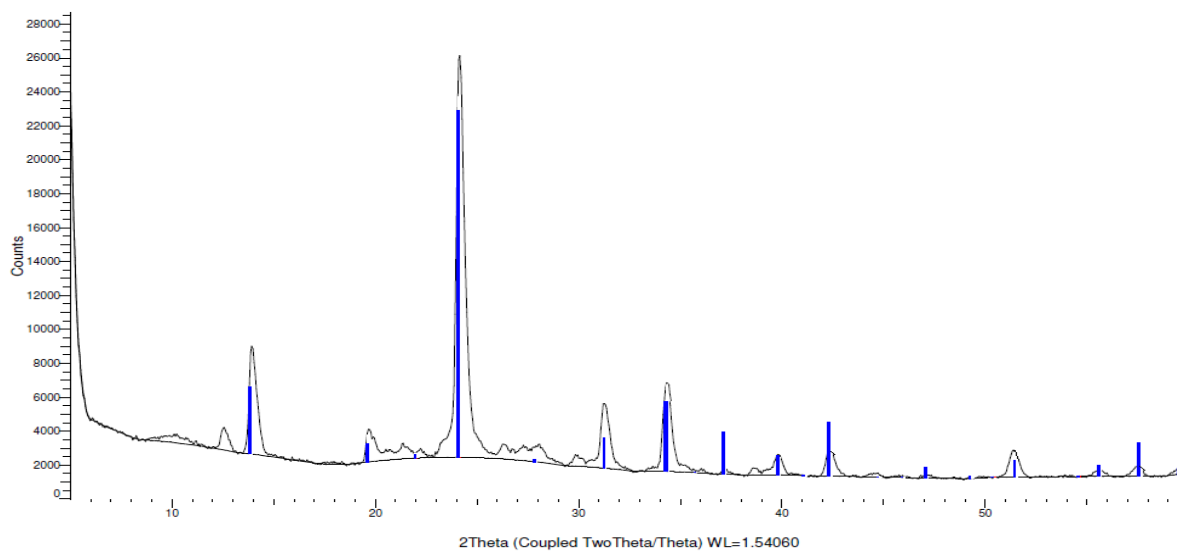


Figure 4.13: Experimental PXRD pattern of oriental blue pigment sample (black line), where the overlaid blue lines indicate 2 theta values for ultramarine (pigment blue 29) from the ICDD database.

4.2.1.3 Phthalo blue (PB)

Phthalocyanine (phthalo) blue's chemical structure contains four isoindole units connected via nitrogen bridges. Phthalo blue is a metal containing phthalocyanine where the metal is copper [41]. The phthalocyanine structure has several reactive sites on the benzene rings which can bond to several different substituents, which affects the colour; for example, a phthalo green contains chlorine substituents. The four nitrogen atoms in the free base phthalocyanine can co-ordinate to various metals which will also affect the colour (Figure 4.14) [37].

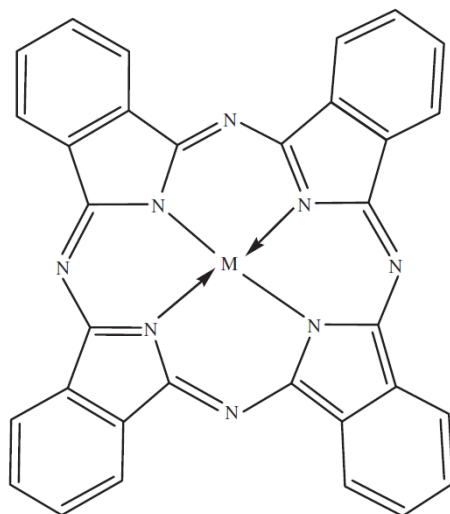


Figure 4.14: Chemical structure of phthalocyanine blue, the metal (M) being copper in the blue variety.

Powders of phthalocyanines are amorphous, and therefore the PXRD pattern provides no valuable information and has no ICDD database match. The XRF results clearly indicate the presence of copper (Figure 4.15). In the FTIR spectrum, the bands at 1620-1420 cm^{-1} correspond to the aromatic rings, and the band at 1737 cm^{-1} corresponds to the imino ($-\text{C}=\text{N}$) groups (Figure 4.16). The FTIR data corresponds to that found in literature [37, 42, 43], confirming that this sample is pigment blue 153 (PB 153).

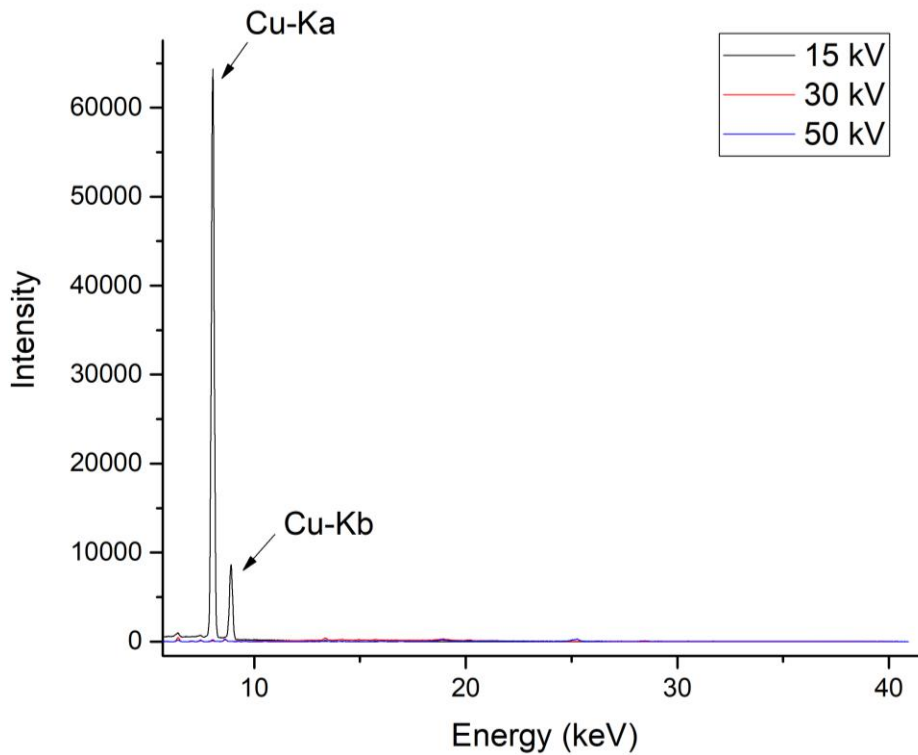


Figure 4.15: X-ray fluorescence spectrum of phthalocyanine blue, using 30 kV excitation energy with a rhodium X-ray tube.

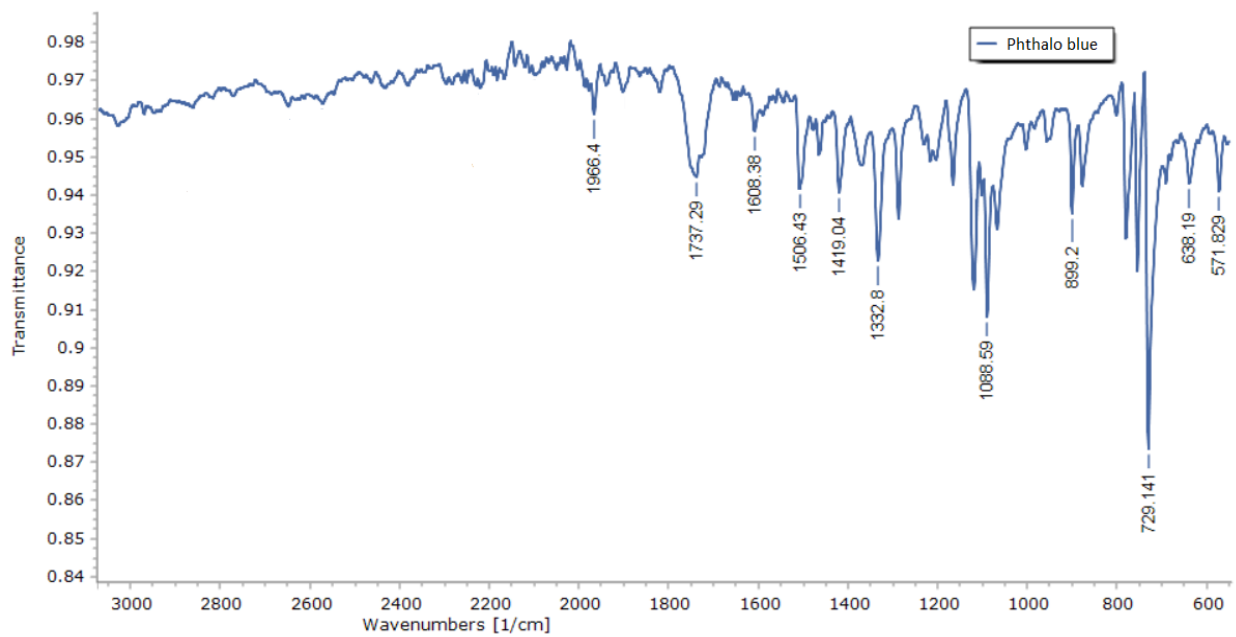


Figure 4.16: FTIR spectrum of phthalocyanine blue. The spectrum was obtained from 4000 cm^{-1} to 400 cm^{-1} but did not show any peaks at higher frequencies ($4000 - 300\text{ cm}^{-1}$).

4.2.1.4 Indian yellow (IY)

Indian yellow (IY) is the historic name of a magnesium complex of euxanthic acid (Figure 4.17a). In the past, IY was only obtainable from farms in India where cows were only fed a diet of only mango leaves. The yellow pigment was collected and precipitated from cow urine [44]. However, due to the high demand for, and price of IY, alternatives were developed. The most common yellow alternative, being pigment yellow 40 (potassium cobalt(III) nitrite) – which is sometimes listed as Indian yellow, and is also known as aureolin – and various azo yellow pigments (Figure 4.17b-d) [44]. For this study it was important to identify the correct chemical structure of the IY, as euxanthic acid fluoresces yellow at 540 nm (λ_{ex} 435 nm) [44] while aureolin fluoresces green at 550 nm (λ_{ex} 337 nm) [45].

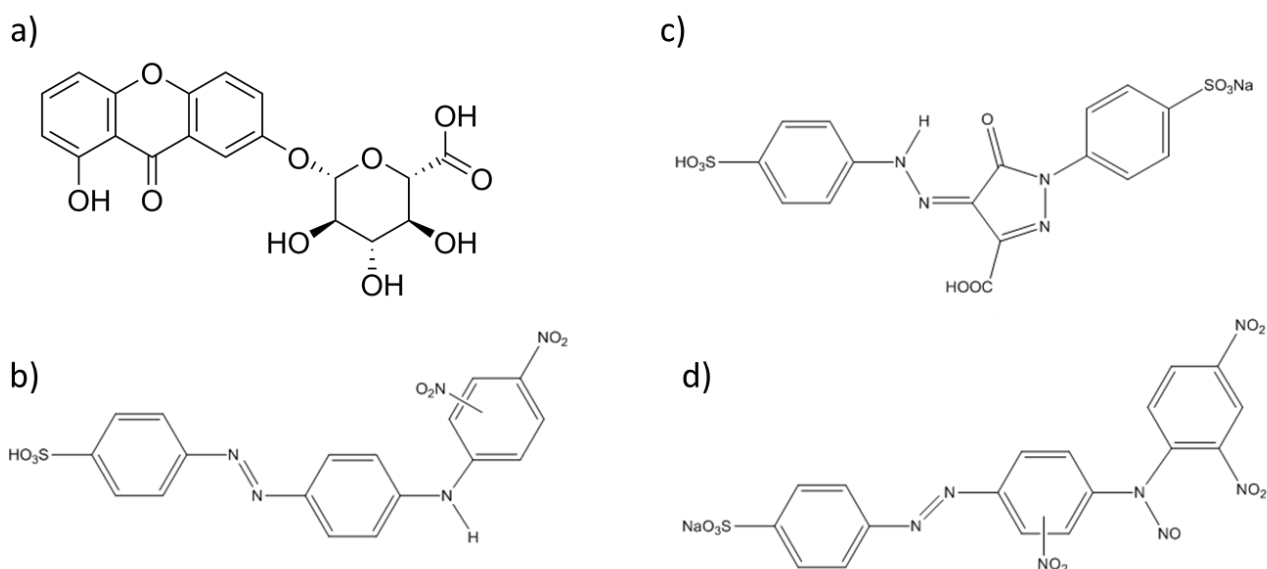


Figure 4.17: Chemical structures of Indian yellow colourants: a) euxanthic acid; b) acid orange 1; c) acid yellow 23; d) acid yellow 63.

The PXRD pattern could not be matched with any known samples in the ICDD database, this could be due to a powder mixture or amorphous powder phase (Addendum B, Figure B6). The XRF spectrum shows no metals, both graphs confirming that the sample is not a crystalline cobalt(III) nitrite (Addendum B, Figure B3). The absence of strong O-H stretching bands ($3500-3000\text{ cm}^{-1}$) in the infrared spectrum, is indicative that the sample is not an euxanthic acid (Figure 4.18). The FTIR spectrum showed a few characteristic peaks of the alternative IY colourants, namely acid orange 1, acid yellow 23 and acid yellow 63 [44]. These peaks are at 1660 cm^{-1} (indicative of an azo or imino group), 1502 cm^{-1} (aliphatic nitro groups) and 1361 cm^{-1} (sulfonates) [38]. It is not possible to distinguish between the azo yellow

alternatives from the FTIR, due to similarities in functional groups present in these compounds. Nevertheless, this fact confirms that the IY sample was neither the expected fluorescent euxanthic acid nor aureolin. The name Indian yellow, therefore refers to the commercial hue and not the chemical composition.

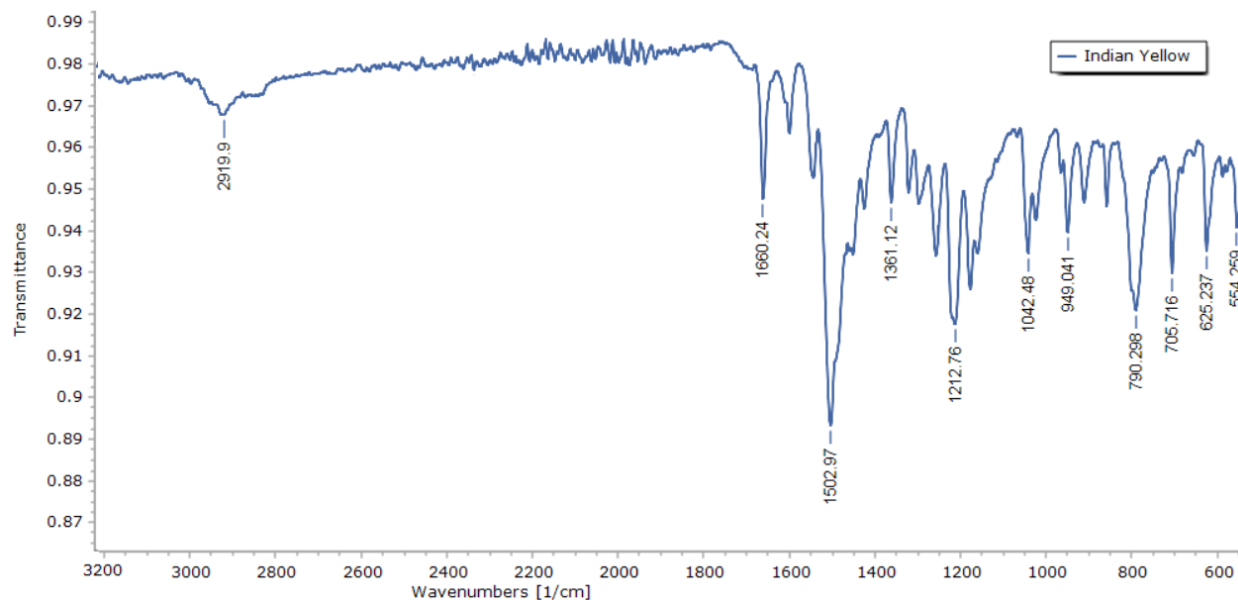


Figure 4.18: FTIR-ATR spectrum of Indian yellow. The spectrum was obtained from 4000 cm^{-1} to 400 cm^{-1} but did not show any peaks at higher frequencies ($4000 - 3200\text{ cm}^{-1}$).

4.2.1.5 Alizarin crimson (AC)

Alizarin crimson (AC) also commonly known as madder lake is a bright red pigment characterised by its orange fluorescence (λ_{em} 630 nm) [41, 46, 47]. The pigment is produced by extracting the colour compounds from madder roots (*Rubia tinctorum* L.) and precipitating them onto a mordant (alumina trihydrate) to form an aluminium lake [48]. These coloured compounds include various anthraquinone derivatives, of which there are three principle coloured compounds: alizarin (1,2-dihydroxyanthraquinone), purpurin (1,2,4-trihydroxyanthraquinone) and pseudopurpurin (1,2,4-trihydroxyquinone-3-carboxylic acid) (Figure 4.19). These three anthraquinone derivatives are responsible for the strong red colour. Alizarin has no UV-induced fluorescent properties, whereas purpurin is a fluorescent orange, and pseudopurpurin, a reddish orange, when illuminated with UV light [48].

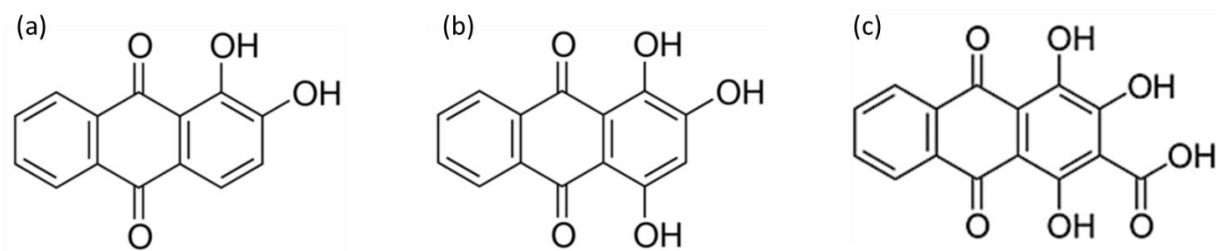


Figure 4.19: Structures of the anthraquinone derivatives responsible for the red colour in madder lake. a) alizarin; b) purpurin; c) pseudopurpurin.

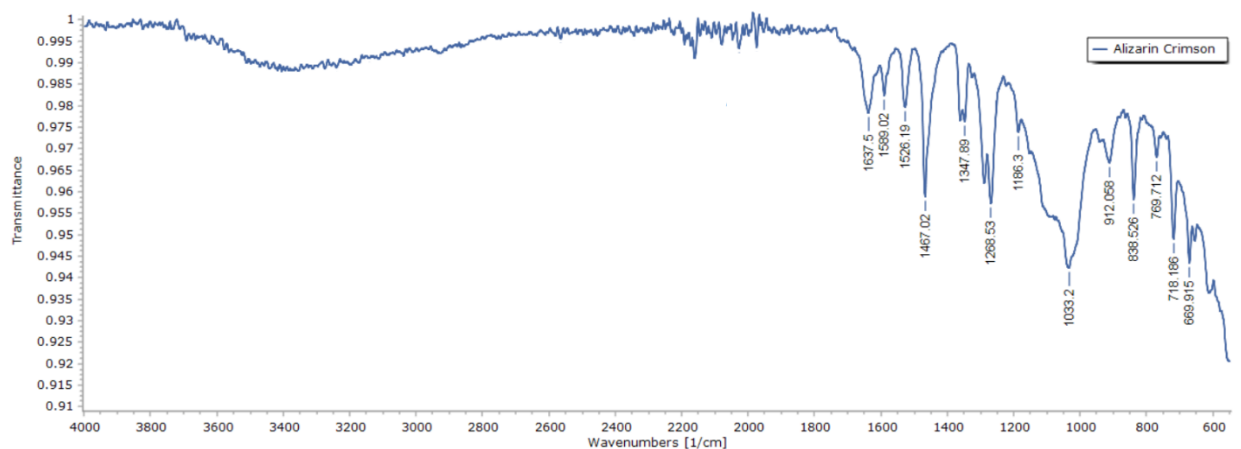


Figure 4.20: FTIR-ATR spectrum of alizarin crimson, obtained from 4000 cm^{-1} to 400 cm^{-1} .

Alizarin crimson did not show any pattern in PXRD, indicating that the sample is amorphous, while the XRF spectrum showed no metal peaks (Addendum B, Figure B4), both indicate that AC is an organic based structure. The FTIR spectrum shows several peaks below 1650 cm^{-1} , and a very broad peak around 3500 cm^{-1} . There have been several studies in which the infra-red peaks of anthraquinones are related to the relative positions of hydroxyl groups in relation to the carbonyls [48, 49]. In all of those spectra there is a strong O-H stretching band between $3200\text{-}2600\text{ cm}^{-1}$ [42, 48, 49] and not the weak peak seen in Figure 4.20. The absence of strong carbonyl stretching bands in the region of $1740\text{-}1640\text{ cm}^{-1}$ is also cause for concern, as all the distinguishing factors of anthraquinones are not present in this sample of AC (Figure 4.20). Therefore, to ensure that the alizarin crimson is indeed an anthraquinone that has fluorescence properties, comparative UPLC-QTOF studies were done.

Three reference samples of madder lake and other alizarin-named pigments from Kremer were used namely; madder lake (NR9), alizarin crimson dark (PR83) and alizarin crimson light (PR112). NR9 is a historically reproduced sample of madder lake, extracted from *Rubia tinctorum L.* and precipitated using aluminium hydroxide. PR83 is an anthraquinone synthetic dye, derived from the colourants of madder lake, purpurin and alizarin. PR112 is also a synthetic dye, derived from alizarin. Although the PR112 (23600 Alizarin crimson light sample from Kremer) shows the same colour saturation and properties as madder lake, Pronti et al. did not detect the presence of anthraquinoid compounds in it [50].

Comparative chromatography analysis confirmed that the BluePrint alizarin crimson sample was identical to PR83, a synthetic derivative of alizarin (Figure 4.21, and Addendum B, Figure B8). This PR83 from Kremer is known to fluoresce at $\lambda_{\text{ex}} 650\text{ nm}$ [50] which is an orange coloured fluorescence.

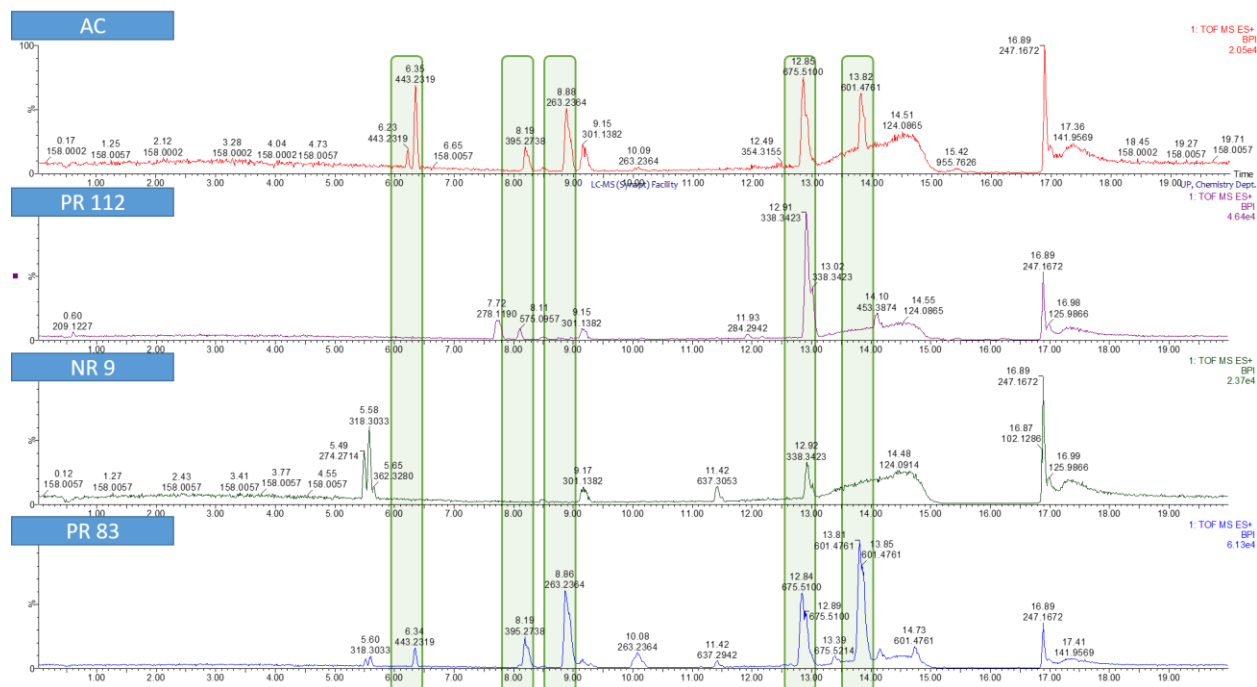


Figure 4.21: Positive ion mass chromatograms, obtained by UPLC-QTOF from red pigments dissolved in methanol. The green blocks indicate similarities between PR83 and the alizarin crimson used in this study. AC - alizarin crimson; PR 112 - pigment red 112; NR 9 - natural red 9; PR 83 - pigment red 83.

4.2.2 Fluorescence spectroscopy of pigments

The five pigments (LB, OB, PB, IY and AC) were tested for fluorescence in the absence of binders. This was achieved by dry packing in a powder sample holder. No UV fluorescence was observed under the UV light, neither at short (λ_{ex} 254 nm) nor long (λ_{ex} 365 nm) wavelengths. However, in the fluorescence spectra of the two blue pigments (OB, PB) a multi-peaked fluorescence structure between 420 and 500 nm was observed, while lamp black (LB), Indian yellow (IY) and alizarin crimson (AC) had a very weak fluorescence response (Figure 4.22 and 4.23). Both oriental and phthalo blue were confirmed to be non-fluorescent by their characterisation (Section 4.2.1.2 and 4.2.1.3), however both show a multi-peaked fluorescence in powder form. This multi-peaked structure is characteristic of dry pigment samples in which the irregular crystal phases reflect the incident light, an effect known as diffuse reflection [51].

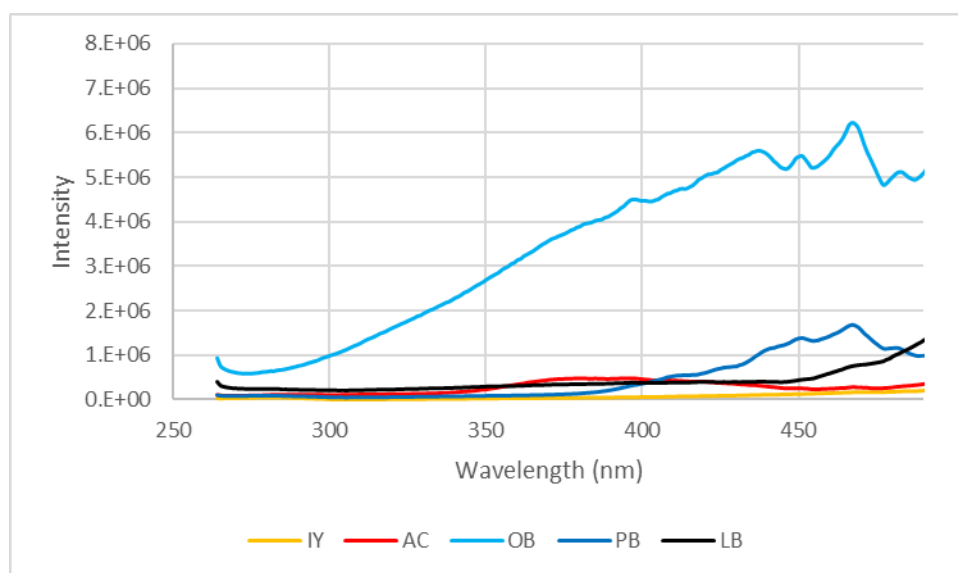


Figure 4.22: Fluorescence spectra of powder pigments under 254 nm excitation (not normalised).

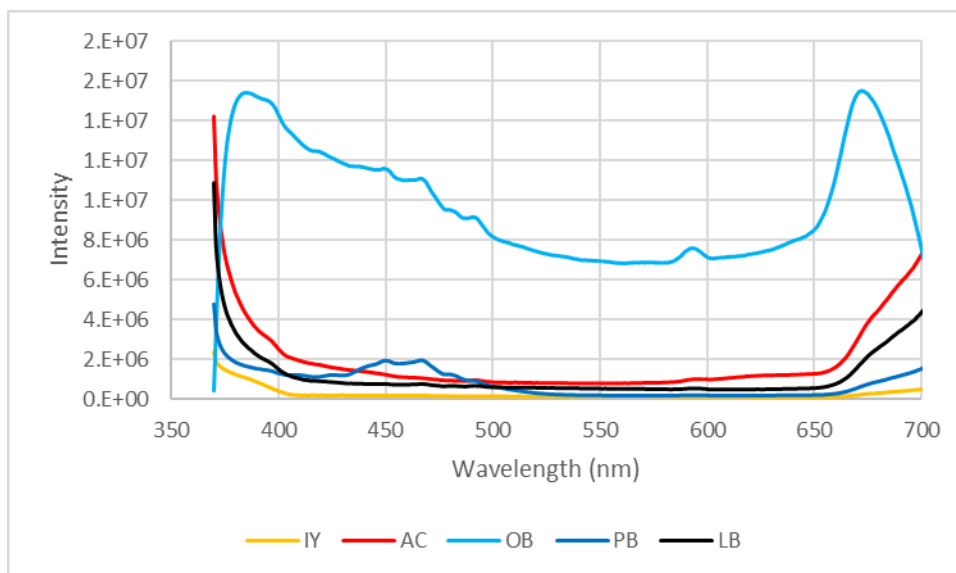


Figure 4.23: Fluorescence spectra of powder pigments under 360 nm excitation (not normalised)

Since the pigments (some of which are organic dyes), are potentially soluble in the binder, their fluorescence in solution was also measured. Hexane and ethanol were selected as nonpolar and polar environments, respectively. None of the pigments fluoresced in hexane while only alizarin crimson fluoresced orange in ethanol (Figure 4.24). No colour correction was done in these photos and thus the colours may appear slightly different to what they were. This orange colour corresponds to the known fluorescence of madder lake pigments [48]. Indian yellow does not fluoresce, once again confirming that the IY used in this study did not contain euxanthic acid [44].

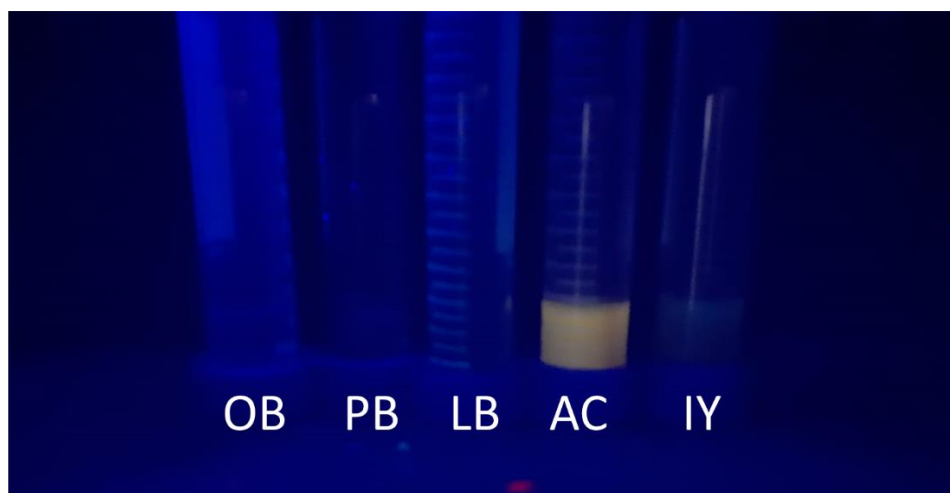


Figure 4.24: The fluorescence image of pigments in ethanol under 365 nm UV light.

The samples shown in Figure 4.24 were supersaturated in their solutions to such an extent that pigment particles were still present in solution, which could have led to colour changes in the fluorescence, due to absorption and scattering effects of the pigment [51]. Further studies were therefore performed on the alizarin crimson in order to accurately characterise the fluorescence. The pigment (AC) was dissolved in a range of solvents (Figure 4.25) and analysed with the spectrofluorometer. There was a small shift in the fluorescence peak (535 – 588 nm) which could not be related to the polarisation orientation of various solvents (Lippert equation; Addendum B, Figure B9). However, there is a distinct increase in the fluorescence intensity of the pigment solution in solvents which allowed for hydrogen bonding (Figure 4.26). Alizarin crimson in ethanol and methanol, respectively, fluoresce a bright yellow-green. However, in DMF which has a higher polarity index and forms no hydrogen bonds, AC does not fluoresce as strongly, and the yellow-green colour is hardly visible. This yellow-green coloured fluorescence does not correspond to results in literature where the fluorescence of alizarin derivatives is characteristic orange to pinkish coloured [47]. However, there is a single study previously done that identifies a green fluorescence (λ_{em} 550 nm) in aluminium-purpurin complexes [52].

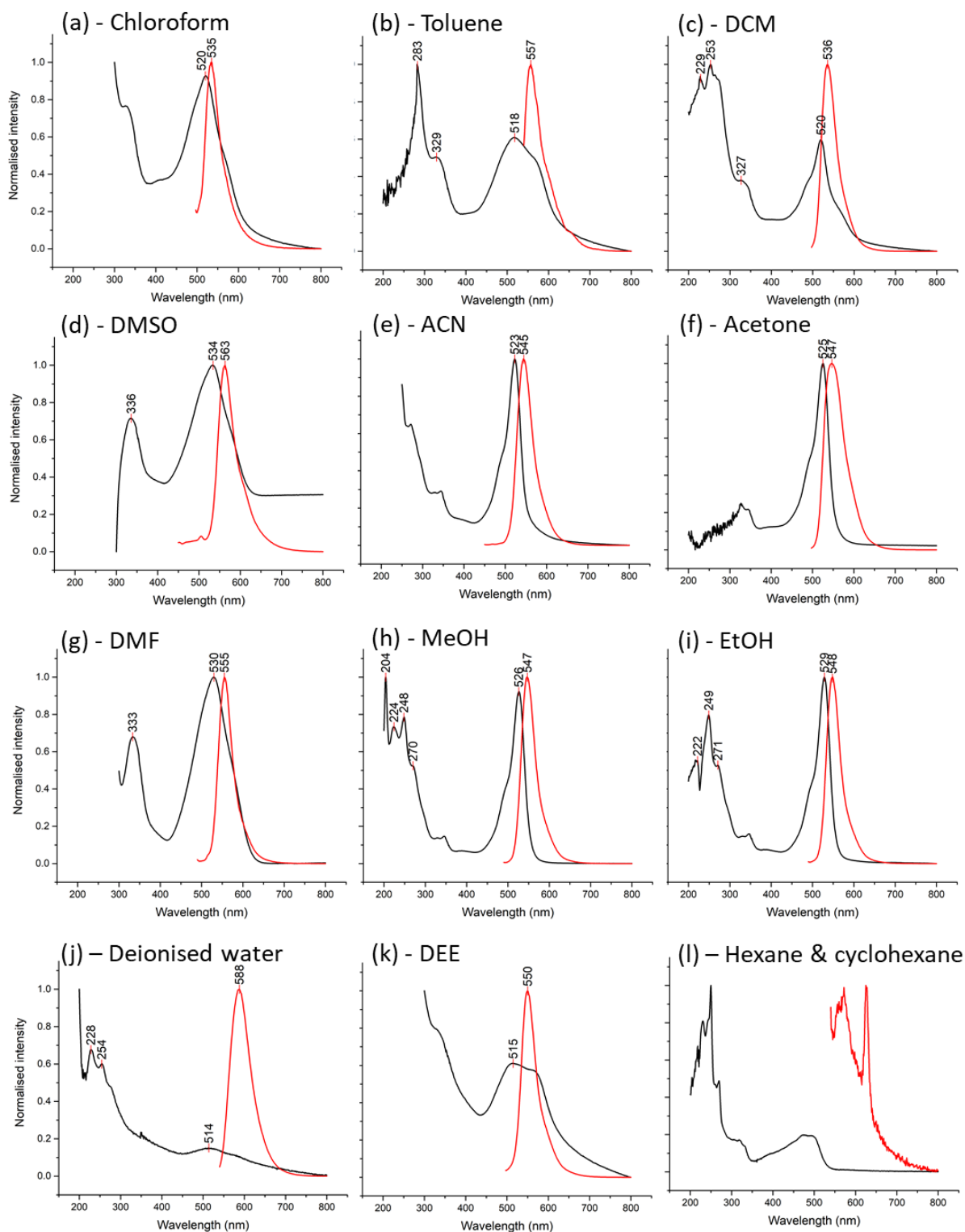


Figure 4.25: The absorption (black) and fluorescence spectra (red) of alizarin crimson in different solvents.

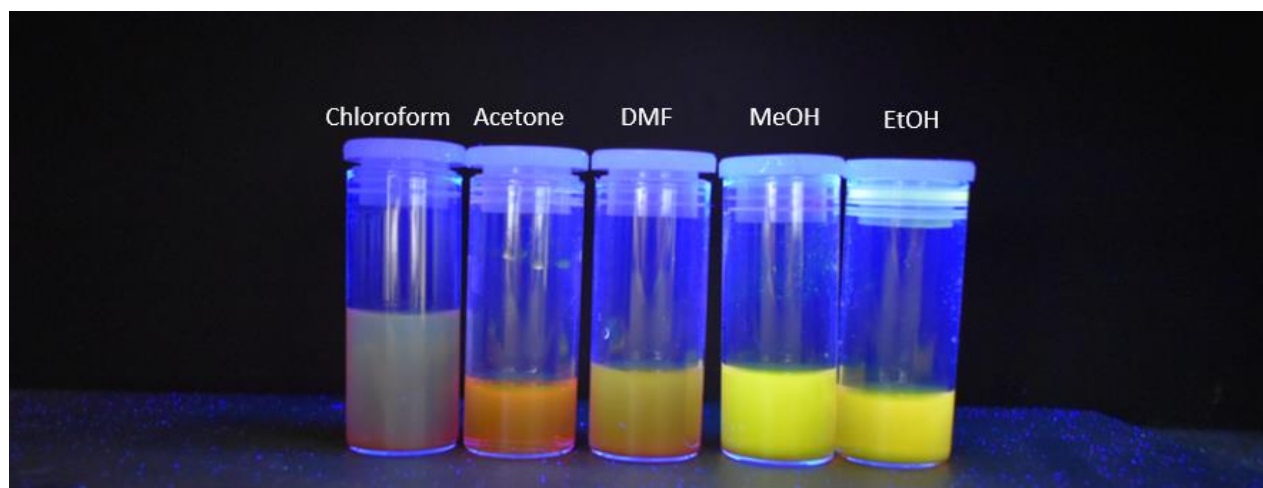


Figure 4.26: Fluorescence image of alizarin crimson (AC) in different solvents under 365 nm UV light.

4.3 Fluorescence study of binder and pigment mixtures

The pigments (LB, OB, PB, IY and AC) were mixed with drying oils, proteinaceous, polysaccharide and synthetic binders to determine if they would interact differently with different fluorophore species in each class of binders. The changes in drying oil fluorescence caused by pigments were compared to the fluorescence results obtained in Section 4.1, while all other binders were compared to spectra obtained in previous studies (Addendum H). A summary of the fluorescence of non-drying oil binders can be found in Section 2.5.

All binders, except for drying oils, were touch-dry within 24 hrs and the fluorescence spectra could be measured. The drying oil-pigment mixtures did not dry significantly faster than the pure oil samples and were touch-dry after three months allowing for the fluorescence to be measured.

4.3.1 Lamp black

The carbon-based black pigment showed no visible fluorescence under UV light (Section 4.2.2). The fluorescence spectra confirmed this, as only the egg samples (WE, EY & EW) and Klusel G showed a weak binder fluorescence peak with λ_{ex} 254 nm (Figure 4.27). This excitation wavelength is where the fluorescence is observed in egg samples, and thus the peak in these spectra is not derived from the LB pigment. From this study, all egg-based samples are slightly hypsochromic shifted when mixed with lamp black pigment, with egg white showing the smallest shift (3 nm; Figure 4.27).

LB appears to quench the fluorescence of drying oils. The fluorescence intensity of drying oils mixed with LB is less than a tenth of the intensity when pure drying oil is measured, even though the LB-drying oil mixtures were applied more thickly. This can also be observed in Figure 4.28, in which the spectra of drying oils have been normalised and smoothed using a 20-point Savitzky-Golay method in Origin Pro 2016. The spectra were still not smooth, indicating a low signal-to-noise ratio.

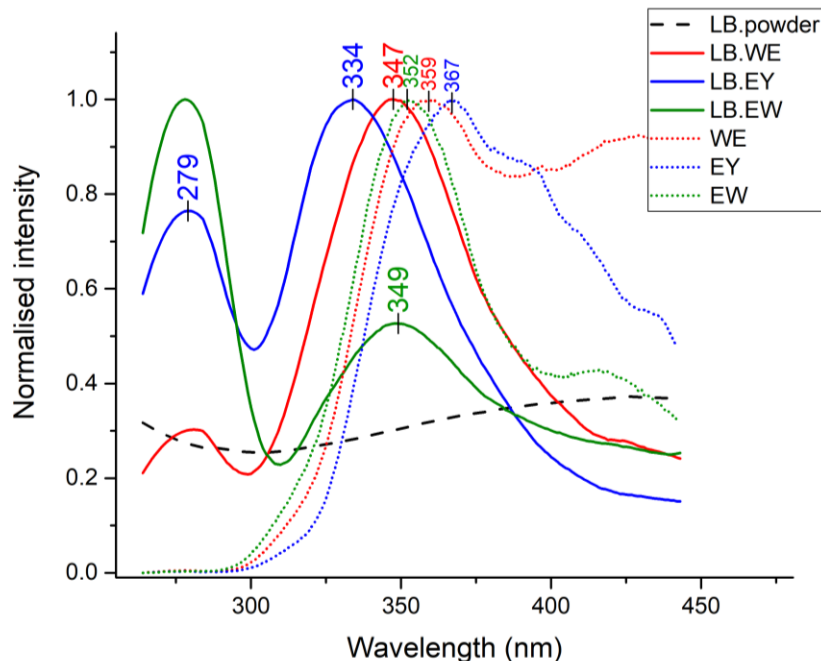


Figure 4.27: Fluorescence spectra of lamp black-binder mixtures at excitation wavelength 254 nm. The graph includes the spectra of lamp black (LB) powder (black dash), lamp black mixed with whole egg (LB.WE - solid red), egg yolk (LB.EY - solid blue) and egg white (LB.EW - solid green) respectively. For comparison, the pure binder fluorescence spectra are shown for whole egg (WE - red dotted), egg yolk (EY - blue dotted) and egg white (EW - green dotted). After 3 months of drying in the dark.

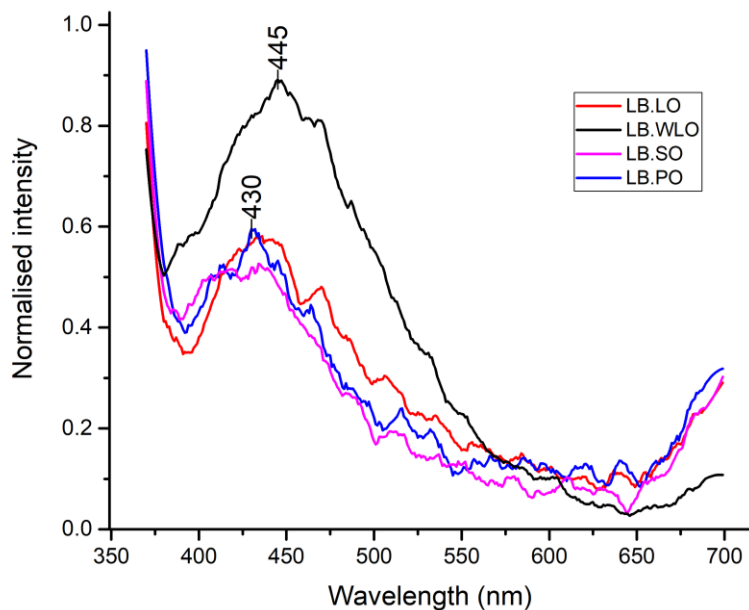


Figure 4.28: Fluorescence spectra of drying oils mixed with lamp black (LB) pigment. LO – linseed oil, PO – poppyseed oil, SO – stand oil, WLO – water-miscible linseed oil. After 3 months of drying in the dark.

4.3.2 Oriental blue

In all OB-binder mixtures excited at 254 nm (λ_{ex}) there is gaussian shaped peak at 450 nm (λ_{em}), the fluorescence images can be found in Addendum E. This falls in the region of the diffuse reflection seen in Figures 4.22 and does not correspond to the fluorescence of any of the binders. This gaussian shaped peak lacks the structured multipeaked fluorescence that is expected from diffuse reflection, indicating that the various binders coat the crystalline pigment particles which then distort the diffuse reflection.

Oriental blue does not have a diffuse reflection peak at λ_{ex} 360 nm, and rather has a fluorescence peak at 384 nm (λ_{em} , Figure 4.29). Therefore, the fluorescence at 450 nm (λ_{em}) can be ascribed to un-yellowed oil (Figure 4.29). Although the drying oils are strongly fluorescent, the fluorescence peak from OB can still be seen between 383 and 395 nm. Poppy seed oil shows a completely different spectrum than is expected and has a strong fluorescent peak at 614 nm and a smaller peak at 543 nm. The peak at 543 nm could be indicative of a severely yellow discoloured oil, while the peak at 614 nm could be resultant of new bond formations between the OB and PO. This result is strange, as the drying oils consist of the same chemical compounds in various ratios and have aged relatively uniformly in all other experiments (Section 4.1), and therefore should be verified by a future repeat experiment.

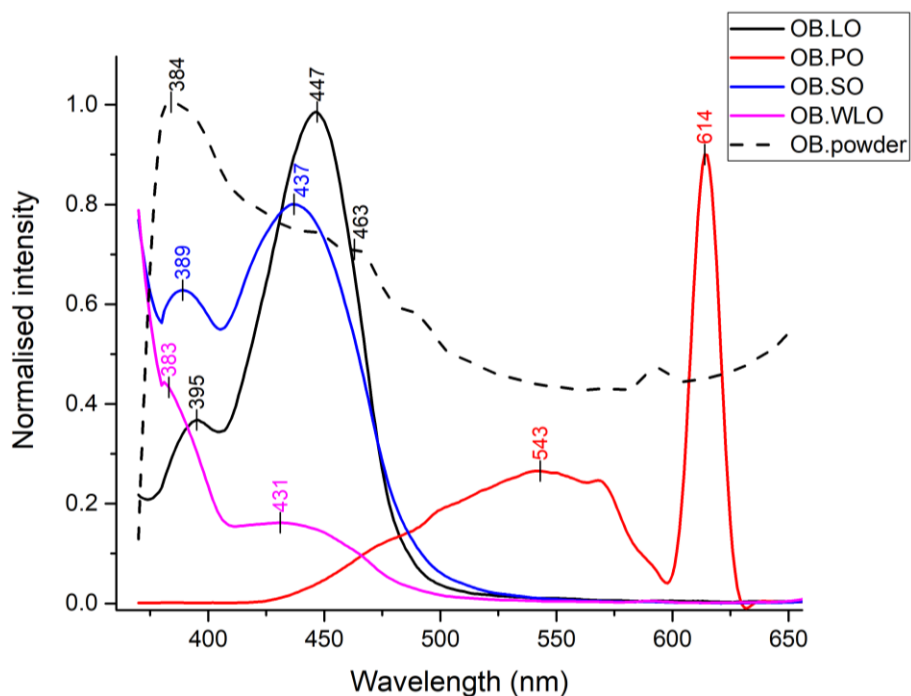


Figure 4.29: Fluorescence of oriental blue (OB) mixed with drying oils (λ_{ex} 360 nm). LO – linseed oil, PO – poppyseed oil, SO – stand oil, WLO – water-miscible linseed oil. After 3 months of drying in the dark.

4.3.3 Phthalo blue

All PB-binder mixtures excited at 254 nm had an emission peak at 280 nm. This peak is seen in all fluorescence spectra taken at λ_{ex} 254 nm (Figure 4.30 and Addendum F). As was seen in the LB-binder mixtures, the egg-based protein samples, once again, have a fluorescence intensity which is strong enough to be seen in these pigment-binder mixtures. Whole egg has the weakest fluorescence intensity, and therefore shows the reflection peaks of the powders very clearly (Figure 4.30). All egg binders have undergone a hypsochromic shift of roughly 10 nm.

The drying oils all had a peak at 450 nm, indicating the presence of young/non-yellowed oils (Figure 4.31). However, with phthalo blue there was a diffuse reflection peak around 450 nm which can cause confusion as to whether the fluorescence is resultant of the binder or the pigment. In this study, the fluorescence of oils has been characterised (Section 4.1) and it is therefore known that this particular fluorescence signal is due to the drying oils. In an *in-situ* application of fluorescence spectroscopy, the conclusion would not be as easily made. Therefore, it is always important to consider that the interference from pigment fluorescence/diffuse reflection can affect the fluorescence result.

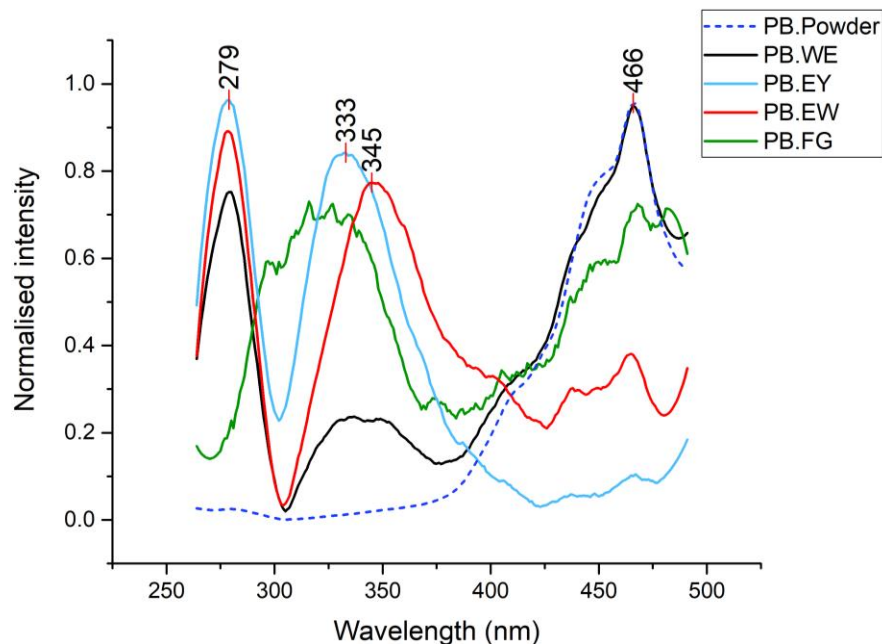


Figure 4.30: Fluorescence spectra of phthalo blue-binder mixtures at excitation wavelength 254 nm. The graph includes the spectra of phthalo blue (PB) powder (blue dash), phthalo blue mixed with whole egg (PB.WE - solid black), egg yolk (PB.EY - solid blue) and egg white (PB.EW - solid red) respectively. After 3 months of drying in the dark.

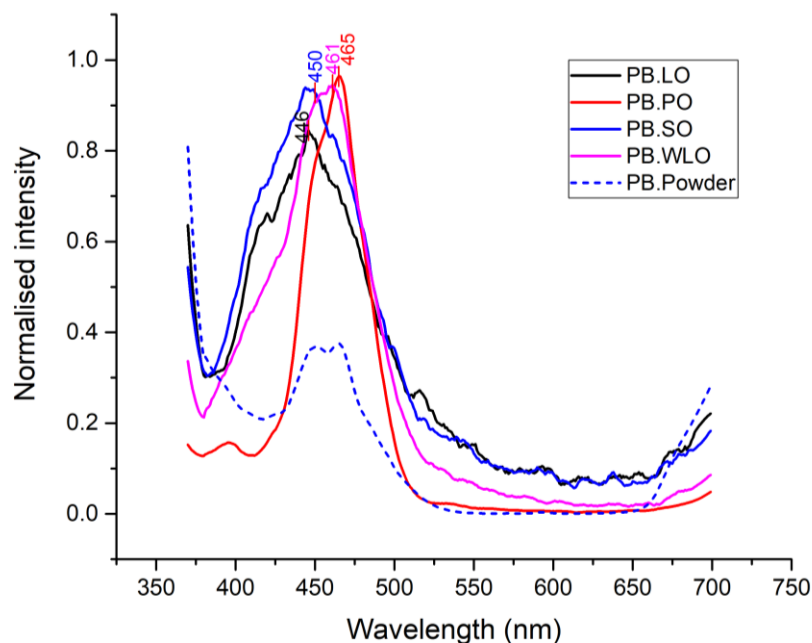


Figure 4.31: Fluorescence spectra of phthalo blue (PB) mixed with drying oils (λ_{ex} 360 nm). LO – linseed oil, PO – poppyseed oil, SO – stand oil, WLO – water-miscible linseed oil. After 3 months of drying in the dark.

4.3.4 Indian yellow

Indian yellow mixed with binders shows very similar trends to the previously discussed pigments where it is only the proteinaceous binders that show fluorescence (Figure 4.32 and Addendum G). Contrary to the previous binders, fish glue shows the strongest fluorescence signal at λ_{em} 326 nm, which is hypsochromic shifted from pure fish glue fluorescence (λ_{em} 406 nm).

Drying oils mixed with Indian yellow do not show the same trends as drying oils mixed with other pigments (Figure 4.33). Instead of these mixtures showing a single peak around 450 nm (λ_{em}), the mixtures show two peaks. One at 430 nm and another around 560 nm. Young and un-yellowed drying oils start to fluoresce at 460 nm and shift towards 560 nm as the sample yellows (Section 4.1). This indicates that the Indian yellow pigment has accelerated the ageing of drying oils and has shifted the fluorescence of the drying oils to 560 nm. The peak at 430 nm, which seems to be the un-yellowed drying oil, is not, and rather should be attributed to the pigment forming new compounds in the binder-pigment mixture.

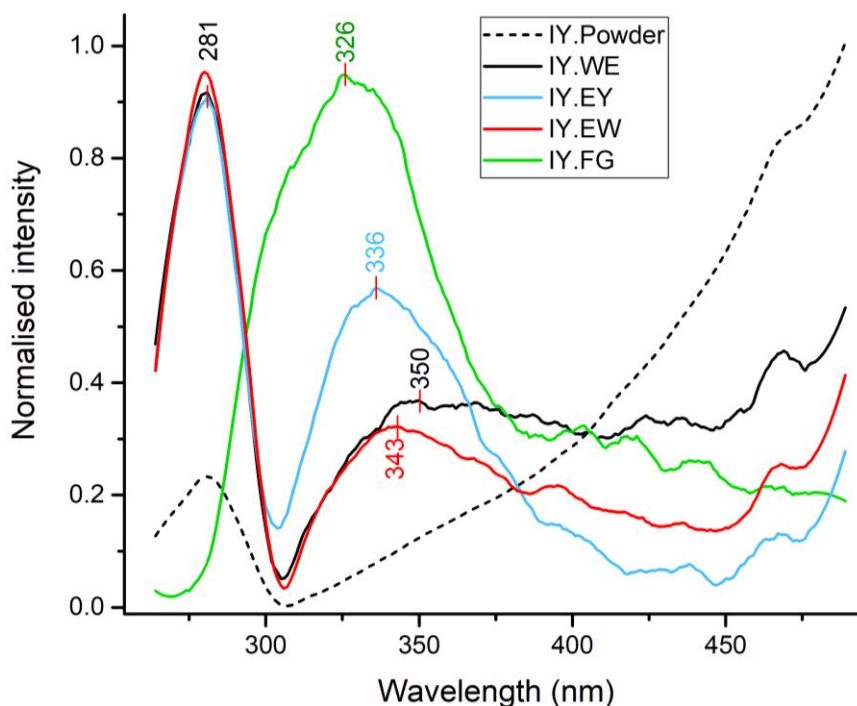


Figure 4.32: Fluorescence spectra of Indian yellow-binder mixtures at excitation wavelength 254 nm. The graph includes the spectra of Indian yellow (IY) powder (black dash), Indian yellow mixed with whole egg (IY.WE - solid black), egg yolk (IY.EY - solid blue), egg white (IY.EW - solid red) and fish glue (IY.FG - solid green) respectively. After 3 months of drying in the dark.

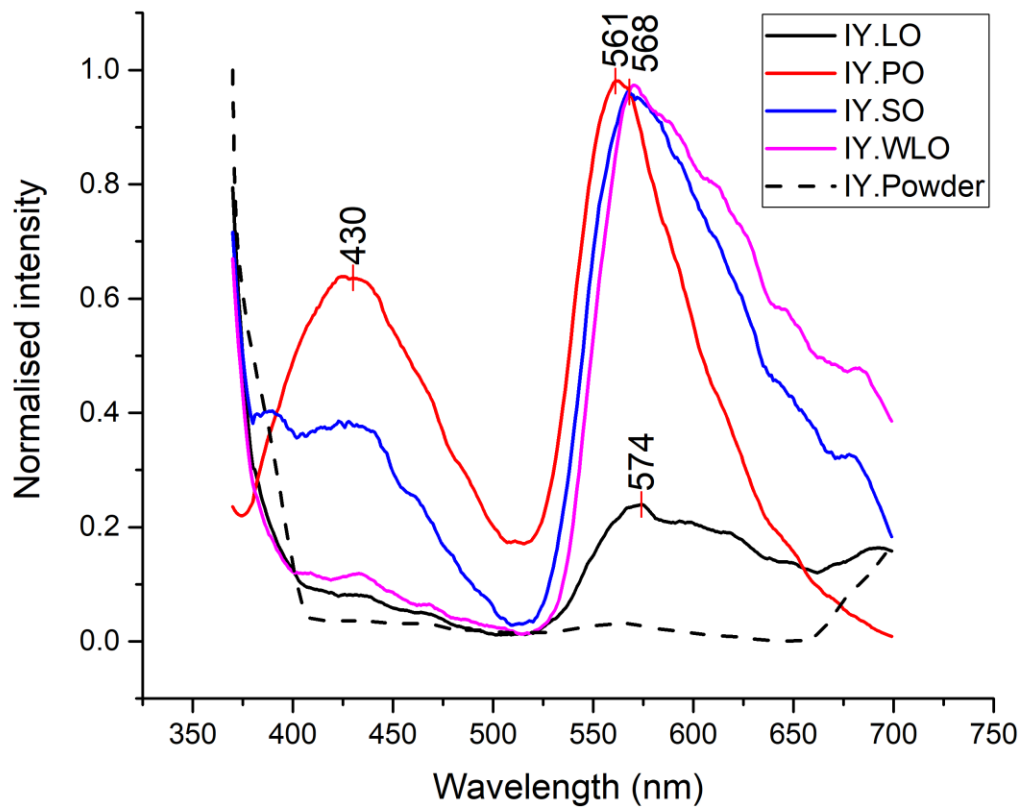


Figure 4.33: Fluorescence spectra of Indian yellow (IY) mixed with drying oils (λ_{ex} 360 nm). LO – linseed oil, PO – poppyseed oil, SO – stand oil, WLO – water-miscible linseed oil. After 3 months of drying in the dark.

4.3.5 Alizarin crimson

After preparing the alizarin crimson samples mixed with various binders, they were observed under both short (254 nm) and long (365 nm) wavelength UV light. Interestingly the alizarin crimson bound in paraloid B72 (AC.P72) and the alizarin crimson in lascoux (AC.LAS) paint were the only samples that showed fluorescence in the freshly painted samples. A green-coloured fluorescence was observed at excitation wavelength 254 nm (Figure 4.34). Interestingly, this indicates that these two binders have strong hydrogen bonding interactions with the alizarin crimson, as the combination of pigment and binder resulted in a bright green luminescence.

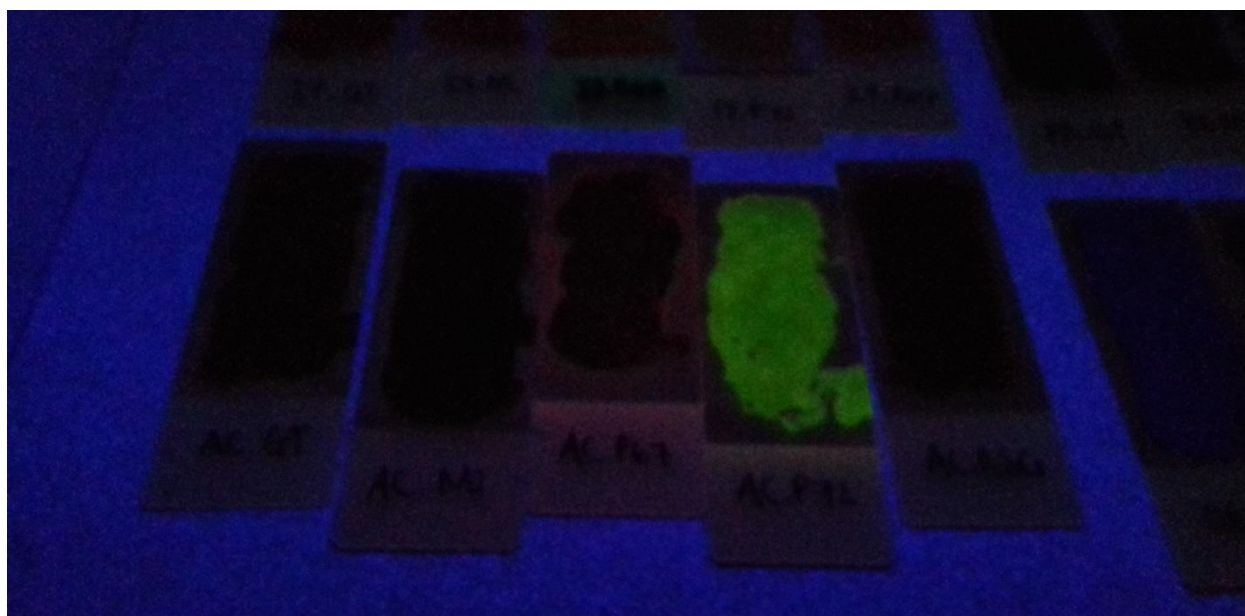


Figure 4.34: *Fluorescence image of alizarin crimson-binder samples painted onto microscope slides visualised under 254 nm ultraviolet light. The green fluorescence of alizarin crimson mixed with paraloid B72 is evident.*

These two samples (AC.P72 and AC.LAS) could not be analysed at this point, as the paint was still wet and would have contaminated the spectrofluorometer. These samples were therefore analysed with the rest of the alizarin crimson paint mixtures, 24 hrs after they were painted. At λ_{ex} 254 nm, the fluorescence of the egg-based binders was seen (similar to all other pigment-binder mixtures). However, the green fluorescence (λ_{em} ~550 nm) that was expected from Figure 4.34 was not observed, as it was masked by the Raman scattering peak.

The Raman scattering peak is an instrumental effect which occurs at double the excitation wavelength. This occurs as the excitation wavelength enters the detector, and gets scattered within the photodiode array detector, which results in the incident light being superimposed and detected at twice the wavelength of the incident light [53]. As the green fluorescence was visibly seen at 254 nm on the samples, the Raman peak in these spectra occurs at 510 nm with a consistent full-width-at-half-maximum (FWHM) of 20 nm. The Raman peak can be removed from the spectra, by placing a light filter that blocks the incident wavelength (254 nm) from entering the detector, without filtering the fluorescent light at longer wavelengths. During this study, this was attempted, however all filters that were tested (XC10, X3C5, C3C25, C3C16 and C3C17) that could block the incident light, had an intrinsic fluorescence, which caused more interference than the Raman peak. Following several more studies it was found that the incident wavelength that resulted in the clearest fluorescence representation was at 360 nm. The green fluorescence from the hydrogen bonding was not as strong, but still appeared in the spectrum (Figure 4.35).

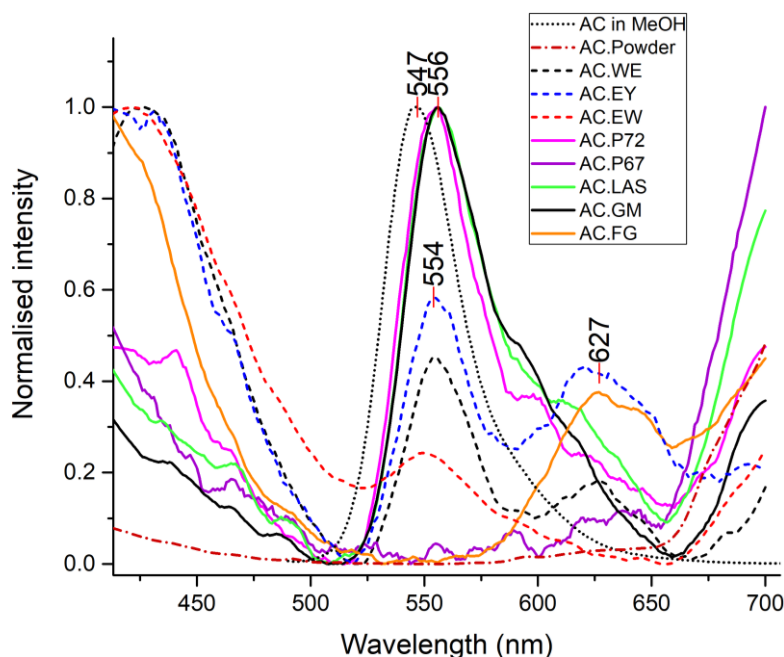


Figure 4.35: Fluorescence spectra of alizarin crimson-binder mixtures at an excitation wavelength of 360 nm. The graph includes the spectra of alizarin crimson (AC) dissolved in methanol (black dotted line); AC powder (red dot-dash line), AC mixed with whole egg (AC.WE - black dash), egg yolk (AC.EY - blue dash), egg white (AC.EW - red dash), paraloid 72 (AC.P72 - solid light pink), paraloid 67 (AC.P67 - solid dark purple), lascoux (AC.LAS - solid green), gilding milk (AC.GM - solid black) and fish glue (AC.FG - solid orange) respectively. After 3 months of drying in the dark.

The alizarin powder does not have any fluorescent peaks, however when it is dissolved in solution it has a sharp peak around 550 nm. As was previously identified, paraloid B72 and lascoux interact with the binder which result in a strong green fluorescence at 556 nm. Paraloid B67 does not develop any fluorescence even though the paraloid pellets were dissolved in methanol, which is strange as it is expected to behave like paraloid B72, which is a similar synthetic polymer.

Interestingly, gilding milk once dry also interacts to create a green fluorescence. This indicates that gilding milk (GM) has no capacity for hydrogen bonding while it is wet, but develops new bonds in the dry form, which allow for hydrogen bonding with the alizarin crimson. Similarly, the egg-based samples (WE, EW & EY) develop a green fluorescence over time, and as the binder dries. These fluorescence images can visually be observed in Addendum C.

In addition to the green fluorescence peak around 550 nm, the binders show a peak around 450 nm, which is resultant of the pure binders fluorescence, and a peak at 630 nm which is a result of a new complex formed between the pigment and binder (more clearly seen in Figure 4.36).

The drying oils mixed with alizarin crimson have three distinct fluorescence peaks. The first being around 430 nm which is the fluorescence of non-yellowed drying oils, the second (λ_{em} 550 nm) being the green fluorescence of alizarin crimson due to hydrogen bonding, and the third (λ_{em} ~630nm) being a peak corresponding to the formation of a new complex. When the AC-drying oil samples were applied, they did not show any fluorescence under UV light, however after 3 months of drying the green fluorescence slowly started appearing. This indicates that liquid drying oils do not have a significant amount of hydroxyl groups which facilitate hydrogen bonding, but rather when the drying oils become cured they develop hydroxyl groups [5] and therefore become more polar leading to the increase of green fluorescence intensity. The third peak which occurs around 630 nm is orange in colour and cannot be seen by the naked eye under UV light. This fluorescence peak corresponds to what has been reported in literature of madder lake in cultural heritage objects [46, 47, 54]. Since paintings are usually a few years old before they are analysed under UV light, it is possible that this orange fluorescence forms over time, and is a product of ageing, and therefore the fluorescence of alizarin crimson is only associated with an orange colour.

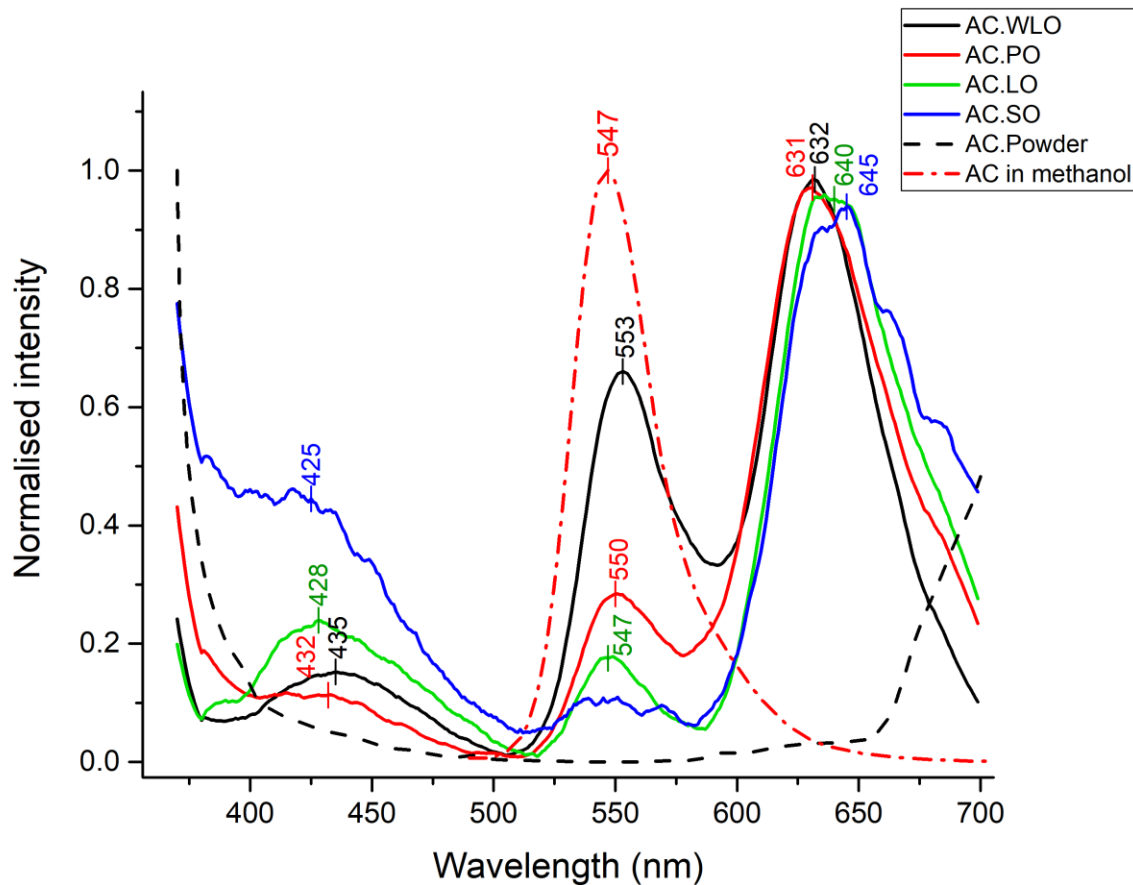


Figure 4.36: Fluorescence spectra of alizarin crimson (AC) mixed with drying oils (λ_{ex} 360 nm). LO – linseed oil, PO – poppyseed oil, SO – stand oil, WLO – water-miscible linseed oil. After 3 months of drying in the dark.

4.3.6 Comparison of pigment effects in different binders

To summarise the fluorescence effect of pigments on the fluorescence of binders, the strongly fluorescent binders, such as egg-based samples and drying oils, continue to fluoresce in pigment mixtures. The effect of pigments varies drastically, as even the pigments that do not fluoresce have different diffuse reflectance spectra.

Of the proteinaceous binders analysed, the egg-based samples have the strongest and most distinct fluorescence. This fluorescence varies from 333 to 367 nm and could be due to various matrix effects. During this study different eggs were used for the initial sample preparation in 2017 compared to the pigment binder mixtures prepared in 2019. The different eggs could have had resulted in somewhat

different matrices and chemical environments, which led to a shift in fluorescence. Alternatively, the fluorescence could be an effect of the age of the egg sample (both before and after the egg has been removed from its casing). The eggs all fluoresce around 340 nm which can be attributed to tryptophan based on literature studies [55, 56]. Interestingly, the fluorescence of crosslinked products (pentosidine or pyridinoline) or oxidation products (N-formylkynurenine and kynurenine) was not observed in the dried egg samples [55]. Additional studies are needed to identify how these chemical compounds would interact with the various pigments, and whether they are quenched by pigment interactions.

The fluorescence of synthetic binders is very weak and could not be seen in any of the pigment-binder mixtures. The fluorescence that was visible from these synthetic binders is in alizarin crimson, where the functional groups on the polymers facilitated the enhancement of the green fluorescence of the alizarin crimson through hydrogen bonding. Therefore, fluorescence studies are not advised in the identification of synthetic binders.

The drying oils, which have a very strong intrinsic fluorescence in their cured form, could be identified in all pigment-binder mixtures, after the comprehensive ageing study was completed. The alizarin crimson pigment, which has its own intrinsic fluorescence, developed a green fluorescence as the drying oils aged, and a new compound was formed in the mixture which fluoresces orange. It is still uncertain what causes this change in fluorescence of alizarin crimson.

4.4 References

1. van den Berg JD, van den Berg KJ, Boon JJ. Identification of non-cross-linked compounds in methanolic extracts of cured and aged linseed oil-based paint films using gas chromatography–mass spectrometry. *Journal of Chromatography A*. 2002;950(1-2):195-211.
2. Udell NA, Hodgkins RE, Berrie BH, Meldrum T. Physical and chemical properties of traditional and water-mixable oil paints assessed using single-sided NMR. *Microchemical Journal*. 2017;133:31-36.
3. Pavia DL, Lampman GM, KRIS G. *Introduction to spectroscopy*. 3rd Edition. Toronto: Thomson Learn Inc; 2001. ISBN 0-03-031961-7.
4. Lakowicz JR. *Principles of fluorescence spectroscopy*. New York: Plenum Press; 1983.

5. van den Berg J. *Analytical chemical studies on traditional linseed oil paints*. PhD Thesis, Univeristy of Amsterdam, Amsterdam; 2002. ISBN 90-801704-7-X.
6. Sutherland K. Solvent-extractable components of linseed oil paint films. *Studies in Conservation*. 2003;48(2):111-135.
7. Zhu S, Song Y, Shao J, Zhao X, Yang B. Non-conjugated polymer dots with crosslink-enhanced emission in the absence of fluorophore units. *Angewandte Chemie International Edition*. 2015;54(49):14626-14637.
8. Bonaduce I, Duce C, Lluveras-Tenorio A, Lee J, Ormsby B, Burnstock A, et al. Conservation issues of modern oil paintings: a molecular model on paint curing. *Accounts of Chemical Research*. 2019;52(12):3397-3406.
9. Van Den Berg JD, Van Den Berg KJ, Boon JJ, editors. Chemical changes in curing and ageing oil paints. . *ICOM Committee for Conservation Triennial meeting (12th)*, Lyon, 29 August-3 September 1999: preprints; 1999:248-253.
10. Bonaduce I, Carlyle L, Colombini MP, Duce C, Ferrari C, Ribechini E, et al. New insights into the ageing of linseed oil paint binder: a qualitative and quantitative analytical study. *PLoS One*. 2012;7(11):e49333.
11. Schaich K. Lipid Oxidation: New Perspectives on an Old Reaction. *Bailey's industrial oil and fat products*. 2020:1-72. doi: 10.1002/047167849X.bio067.pub2.
12. Schaeffer TT. *Effects of light on materials in collections: data on photoflash and related sources*. Los Angeles: The Getty Conservation Institute; 2001.
13. Feller RL. *Accelerated aging: photochemical and thermal aspects*. Los Angeles: The Getty Conservation Institute; 1995.
14. de la Rie ER. Fluorescence of paint and varnish layers (Part II). *Studies in Conservation*. 1982;27(2):65-69.
15. Pelagotti A, Pezzati L, Bevilacqua N, Vascotto V, Reillon V, Daffara C, editors. A study of UV fluorescence emission of painting materials. *Art '05–8th International Conference on Non-Destructive Investigations and Microanalysis for the Diagnostics and Conservation of the Cultural and Environmental Heritage Lecce, Italy*; 2005.

16. Comelli D, Nevin AB, Verri G, Valentini G, Cubeddu R. Time-resolved fluorescence spectroscopy and fluorescence lifetime imaging for the analysis of organic materials in wall painting replicas. In: Pique F, Verri G. *Organic Materials in Wall Paintings*. Los Angeles: The Getty Conservation Institute; 2015.
17. Larson LJ, Shin K-SK, Zink JI. Photoluminescence spectroscopy of natural resins and organic binding media of paintings. *Journal of the American Institute for Conservation*. 1991;30(1):89-104.
18. Miyoshi T. Fluorescence from oil colours, linseed oil and poppy oil under N₂ laser excitation. *Japanese Journal of Applied Physics*. 1985;24(3):371-372.
19. de la Rie ER. Fluorescence of paint and varnish layers (Part I). *Studies in Conservation*. 1982;27(1):1-7.
20. Chio K, Tappel AL. Synthesis and characterization of the fluorescent products derived from malonaldehyde and amino acids. *Biochemistry*. 1969;8(7):2821-2827.
21. Itakura K, Uchida K. Evidence that malondialdehyde-derived aminoenimine is not a fluorescent age pigment. *Chemical Research in Toxicology*. 2001;14(5):473-475.
22. O'Neill L, Rybicka S, Robey T. Yellowing of drying oil films. *Chemistry and Industry*. 1962:1796-1797.
23. Levison HW. Yellowing and bleaching of paint films. *Journal of the American Institute for Conservation*. 1985;24(2):69-76.
24. Rakoff H, Thomas F, Gast L. Reversibility of yellowing phenomenon in linseed-based paints. *Journal of Coatings Technology*. 1979;51(649):25-28.
25. Carlyle L, Binnie N, Kaminska E, Ruggles A. The yellowing/bleaching of oil paintings and oil paint samples, including the effect of oil processing, driers and mediums on the colour of lead white paint. *ICOM Committee for Conservation Triennial meeting (13th)*, Rio de Janeiro, 22-27 September 2002: preprints; 2002:328-337.
26. Berns RS, Byrns S, Casadio F, Fiedler I, Gallagher C, Imai FH, et al. Rejuvenating the color palette of Georges Seurat's *A Sunday on La Grande Jatte—1884*: A simulation. *Color Research & Application*. 2006;31(4):278-293.

27. Geldof M, Gaibor ANP, Ligterink F, Hendriks E, Kirchner E. Reconstructing Van Gogh's palette to determine the optical characteristics of his paints. *Heritage Science*. 2018;6(1:17):1-20. doi:10.1186/s40494-018-0181-6.
28. Kirchner E, van der Lans I, Ligterink F, Hendriks E, Delaney J. Digitally reconstructing van Gogh's field with irises near Arles. Part 1: varnish. *Color Research & Application*. 2018;43(2):150-157.
29. Kirchner E, van der Lans I, Ligterink F, Geldof M, Ness Proano Gaibor A, Hendriks E, et al. Digitally reconstructing van Gogh's field with irises near Arles. Part 2: pigment concentration maps. *Color Research & Application*. 2018;43(2):158-176.
30. Kirchner E, van der Lans I, Ligterink F, Geldof M, Megens L, Meedendorp T, et al. Digitally reconstructing Van Gogh's Field with Irises near Arles part 3: Determining the original colors. *Color Research & Application*. 2018;43(3):311-327.
31. Monico L, Janssens K, Miliani C, Brunetti BG, Vagnini M, Vanmeert F, et al. The degradation process of lead chromate in paintings by Vincent van Gogh studied by means of spectromicroscopic methods. 3: Synthesis, characterization and detection of different crystal forms of the chrome yellow pigment. *Analytical Chemistry*. 2013;85:851-859. Doi: 10.1021/ac302158b.
32. Mallégol J, Lemaire J, Gardette J-L. Yellowing of oil-based paints. *Studies in Conservation*. 2001:121-131.
33. Privett O, Blank M, Covell J, Lundberg W. Yellowing of oil films. *Journal of the American Oil Chemists' Society*. 1961;38(1):22-27.
34. Miliani C, Monico L, Melo MJ, Fantacci S, Angelin EM, Romani A, et al. Photochemistry of artists' dyes and pigments: towards better understanding and prevention of colour change in works of art. *Angewandte Chemie International Edition*. 2018;57(25):7324-7334.
35. Nicolaus K. *Restoration of Paintings*. Cologne: Konemann; 1999.
36. Wich E. The colour index. *Color Research & Application*. 1977;2(2):77-80.
37. Eastaugh N, Walsh V, Chaplin T, Siddall R. *Pigment compendium: A dictionary of historical pigments*. Oxford: Elsevier Butterworth-Heinemann; 2004.

38. Coates J. Interpretation of infrared spectra, a practical approach. *Encyclopedia of analytical chemistry: applications, theory and instrumentation*. 2006. doi: 10.1002/9780470027318.a5606.
39. Lazar P, Karlicky F, Jurečka P, Kocman Ms, Otyepková E, Šafářová Kr, et al. Adsorption of small organic molecules on graphene. *Journal of the American Chemical Society*. 2013;135(16):6372-6377.
40. Roy A. *Artist's pigments: a handbook of their history and characteristics, Vol. 2*. London: Archetype Publications; 1993. ISBN: 978-1-904982-75-3.
41. Smith R. *The artist's handbook*. London: Dorling Kindersley; 1990.
42. Derrick MR, Stulik D, Landry JM. *Infrared spectroscopy in conservation science*. Los Angeles: The Getty Conservation Institute; 2000.
43. Defeyt C, Vandenabeele P, Gilbert B, Van Pevenage J, Cloots R, Strivay D. Contribution to the identification of α -, β - and ϵ -copper phthalocyanine blue pigments in modern artists' paints by X-ray powder diffraction, attenuated total reflectance micro-fourier transform infrared spectroscopy and micro-Raman spectroscopy. *Journal of Raman Spectroscopy*. 2012;43(11):1772-1780.
44. Feller RL. *Artist's pigments: a handbook of their history and characteristics, Vol. 1*, London: Archetype Publications: 1986. ISBN: 978-1-904982-74-6.
45. Miyoshi T, Ikeya M, Kinoshita S, Kushida T. Laser-induced fluorescence of oil colours and its application to the identification of pigments in oil paintings. *Japanese Journal of Applied Physics*. 1982;21(7R):1032-1036.
46. Fiocco G, Rovetta T, Gulmini M, Piccirillo A, Canevari C, Licchelli M, et al. Approaches for detecting madder lake in multi-layered coating systems of historical bowed string instruments. *Coatings*. 2018;8(5)(171);1-16. doi:10.3390/coatings8050171.
47. Cosentino A. Identification of pigments by multispectral imaging; a flowchart method. *Heritage Science*. 2014;2(1):8.
48. Fitzhugh EW. *Artists' pigments: a handbook of their history and characteristics, Vol. 3*. London: Archetype Publications; 1997. ISBN: 978-1-904982-76-0.

49. Bloom H, Briggs L, Cleverley B. 33. Physical properties of anthraquinone and its derivatives. Part I. Infrared spectra. *Journal of the Chemical Society (Resumed)*. 1959:178-185.
50. Pronti L, Felici AC, Ménager M, Vieillescazes C, Piacentini M. spectral behavior of white pigment mixtures using reflectance, ultraviolet—fluorescence spectroscopy, and multispectral imaging. *Applied Spectroscopy*. 2017;71(12):2616-2625.
51. Roduner E, Forbes P, Kruger T, Kress K. *Optical Spectroscopy: Fundamentals and Advanced Applications*. New Jersey: World Scientific; 2018.
52. Claro A, Melo MJ, de Melo JSS, van den Berg KJ, Burnstock A, Montague M, et al. Identification of red colorants in van Gogh paintings and ancient Andean textiles by microspectrofluorimetry. *Journal of Cultural Heritage*. 2010;11(1):27-34.
53. Zepp RG, Sheldon WM, Moran MA. Dissolved organic fluorophores in southeastern US coastal waters: correction method for eliminating Rayleigh and Raman scattering peaks in excitation–emission matrices. *Marine Chemistry*. 2004;89(1)(4):15-36.
54. Zaffino C, Bertagna M, Guglielmi V, Dozzi MV, Bruni S. In-situ spectrofluorimetric identification of natural red dyestuffs in ancient tapestries. *Microchemical Journal*. 2017;132:77-82.
55. Nevin A, Cather S, Anglos D, Fotakis C. Analysis of protein-based binding media found in paintings using laser induced fluorescence spectroscopy. *Analytica Chimica Acta*. 2006;573:341-346.
56. Gaspard S, Oujja M, Moreno P, Méndez C, García A, Domingo C, et al. Interaction of femtosecond laser pulses with tempera paints. *Applied Surface Science*. 2008;255(5):2675-2681.

Chapter 5: Conclusion

5.1 Final remarks and conclusion

In this study, the fluorescence of drying oils was extensively investigated, and was found to be largely dependent on the physical state of the oil. Liquid oils fluoresce in the ultraviolet range, a phenomenon not visible to the naked eye. Cured oils fluoresce in the blue range, but the fluorescence shifts to green (and sometimes yellow), as the oil yellows. It is proposed that the fluorescence of drying oils is a result of the presence of subfluorophores, which are poorly fluorescent in the liquid phase, but become fluorescent once they are immobilised in a cured oil matrix. The bathochromic shift, from blue to green, observed in the spectra of the cured oils, is a result of increased rigidity in the cured oil matrix. The yellowing, which can be correlated to the fluorescence of the oil, is not a result of age, but of storage conditions, as was identified by the use of extreme experimental storage conditions in this study. Exposure to ammonia vapour rapidly increases the degree of yellowing, and therefore ammonia-based cleaning products should be avoided in museum environments, as the discolouration affects the aesthetic value of artworks. Sunlight bleaches drying oil and thus reverses the fluorescence shift associated with yellowing, while dark storage conditions promote yellowing and fluorescence changes. Although light bleaches the yellowing of drying oils, this is not advised as it may cause irreversible photodegradation of certain pigments.

The yellow discolouration of oils is not always visible when pigments are present in the drying oil, and in mixtures with non-fluorescent pigments, the fluorescence can be used to identify the degree of discolouration. The colour associated with the peak in the fluorescence spectrum provides a measure of yellowing, and could therefore potentially be used for digital colour correction of paintings. Colour corrections are a common technique used to determine the change in colour due to ageing, such that paintings can be viewed as the artist originally envisioned the painting. As fluorescence spectroscopy is non-destructive, it can be used to determine the extent of yellowing without the need for sampling, and is thus an advisable method for the monitoring of discolouration in paintings.

In addition to being stored for ageing studies, the drying oils were mixed with pigments of which only one, alizarin crimson (AC) was fluorescent. The intrinsic fluorescence intensity of the drying oils is high

enough to be visible in all paint mixtures. This confirmed the validity of using fluorescence spectroscopic measurements to identify the degree of yellowing of drying oils.

The pigments were also mixed with various binders, namely the proteinaceous, polysaccharide and synthetic binders. An extensive ageing study of the fluorescence of these binders was not performed. Instead, they were mixed with pigments and the relative change in fluorescence was compared to that of the drying oils.

In this study, the fluorescence of synthetic binders was found to be minimal to non-existent. Synthetic binders are polymeric structures that do not contain fluorophores or subfluorophores. When a synthetic binder fluoresces, it is typically caused by a heterogeneity in the polymer matrix. However, this heterogeneity occurs at random, and would not be a guaranteed feature that would help with the characterisation of synthetic binders through fluorescence spectroscopy.

The effects of pigments on the fluorescence of the various binders were diverse, as they led to diffuse reflection when the pigment was a crystallised powder. In addition, pigments led to quenching or masking of the binder's fluorescence, as well as the formation of new fluorescent species in alizarin crimson samples. Most binders were non- to poorly fluorescent, and therefore only showed diffuse reflection in fluorescence measurements. The way the binders coated the pigment particles affected the extent of the diffuse reflection from the pigment powder. The fluorescence spectra of the pigment powders showed a multi-peaked diffuse reflection, but after mixing the pigment with binders, the pigment became covered with binder and a broad single peak was observed. This was most prominent in the non-fluorescent pigment powders (oriental blue, phthalo blue, Indian yellow and lamp black).

Alizarin crimson (AC) has a green fluorescence in solutions which facilitates hydrogen bonding. In pigment-binder mixtures, only certain binders form these hydrogen bonds with AC, which produces a green fluorescence. However, in drying oils, this green fluorescence is masked by the formation of a fluorescent compound which led to an intense orange fluorescence. These results indicate that the pigments have a range of effects and cannot be summarised into a general trend.

5.2 Recommendations and future work

An extensive study of drying oils and their discolouration was performed, but since research is always developing, recommendations for future work are provided. A follow up study should be conducted in which colourimetry measurements of drying oils are done. Colourimetry makes use of the RGB (red-

green-blue) or the abc method of characterising the specific hue and colour. Unlike fluorescence spectroscopy, colourimetry is based on the principle of colour detection by eye and thus does not measure a single wavelength of fluorescence emission. The monitoring of the exact yellow colour changes in drying oils can be done with colourimetry to correlate with the fluorescence changes, which would result in a quantitative method in which the yellowing of drying oils can be monitored.

In addition to investigations into the ageing process of oils, a complete study of the fluorophores in proteinaceous samples is recommended, in order to determine whether natural and artificial ageing results in bathochromic or hypsochromic shifts in proteinaceous binders, as well as the identity of the chemical compounds in the samples which incur these changes. In particular, it could be determined whether egg samples from different farms produce different fluorescence spectra, due to the different chemical matrix of each egg, arising from differences in diets of the chickens. Additionally, the age of the egg should be monitored before removing the egg yolk/white from the shell, and the age of the egg film after it is applied to a substrate. It is possible that eggs could undergo large changes in fluorescence due to the chemical complexity of an egg sample which does not solely consist of amino acids.

Furthermore, to use fluorescence measurements accurately and confidently for the identification of binders, an extensive study could be done using a wider range of binders and pigments. This could include paint mixtures intended to imitate historic paint mixtures, with multiple pigments added to individual binders, and mixtures of binders. The fluorescence spectra of these mixtures could then be added to a database for applications of machine learning, in which a deconvolution algorithm could be established to predict the binder and paint mixture that was analysed. Without more extensive research, binders should not be identified solely on the basis of fluorescence emission peaks, as these emission peaks are changed by the paint matrix.

Colour changes, changes in transparency and other optical properties such as fluorescence are largely dependant on the nature of the painting. Paintings are extensive, complex mixtures which can contain various pigments and binders. The study focused solely on fluorescent changes, however further research should be done to compare the fluorescent changes with other optical properties (such as transparency and opacity changes) and metal complex formations (metal soaps) which lead to transparency changes. Further studies also need to be done to determine the sampling depth of fluorescence studies, especially on paintings which do not have a smooth paint layer.

Addendum A

Lippert equation calculations for drying oils

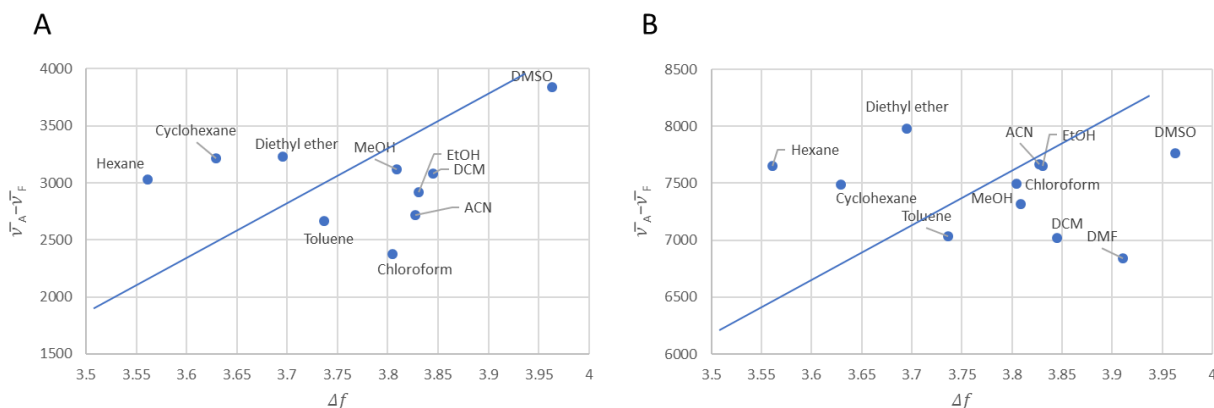


Figure A1: Lippert equation applied to linseed oil in different solvents, the first plot relates to the peak at 315 nm (λ_{em}) which arises with 300 nm incident light (λ_{ex}) and the second plot being the peak at 330 nm (λ_{em}) which arises with 315 nm excitation light (λ_{ex}). The lines are estimates of how the plots should be distributed if the fluorescence obeys the Lippert equation.

In solution, the fluorophore is stabilized by the presence of dipole moments in the solvent that orientate around the dipole moment of the fluorophore. Solvents are known to shift the emission peak to longer wavelengths (higher energy) due to the stabilization of the excited state by polar solvent molecules [1]. Some fluorophores are significantly affected by changes in polarity, for example trans-4-dimethylamino-4'-(1-oxobutyl) stilbene (DOS), where a change in solvent can lead to a shift to 200 nm longer emission wavelengths. Solvent effects can be interpreted by the Lippert equation (eq 1.1).

$$\bar{\nu}_A - \bar{\nu}_F = \frac{2}{hc} \left(\frac{\epsilon - 1}{2\epsilon + 1} - \frac{n^2 - 1}{2n^2 + 1} \right) \frac{(\mu_E - \mu_G)^2}{a^3} + constant \quad (1.1)$$

$$\Delta\bar{\nu} = \frac{2}{hc} \Delta f \frac{(\mu_E - \mu_G)^2}{a^3} + constant \quad (1.2)$$

Where $\bar{\nu}_A$ and $\bar{\nu}_F$ are the wavenumbers (cm^{-1}) of the absorption and fluorescence, respectively. Planck's constant (h) and the speed of light (c) are the two constants. The values that describe the properties of the fluorophore are: a^3 , the area of the cavity in which the fluorophore resides, along with the excited- (μ_E) and ground-state (μ_G) dipole moments. The properties of the solvent, dielectric constant (ϵ) and the refractive index (n) will cause a change in the energy gap. The dielectric constant is a static property of the solvent which describes the molecular polarizability, which results in the reorientation of the solvent dipoles around the excited state. In contrast, the refractive index is a high-frequency response and depends on the motion of electrons within the solvent molecules. An increase in the refractive index would result in both the ground and excited states to be instantaneously stabilized from the movements of electrons in the solvent molecules, thus decreasing the energy gap. An increase in the

dielectric constant will also result in a stabilization of the ground and excited states, and thus decrease the band gap energy. However, where the refractive index results in an instantaneous stabilization, the stabilization from the dielectric constant only occurs after a reorientation of the solvent dipoles. In the Lippert equation, it is assumed that the solvent relaxation is complete prior to emission.

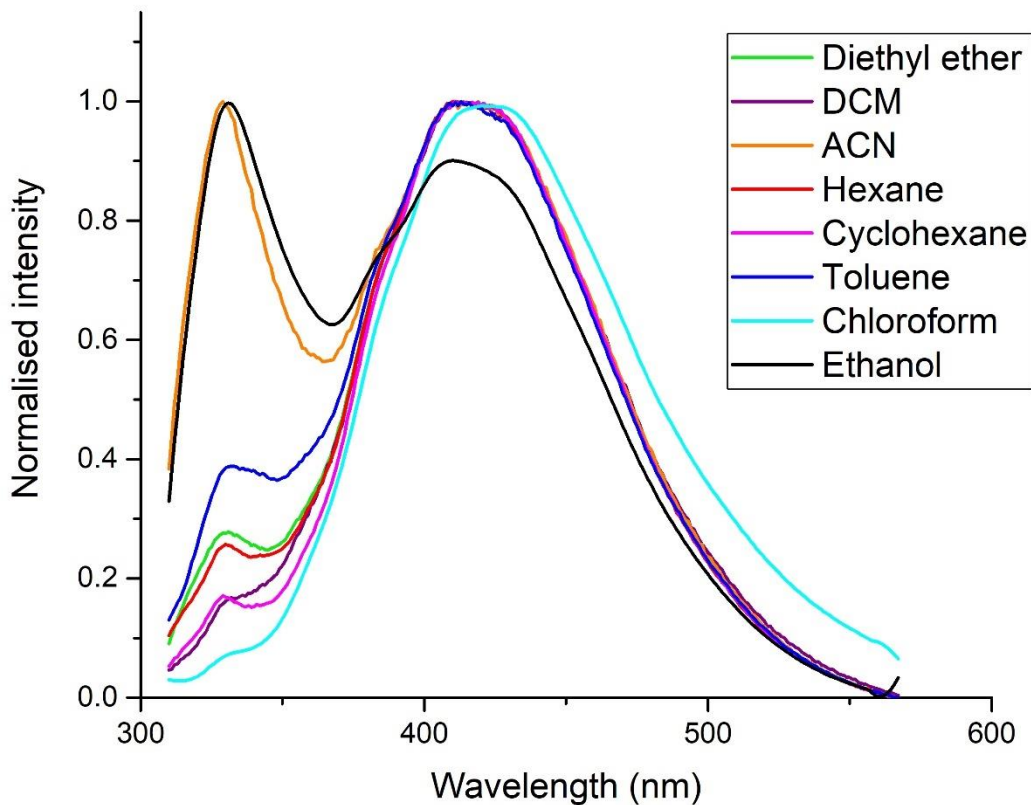


Figure A2: Fluorescence intensity of liquid linseed oil in various solvents using an excitation wavelength of 300 nm.

Ageing of Drying oils

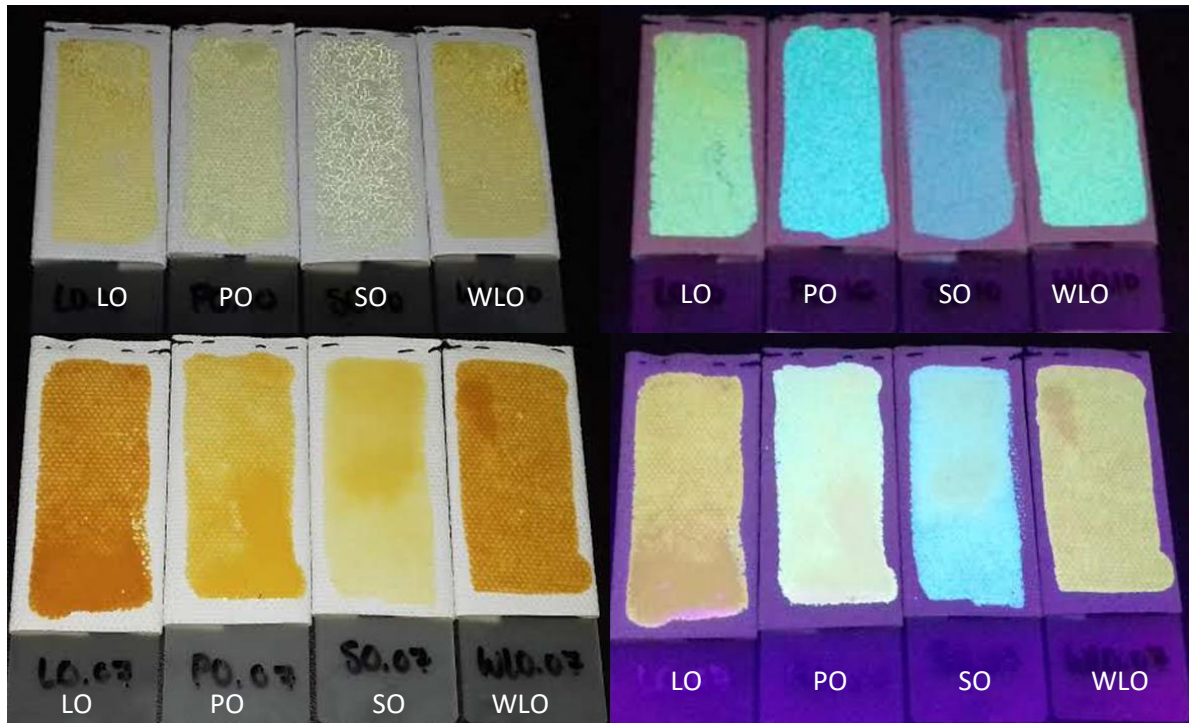


Figure A3: Fluorescence colours of the different oils after 1 week of UV exposure (top) and after 24 hr exposure to ammonia vapour (bottom). LO- Linseed oil; PO- Poppy seed oil; SO- Stand oil; WLO- water-miscible linseed oil.

Fluorescent changes in Poppy seed oil

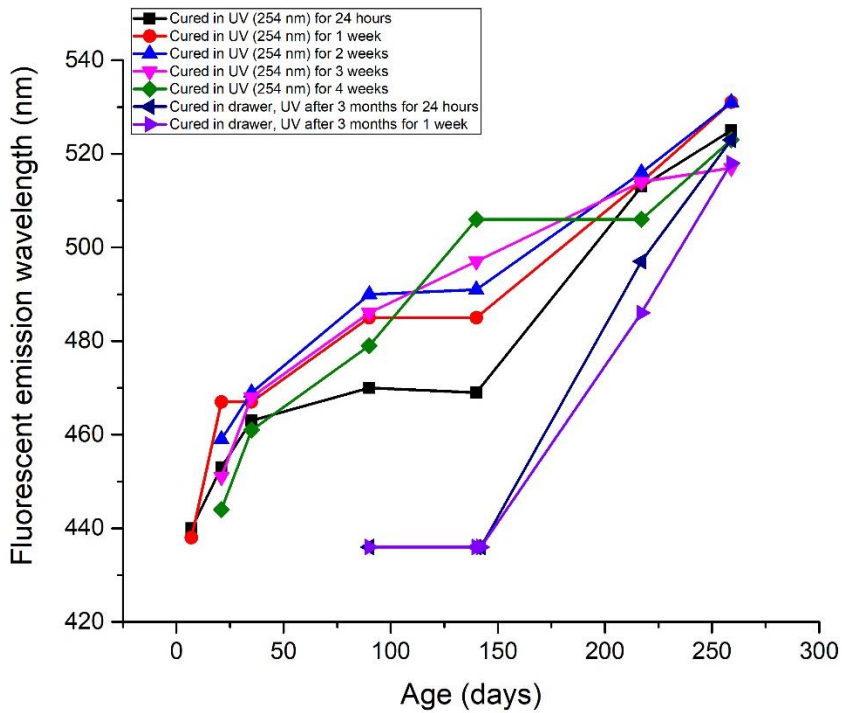


Figure A4: Rate of the fluorescence emission maximum changes of poppy seed oil various exposure times to UV light (254 nm) and then subsequent storage in dark drawers. The excitation wavelength was 360 nm for all measurements.

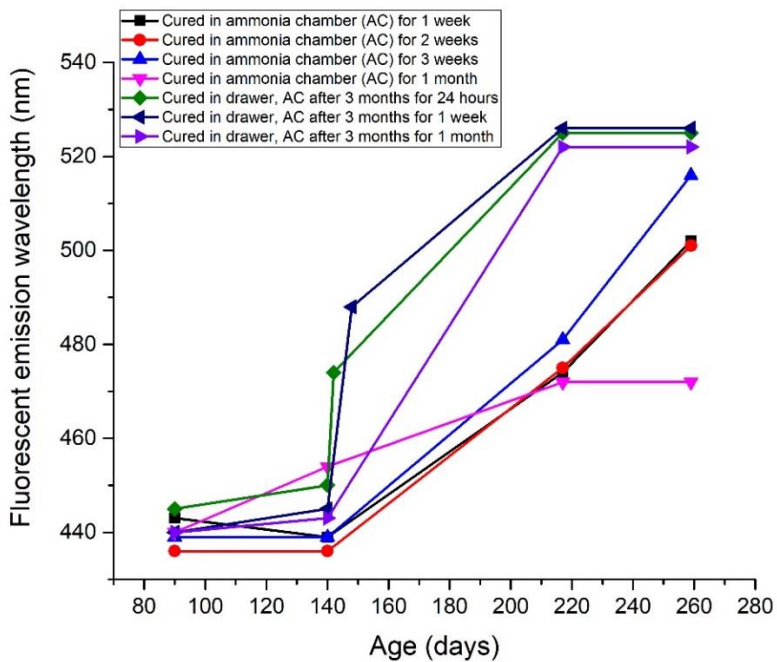


Figure A5: Rate of fluorescent changes of poppy seed oil after exposure to ammonia vapor, and subsequent storage in a dark drawer. The excitation wavelength was 360 nm for all measurements.

Fluorescent changes in Stand oil

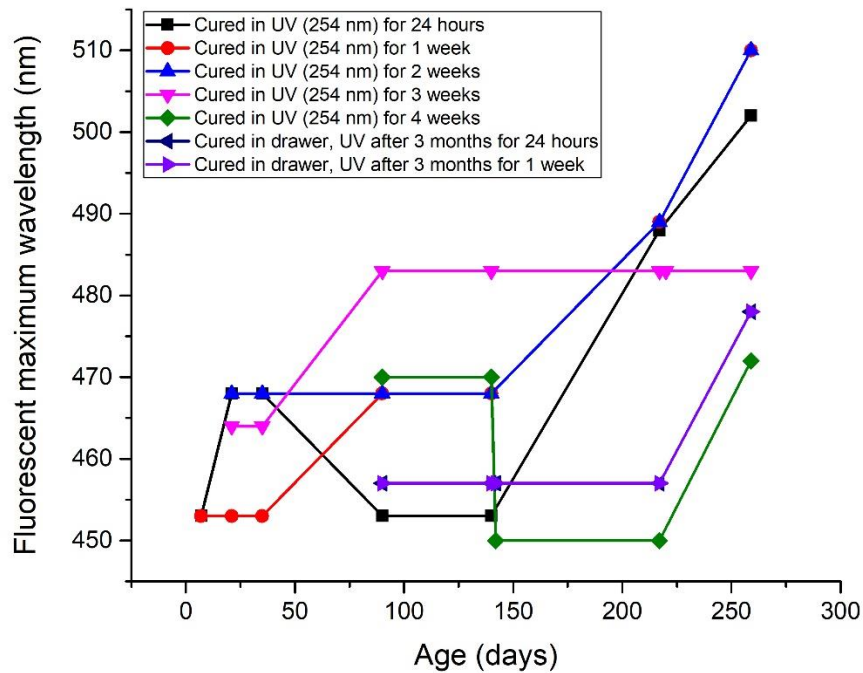


Figure A6: Rate of the fluorescence emission maximum changes of stand oil various exposure times to UV light (254 nm) and then subsequent storage in dark drawers. The excitation wavelength was 360 nm for all measurements.

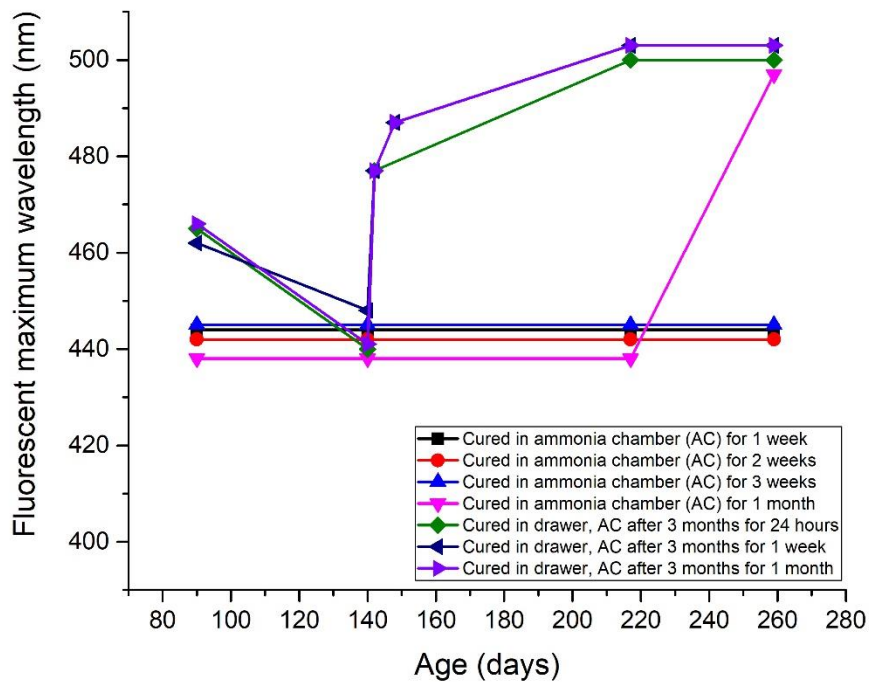


Figure A7: Rate of fluorescent changes of stand oil after exposure to ammonia vapor, and subsequent storage in a dark drawer. The excitation wavelength was 360 nm for all measurements.

Fluorescent changes in water-miscible linseed oil

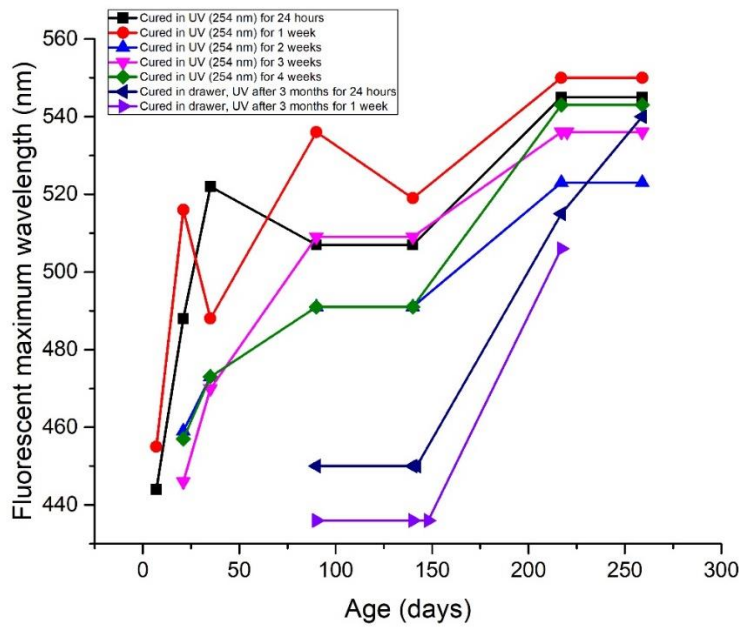


Figure A8: Rate of the fluorescence emission maximum changes of water-miscible linseed oil various exposure times to UV light (254 nm) and then subsequent storage in dark drawers. The excitation wavelength was 360 nm for all measurements.

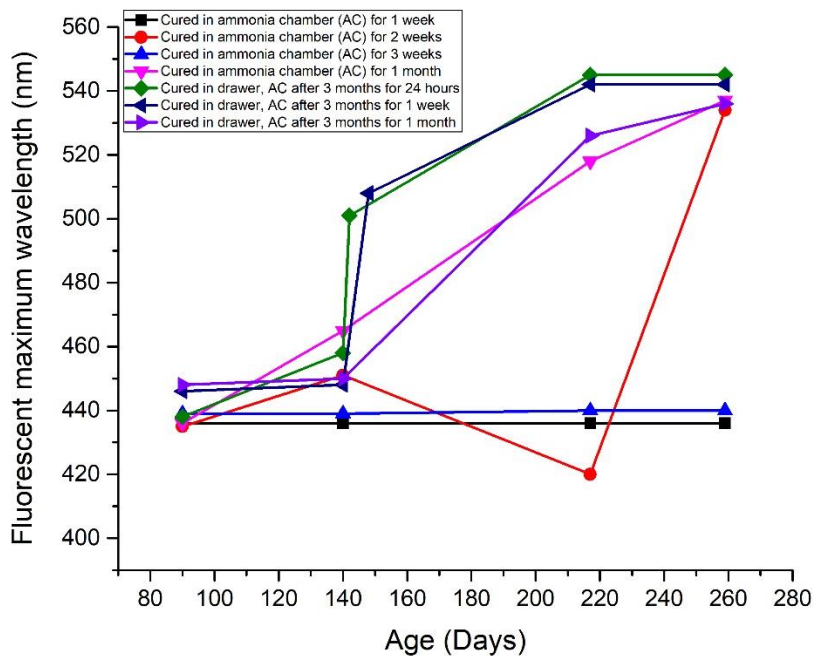


Figure A9: Rate of fluorescent changes of stand oil after exposure to ammonia vapor, and subsequent storage in a dark drawer. The excitation wavelength was 360 nm for all measurements.

Linseed oil and poppy seed oil showed the most homogenous yellow discoloration over the painted area. As the water-miscible oil dried, the painted surface started forming drops instead of drying as painted. These drops formed an agglomerate of linseed oil, that yellow much faster than other oils once dried. This heterogeneity of the surface discoloration causes variation in the fluorescence intensity as the exact position at which the fluorescence is measured could not be perfectly reproduced. Stand oil did not form drops but had sections where the stand oil was applied thicker; due to the viscosity of the oil it did not roll out to form a uniform surface.

Addendum B

Additional graphs for pigment characterisation

XRF spectra

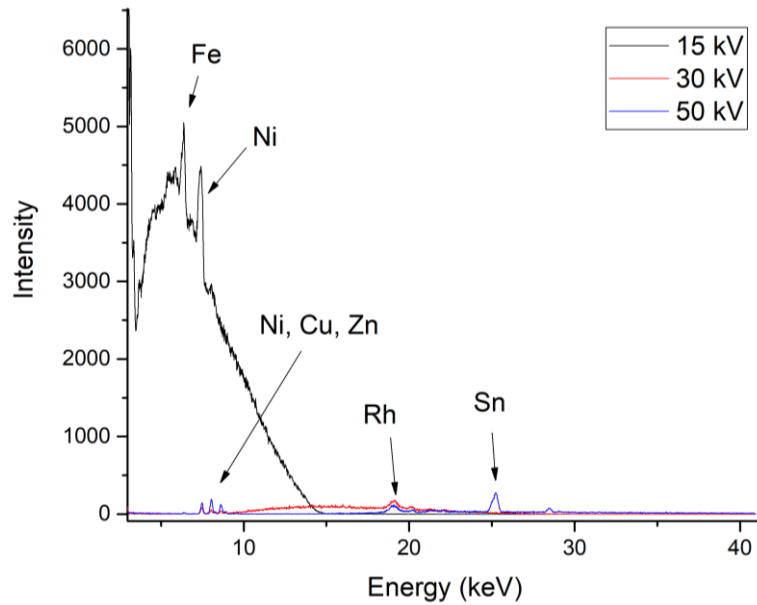


Figure B1: X-ray fluorescence spectrum of a blank polyester plastic sleeve.

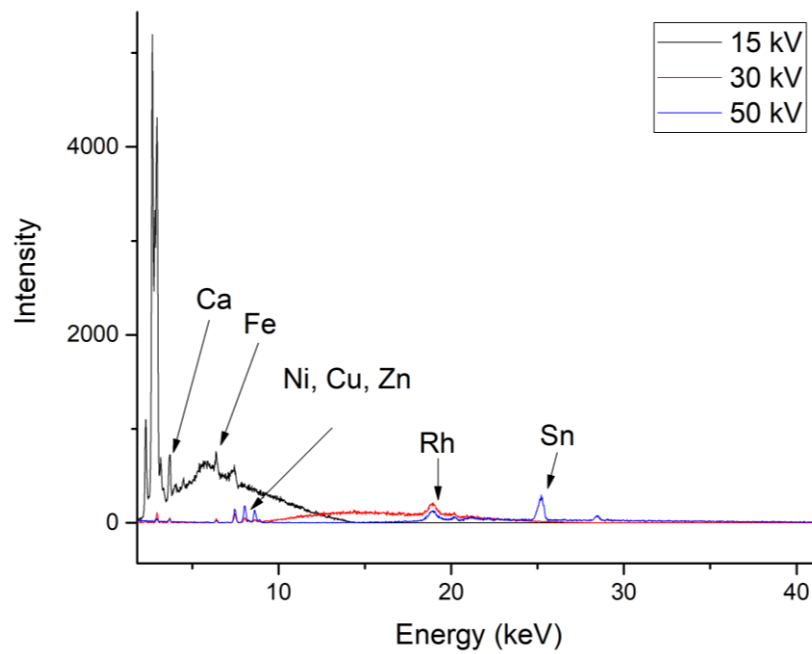


Figure B2: X-ray fluorescence spectrum of lamp black pigment.

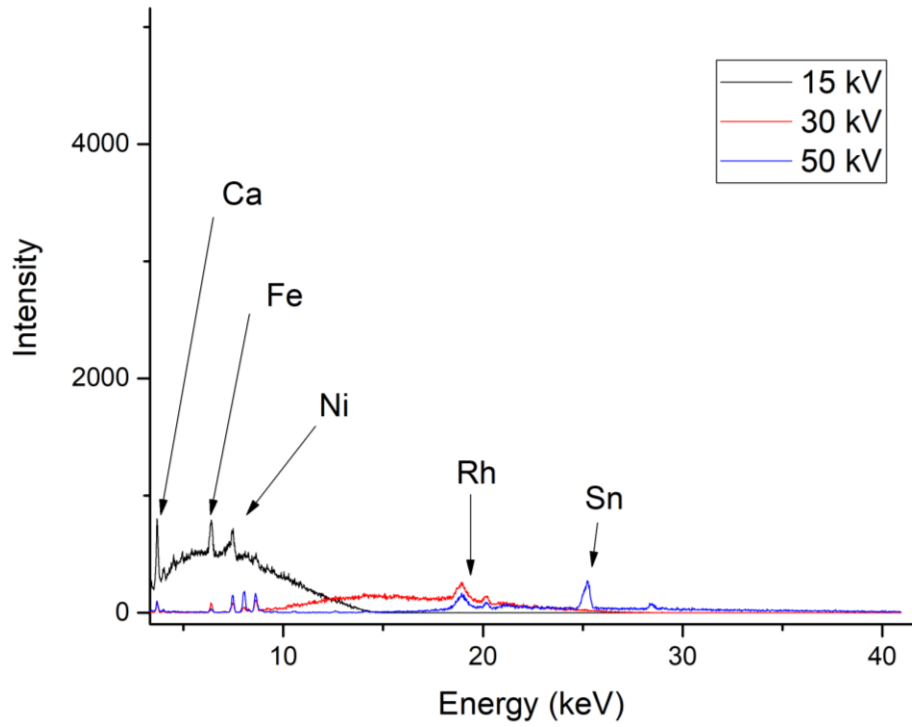


Figure B3: X-ray fluorescence spectrum of Indian yellow.

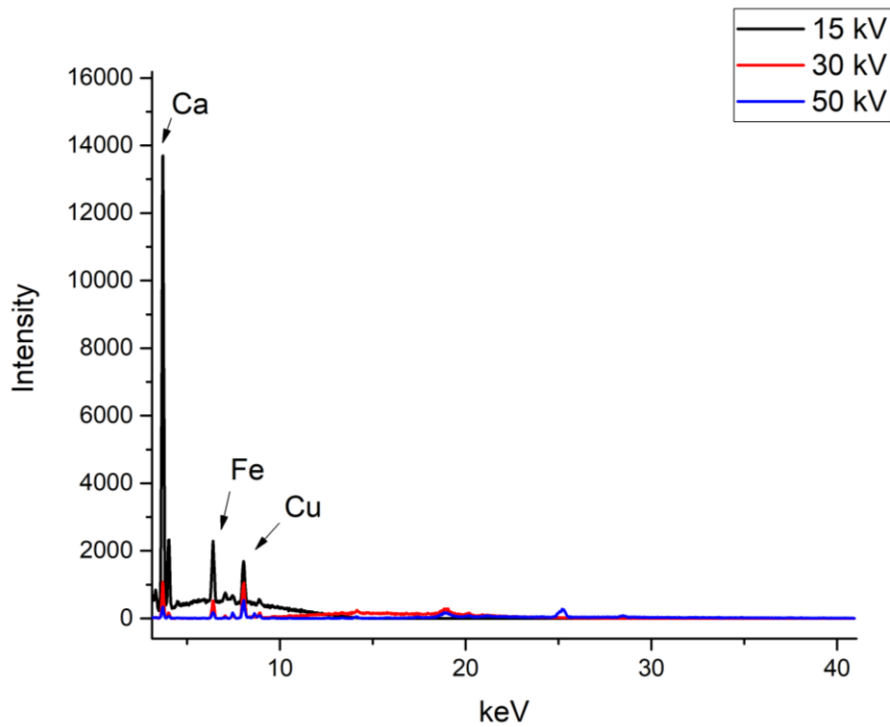


Figure B4: X-ray fluorescence spectrum of alizarin crimson.

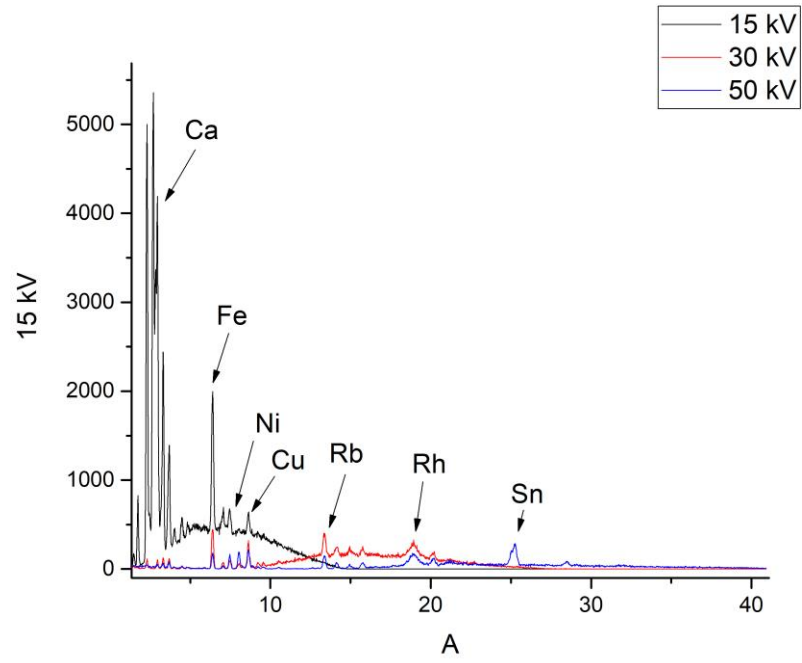


Figure B5: X-ray fluorescence spectrum of oriental blue.

PXRD

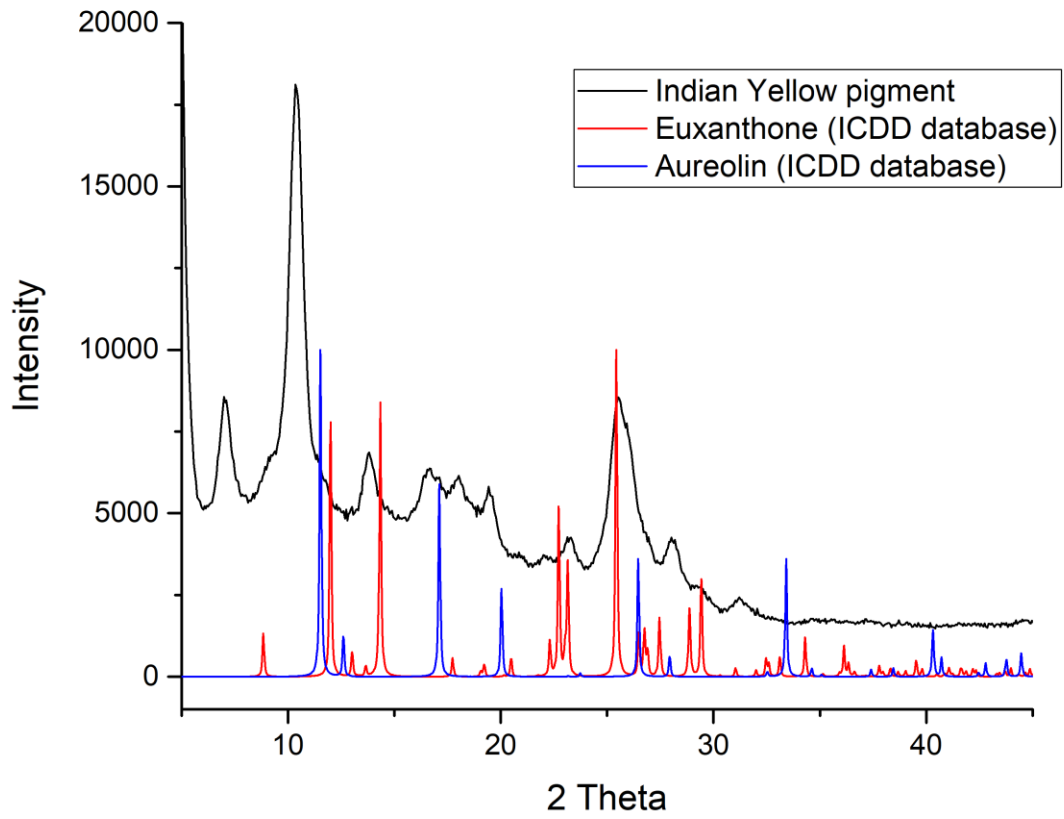


Figure B6: Powder X-ray diffraction pattern for Indian yellow.

FTIR spectra

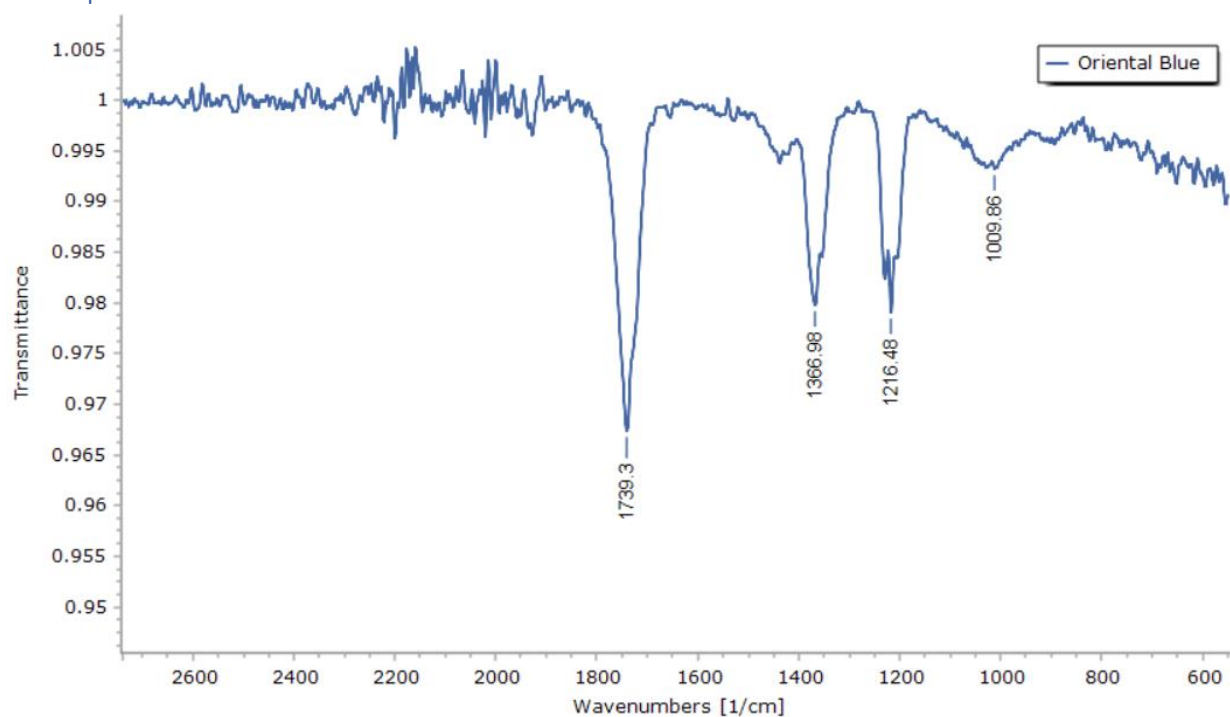


Figure B7: The ATR-FTIR spectrum of oriental blue powder. The spectrum was obtained from 4000 cm^{-1} to 400 cm^{-1} but did not show any peaks at the higher frequencies ($4000 - 2500 \text{ cm}^{-1}$).

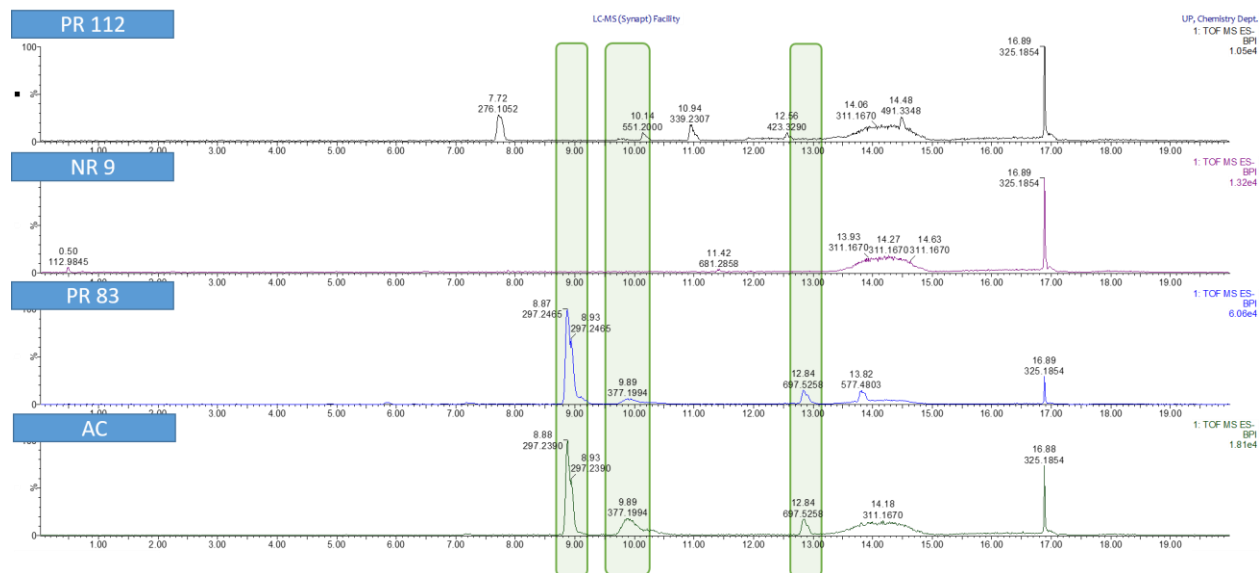


Figure B8: Negative ion mass chromatograms of red pigments dissolved in methanol. The green blocks indicate the similarities between PR83 and the alizarin crimson used in this study.

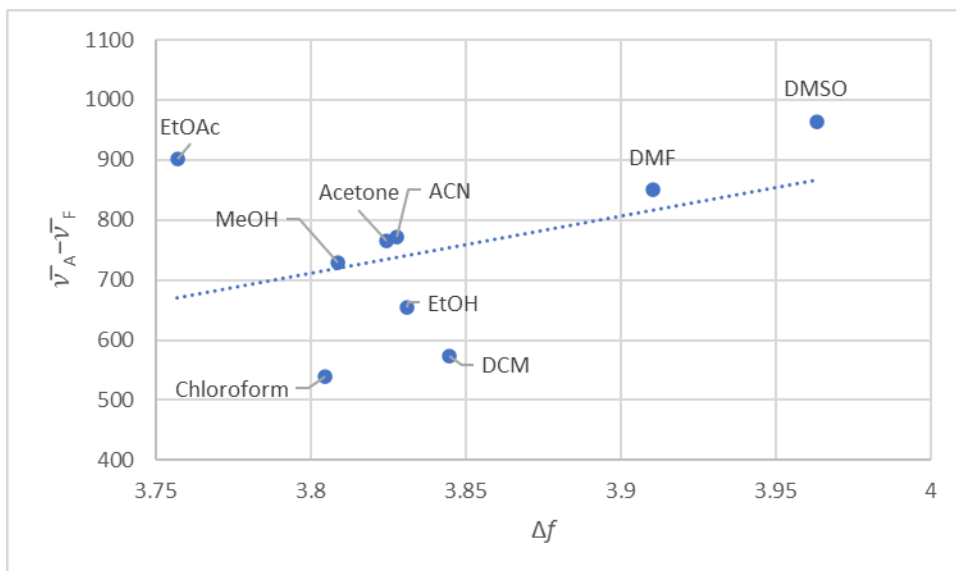


Figure B9: Lippert equation applied to alizarin crimson (AC) in different solvents.

Addendum C

Fluorescence images of alizarin crimson (AC) samples

Each pigment-binder mixture was photographed under normal ambient white light, and under a UV lamp. Two wavelengths were used with UV light, namely 254 nm (the middle image) and 365 nm (the right-hand side image).

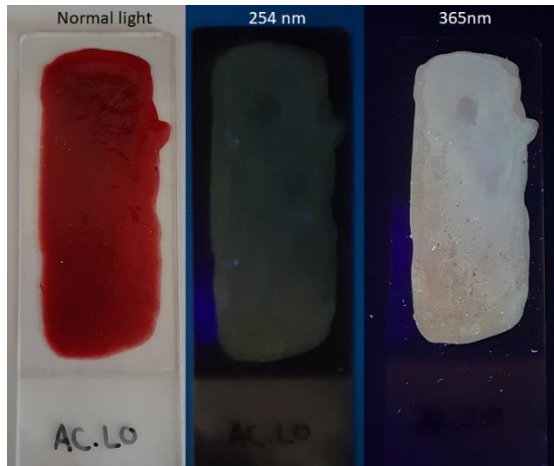


Figure C1: AC mixed with linseed oil (LO)

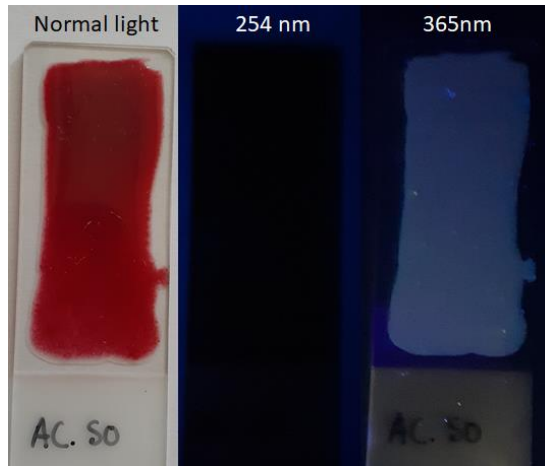


Figure C2: AC mixed with stand oil (SO)

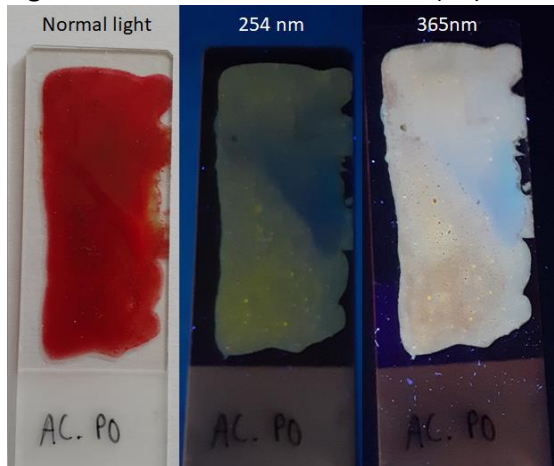


Figure C3: AC mixed with poppyseed oil (PO)

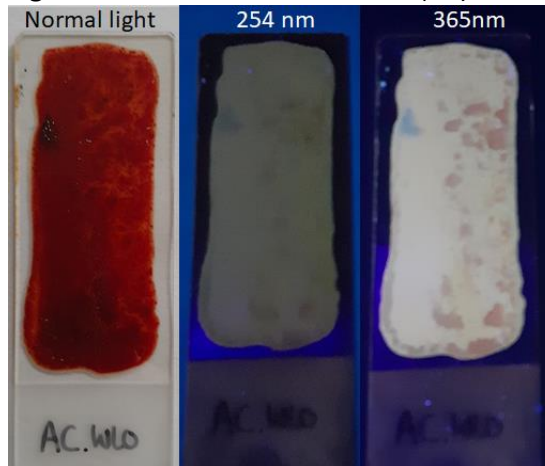


Figure C4: AC mixed with water-miscible linseed oil (WLO)

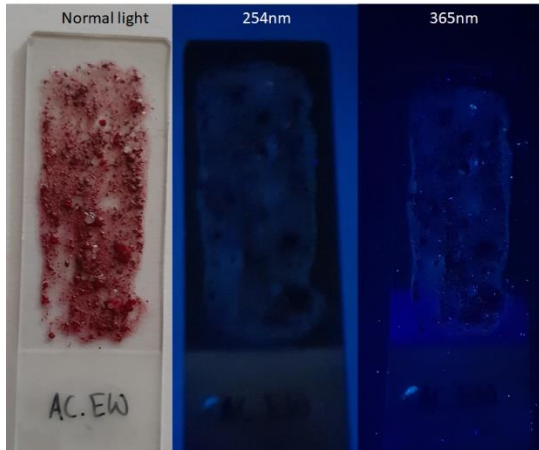


Figure C5: AC mixed with egg white (EW)

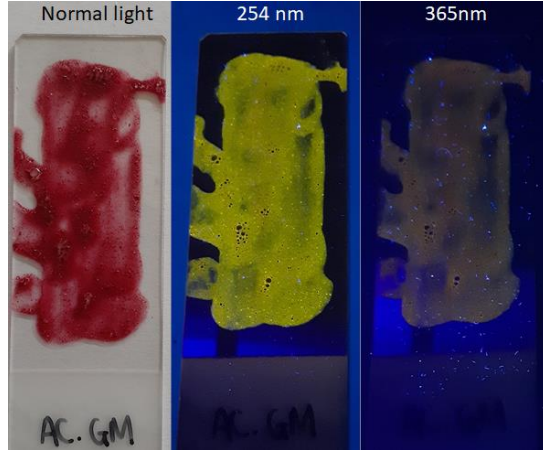


Figure C6: AC mixed with gilding milk (GM)

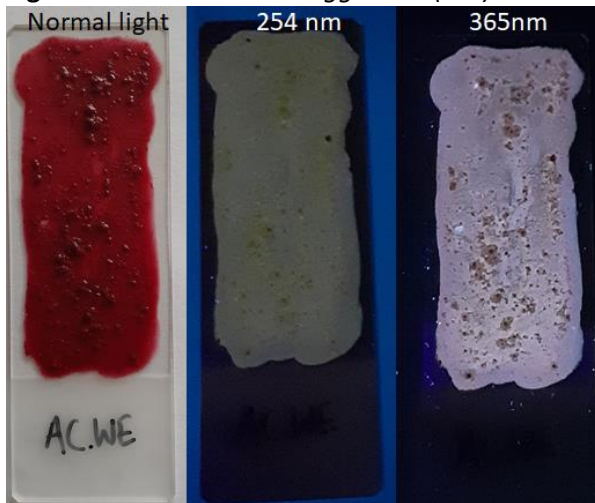


Figure C7: AC mixed with whole egg (WE)

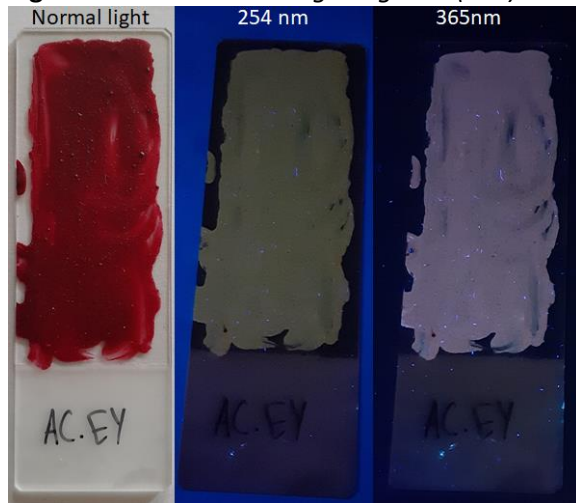


Figure C8: AC mixed with egg yolk (EY)

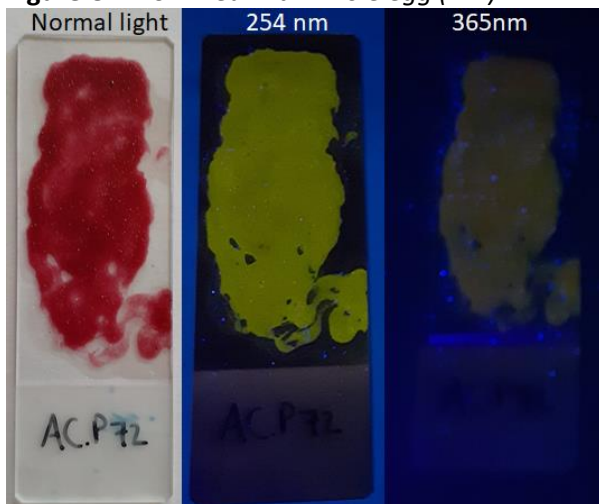


Figure C9: AC mixed with paraloid B72 (P72)

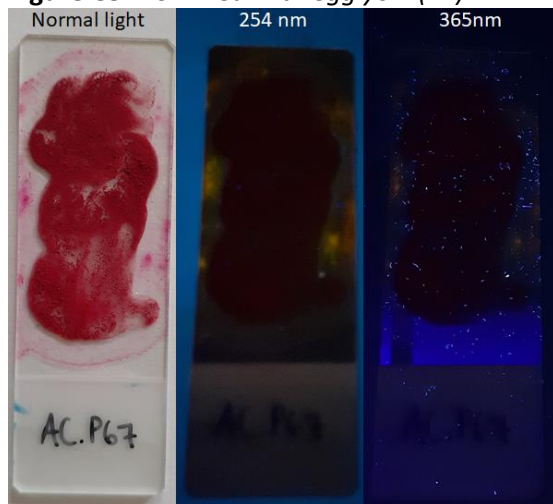


Figure C10: AC mixed with paraloid B67 (P67)

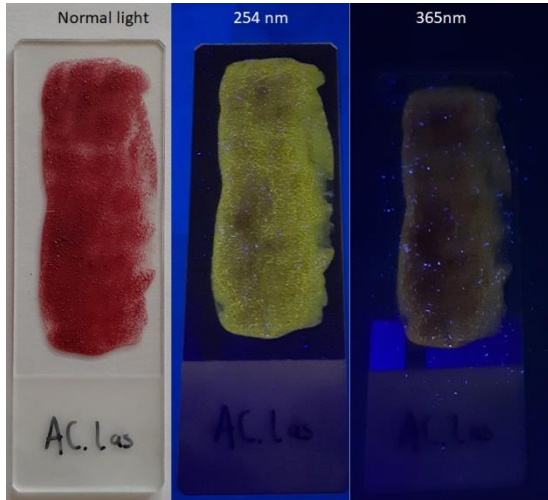


Figure C11: AC mixed with lascoux (Las)

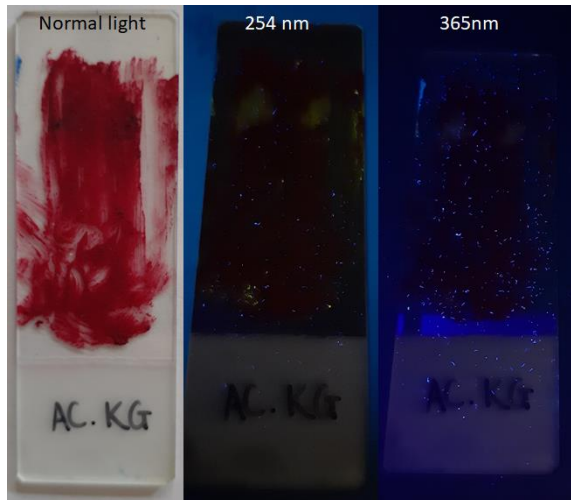


Figure C12: AC mixed with klusel G (KG)

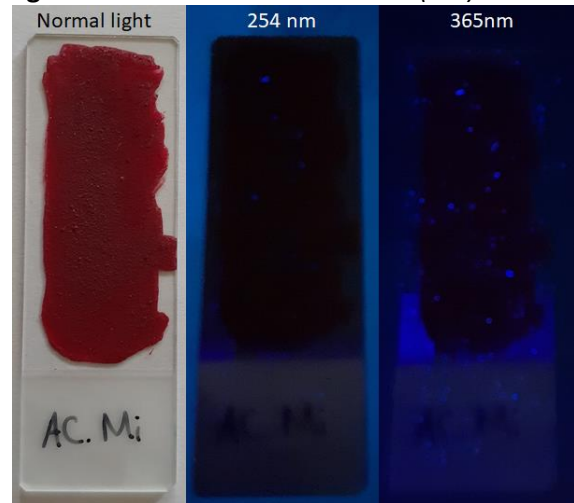


Figure C13: AC mixed with mowiol (Mi)

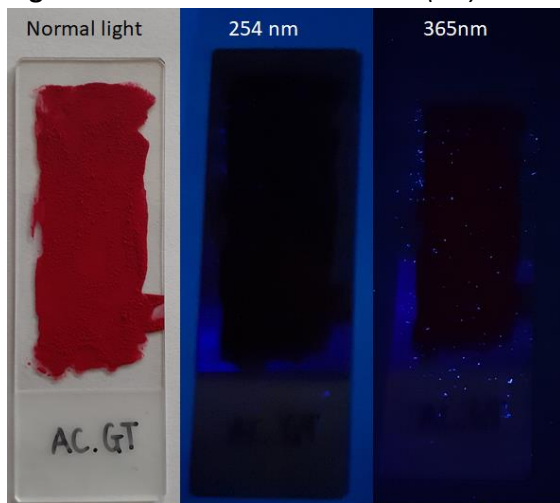


Figure C14: AC mixed with gum Tragacanth (GT)

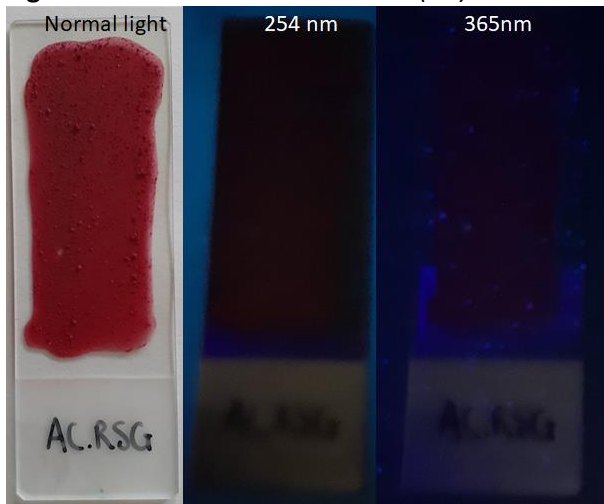


Figure C15: AC mixed with rabbit skin glue (RSG)

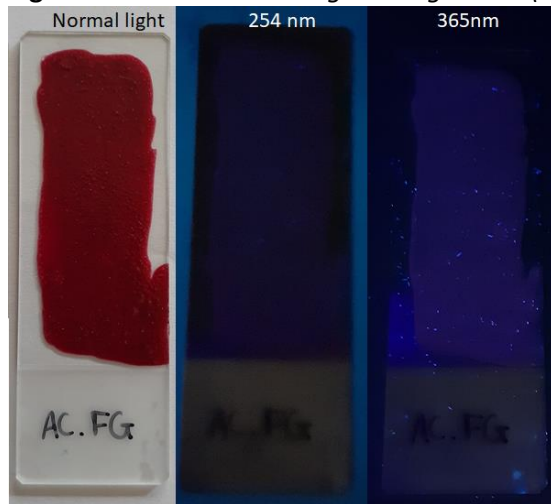


Figure C16: AC mixed with fish glue (FG)

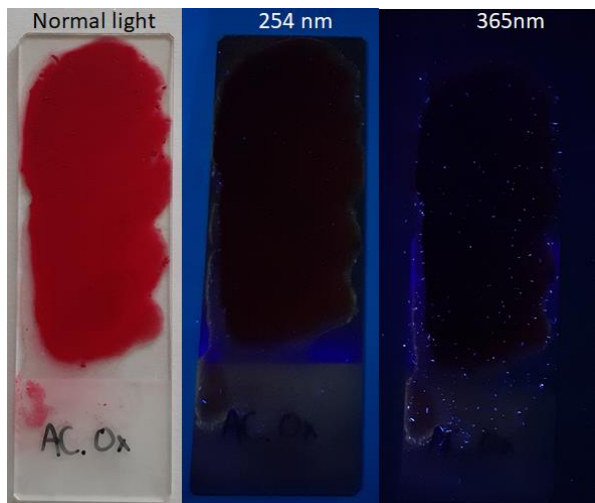


Figure C17: AC mixed with ox gall (OX)

Addendum D

Fluorescence images of lamp black (LB) samples

Each pigment-binder mixture was photographed under normal ambient white light, and under a UV lamp. Two wavelengths were used with UV light, namely 254 nm (the middle image) and 365 nm (the right-hand side image).

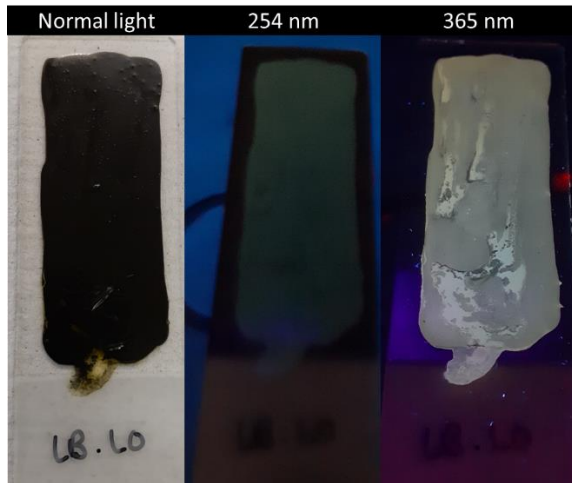


Figure D1: LB mixed with linseed oil (LO)

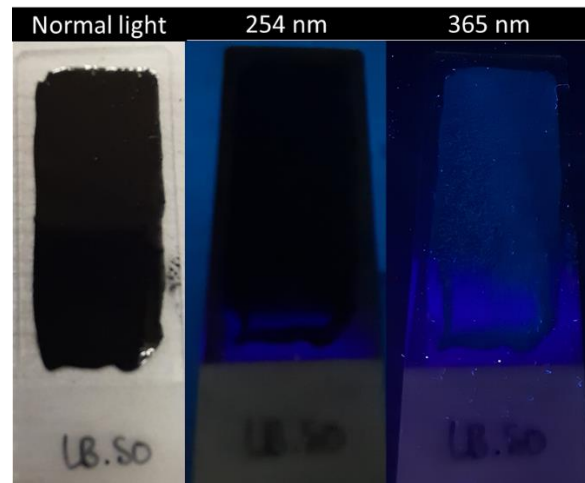


Figure D2: LB mixed with stand oil (SO)

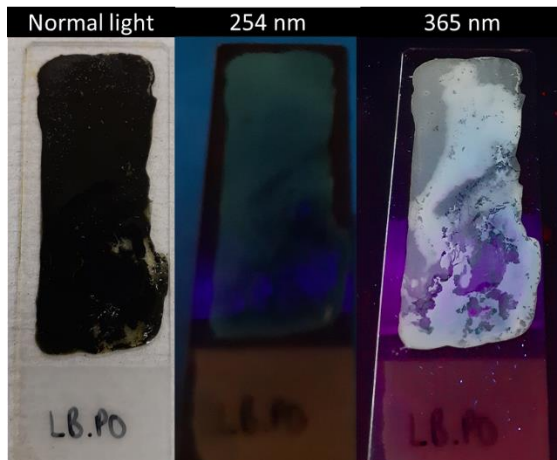


Figure D3: LB mixed with poppyseed oil (PO)

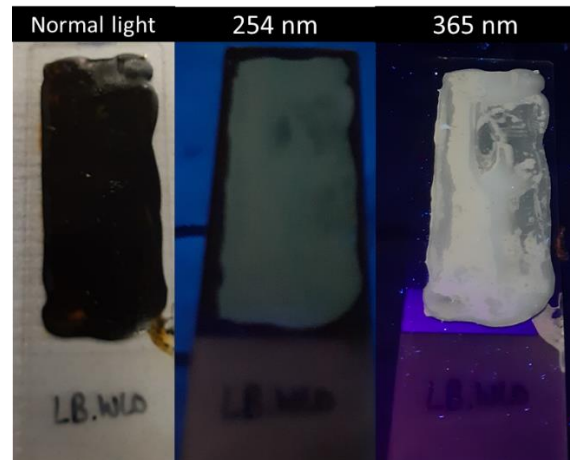


Figure D4: LB mixed with water-miscible linseed oil (WLO)

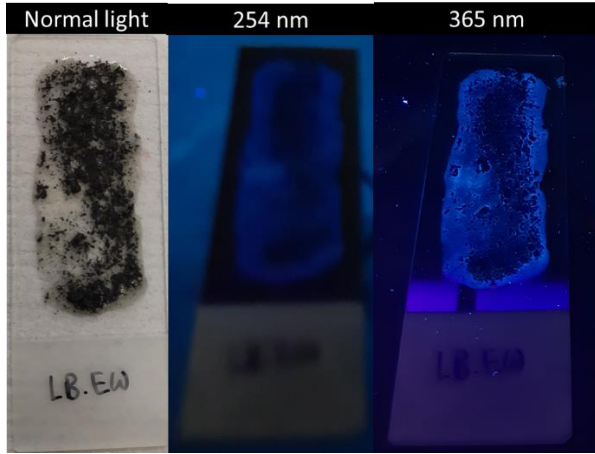


Figure D5: LB mixed with egg white (EW)

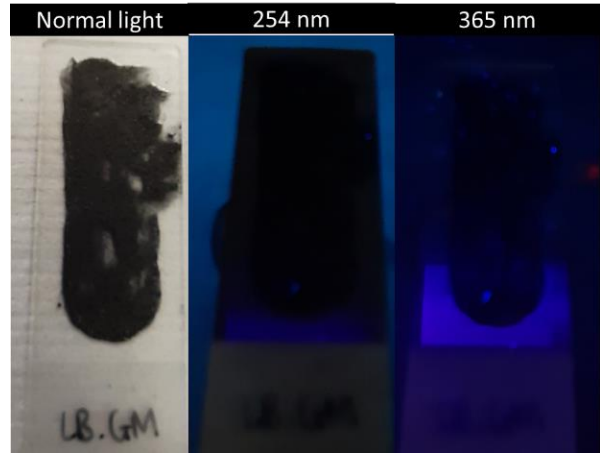


Figure D6: LB mixed with gilding milk (GM)

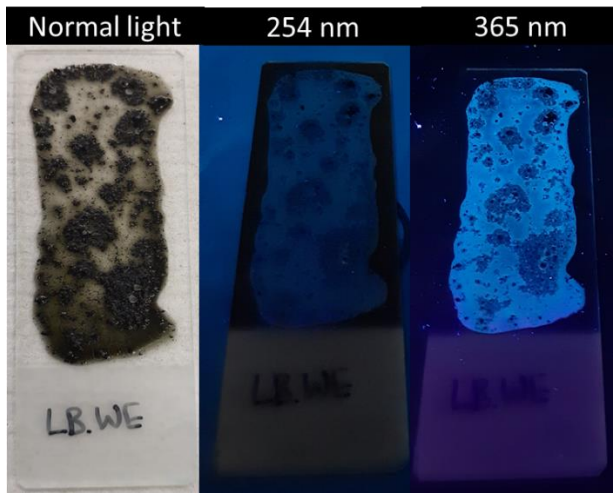


Figure D7: LB mixed with whole egg (WE)

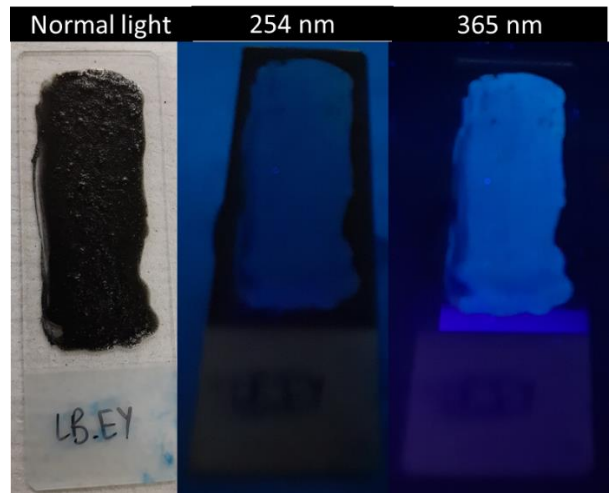


Figure D8: LB mixed with egg yolk (EY)

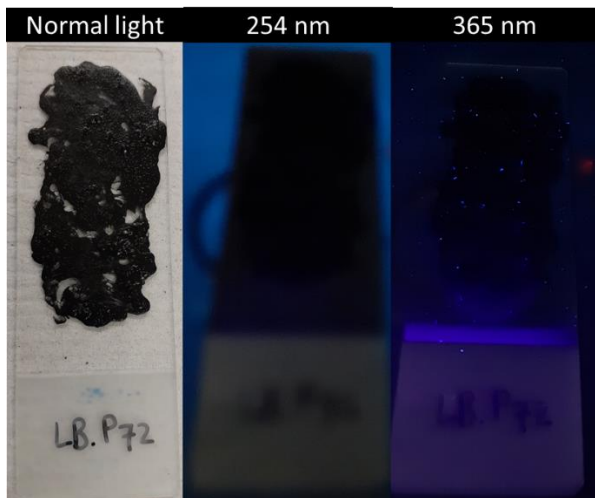


Figure D9: LB mixed with paraloid B72 (P72)

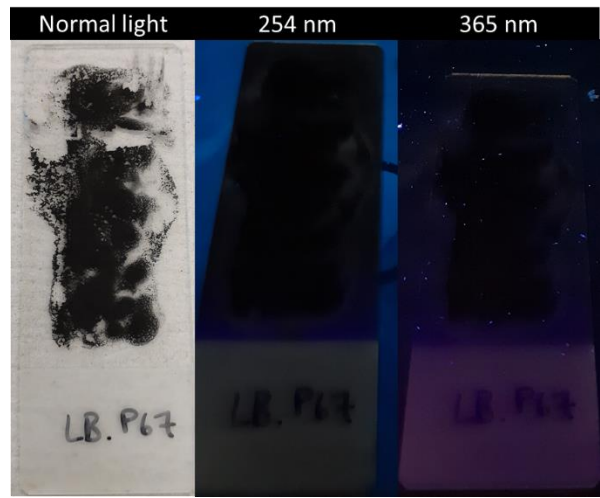


Figure D10: LB mixed with paraloid B67 (P67)

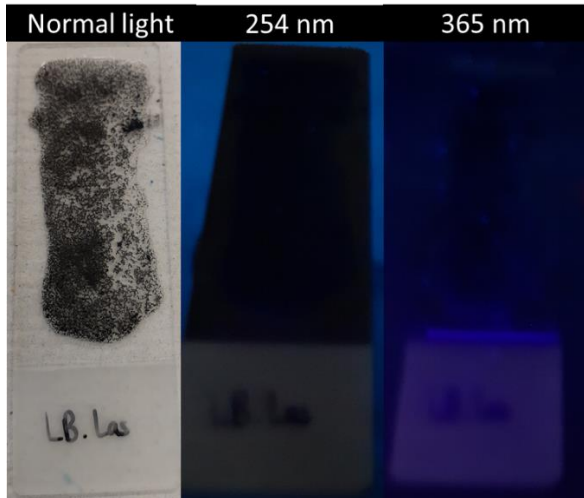


Figure D11: LB mixed with lascoux (*Las*)

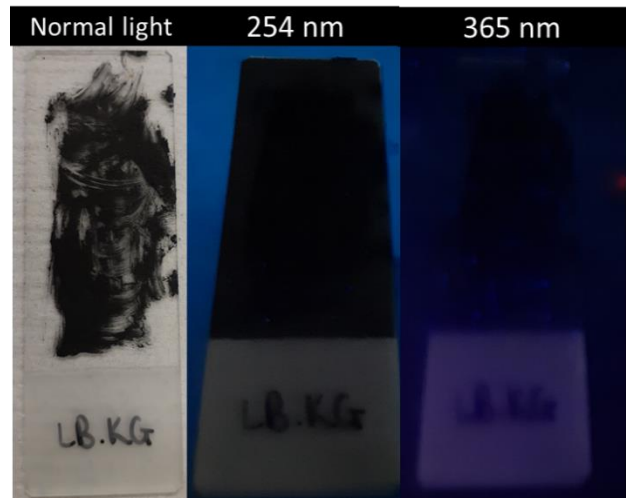


Figure D12: LB mixed with klusel G (*KG*)

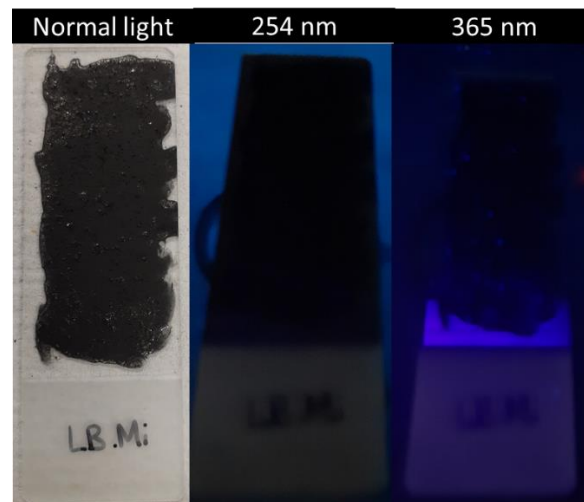


Figure D13: LB mixed with mowiol (*Mi*)

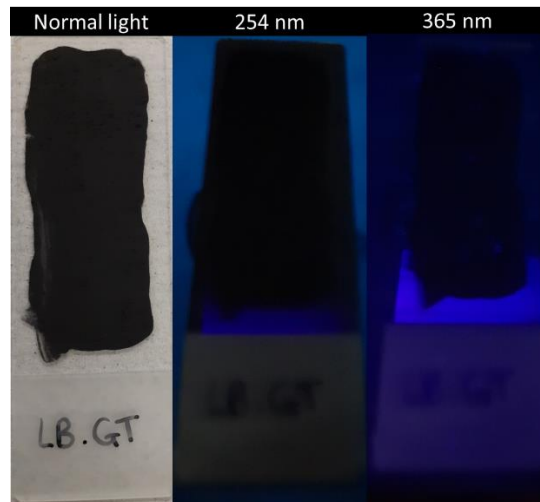


Figure D14: LB mixed with gum Tragacanth (*GT*)

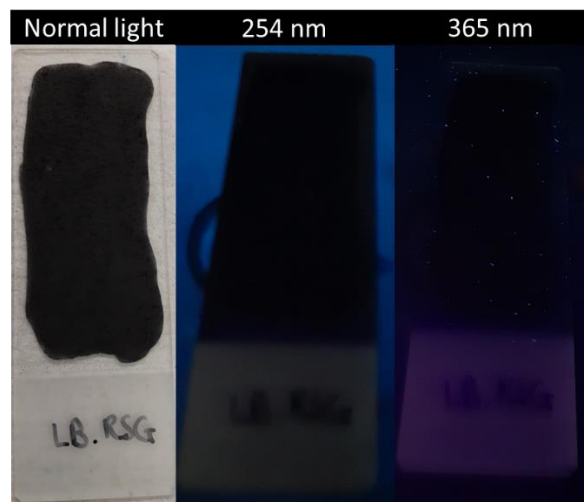


Figure D15: LB mixed with rabbit skin glue (*RSG*)

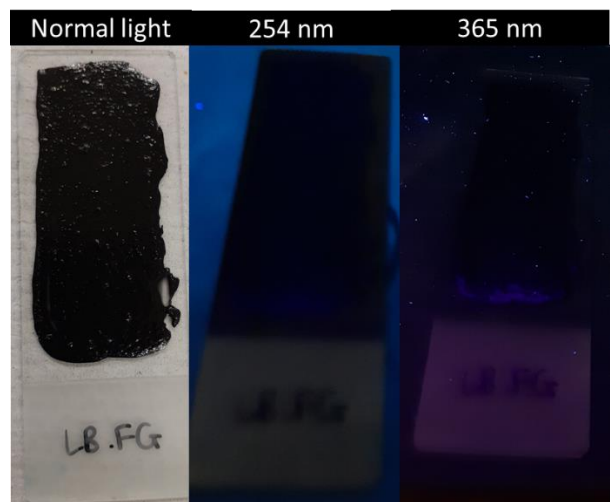


Figure D16: LB mixed with fish glue (*FG*)

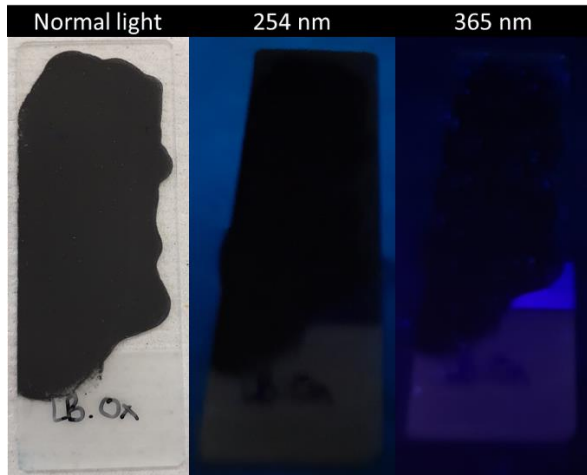


Figure D17: LB mixed with ox gall (OX)

Addendum E

Fluorescence images of oriental blue (OB) samples

Each pigment-binder mixture was photographed under normal ambient white light, and under a UV lamp. Two wavelengths were used with UV light, namely 254 nm (the middle image) and 365 nm (the right-hand side image).

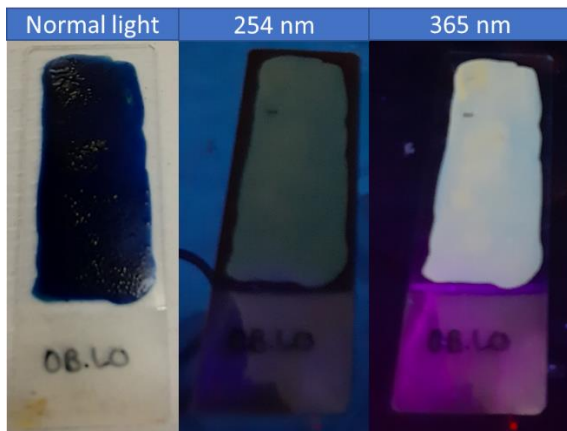


Figure E1: OB mixed with linseed oil (LO)

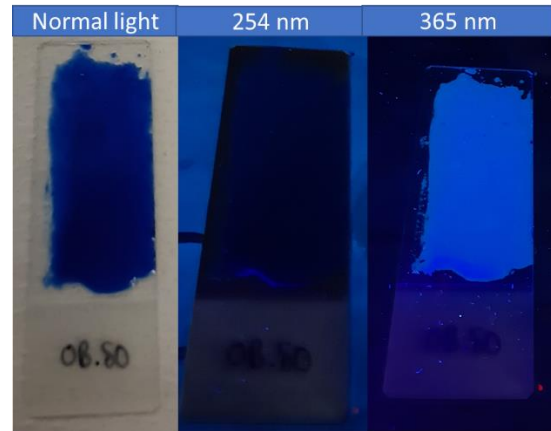


Figure E2: OB mixed with stand oil (SO)

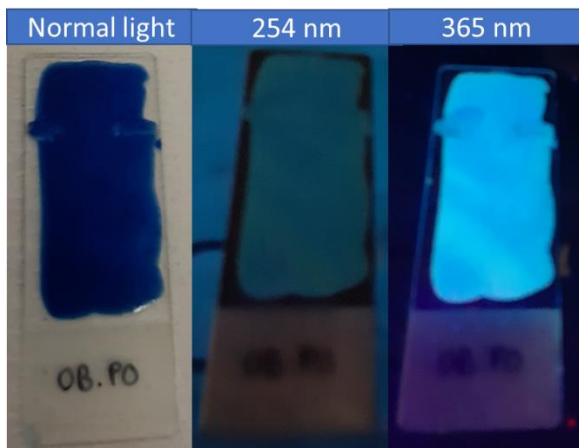


Figure E3: OB mixed with poppyseed oil (PO)

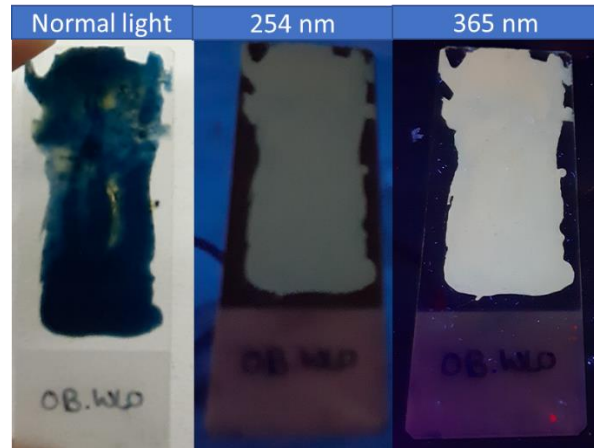


Figure E4: OB mixed with water-miscible linseed oil (WLO)

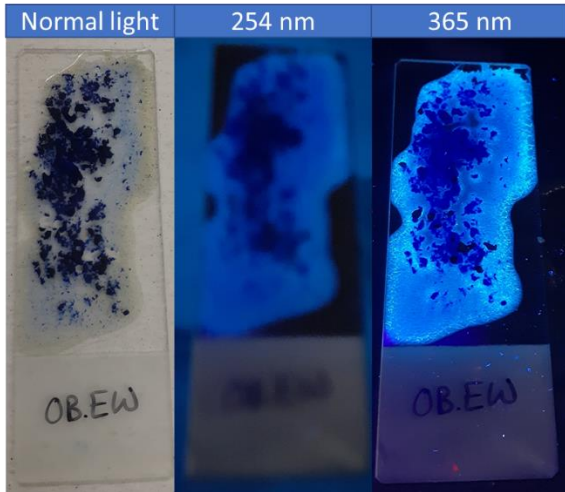


Figure E5: OB mixed with egg white (EW)

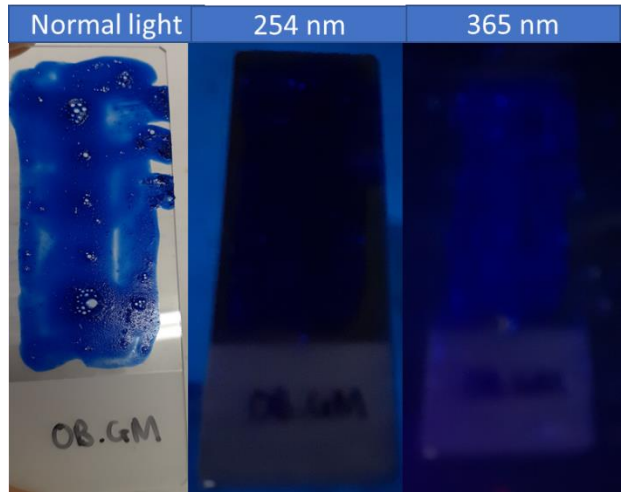


Figure E6: OB mixed with gilding milk (GM)

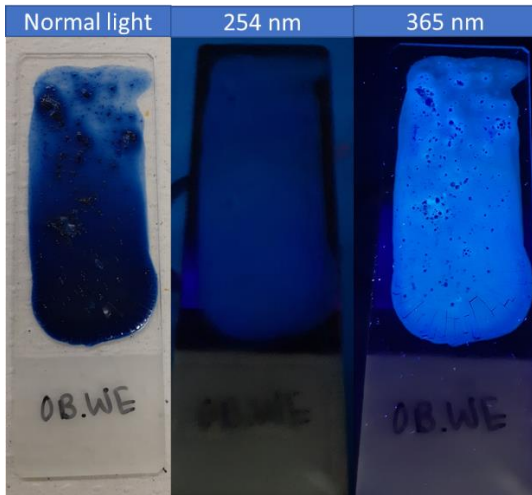


Figure E7: OB mixed with whole egg (WE)

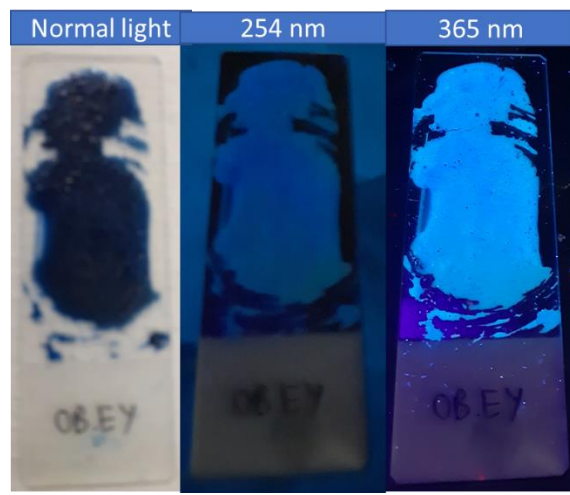


Figure E8: OB mixed with egg yolk (EY)

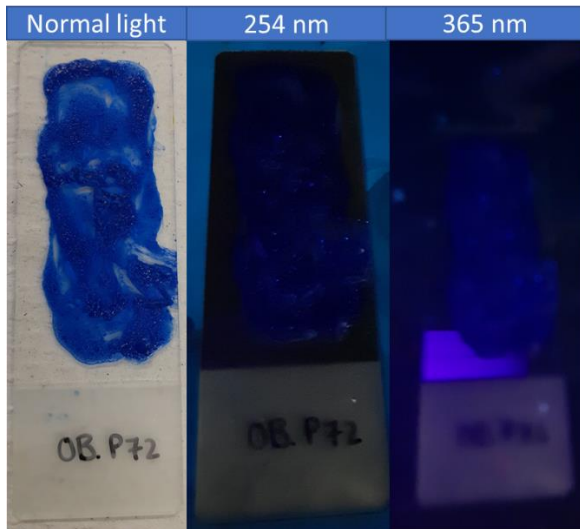


Figure E9: OB mixed with paraloid B72 (P72)

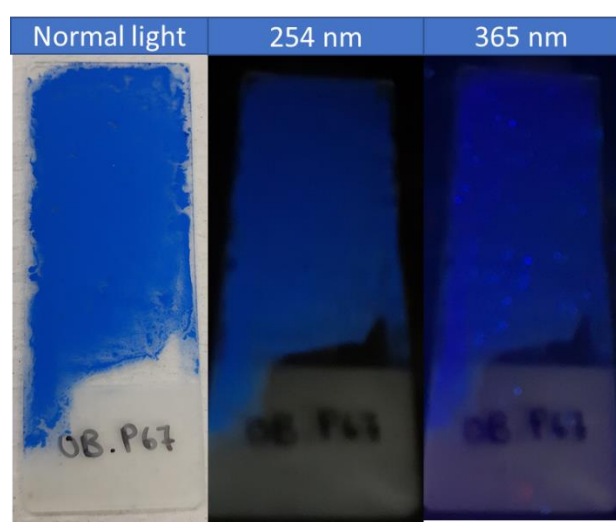


Figure E10: OB mixed with paraloid B67 (P67)

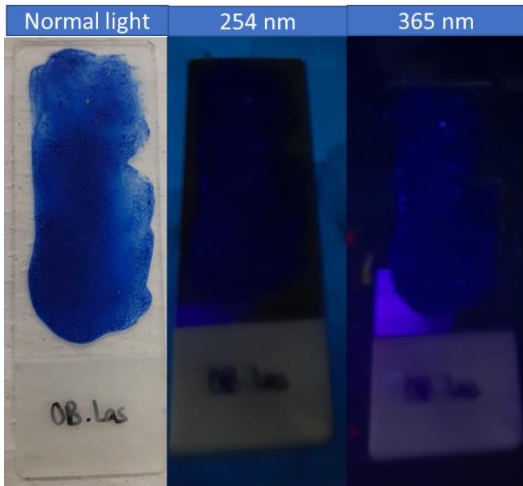


Figure E11: OB mixed with *lascoux (Las)*

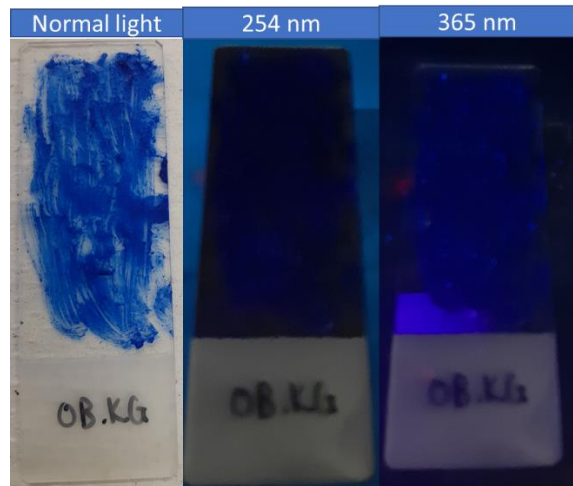


Figure E12: OB mixed with *Klusel G (KG)*

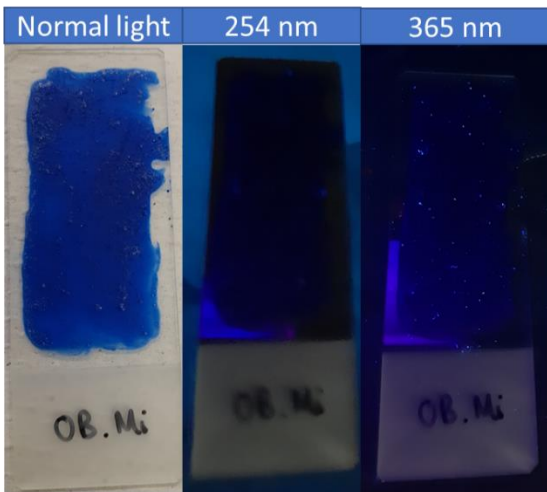


Figure E13: OB mixed with *mowiol (Mi)*

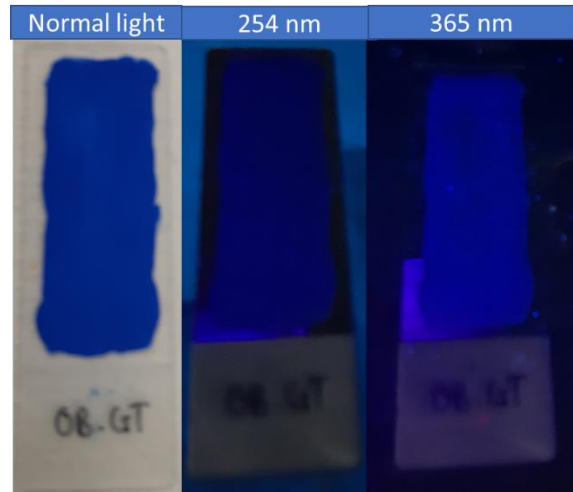


Figure E14: OB mixed with *gum Tragacanth (GT)*

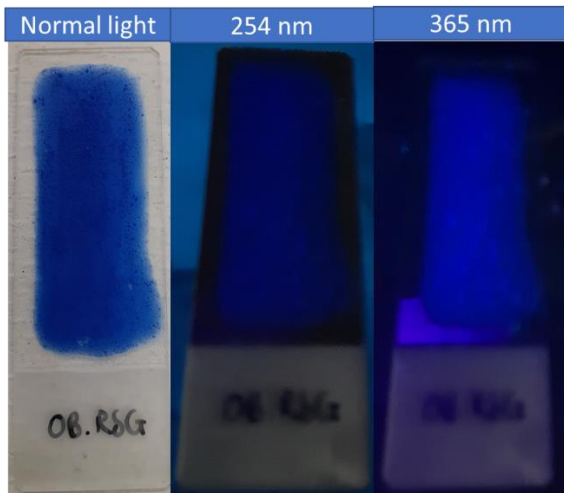


Figure E15: OB mixed with *rabbit skin glue (RSG)*

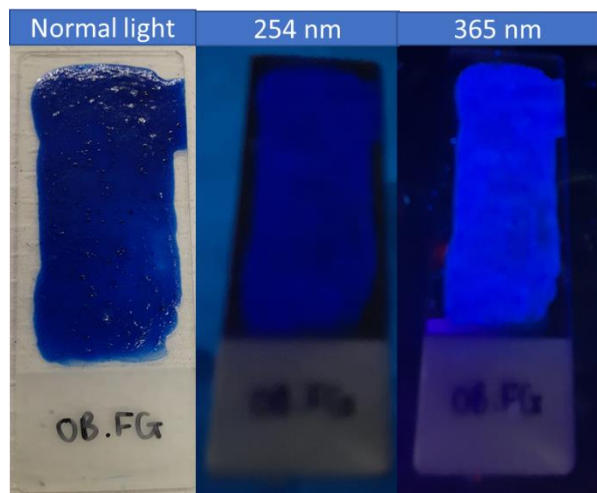


Figure E16: OB mixed with *fish glue (FG)*

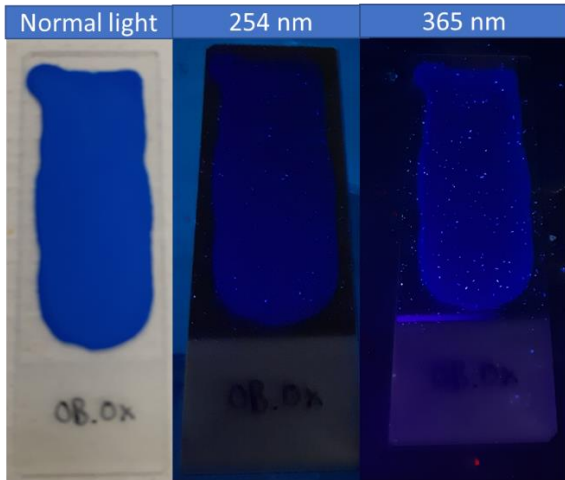


Figure E17: *OB mixed with ox gall (OX)*

Addendum F

Fluorescence images of phthalo blue (PB) samples

Each pigment-binder mixture was photographed under normal ambient white light, and under a UV lamp. Two wavelengths were used with UV light, namely 254 nm (the middle image) and 365 nm (the right-hand side image).

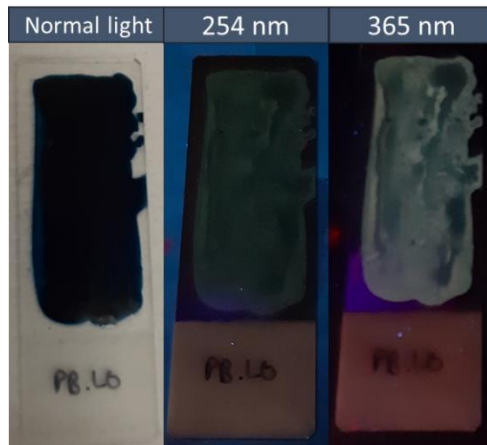


Figure F1: PB mixed with linseed oil (LO)

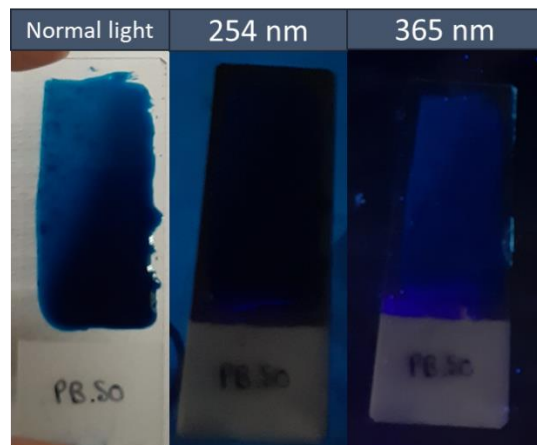


Figure F2: PB mixed with stand oil (SO)

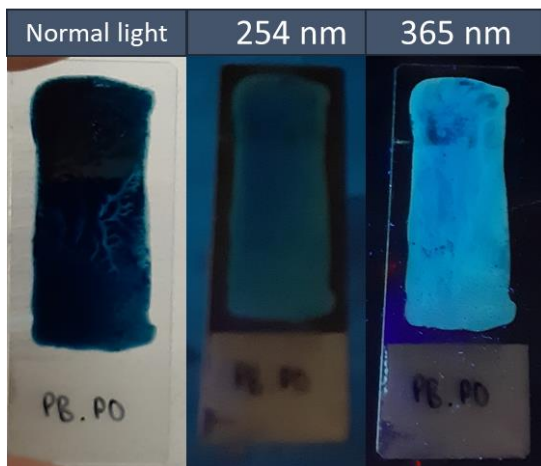


Figure F3: PB mixed with poppyseed oil (PO)

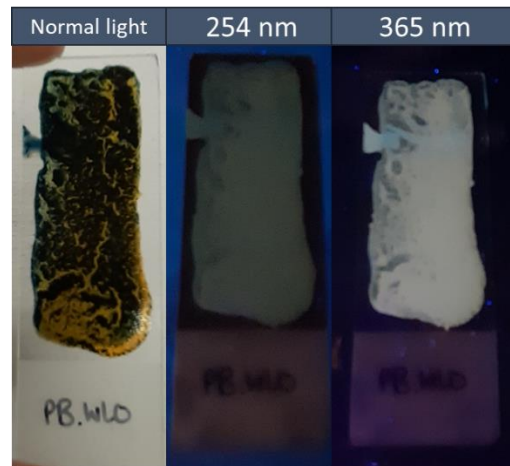


Figure F4: PB mixed with water-miscible linseed oil (WLO)

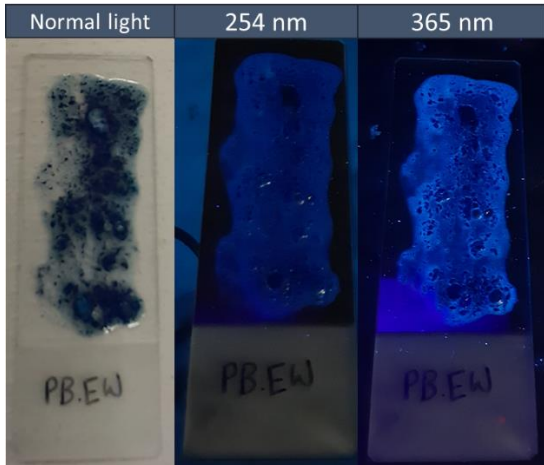


Figure F5: PB mixed with egg white (EW)

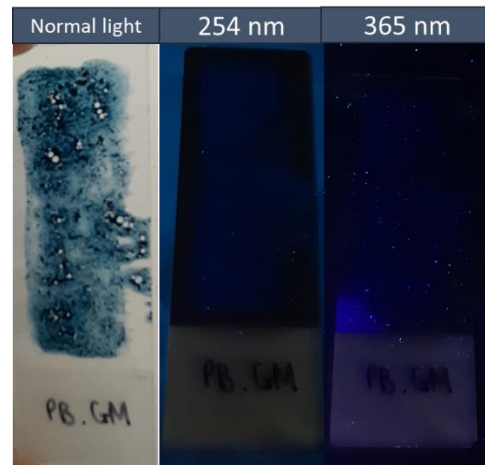


Figure F6: PB mixed with gilding milk (GM)

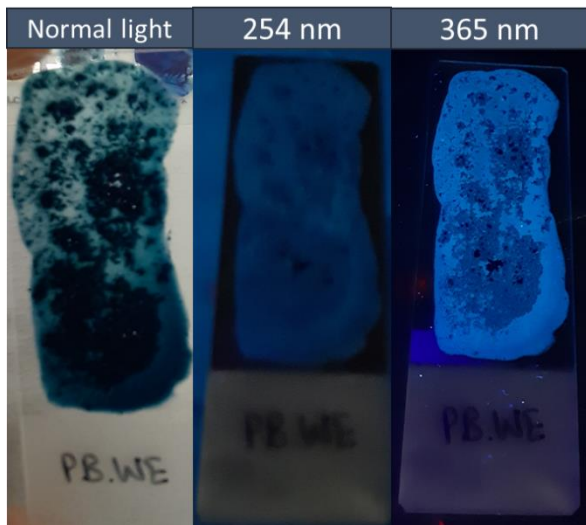


Figure F7: PB mixed with whole egg (WE)

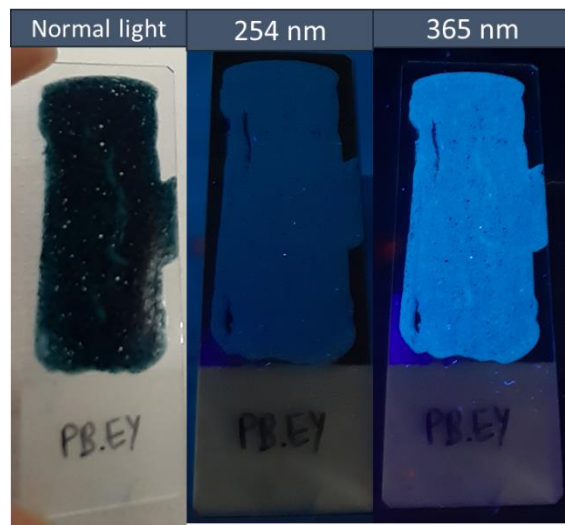


Figure F8: PB mixed with egg yolk (EY)

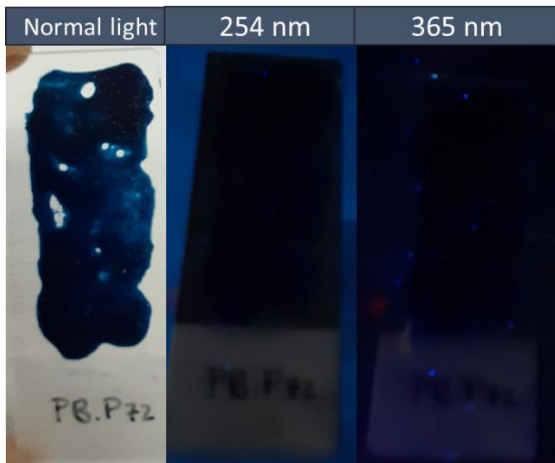


Figure F9: PB mixed with paraloid B72 (P72)

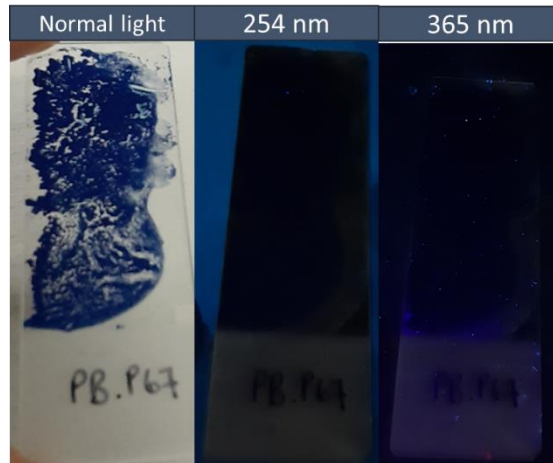


Figure F10: PB mixed with paraloid B67 (P67)

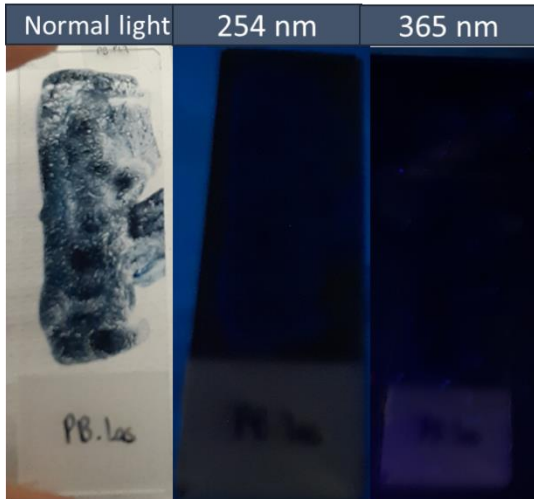


Figure F11: PB mixed with *lascarou (Las)*

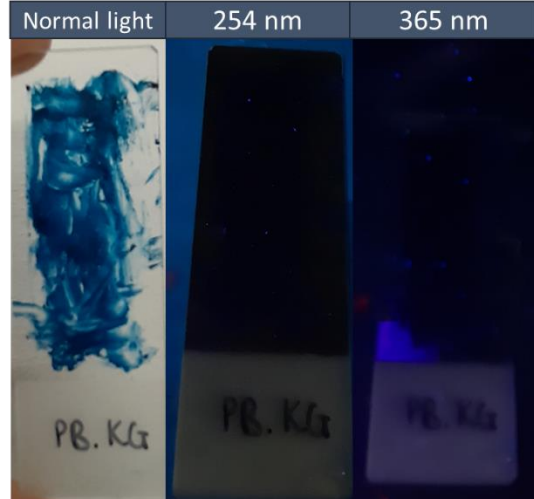


Figure F12: PB mixed with *Klusel G (KG)*

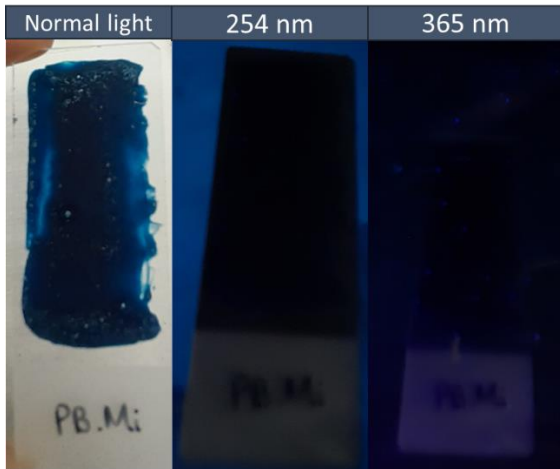


Figure F13: PB mixed with *mowiol (Mi)*

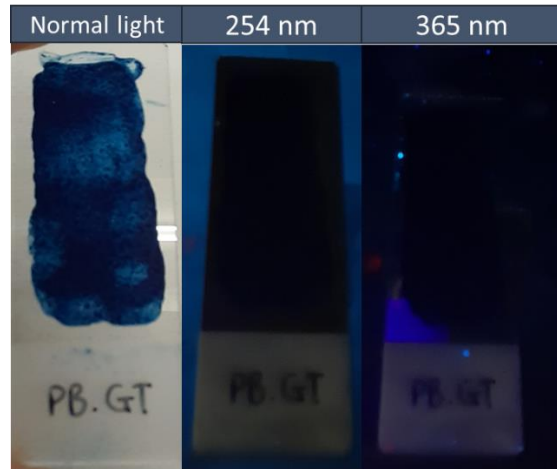


Figure F14: PB mixed with *gum Tragacanth (GT)*

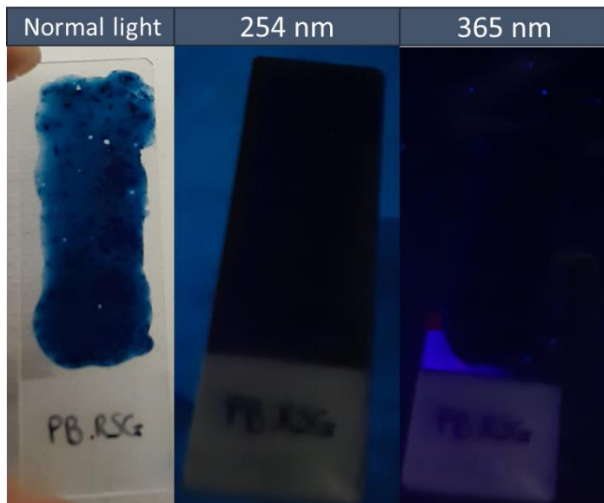


Figure F15: PB mixed with *rabbit skin glue (RSG)*

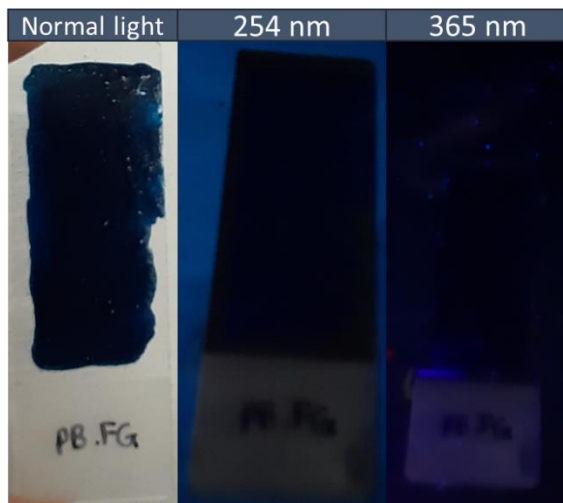


Figure F16: PB mixed with *fish glue (FG)*

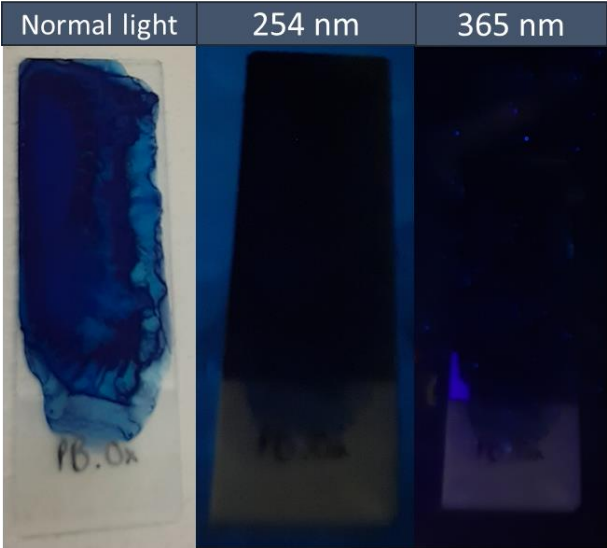


Figure F17: PB mixed with ox gall (OX)

Addendum G

Fluorescence images of Indian yellow (IY) samples

Each pigment-binder mixture was photographed under normal ambient white light, and under a UV lamp. Two wavelengths were used with UV light, namely 254 nm (the middle image) and 365 nm (the right-hand side image).

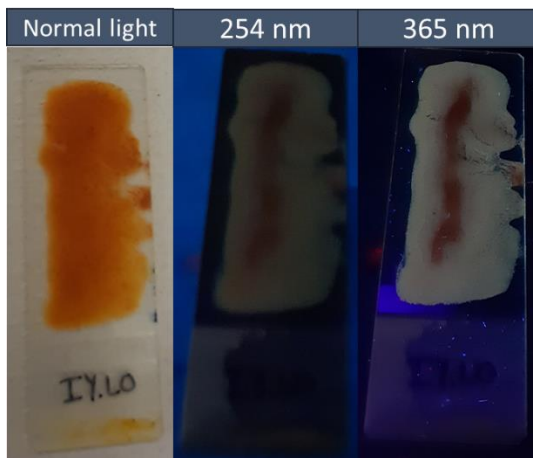


Figure G1: IY mixed with linseed oil (LO)

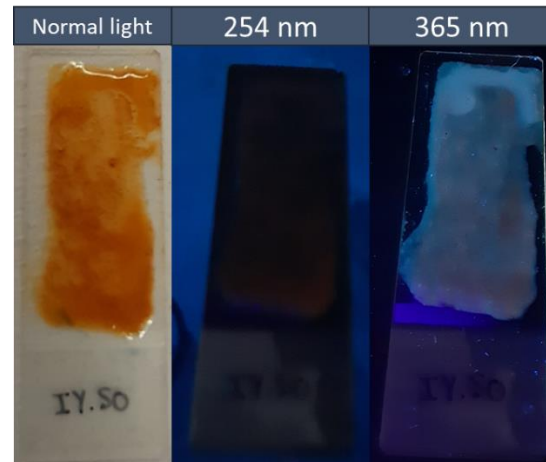


Figure G2: IY mixed with stand oil (SO)

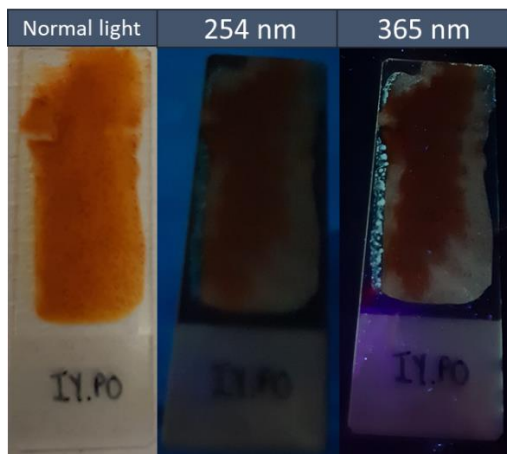


Figure G3: IY mixed with poppyseed oil (PO)

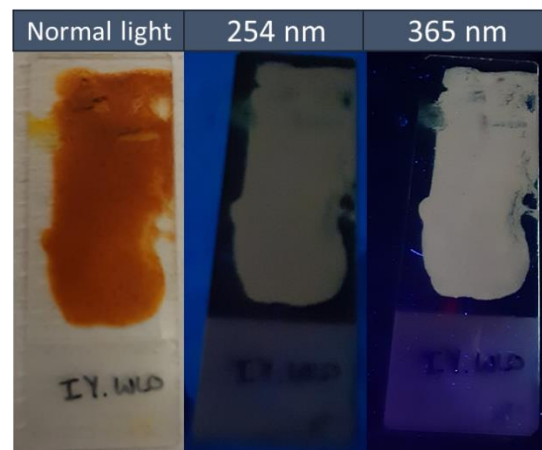


Figure G4: IY mixed with water-miscible linseed oil (WLO)

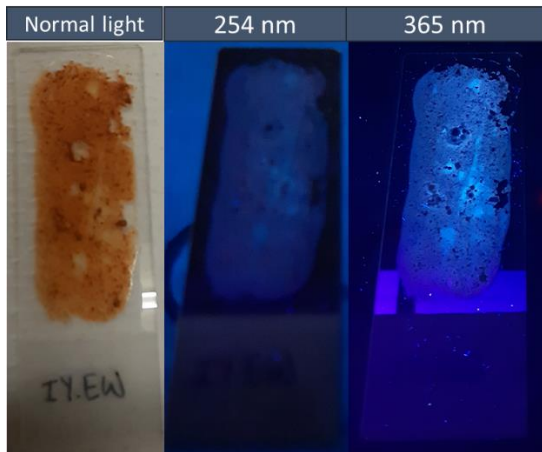


Figure G5: IY mixed with egg white (EW)

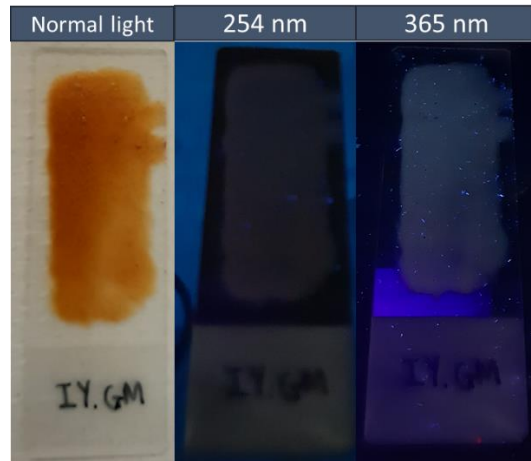


Figure G6: IY mixed with gilding milk (GM)

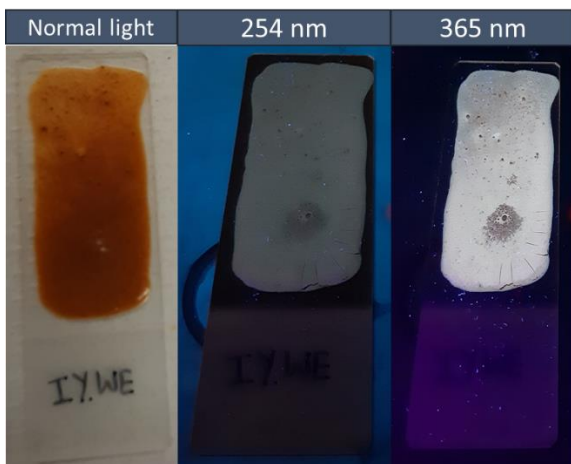


Figure G7: IY mixed with whole egg (WE)

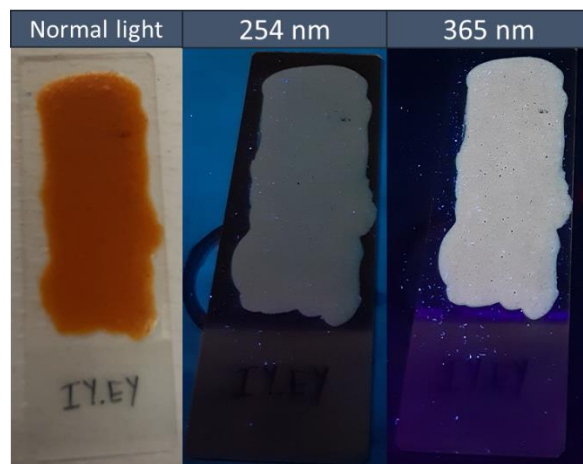


Figure G8: IY mixed with egg yolk (EY)

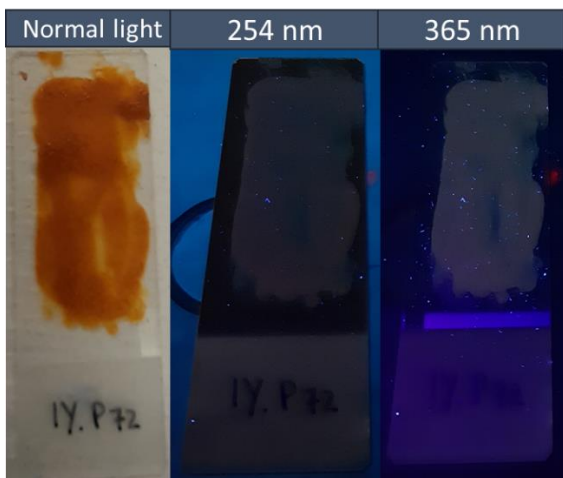


Figure G9: IY mixed with paraloid B72 (P72)

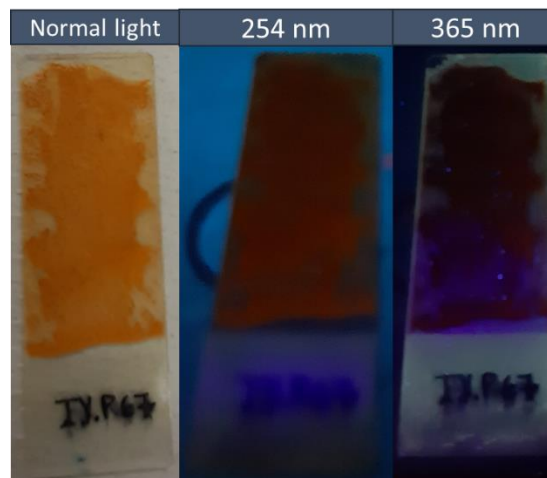


Figure G10: IY mixed with paraloid B67 (P67)

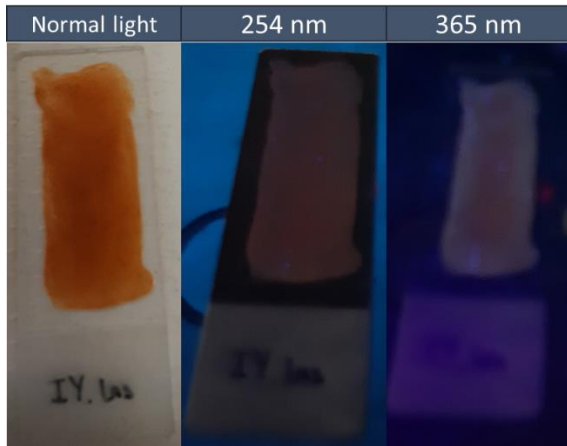


Figure G11: IY mixed with *lascoux* (Las)

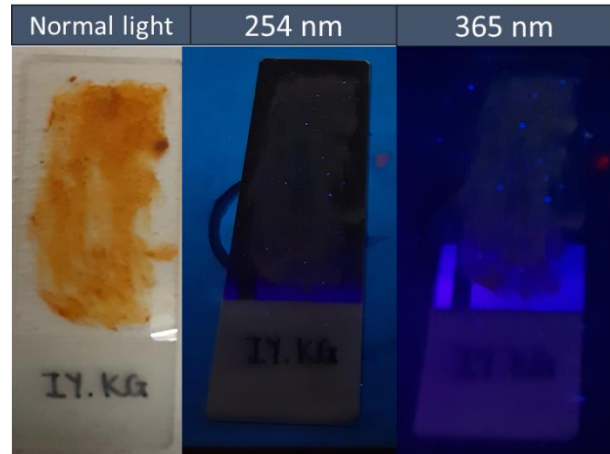


Figure G12: IY mixed with *Klusel G* (KG)

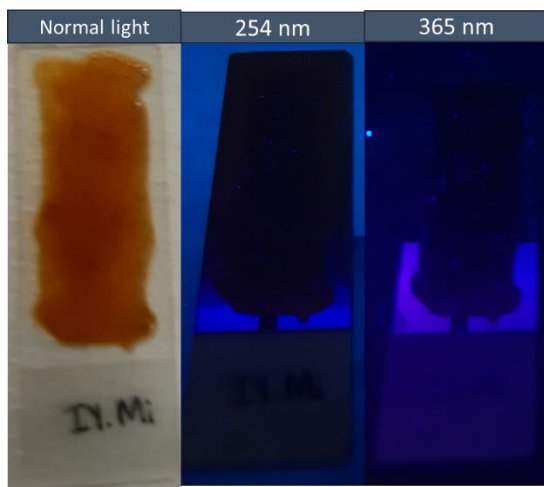


Figure G13: IY mixed with *mowiol* (Mi)

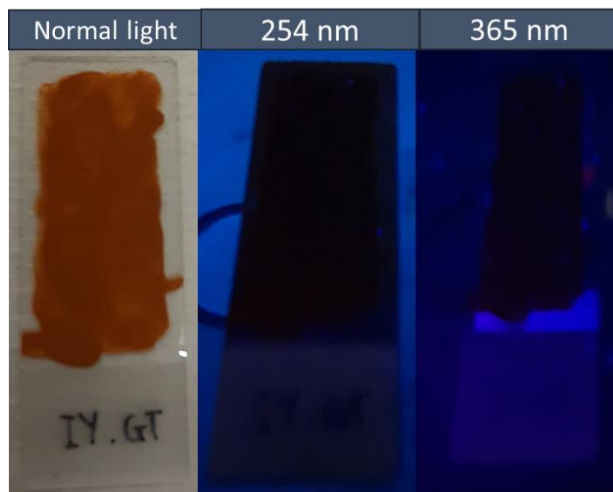


Figure G14: IY mixed with *gum Tragacanth* (GT)

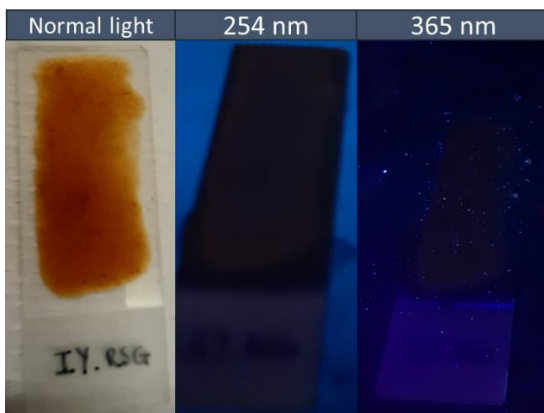


Figure G15: IY mixed with *rabbit skin glue* (RSG)

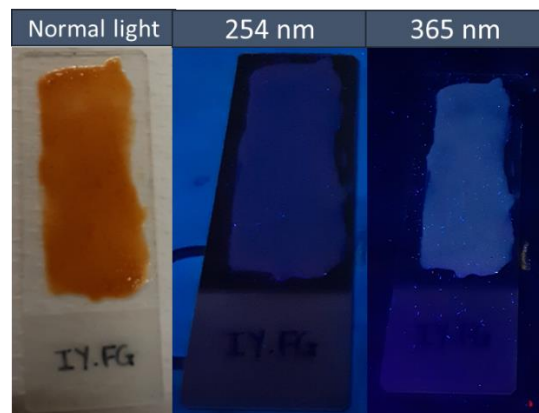


Figure G16: IY mixed with *fish glue* (FG)

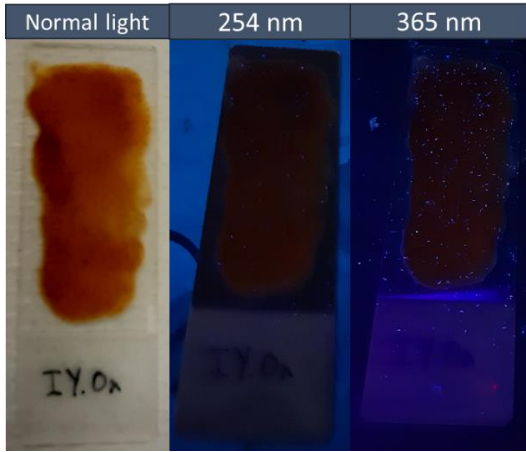


Figure G17: IY mixed with ox gall (OX)

Addendum H

Summary of fluorescence of binders from previous studies

	Peak position (nm)	Description of curve	Half width (nm)
Rabbit Skin Glue			
Pure binder	395	Broad, Symmetrical	349-453 (104)
Fish Glue			
Pure binder	406	Broad, right handed skew	366-485 (119)
Whole egg			
Pure binder	355	One very broad peak	324-440 (116)
Egg yolk			
Pure binder	357	One peak	330-405 (75)
Egg White			
Pure binder	352	Sharp peak	326-384 (58)
Ox gall			
Pure binder	395	Very broad peak	To broad to measure
Gilding milk			
Pure binder	391	One peak	352-444 (92)
Gum Arabic			
Pure binder	Could not be measured due to flaking of paint on microscope slide.		
Gum Tragacanth			
Pure binder	394	Broad peak	To broad to measure
Klusel G			
Pure binder	397		353-437 (84)
Mowiol			
Pure binder	394		353-444 (91)
Paraloid B72			
Pure binder	393		354-442 (88)
Paraloid B67			
Pure binder	395		Too broad to measure

Addendum I

Outputs from this Project

Published paper:

Cairns L, Forbes P. Insights into the yellowing of drying oils using fluorescence spectroscopy. *Heritage Science*. 2020;8(59):1-11. Doi: 10.1186/s40494-020-00403-1

Oral presentation:

Cairns L. The South African Spectroscopy Society's Young student Symposium (SASS-YSS), Midrand: 2019. Oral presentation on research entitled: *Insights into the yellowing of drying oils using fluorescence spectroscopy*.

Poster presentation:

Cairns LK. Forbes PBC. *Exploring the surface of paintings using fluorescence spectroscopy*. [Poster]. Exhibited at the summer school for Advanced Mass Spectrometry Applied in Cultural Heritage, Bordeaux, France: 2019.

Addendum J

Published journal paper in *Heritage Science*

Cairns and Forbes *Herit Sci* (2020) 8:59
<https://doi.org/10.1186/s40494-020-00403-1>

 Heritage Science

RESEARCH ARTICLE

Open Access

Insights into the yellowing of drying oils using fluorescence spectroscopy



L. K. Cairns and P. B. C. Forbes* 

Abstract

Drying oils are commonly used in paintings and are prone to yellow discolouration from aging. Although there are numerous studies aimed at understanding their chemical composition, the yellowing process and its effects on the underlying fluorescence emission of the oils are not fully understood. In this study, four different commercially available oils, namely linseed, water-miscible linseed-, stand- and poppy seed oil, were analysed using UV-visible absorption and fluorescence spectroscopy. Both liquid and cured, solid film oils were analysed. Liquid oils show a structured absorption pattern, of which only two weakly absorbing peaks (λ_{ex} 300 and 315 nm) result in fluorescence emission (λ_{em} 330 and 410 nm). The solid film lacks the structured pattern seen in the liquid oil's absorption spectrum, showing instead a broad absorption peak. At an excitation wavelength (λ_{ex}) of 365 nm the cured film normally fluoresces at λ_{em} 440 nm but is seen to shift to λ_{em} 550 nm as a result of yellowing. Artificial aging techniques, applied to the oils in order to cause a large degree of yellow discolouration, were seen to induce a large bathochromic shift in their fluorescence spectra. A correlation between the degree of discolouration and the shift in fluorescence is demonstrated, giving rise to a quantitative method that can be used to monitor the yellow discolouration. By non-destructively quantifying the degree of discolouration, colour-reconstruction of paintings could be performed to identify what the paintings looked like before degradation.

Keywords: Drying oils, Yellowing, Fluorescence spectroscopy, Absorption spectroscopy, Artificial aging, Painting

Introduction

Drying oils have been used in paintings as a binding medium since the 15th century [1–3]. Their ability to dry and form a solid film under ambient conditions [4] can be attributed to the unsaturation in oils, which facilitates polymerization [2]. The properties of each oil are largely dependent on the type of fatty acids present; for example, oils with a high unsaturated fatty acid content dry faster but have a greater tendency to yellow with age [3, 5–8]. Linseed-, poppy seed-, as well as walnut- or safflower-oil, which are commonly used in paintings, contain high concentrations of the unsaturated fatty acids, linolenic and linoleic acid (Table 1) [9]. Linseed oil is extracted from the flax plant (*Linum usitatissimum*), which contains

large amounts of unsaturated fatty acids [3]. Water-miscible linseed oil contains the same oil content as linseed oil with an added emulsifier that increases hydrophilicity and thereby allows for water to rinse paint brushes, instead of toxic organic solvents [2]. Water-miscible oil paints were introduced to the artist's palette around the 1990s [10] although oil and water paint mixtures had previously been used for centuries [11]. Stand oil is a form of linseed oil that has been pre-polymerised through heat treatment. Poppy seed oil is extracted from *Papaver somniferum* seeds and has a lower degree of unsaturation [1]. There are numerous manufacturing processes, and thus numerous historical formulations, for the production of drying oils [12, 13], however, the oils used for this study are representative of the 21st century artist's palette, and therefore commercially available drying oils used were tested.

*Correspondence: patricia.forbes@up.ac.za
Department of Chemistry, Faculty of Natural and Agricultural Sciences,
University of Pretoria, Pretoria 0002, South Africa



©The Author(s) 2020. This article is licensed under a Creative Commons Attribution 4.0 International License, which permits use, sharing, adaptation, distribution and reproduction in any medium or format, as long as you give appropriate credit to the original author(s) and the source, provide a link to the Creative Commons licence, and indicate if changes were made. The images or other third party material in this article are included in the article's Creative Commons licence, unless indicated otherwise in a credit line to the material. If material is not included in the article's Creative Commons licence and your intended use is not permitted by statutory regulation or exceeds the permitted use, you will need to obtain permission directly from the copyright holder. To view a copy of this licence, visit <http://creativecommons.org/licenses/by/4.0/>. The Creative Commons Public Domain Dedication waiver (<http://creativecommons.org/publicdomain/zero/1.0/>) applies to the data made available in this article, unless otherwise stated in a credit line to the data.

Table 1 The fatty acid content of drying oils typically present in paintings [6, 14, 15]

Fatty acids		Linseed oil (%)	Poppy seed oil (%)	Walnut oil (%)	Safflower oil (%)
Palmitic acid	(C16:0*)	6–8	8–12	3–7	5.5–7
Stearic acid	(C18:0)	3–6	2–3	0.5–3	2–3
Oleic acid	(C18:1)	14–24	12–17	9–30	10–35
Linoleic acids	(C18:2)	14–19	55–65	57–76	55–81
Linolenic acid	(C18:3)	48–60	3–8	2–16	0–1

* C16 indicates the number of carbons in the chain (in this case, 16 carbons), while the second number indicates the degree of unsaturation (number of double bonds)

The discolouration of paintings is of concern, as we can no longer appreciate a painting for its original colours. There are several factors that lead to discolouration such as the degradation of pigments [16–19], formation of lead soaps [20–23], the yellowing of varnish [24, 25] and oil binding media [26–28]. This study focuses on the discolouration of drying oils. Drying oils are clear or faintly coloured when applied to paintings, but gradually develop a strong yellow discoloration over time. This discoloration is an unavoidable property of oil paint [2]. The basis of the yellow colour remains poorly understood, despite the wide range of reported chemical compounds that are suspected to play a role in this regard [2, 4, 26–32]. The currently accepted view is that the yellowing is a result of two compounds, one which reflects yellow light, and another which fluoresces yellow, however, their identities are still unknown. Together these two compounds are thought to make up the characteristic intense yellow colour [29].

Although little is known of the yellowing of oils, there are a few trends associated with the yellowing process. Firstly, a high degree of unsaturation in the oil leads to significant discolouration. Therefore, linseed oil will yellow to a greater extent than poppy seed oil, which is less unsaturated [2, 33]. Secondly, the yellowing has been found to be accelerated by certain metal-containing pigments, such as lead white, copper carbonate and various cobalt pigments [26, 33–36]. Thirdly, the discolouration can be bleached and can go through cycles of yellowing and bleaching, depending on the storage conditions; light exposure reverses the yellowing, while dark conditions promote yellowing, which suggests that photodegradation reactions reverse the discolouration [26, 36]. Lastly, there is a correlation between the fluorescence of drying oils and the degree of yellowing: fluorescence emission shifts from blue to green as the samples yellow [26, 29, 37].

In contrast to yellowing, the fluorescent property of oils is beneficial as it can aid in diagnostic tests that identify areas of previous restoration [38–40].

Fluorescence imaging of a painting is obtained by illuminating its surface with ultra-violet (UV) light and observing the visible-light fluorescence. The development of the LED micro-spectrofluorometer (LED μ SF) and other handheld spectrofluorometers has allowed for more sophisticated spectroscopic analysis [41–45]. The fluorescence of a painting can now be measured as a spectrum, with exact emission wavelengths, instead of a single colour determined subjectively by the eye.

This study aimed to identify changes in yellowing, during the curing of drying oils, through the use of high-sensitivity fluorescence spectroscopy. Four commercially available drying oils were exposed to different light conditions (sun light, UV-light and dark) during the curing process, and afterwards were exposed to artificial aging mechanisms (UV-light and an ammonia vapour chamber respectively) to accelerate yellowing. By correlating the fluorescence changes with the degree of yellowing, digital colour corrections can be performed on paintings without the need to sample. This allows a viewer to see what the colours would likely have looked like before age-related degradation occurred.

Experimental methods

Sample preparation

Solid film samples were prepared by painting the drying oils onto glass microscope slides which were allowed to dry in order for film formation to occur. Four drying oils were tested: linseed oil (LO), water-miscible linseed oil (WLO), stand oil (SO) and poppy seed oil (PO), all from Winsor & Newton, UK. The solid samples were naturally aged for 2 years under ambient temperature (20 ± 5 °C) and humidity ($50 \pm 20\%$ RH) in a drawer. Fluctuations in temperature and humidity are resultant of seasonal changes. Liquid samples were prepared by dissolving 10 μ L of the liquid oil in 1000 μ L of ethanol (99.9% from ACE, South Africa) or other solvent. The solvents used were diethyl ether (90% SAR Chem, South Africa), ethanol, dichloromethane and toluene at 95% purity (ACE, South Africa). Acetonitrile, hexane and toluene were HPLC grade (Sigma Aldrich, South Africa), while

cyclohexane and chloroform were 99.5% purity (Rad-Chem, South Africa).

Solid-liquid extraction was performed on the dried oils by placing 0.500 mg cured oil into a vial with 1000 μ L ethanol. The vial was then ultrasonicated at a high frequency (50 Hz) for 30 min using a Scientech ultrasonic cleaner (Labtec, South Africa). Additionally, the solid film on a microscope slide was extracted through Soxhlet extraction, using 100 mL ethanol for 24 h. The liquid extract was yellow coloured, while the remaining solid film was severely cracked.

Samples for artificial aging were prepared by painting the drying oils onto microscope slides covered with pieces of painter's canvas to facilitate the accelerated aging with minimal alligator-skin formation (wrinkling of paint caused by rapid drying of the upper layers of the oil). These samples were solely used for fluorescence studies and to monitor the changes in fluorescence during artificial aging.

Artificial ageing and curing

Artificial ageing was achieved by exposing the samples to elevated temperatures, artificial light and a saturated chamber of ammonia. An ammonia chamber was prepared to induce yellowing. The wooden chamber (25 \times 25 \times 60 cm) was sealed with rubber and had a glass window through which the colour change could be monitored. A beaker containing 40 mL of 25% ammonia solution was placed in the chamber to saturate the air with ammonia vapour. Two main sets of samples were treated, the first set of samples was exposed to various ageing environments while wet, and the samples were cured under the ageing conditions. The second set was first cured in a dark chamber for 3 months after which the samples were exposed to the artificial ageing conditions.

Within each set, there were various times for which a sample was exposed to the ageing conditions. The first set of 44 samples were cured under the ageing conditions: two samples for each oil (a total of 8 samples) were cured exposed to an elevated temperature (80 $^{\circ}$ C), with one sample exposed for 3 h and the other for 6 h. Another set of 5 samples per oil were cured for either 24 h, 1 week, 2 weeks, 3 weeks or 1 month under a UVC lamp (254 nm), thereafter they were placed in a dark drawer. Another set of 4 samples for each oil were cured in the ammonia chamber under ambient indoor light conditions, for either 24 h, 1 week, 2 weeks or 1 month, and thereafter placed in a dark drawer.

The second set of 24 samples was cured in a dark drawer for 3 months before exposing the samples to the different ageing conditions. Two samples for each oil were placed under the UV lamp for either 24 h or 1 week, and thereafter were placed in a dark drawer. Another set

of 4 samples for each oil were placed in the ammonia chamber for either 24 h, 1 week, 2 weeks or 1 month and thereafter were stored in a dark drawer prior to analysis.

Absorption and fluorescence spectroscopy

During both absorption and fluorescence studies, liquid samples were held in 10 mm quartz cuvettes, which were washed between each experiment using 10% Piranha solution. For fluorescence studies, painted samples on microscope slides were analysed in a slide-holder at a 30 $^{\circ}$ angle to the incident light, to prevent reflected incident light from entering the detector.

UV-visible light absorption spectrophotometer

UV-visible absorption was done using a Cary 100-Bio UV-visible spectrophotometer (Varian, USA) equipped with a visible light source lamp and a deuterium lamp, which switched at 350 nm. Scans were measured from 800–200 nm with a Czerny-Turner 0.28 m monochromator equipped with a R928 photomultiplier tube (PMT) detector.

Fluorescence spectrophotometer

Fluorescence measurements were made on a Fluoromax-4 Spectrofluorometer (Horiba, Japan) with a continuous 150 W xenon lamp and photodiode detector. A single monochromator was used for excitation and emission wavelengths, with a slit width of 5 nm for both the light source and the detector.

Chromatographic fractionation

Samples were analysed using a 1260 Infinity binary high-performance liquid chromatography (HPLC) system (Agilent, USA), equipped with an Agilent 1260 auto sampler and a XSelect[®] HSS T3 5 μ m (4.6 mm \times 150 mm) reverse phase column (Waters, South Africa). The 1260 Infinity Photodiode-Array Detector (PDA) (Agilent, USA) used a deuterium lamp (wavelength range 190 to 640 nm), with optical slit of 4 nm. Chromatograms were monitored using select wavelengths: 240, 260, 280, 300, 315 and 400 nm.

Separation was achieved by means of a reverse phase step gradient using acetonitrile (A) and water (B) both with 0.1% formic acid, at a 4.00 μ L/min flow rate. Initial conditions were: 20% A: 80% B, ramped up to 100% A within 12 min, held constant for 14 min. Thereafter, the gradient was rapidly changed back to the initial conditions of 20% A in 2 min and then held constant for 2 min. The HPLC system was fitted with a re-usable online micro solid phase extraction (μ SPE) collection unit. Two fractions were manually collected onto the Hysphere-GP 20 \times 2 mm μ SPE cartridges (Spark Holland, The

Netherlands) and were then eluted using HPLC grade methanol (Sigma Aldrich, South Africa).

Results and discussion

UV-absorption and fluorescence spectroscopic changes due to curing

The absorption spectra of drying oils were recorded for the liquid oils (dissolved in ethanol) and the solid films. There were few differences in the absorption between the four different drying oils in solution (Fig. 1). All oils have two strongly UV-absorbing peaks, one between 200 and 215 nm while the second, less intense peak occurred at 230 nm. The absorption at 200–215 nm indicates the presence of polyenes and unsaturated α,β -ketones [46, 47]. Between 250 and 350 nm, the oils show weak absorptive peaks indicating the presence of an unconjugated chromophore containing a heteroatom [46].

The spectra of linseed oil (LO) and water-miscible linseed oil (WLO) are the most similar: both show peaks at about 280, 300 and 315 nm, while the peak at 269 nm (in the presence of another peak at 315 nm) is characteristic of WLO. The spectral similarity between LO and WLO are not surprising, considering the fact that WLO is LO with an emulsifier that increases its solubility in water, but other than that, the two are chemically identical [48]. Poppy seed oil (PO) has three additional moderately absorbing peaks, at 258, 269 and 279 nm, of which the first peak is characteristic of PO and does not appear in either LO or WLO. Stand oil (SO) does not have any peaks in the range between 250 and 350 nm, suggesting that the compounds that would normally give rise to peaks in this area may have reacted during the pre-polymerization process [3]. In contrast to the absorption

spectra of samples in solution, the cured films show only a broad peaked absorption at 300 nm (Fig. 2).

The absorption patterns give an indication of the excitation wavelength which will result in optimal fluorescence. Of the 5 distinct absorption peaks in liquid linseed oil, only two resulted in fluorescence. Excitation (λ_{ex}) at 300 nm gives a two-peaked fluorescence signal (Fig. 3) while excitation at 315 nm gives only one. The emission at 330 nm only appears upon excitation at 300 nm, while the peak at 412 nm appears when both excitation wavelengths (λ_{ex} 300 and 315 nm) are used. Although PO and SO show no absorption at 300 and 315 nm, both

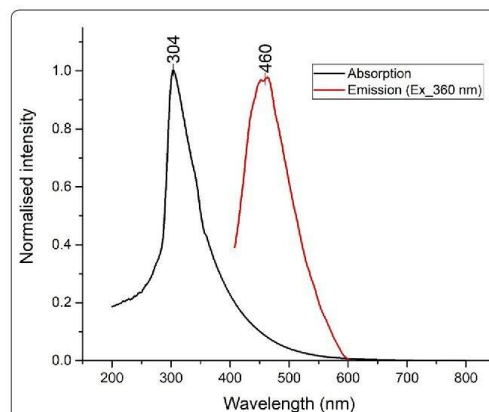


Fig. 2 Fluorescence and absorption spectra of cured drying oils (once they formed a solid film). All oils showed the same peaks

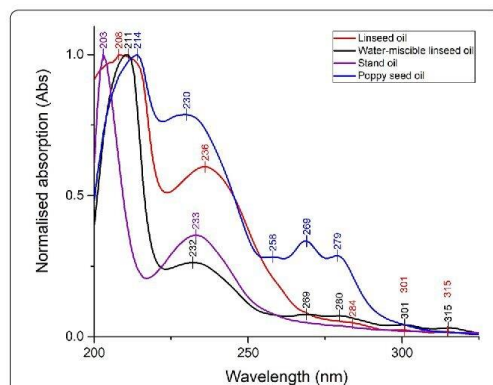


Fig. 1 Absorption spectra of the liquid drying oils dissolved in ethanol. All spectra were blank corrected and normalised to 1

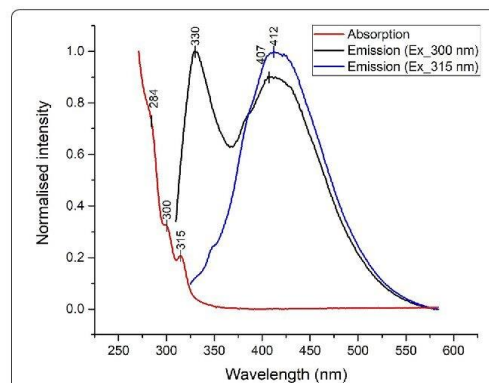


Fig. 3 Absorption spectra of liquid linseed oil dissolved in ethanol (red) and corresponding fluorescence spectra, at an excitation wavelength (λ_{ex}) 300 nm (black) and λ_{ex} 315 nm (blue), respectively

excitation wavelengths give the same fluorescence spectra as LO, and no additional fluorescence is observed.

Curing of the liquid-phase samples shifts the fluorescence from a weak ultraviolet emission (330 and ~410 nm) to a strong blue-green fluorescence in the solid film (Fig. 2). Bathochromic shifts (shifts to longer wavelengths) of such magnitude (50 to 100 nm) are not uncommon and are often induced through changes in solvent polarity or hydrogen bonding [49]. Drying oils are cured through an auto-oxidation process which results in a change from a non-polar liquid oil to a polar polymer network [47]. To determine whether the bathochromic shift is a result of a polarity change, the Lippert equation can be used [49]. The equation assumes that no external factors interact with the fluorophore; additional interactions, such as hydrogen bonding or the formation of charge-transfer states, can be detected as deviations from this generalised state. In this case, applying the Lippert equation reveals no trend, indicating that the bathochromic shift is not a result of polarity changes (Additional file 1: Figure S1). Interestingly, the intensity of the two fluorescent peaks from the liquid samples is found to be solvent-dependent. Polar solvents result in both peaks having similar fluorescence intensities, whereas non-polar solvents halve the intensity of the first peak (330 nm) while the second peak (410 nm) remains at a reasonably constant intensity (Additional file 1: Figure S2).

The solvent-extractable components of the cured oil were analysed. The cured linseed oil film does not fully dissolve, regardless of the polarity of solvent used. Ethanol proves to yield the largest fluorescent intensity, confirming literature reports of ethanol being the most efficient solvent for extracting compounds from LO [50].

The extracts (Soxhlet- and ultrasonic-extractions) show a single absorption peak (315 nm) which corresponds to that of the liquid oil, with the absence of the absorption peak at 300 nm. The yellow extract was found to be stable with no noticeable colour changes after a period of a month. The fluorescence of the extract was tested directly after extraction and a month later to determine whether any degradation or instability had occurred, and the fluorescence was found to remain stable at 418 nm.

The fluorescence peak of the extract at 418 nm corresponds to liquid LO and not its solid phase (Table 2). The remaining solid film remains strongly fluorescent under UV light, and shows no change in fluorescence emission. However, the film was severely cracked and could not be used for further absorption studies.

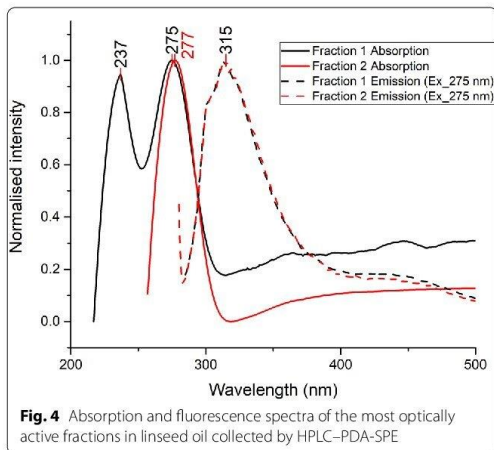
The ethanol extract of the cured oil was fractionated using high performance liquid chromatography (HPLC) coupled to a photodiode array detector (PDA) to identify the most optically active fractions. The chromatograms were monitored using a range of absorption wavelengths, as no peaks were seen using 315 nm. Interestingly, only 280 nm show peaks on the chromatogram. Two fractions were collected corresponding to the detection of two large absorption peaks, at 12.8 min (fraction 1) and 13.2 min (fraction 2; Additional file 1: Figure S3) respectively. These two peaks were found upon analysis of both the liquid oil and cured oil extracts.

Both fraction 1 and 2 have the same strong absorption peak at 275 nm, while fraction 1 has an additional peak at 232 nm (Fig. 4 and Table 2). The fluorescence emission of the two fractions are both at 315 nm (λ_{ex} 275 nm; Δ 40 nm), which does not correspond to that of the liquid or cured oil (Table 2). This suggests that the absorption at 315 nm is highly dependent on the oil matrix, and that

Table 2 Shifts in absorption and emission bands of the liquid sample, cured film, ethanol extract and the oil film after ethanol extraction, as well as the two purified HPLC fractions in methanol

	Absorption band maximum; λ_{ex} (nm)	Emission band maximum; λ_{em} (nm)	Stokes shift; Δ (nm)
Liquid	207	–	–
	236	–	–
	283	–	–
	300	329, 412	29, 112
	315	412	97
Cured oil film	300	445 → 550*	145 → 250*
Ethanol extract from cured oil	318	418	100
Cured oil film after ethanol extraction	–	445	–
Fraction 1	232	–	–
	275	315	40
Fraction 2	275	315	40

* Fluorescence of cured oil changes upon ageing; discussed in "Artificial ageing" section



once the compounds are isolated, they show different excitation spectra. The fractions have a smaller Stokes shift than the liquid oil and the extract of cured oil, suggesting that the isolated compound is not the same as the compound that results in the fluorescence in the cured oil.

The preceding findings indicate that the compound giving rise to the first peak in liquid oil, at λ_{ex} 300 nm; λ_{em} 330 nm, reacts as part of a polymer structure, and cannot be extracted. While the second compound, which gives rise to the second peak at λ_{ex} 315 nm; λ_{em} 410 nm, remains unreacted in the cured oil, and emits only in solution. This could be interpreted to mean that the first peak contributes significantly to the strong blue fluorescence in the solid phase, which is stabilised during the polymerization process. This is commonly seen in non-conjugated polymer dots (NCPDs) where poorly fluorescent subfluorophores (heteroatom-containing double bonds; C=O, C=N, N=O) are enhanced through chemical linking or physical immobilisation [51]. Subfluorophores have intrinsically weak fluorescence, although it increases drastically with vibrational and rotational restriction. NCPDs have characteristic blue fluorescence and can develop a bathochromic shift when the electron density over the subfluorophore increases [52]. This bathochromic shift in drying is seen as the oil ages (as is further explained in “Artificial ageing” section).

Artificial ageing

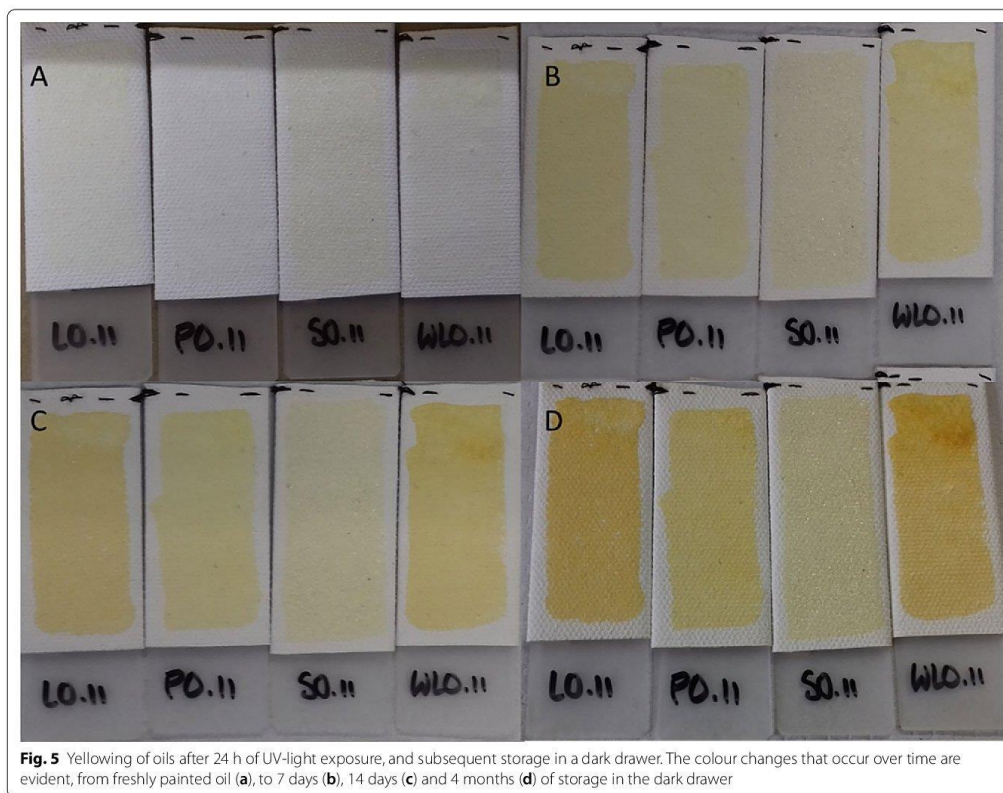
Oils that were cured under UVC light (254 nm) showed immediate alligator skin formation and bleaching. The accelerated curing of oils exposed to UV light is due to the radical mechanism of curing which is initiated

through light [52–54]. After exposure to UV light, the cured samples were placed in dark drawers, which visibly accelerated the yellowing of the oils (Fig. 5). As the samples aged, the fluorescence was measured in weekly intervals, for 2 months, and then monthly, for another 6 months. It is important to note that the ageing methods employed in this study were extreme exposure to light and dark, which does not represent the typical light conditions in museums. However, the dark conditions could represent the storage areas of museum where paintings will reside for months in the dark. The extreme light conditions accelerated all ageing reactions, which allowed for a short-term monitoring of fluorescence changes [55, 56].

With aging, a bathochromic shift is observed, which can be related to the yellowing effect (Fig. 6) [29, 39, 57–59]. The fluorescence emission maximum is initially at 460 nm but increases exponentially to 500–510 nm (a green colour), where it reaches a plateau (Fig. 7). An additional few months in the dark drawer increases the emission further to 550 nm, imparting a yellow-green fluorescent colour (Additional file 1: Figure S4) to the sample. This is the general trend for samples cured under ultra-violet light. The formation of a plateau of constant emission indicates that there are two processes that cause the bathochromic shift. This confirms that oil paintings are not only continuously changing, but that there are multiple steps in the process that can occur over a period of months.

Drying oils that have been cured under ambient conditions (dark drawer at 20 ± 5 °C and $50 \pm 20\%$ RH) and then exposed to UV light after 3 months, show a different trend. Instead of reaching a plateau, a steadily increasing emission wavelength is observed, that passes from blue (450–490 nm), to green (495–570 nm) and to yellow (570–590 nm) fluorescence (Fig. 7). Samples that were cured in sunlight did not show any yellowing, and thus no changes in fluorescence. Aging under dark conditions causes discolouration, however, without sunlight or UV-light exposure, the discolouration takes much longer to develop. Natural aging can take up to 2 years to develop the same kind of discolouration that UV-light causes within 2 weeks.

The curing of drying oils in an ammonia chamber appears to inhibit the drying process, as the oils appeared to be as viscous as when they were initially applied. Drying oils that were cured in the dark showed some degree of drying within the same time frame as those kept in the ammonia chamber. Interestingly, uncured samples that were in the ammonia chamber for a longer period (1 month) showed accelerated yellowing once cured (after 4 months), while a short exposure time to ammonia does not affect the yellowing rate (Fig. 8). This could be because the ammonia is absorbed into the liquid, and

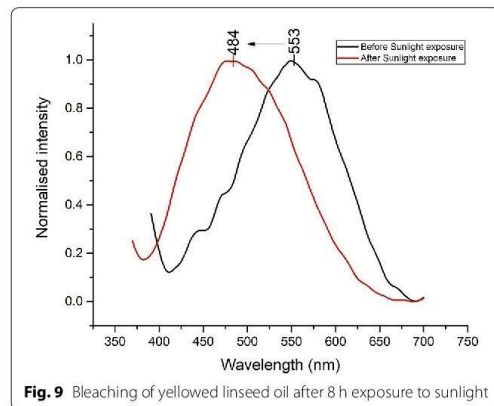
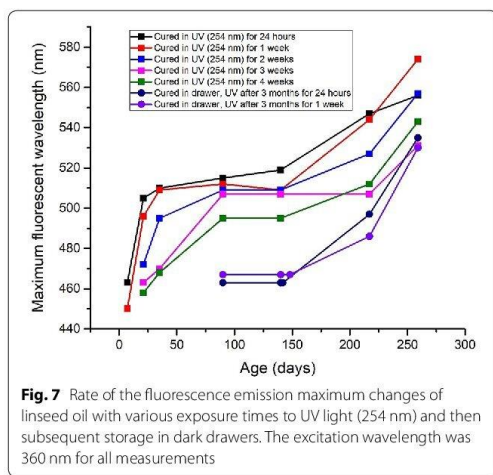
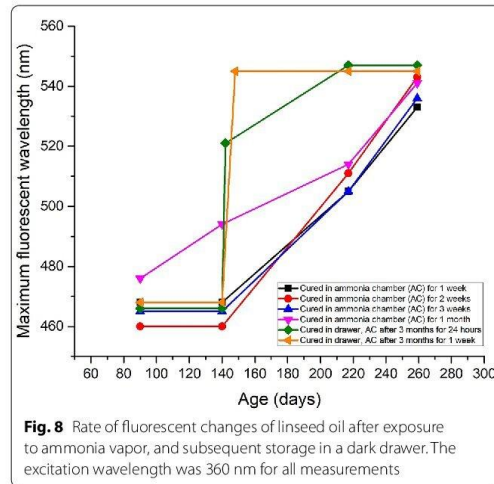
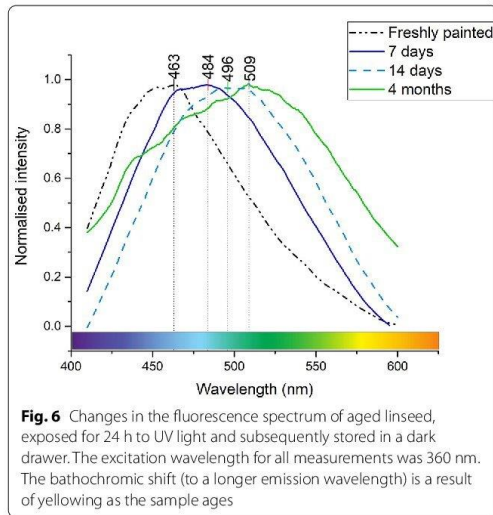


when the oils are cured, the ammonia becomes more readily available, which accelerates the rate of yellowing.

When the ambiently cured oils were placed (after 3 months of curing) in the ammonia chamber, the colour of the oil changed rapidly. Within 24 h, the saturated ammonia chamber changed all four oils to an orange-brown colour. The ammonia chamber caused the same degree of yellowing as UV-light treatment did, but within a 24-h period, rather than a month (Fig. 8). This supports the hypothesis that the presence of ammonia is a main cause for the acceleration of the yellowing found in oil paintings [29], and thus stresses the need to use ammonia-free cleaning products in museum environments. Previous studies have suggested the formation of a fluorescent aminoenamine in oils, which is responsible for bathochromic shifts [29, 30]. However, recent studies have shown that these isolated adducts may in fact not be fluorescent [60]. It is, however, still possible that the nitrogen-containing vapours are responsible for the colour changes through the formation of a fluorescent

compound, as there have been studies that demonstrate through infrared spectroscopy that the nitrogen content in drying oils increases as the oils age [32].

All stages of yellowing (identified by green and yellow fluorescence) were reversible in sunlight within 8 h of exposure, as is evident from the hypsochromic shift in fluorescence (Fig. 9). The yellowing is reversed in neither 254 nor 365 nm UV light (in a 24-h period), indicating that a broad light spectrum is needed to reverse the yellowing effects. Artificial aging under UV light accelerates the rate of yellowing but yellowing cannot be used as a measure of age as the painting can be bleached. A bleached painting will thereby appear younger while a freshly painted portrait might look old if stored in the dark. The yellowing cycle can be repeated numerous times and still undergo the same degree of yellowing and bleaching [8], the bleaching process is faster than the yellowing. This suggests a hysteresis curve, in which the extent of yellowing is related to the light exposure history of the painting. Previous studies that have monitored the



discolouration over several years have found a repetitive nature of the yellowing and bleaching of oils [33, 61]. Even though the bleaching is cyclic, it is important to stress that it is a photodegradation reaction and therefore affects the integrity of the paint and should be avoided.

Although all drying oils showed a similar trend in their rate of yellowing, they did not all yellow to the same extent. Linseed oil (both LO and WLO) shows the most intense colour changes, while poppy seed oil yellows less,

and stand oil hardly shows any yellowing. Poppy seed oil reaches a maximum fluorescence emission at 530 nm as a result of yellowing, while stand oil remains at 510 nm (Additional file 1: Figures S5, S6 for poppy seed oil and Additional file 1: Figures S7, S8 for stand oil). WLO takes longer to cure, but once cured, yellows much more rapidly than LO, reaching its maximum fluorescence emission at 570 nm (the same as LO; Additional file 1: Figures S9, S10). During the curing process of all oils, no noticeable yellowing occurred, whereas once cured, the rate of change in yellowing and fluorescence were a result of the aging mechanism employed.

The two-step process in fluorescence development was also observed in the colour changes, whereby the first incline lead to a yellow (Fig. 5a–d) and the second to a brown discolouration (Additional file 1: Figure S4). The brown discolouration became evidently visible with the discolouration from ammonia vapour, but occurred over several months in all samples. A shorter wavelength fluorescence (blue, 460 nm) indicates a yellow discolouration, while a longer wavelength (green or yellow; 500–550 nm) indicates that the oil has started to turn brown in colour. Although these observed changes were drastic, they are not unknown—paintings degrade over time [28, 62], which leads to colour changes. These colour changes can be a result of varnish discolouration [24], pigment degradation [16–18], or binder discolouration [26–28]. Pigments are commonly used for colour reconstructions, as they have been found to be irreversible [63]. Varnish is also known to be a major factor in the discolouration of paintings due to its yellowing tendencies and the formation of micro-cracks which turn the varnish a milky colour [25]. This can be accounted for by having a conservator remove the varnish layer. However, the process to determine the original colour of the binding medium is not as easily achieved, due to the cyclic nature of the discolouration.

Drying oils are found to bleach in light, whereas dark conditions accelerate discolouration. As there is no measure of the amount of ‘darkness’ a painting receives, the measure of the discolouration of binder is often misinterpreted. By relating the discolouration of drying oils to the fluorescence, the discolouration of drying oils can be accurately calculated regardless of the age of the painting or the light conditions to which it has been exposed.

Conclusion

The fluorescence of drying oils is largely dependent on the physical state of the oil. Liquid oils fluoresce in the ultra-violet range, and therefore cannot be seen by the naked eye. Cured oils fluoresce in the blue range, and shift to green (and sometimes yellow) fluorescence, as the oil yellows. Contrary to previous findings it is proposed that the fluorescence of drying oils is a result of subfluorophores which are poorly fluorescent in the liquid phase but become fluorescent once immobilised in the cured oil matrix. The bathochromic shift in fluorescence (from blue to green) is a result of increased rigidity in the cured oil matrix. The yellowing which is linked to the fluorescence of the oil is not a result of age, but rather of storage conditions, as was identified by the extreme storage conditions used in this study. Exposure to ammonia vapour rapidly increases the degree of yellowing, and therefore ammonia-based cleaning products should be avoided in museum environments, as the discolouration affects the

aesthetic value of artworks. Light bleaches the oil and thus reverses the fluorescence shift, while dark storage conditions promote yellowing and fluorescence changes. Although light bleaches the yellowing of drying oils, this is not advised as it could simultaneously cause irreversible photodegradation of certain pigments.

The yellow discolouration of oils is not always visible when pigments are present, and in mixtures with non-fluorescent pigments, the fluorescence can be used to identify the degree of discolouration. The fluorescence peak colour provides a measure of yellowing and can therefore, be used to do digital colour corrections of paintings. As fluorescence spectroscopy is non-destructive, it can be used to determine the extent of yellowing without the need of sampling and is thus an advisable method for the monitoring of discolouration in paintings.

Supplementary information

Supplementary information accompanies this paper at <https://doi.org/10.1186/s40494-020-00403-1>.

Additional file 1. Supplementary information.

Abbreviations

LO: Linseed oil; WLO: Water-miscible linseed oil; SO: Stand oil; PO: Poppy seed oil; λ_{em} : Emission wavelength; λ_{ex} : Excitation wavelength.

Acknowledgements

The authors would like to thank Isabelle McGinn and Maggi Loubser from the Tangible Heritage Conservation program at the University of Pretoria for their continual support throughout this project. The authors would also like to acknowledge and thank Dr Mamoalosi Selepe for assisting with HPLC analyses and Daniel Pretorius' contribution in editing the manuscript.

Authors' contributions

The whole database construction and analysis presented in the manuscript had been achieved by the first author. The second author provided samples and equipment and made significant contributions to the content, reviewed the whole text and made valuable comments and suggestions. All authors read and approved the final manuscript.

Funding

The authors confirm that they are not currently in receipt of any research funding relating to the research presented in this manuscript.

Availability of data and materials

The dataset generated and analysed during the current study is available from the corresponding author on reasonable request.

Competing interests

The authors declare that they have no competing interests.

Received: 18 February 2020 Accepted: 11 June 2020

Published online: 19 June 2020

References

1. Izzo FC. 20th century artists' oil paints: a chemical-physical survey. (Thesis) 2011.
2. Poth U. Drying oils and related products. Ullmann's Encyclopedia of Industrial Chemistry. 2001.

3. Van den Berg J. Analytical chemical studies on traditional linseed oil paints. (Thesis) 2002.
4. White R. The organic chemistry of museum objects. London: Butterworth; 1994.
5. Van Dam EP, van den Berg KJ, Gaibor ANP, van Bommel M. Analysis of triglyceride degradation products in drying oils and oil paints using LC-ESI-MS. *Int J Mass Spectrom*. 2017;413:33–42.
6. Colombini MP, Modugno F. Organic mass spectrometry in art and archaeology. Hoboken: Wiley; 2009.
7. Van der Doelen GA, van den Berg KJ, Boon JJ. Comparative chromatographic and mass-spectrometric studies of triterpenoid varnishes: fresh material and aged samples from paintings. *Stud Conserv*. 1998;43(4):249–64.
8. Levison HW. Yellowing and bleaching of paint films. *Journal of the American Institute for Conservation*. 1985;24(2):69–76.
9. Smith R. The artist's handbook. London: Dorling Kindersley; 1990.
10. Schilling MR, Mazurek J, Learner TJ. Studies of modern oil-based artists' paint media by gas chromatography/mass spectrometry. *Modern paints uncovered: proceedings from the modern paints uncovered symposium*, Getty Conservation Institute symposium proceedings series Getty Conservation Institute, Los Angeles; 2007: 129–139.
11. Foster A. The performance and properties of artisan water mixable oil colour compared with other oil-based paints by Winsor & Newton. *Modern paints uncovered: proceedings from the modern paints uncovered symposium*; 2007: 53–57.
12. Carlyle L. Historical reconstructions of artists' oil paint: an investigation of oil processing methods and the use of selected artists' mediums. *Deterioration of artists' paints: effects and analysis A joint meeting of ICOM-CC working groups 1 & 2 and the Paintings Section, UKIC, British Museum, London, September 10–11, 2001* Extended abstracts of publications; 2001.
13. Carlyle L. Historically accurate reconstructions of oil painters' materials: an overview of the Hart project 00-005. *Reporting Highlights of the De Mayerne Programme*, (Jaap J Boon and Esters SB Ferrera), Den Haag. 2006:63–76.
14. Katkade M, Syed H, Andhale R, Sontakke M. Fatty acid profile and quality assessment of safflower (*Carthamus tinctorius*) oil. *J Pharmacogn Phytochem*. 2018;7:3581–5.
15. Coşge B, Gürbüz B, Kiralan M. Oil content and fatty acid composition of some Safflower (*Carthamus tinctorius* L.) varieties sown in Spring and Winter. *Int J Nat Eng Sci*. 2007;1(3):11–5.
16. Kirchner E, van der Lans I, Ligterink F, Geldof M, Ness Proano Gaibor A, Hendriks E, et al. Digitally reconstructing van Gogh's field with irises near Arles. Part 2: pigment concentration maps. *Color Res Appl*. 2018;43(2):158–76.
17. Kirchner E, van der Lans I, Ligterink F, Geldof M, Megens L, Meedendorp T, et al. Digitally reconstructing Van Gogh's Field with Irises near Arles part 3: determining the original colors. *Color Res Appl*. 2018;43(3):311–27.
18. Monico L, Janssens K, Miliani C, Brunetti BG, Vagnini M, Vanmeert F, et al. The degradation process of lead chromate in paintings by Vincent van Gogh studied by means of Spectromicroscopic methods. 3: synthesis, characterization and detection of different crystal forms of the chrome yellow pigment. *Anal Chem*. 2012;85:851–9.
19. Centeno SA, Mahon D. The chemistry of aging in oil paintings: metal soaps and visual changes. *Metrop Mus Art Bull*. 2009;67(1):12–9.
20. Centeno SA, Hale C, Carò F, Cesaratto A, Shibayama N, Delaney J, et al. Van Gogh's Irises and Roses: the contribution of chemical analyses and imaging to the assessment of color changes in the red lake pigments. *Herit Sci*. 2017;5(1):18.
21. Shimadzu Y, Van Den Berg K. On metal soap related colour and transparency changes in a 19th C painting by Millais. *Reporting Highlights of the De Mayerne Programme*. Netherlands Organisation for Scientific Research (NWO); 2006. P.43–52.
22. Hermans J, Osmond G, van Loon A, Iedema P, Chapman R, Drennan J, et al. Electron microscopy imaging of zinc soaps nucleation in oil paint. *Microsc Microanal*. 2018;24(3):318–22.
23. Hermans JJ, Keune K, van Loon A, Corkery RW, Iedema PD. Ionomer-like structure in mature oil paint binding media. *RSC Adv*. 2016;6(96):93363–9.
24. Kirchner E, der Lans I, Ligterink F, Hendriks E, Delaney J. Digitally reconstructing van Gogh's field with irises near Arles. Part 1: varnish. *Color Res Appl*. 2018;43(2):150–7.
25. Nicolaus K. *Restoration of Paintings*. New York: Konemann; 1999.
26. Mallégol J, Lemaire J, Gardette J-L. Yellowing of oil-based paints. *Stud Conserv*. 2001;46:121–31.
27. Privett O, Blank M, Covell J, Lundberg W. Yellowing of oil films. *J Am Oil Chem Soc*. 1961;38(1):22–7.
28. Geldof M, Gaibor ANP, Ligterink F, Hendriks E, Kirchner E. Reconstructing Van Gogh's palette to determine the optical characteristics of his paints. *Herit Sci*. 2018;6(1):17.
29. de la Rie ER. Fluorescence of paint and varnish layers (Part II). *Stud Conserv*. 1982;27(2):65.
30. Chio K, Tappel AL. Synthesis and characterization of the fluorescent products derived from malonaldehyde and amino acids. *Biochemistry*. 1969;8(7):2821–7.
31. Franks F, Roberts B. Quantitative study of the oxidative discoloration of ethyl linoleate. I. Oxidation in the bulk phase. *J Appl Chem*. 1963;13(7):302–9.
32. O'Neill L, Rybicka S, Robey T. Yellowing of drying oil films. *Chemistry and industry*. 1962; 1796–7.
33. Rakoff H, Thomas F, Gast L. Reversibility of yellowing phenomenon in linseed-based paints. *J Coat Technol*. 1979;51(649):25–8.
34. Mounier A, Belin C, Daniel F. Spectrofluorimetric study of the ageing of mixtures used in the gildings of mediaeval wall paintings. *Environ Sci Pollut Res*. 2011;18(5):772–82.
35. Ioakimoglou E, Boyatzis S, Argitis P, Fostiridou A, Papapanagiotou K, Yanovits N. Thin-film study on the oxidation of linseed oil in the presence of selected copper pigments. *Chem Mater*. 1999;11(8):2013–22.
36. Kumarathasan R, Rajkumar AB, Hunter NR, Gesser HD. Autoxidation and yellowing of methyl linolenate. *Prog Lipid Res*. 1992;31(2):109–26.
37. Bayliss S, van den Berg KJ, Burnstock A, de Groot S, van Keulen H, Sawicka A. An investigation into the separation and migration of oil in paintings by Erik Oldenof. *Microchem J*. 2016;124:974–82.
38. Cosentino A. Practical notes on ultraviolet technical photography for art examination. *Conserv Património*. 2015. <https://doi.org/10.14568/cp2015006>.
39. Pelagotti A, Pezzati L, Bevilacqua N, Vascotto V, Reillon V, Daffara C, editors. *A study of UV fluorescence emission of painting materials*. Art '05–8th International Conference on Non-Destructive Investigations and Microanalysis for the Diagnostics and Conservation of the Cultural and Environmental Heritage Lecce, Italy; 2005.
40. Rorimer JJ. *Ultra-violet rays and their use in the examination of works of art*. New York: Metropolitan Museum of Art; 1931.
41. Mounier A, Lazare S, Le Bourdon G, Aupetit C, Servant L, Daniel F. LEDµSF: a new portable device for fragile artworks analyses. Application on medieval pigments. *Microchem J*. 2016;126:480–7.
42. Romani A, Clementi C, Miliani C, Favaro G. Fluorescence spectroscopy: a powerful technique for the noninvasive characterization of artwork. *Acc Chem Res*. 2010;43(6):837–46.
43. Romani A, Clementi C, Miliani C, Brunetti B, Sgamellotti A, Favaro G. Portable equipment for luminescence lifetime measurements on surfaces. *Appl Spectrosc*. 2008;62(12):1395–9.
44. Fuster-López L, Stols-Witlox M, Picollo M. UV-Vis Luminescence imaging techniques/Técnicas de imagen de luminiscencia UV-Vis. *Colección Conservación 360º*. 2020.
45. Comelli D, Valentini G, Nevin A, Farina A, Toniolo L, Cubeddu R. A portable UV-fluorescence multispectral imaging system for the analysis of painted surfaces. *Rev Sci Instrum*. 2008;79(8):086112.
46. Pavia DL, Lampman GM, Kriss G. *Introduction to spectroscopy Third Edition*. Thomson Learn Inc. 2001;15:579.
47. Van den Berg JD, van den Berg KJ, Boon JJ. Identification of non-cross-linked compounds in methanolic extracts of cured and aged linseed oil-based paint films using gas chromatography–mass spectrometry. *J Chromatogr A*. 2002;950(1–2):195–211.
48. Udell NA, Hodgkins RE, Berrie BH, Meldrum T. Physical and chemical properties of traditional and water-mixable oil paints assessed using single-sided NMR. *Microchem J*. 2017;133:31–6.
49. Lakowicz JR. *Principles of fluorescence spectroscopy*. New York: Plenum Press; 1983.
50. Sutherland K. Solvent-extractable components of linseed oil paint films. *Stud Conserv*. 2003;48(2):111–35.

51. Zhu S, Song Y, Shao J, Zhao X, Yang B. Non-conjugated polymer dots with crosslink-enhanced emission in the absence of fluorophore units. *Angew Chem Int Ed*. 2015;54(49):14626–37.
52. Bonaduce I, Duce C, Lluveras-Tenorio A, Lee J, Ormsby B, Burnstock A, et al. Conservation issues of modern oil paintings: a molecular model on paint curing. *Acc Chem Res*. 2019;52(12):3397–406.
53. Bonaduce I, Carlyle L, Colombini MP, Duce C, Ferrari C, Ribechini E, et al. New insights into the ageing of linseed oil paint binder: a qualitative and quantitative analytical study. *PLoS ONE*. 2012;7(11):e49333.
54. Schaich K. Lipid Oxidation: New Perspectives on an Old Reaction. Bailey's industrial oil and fat products. 2020.
55. Schaeffer TT. Effects of light on materials in collections: data on photo-flash and related sources. Los Angeles: Getty Publications; 2001.
56. Feller RL. Accelerated aging: photochemical and thermal aspects. Los Angeles: Getty Publications; 1995.
57. Comelli D, Nevin AB, Verri G, Valentini G, Cubeddu R. Time-resolved fluorescence spectroscopy and fluorescence lifetime imaging for the analysis of organic materials in wall painting replicas. 2015.
58. Larson LJ, Shin K-SK, Zink JI. Photoluminescence spectroscopy of natural resins and organic binding media of paintings. *J Am Inst Conserv*. 1991;30(1):89–104.
59. Miyoshi T. Fluorescence from oil colours, linseed oil and poppy oil under N₂ laser excitation. *Jpn J Appl Phys*. 1985;24(3):371–2.
60. Itakura K, Uchida K. Evidence that malondialdehyde-derived aminoenimine is not a fluorescent age pigment. *Chem Res Toxicol*. 2001;14(5):473–5.
61. Carlyle L, Binnie N, Kaminska E, Ruggles A, editors. The yellowing/bleaching of oil paintings and oil paint samples, including the effect of oil processing, driers and mediums on the colour of lead white paint. Triennial meeting (13th), Rio de Janeiro, 22–27 September 2002: preprints; 2002.
62. Berns RS, Byrns S, Casadio F, Fiedler I, Gallagher C, Imai FH, et al. Rejuvenating the color palette of Georges Seurat's *A Sunday on La Grande Jatte—1884*: a simulation. *Color Res Appl*. 2006;31(4):278–93.
63. Miliani C, Monaco L, Melo MJ, Fantacci S, Angelin EM, Romani A, et al. Photochemistry of Artists' Dyes and Pigments: towards better understanding and prevention of colour change in works of art. *Angew Chem Int Ed*. 2018;57(25):7324–34.

Publisher's Note

Springer Nature remains neutral with regard to jurisdictional claims in published maps and institutional affiliations.

Submit your manuscript to a SpringerOpen® journal and benefit from:

- Convenient online submission
- Rigorous peer review
- Open access: articles freely available online
- High visibility within the field
- Retaining the copyright to your article

Submit your next manuscript at ► [springeropen.com](https://www.springeropen.com)